Stanley Meyer's Hydrogen Fracturing Process

An Electronic Circuit Analysis

With Additional Mechanical Dimensions

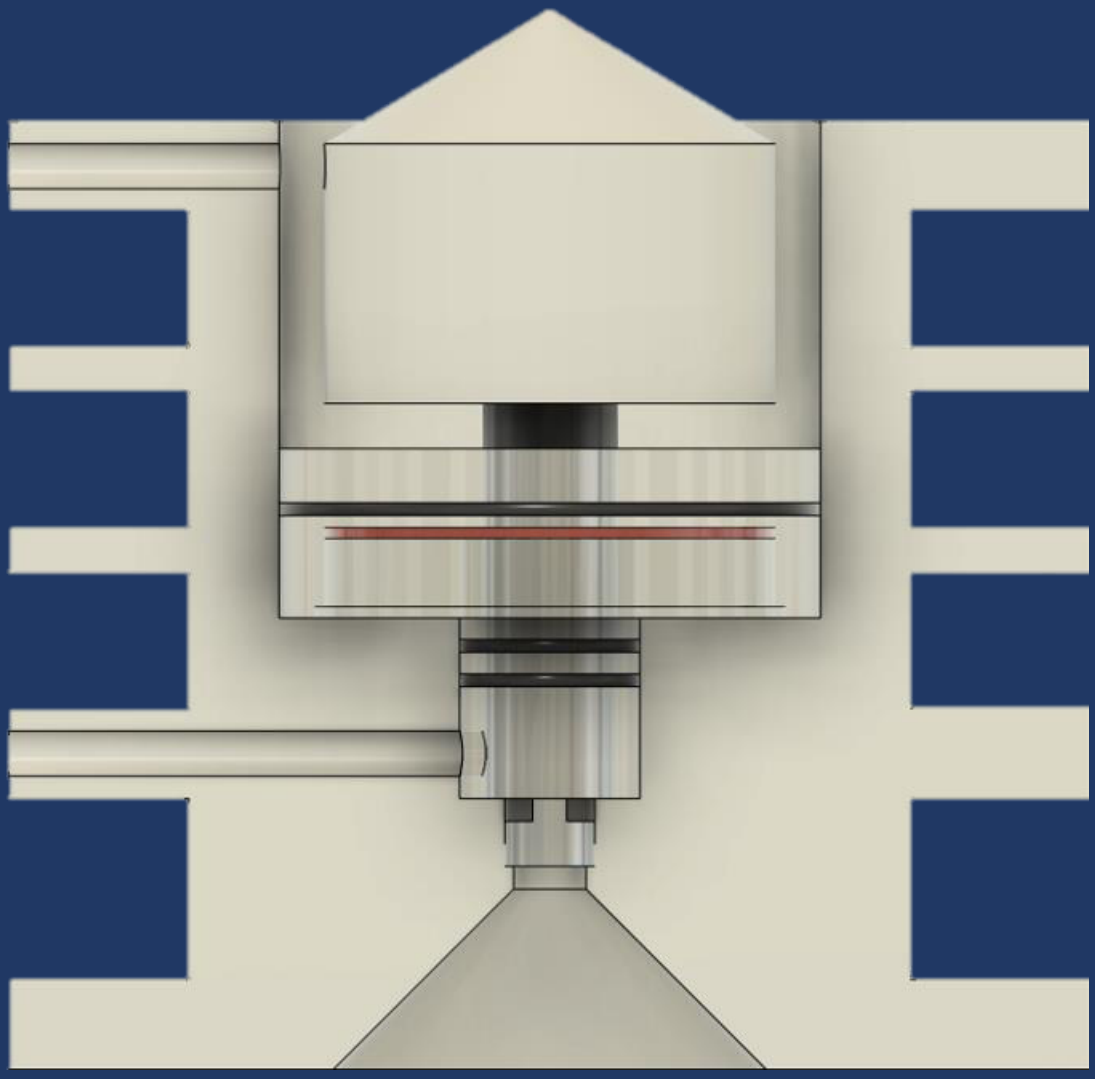

Ethan Crowder

Introduction & Acknowledgements:

Stan Meyer's technology encompasses a multitude of avenues, often overshadowed by the iconic water-powered car. While this vehicle remains a remarkable achievement, it represents only a culmination of numerous separate discoveries made throughout Meyer's extensive research and development career. The focus of this book is to bridge the gap in understanding by providing technical analysis of the electronic circuitry employed by him. This analysis is drawn from his literature and publicly released photographs, offering a detailed examination of the methodologies he described. By delving into these technical aspects, this book aims to shed light on the broader scope of Meyer's work.

The lack of comprehensive technical analysis has led to numerous misconceptions, and a general dismissal of Stan's accomplishments. This deficiency has fostered an environment where the true significance of Stan's work is often misunderstood. Inspired by this critical gap in understanding, this book was written with the intention of preserving the knowledge surrounding Stan's contributions and ensure that Stan's achievements receive the recognition they rightfully deserve.

Special Thanks:

1.) Stanley Allen Meyer, in who's memory this work is dedicated to.
2.) To our core research team members consisting of: Simon Beausoleil, Paul Butcher and Chris Bake for replication and numerous other contributions.
3.) Don Gabel who publicly released Stan's estate photographs, providing invaluable evidentiary proof of his technology and generously permitting their inclusion in this work.
4.) James Miner who has generously contributed to an expanding knowledgebase of Stan Meyer's work.
5.) Max Miller who has replicated, shared, demonstrated and proved Stan's concepts are viable.
6.) Frank Sullivan who replicated and shared Stan's work.

Notes From the Author:

Disclaimer: Due to the potentially dangerous nature of this technology, everything contained herein is meant for educational purposes only. The author does not accept any liabilities if replications are pursued.

Mechanical Dimensions: Appendix A through H contain dimensions for devices covered herein. The dimensions are based on photographic analysis and limited literature from Stan. While the best effort was made for accuracy, there may be some discrepancies. Unfortunately, original dimensions were not known at the time of this writing. Dimensions and some design features are tailored towards additive manufacturing techniques (3D printing). Traditional machining operations/techniques may warrant revision.

Open Source: The author believes Stan's technology belongs to all of humanity. This literary work may be disseminated freely, so long as monetary profit is not gained nor sought after. This literary work may also be translated into other languages by those who may be inspired to do so.

Supplemental Additions: While this book provides technical analysis of the electronic circuit functionality, it is not all encompassing. Further lab work may be added as a follow up at a later date.

Table of Contents:

Section One: The Hydrogen Fracturing Process	Page 3
Section Two: System Overview	Page 5
Section Three: PC9XA – VIC Driver Circuit	Page 14
Section Four: PC9XB – Variable Frequency Generator	Page 15
Section Five: PC9XC – Variable Gate Circuit	Page 26
Section Six: PC9XD – Regulated Voltage Supply Circuit	Page 38
Section Seven: PC9XE – Sequential Gate Circuit	Page 39
Section Eight: 20YJJ2 LED Light Module	Page 74
Section Nine: 20JX Gas Resonant Cavity	Page 76
Section Ten: Water Tank	Page 79
Appendix A: Gas Resonant Cavity Dimensions	Page 80
Appendix B: Water Resonant Cavity Dimensions	Page 103
Appendix C: Water Resonant Cavity Bottom Mount Dimensions	Page 108
Appendix D: Acrylic LED Lens Dimensions	Page 110
Appendix E: Colored Lens Dimensions	Page 113
Appendix F: Base Board & Rubber Feet Dimensions	Page 114
Appendix G: Insulative Cone Dimensions	Page 116
Appendix H: Water Tank Dimensions	Page 117

SECTION ONE: Hydrogen Fracturing Process

The hydrogen fracturing technology was a summation of several stages that are described below. Diagram 1 on page 4 provides a visual representation of each stage's progression and respective energy level.

Natural State: Prior to voltage stimulation, the water molecules are randomly dispersed (A) throughout the water medium inside each resonant cavity.

Analog Voltage Formation: When a variable voltage unipolar pulse train is applied to the voltage intensifier circuit, it produces an analog voltage pulse train that increases linearly. Each pulse causes the voltage to rise from a low to a high energy state. The voltage typically ranges from 0 to over 5,000 volts. The voltage remains positive relative to the negative ground throughout each pulse. The polarity on the excitor plates remains constant, and are generated simultaneously.

Water Molecule Alignment: Water molecules have opposite electrical charges within them. When an analog voltage pulse is applied, these molecules align with the voltage fields: positive hydrogen atoms move toward the negative plate, and negative oxygen atoms move toward the positive plate. Only a few nano-volts (B) are needed to start this molecular alignment.

Polarization Charge: The analog voltage causes the aligned water molecules to arrange end-to-end between the voltage plates, following the increasing positive voltage field. As the voltage level raises to the microvolt range (C), molecular alignment is achieved and movement stops. This alignment creates a polar charge between the voltage plates, with positive hydrogen atoms aligned in one direction and negative oxygen atoms in the opposite direction.

Molecular Elongation: As the analog voltage approaches the milli-volt range (D), the stationary water molecules begin to stretch because the positively and negatively charged atoms are attracted to opposite voltage zones, disrupting the equilibrium of the water molecules.

Atom Liberation: As the analog voltage increases (E), it disrupts the electrical equilibrium of the water molecules, causing the atoms to shift. Higher voltage intensifies the electrical charge on the atoms, eventually breaking the covalent bonds. Electrons are attracted to the positive hydrogen atoms and repelled by the negative oxygen atoms. This leads to electrical polarization and the disassociation of water molecules, which is directly related to the applied voltage. Higher voltages result in more gas production. During fuel cell operation, voltage fields can reach hundreds of volts.

Liquid To Gas Ionization: When the voltage reaches a certain threshold (F), the exposed water molecules, along with released hydrogen, oxygen, and other gases, begin to ionize. This ionization process causes the atoms to lose or gain electrons, destabilizing them and disrupting their electrical and mass equilibrium. Positive voltage fields attract negatively charged electrons, while positive nuclei are drawn to the negative voltage field. Because the voltage fields are continuous and unchanging in polarity, atoms do not stabilize. Ionization occurs at voltages of several thousand volts.

Electrical Charging Effect: As the ionized gases are allowed to accumulate inside said fuel cell, the electrical charging effect (G) can be greater than said applied voltage speeding up the Electrical Polarization Process still further.

Particle Impact: Particle impact (H) occurs when the liberated ionized gases are voltage deflected through the Electrical Polarization Process.

Laser of Photon Injection: To achieve gas ionization (I) and energize the atomic nuclei, a laser or photon energy of a specific wavelength and intensity is directed at the gas ions. The absorbed energy excites the nuclei, causing electrons to move to higher energy levels. The laser or light pulse's wavelength and intensity are adjusted to match the absorption characteristics of the gas nuclei.

Atomic Destabilization: Continued exposure of said gas ions (F) to said laser or light energy (I), during voltage stimulation (A through H) prevents atomic stabilization (J).

Atomic Triggering on Demand: Since the liberated atoms are highly energized combustible gas ions, having been electrically charged and laser primed (exposure to pulsed electromagnetic light energy), the atomic energy yield from water is simply controlled by varying the applied voltage pulse-train. When these gases flow into and through a quenching disc assembly, an immense amount of energy is released in the form of heat energy, up to and beyond 3,000 degrees Fahrenheit.

Diagram 1:

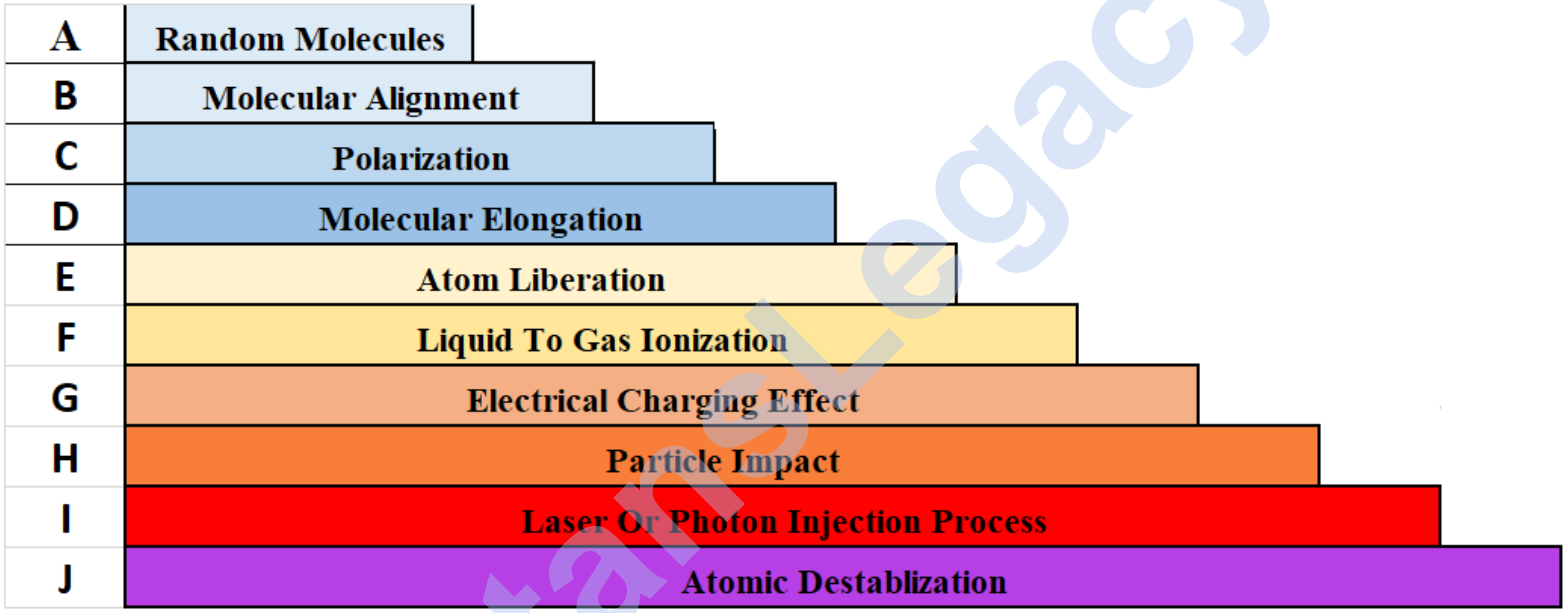

System Components:

- The hydrogen fracturing process electronic control unit.
- Resonant cavities with photon injection, stacked.
- Water recycling tank.
- Gas resonant Cavity.

SECTION TWO: System Overview

The Hydrogen Fracturing Process was the integration of several technological developments. In short, the process released atomic energy contained within Hydrogen and Oxygen gases from any natural water source. This was accomplished by utilizing electronic resonance circuitry, coupled with photon injection, reduced power consumption to a minimum. Particle impacts, referred to as "resonant action", increased the efficiency by producing ionization, leading to an increase in potential. Finally, fuel gases were ionized, having electrons removed, destabilizing their respective atoms, leading to greater energy release. The photo below shows the system unit front control panel.

(Source: photo courtesy Don Gabel)

Working left to right, a description of each of the control interface is below:

1.) **CONTROL UNIT:**
   a. POWER/HGG VOLTAGE LEVEL: Provides selection of 1V-4V (or higher) applied to the VIC associated with the Gas Resonant Cavity.
   b. "CP" (Constant Pulse): Provides constant train of pulses (frequency variable) to Dual Voltage Driver.
   c. "GP" (Gated Pulses): Provides gated pulse train (frequency variable) to Dual Voltage Driver.
   d. "SP" (Sequenced Pulses): Provides sequenced pulse train (frequency variable)

2.) **CAVITY ARRAY:**
   a. LIGHT: Controls the frequency of pulses driving LED array circuits contained within each resonant cavity, exposing water and releases gases to various colors of light, depending on plastic lens color.

3.) **HYDROGEN GAS GUN ASSEMBLY:**
   a. VOLTAGE: Controls the frequency of pulses to VIC stage from 1V-4V selection switch.
   b. LIGHT: Controls the frequency of pulses applied to 660nm LEDs on Gas Resonant Cavity.

4.) **PF1:** Variable frequency generator, 50% fixed duty cycle.
5.) **GATE:** Variable frequency flip-flop circuit and provides adjustable gate time to PF1 pulse train.
6.) **SEQ:** Variable frequency sequencing circuit to allow independent selection of resonant cavity stages.
7.) **PF2:** Variable frequency generator, 50% fixed duty cycle.
8.) **GAS RATE CONTROL/RESONANT AMPLITUDE:** Variable transformers providing independently adjustable voltages.

The photo below provides a rear view of the unit's internal layout.

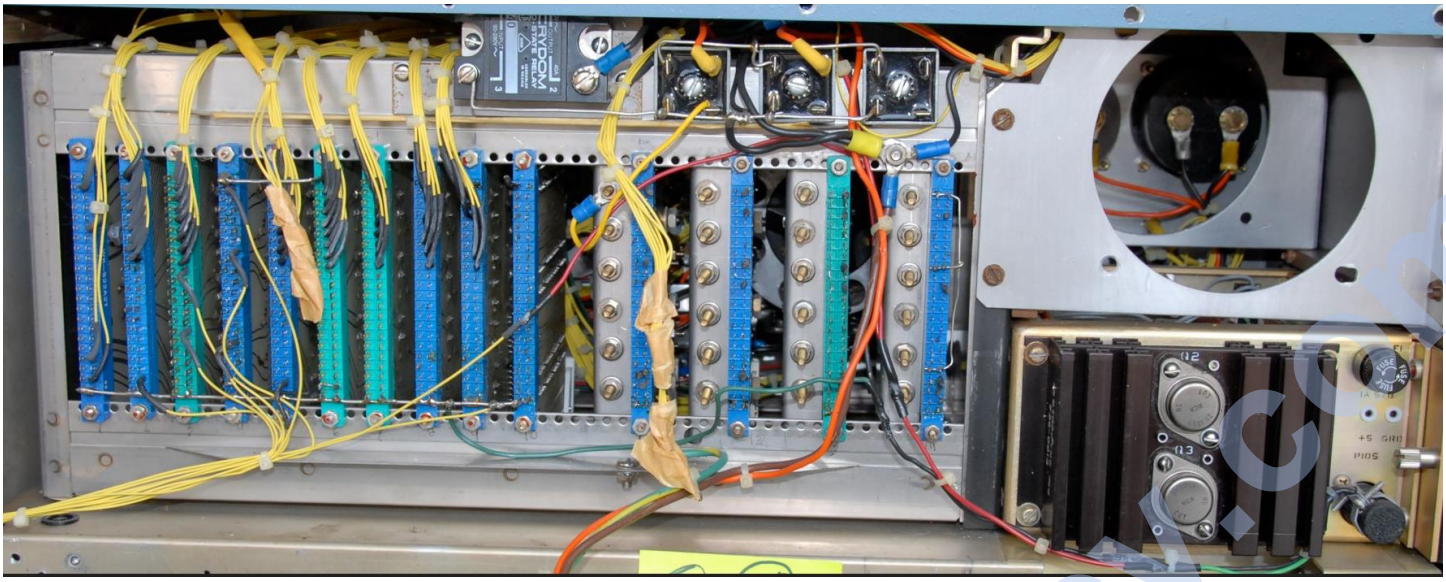

(Source: photo courtesy Don Gabel)

System Flow Chart:

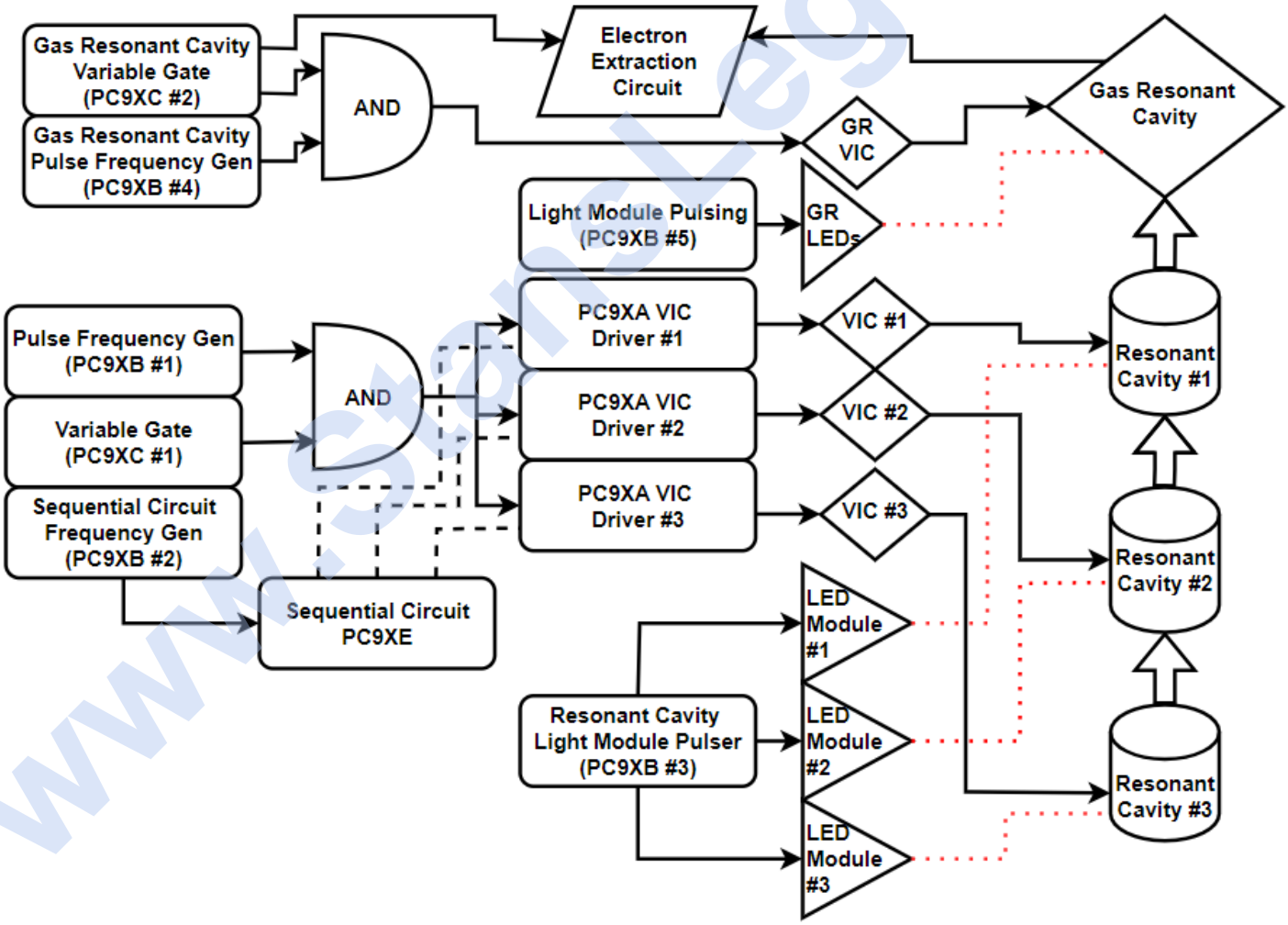

A brief discussion with CAD models of each component will now be presented. Full dimensions are provided in the appendices. Each resonant cavity housing was made of Delrin to provide the highest level of electrical insulation value. The CAD model below shows a cut-away view of a single cavity. Three channels were machined to provide slots for the external winding of the VIC coils, an interesting design characteristic of this device. An inner and outer electrode, coaxially orientated, extend upwards through a sealed light lens towards the middle of the chamber. The light lens contains an area for a PCB comprised of 5mm LEDs. Colored translucent plastic lenses were placed on top to provide different colored light, which was pulsed into the inner chamber. A Delrin cone was placed on top of the electrode pair to perform momentary entrapment, extending the exposure time of the Hydrogen & Oxygen gases to the pulsating light energy. These gases moved upwards into the next stacked cavity. Upwards movement produced a pumping action.

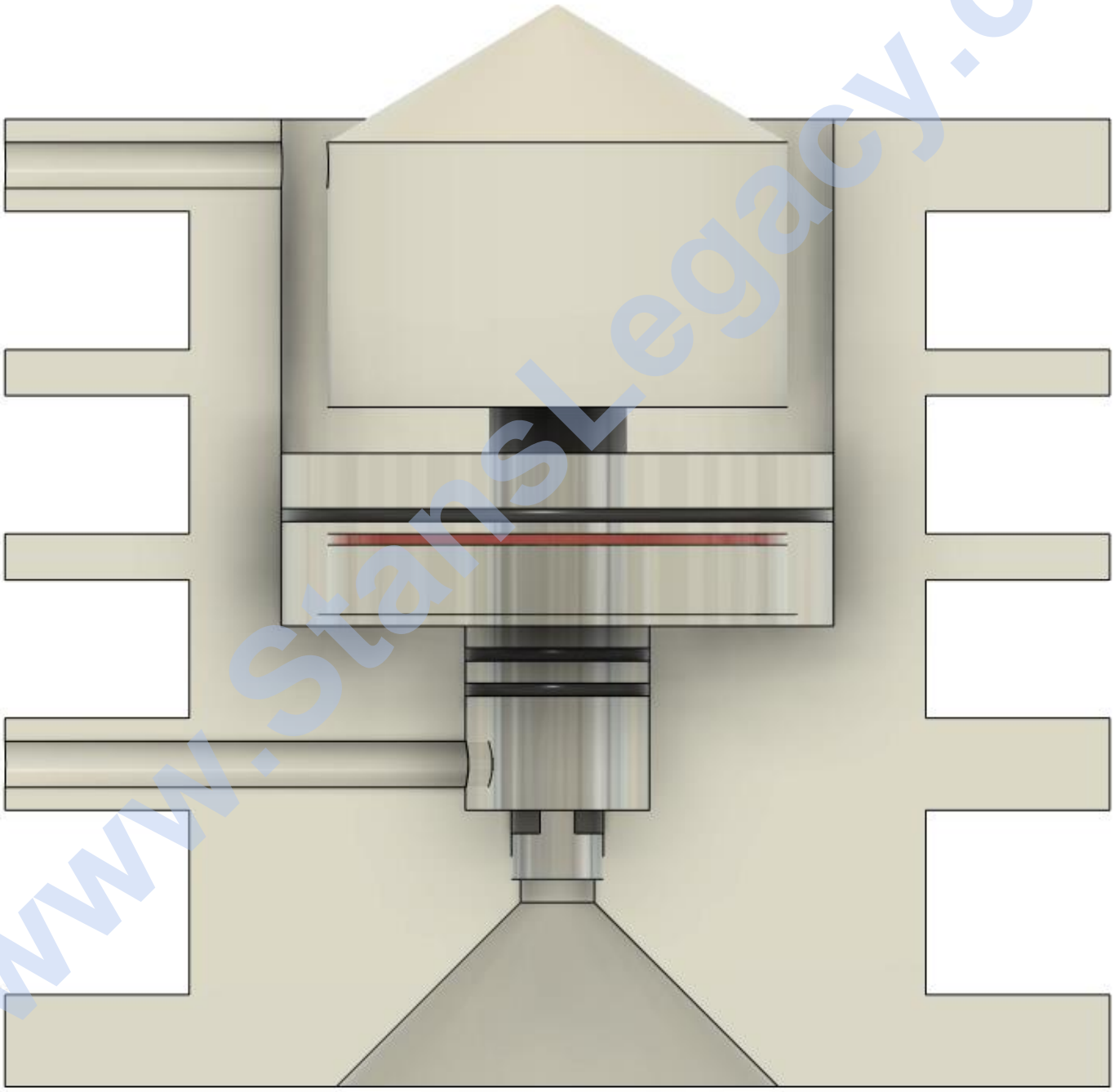

The CAD model below shows how the triple stack arrangement would be accomplished. From a machining viewpoint, depending on the quality of facing operations, sealing may be accomplished by simple joining of each section. However, pressurized sealing may be better accomplished by the employment of rubber gaskets between layers.

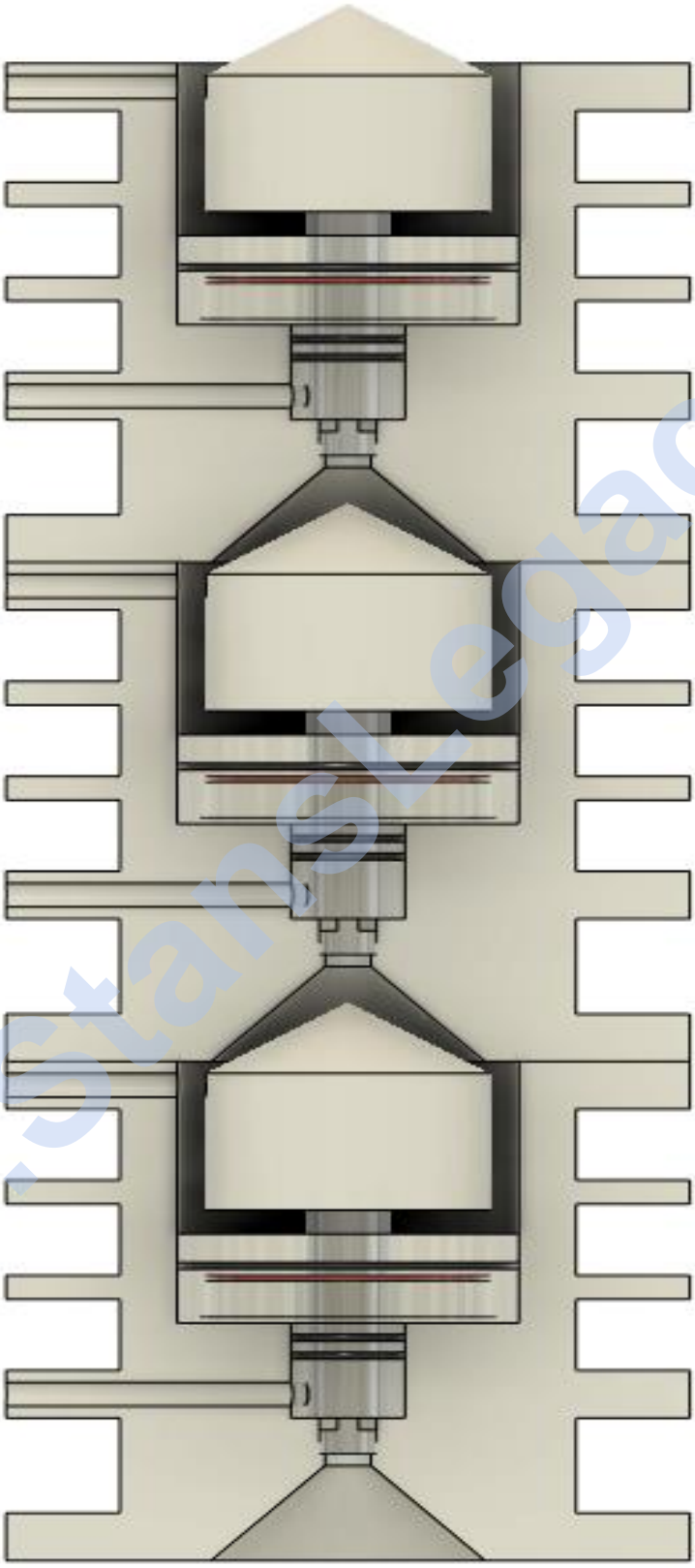

Each resonant cavity had a pair of tubular electrodes. Both are T-304 stainless steel. CAD models below illustrate how they're assembled. Working left to right, the solid inner electrode, with fluting at one end, is pressed fit inside an insulative Delrin cap. A hole is cut out of the side to allow connection via a screw. This pair is then pressed fit into the inner diameter of the outer electrode. The resultant arrangement is shown on the far right. Alignment for both is maintained when fluted end is placed into its corresponding recession within the resonant cavity. The gapping between the two is ideally 0.100", but this requires machining of a standard 0.75" tube with a 0.035" wall. Without machining, the gap measures 0.090"

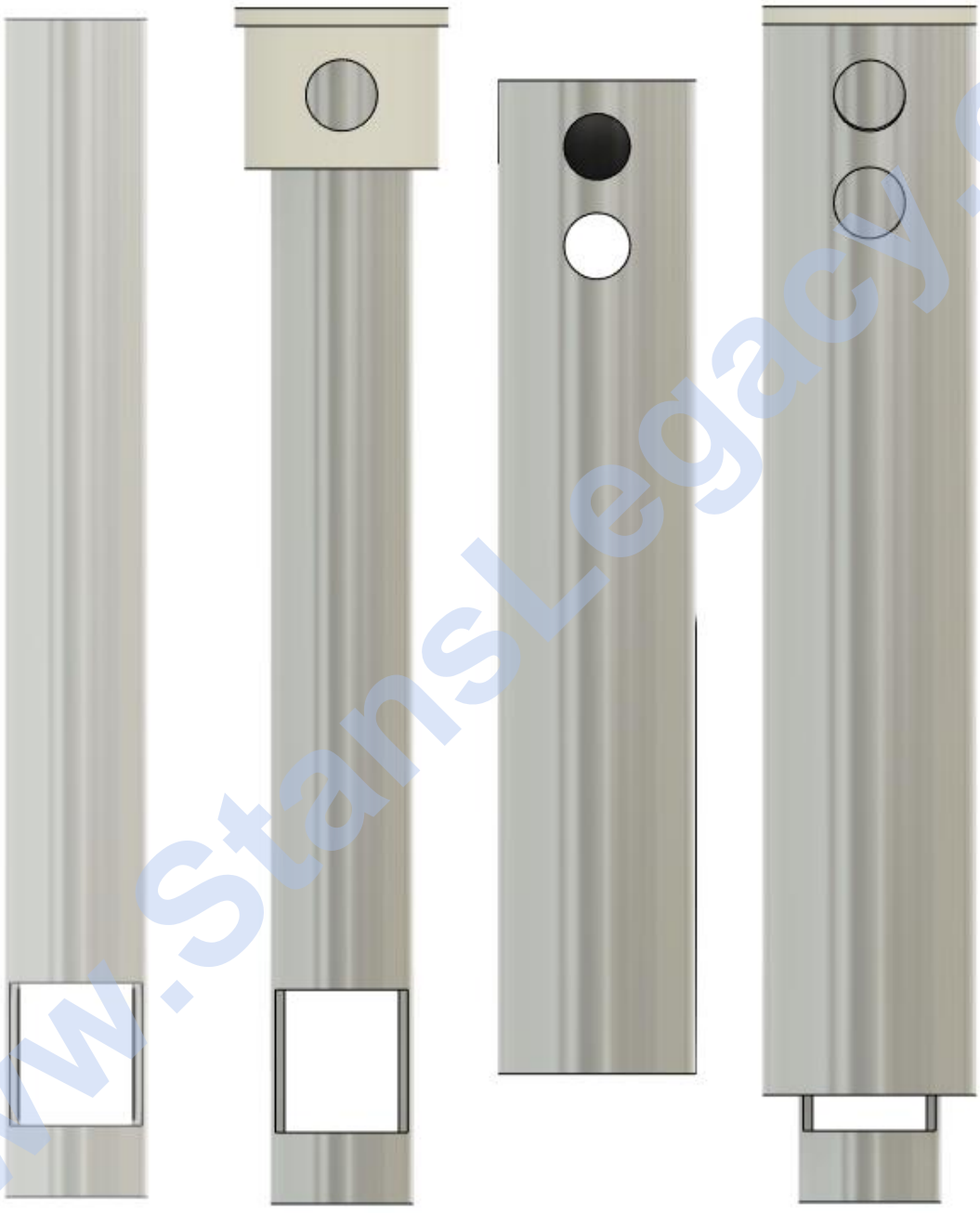

Stan's use of different colored lenses was to investigate potential effects on the liberated gases via exposure to monochromatic light. CAD models and photos below illustrate the location within the lens housing and differing colored plastic lenses that could've been used. The lenses would've been more translucent than the ones shown as examples.

Momentary entrapment is achieved in conjunction with the cone. The natural white surface of the Delrin provides optimum reflectivity, increasing the overall exposure of the gases to the light energy.

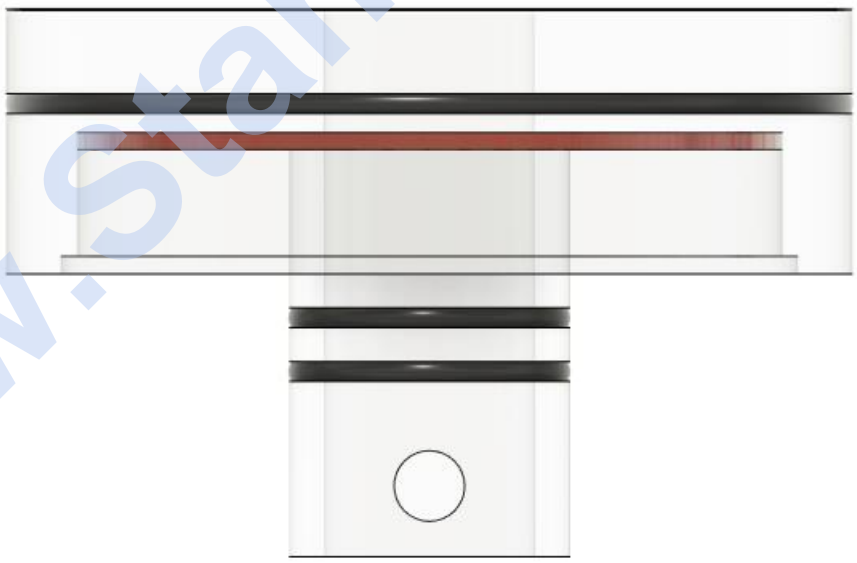

A water tank was located on top of the triple stack assembly. The center tube permitted gases to flow upwards, isolated from the volume of water. A fill port was located on the top cap. Not shown, a ½" diameter tubing extended from bottom of the water tank down to the bottom mount, utilizing gravity, for water replenishing within resonant cavities.

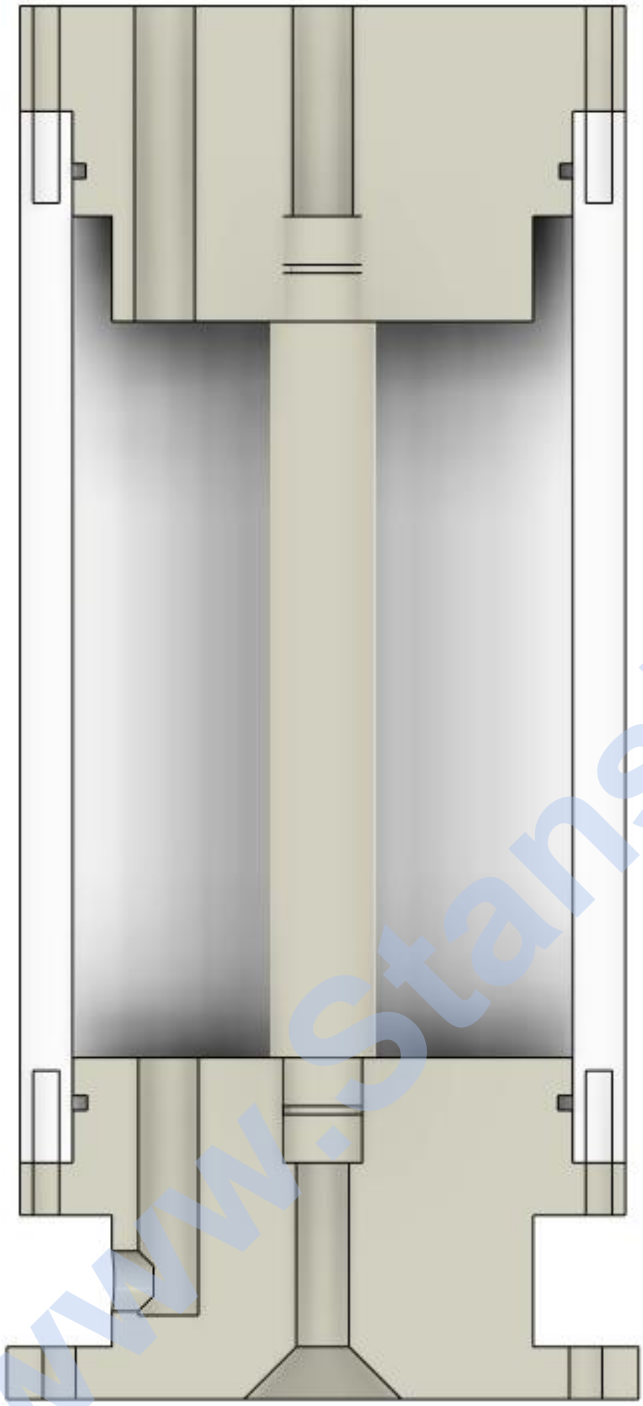

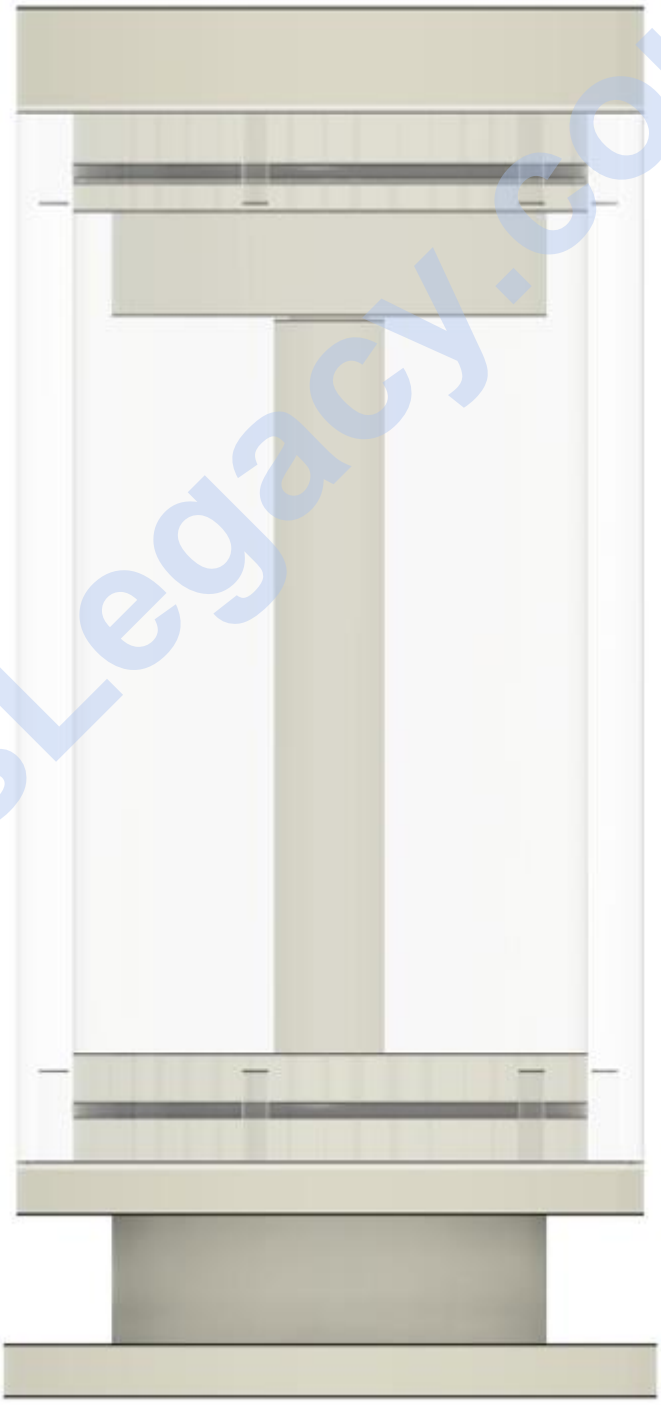

The final component, the Gas Resonant Cavity (also referred to as the Hydrogen Gas Gun) was affixed on top of the water tank. The liberated gases would pass through this device and become destabilized by having their electrons extracted. This destabilization process, or fracturing of atomic structures, produced a greater release of energy compared to combustion of the gases in their natural stable form. Similar to the resonant cavities, this device had VIC coils wrapped around the resonant electrode pair. From this observation, one can extrapolate that the outer electrode behaved as a core, although the coils position relative to one another would have loose coupling.

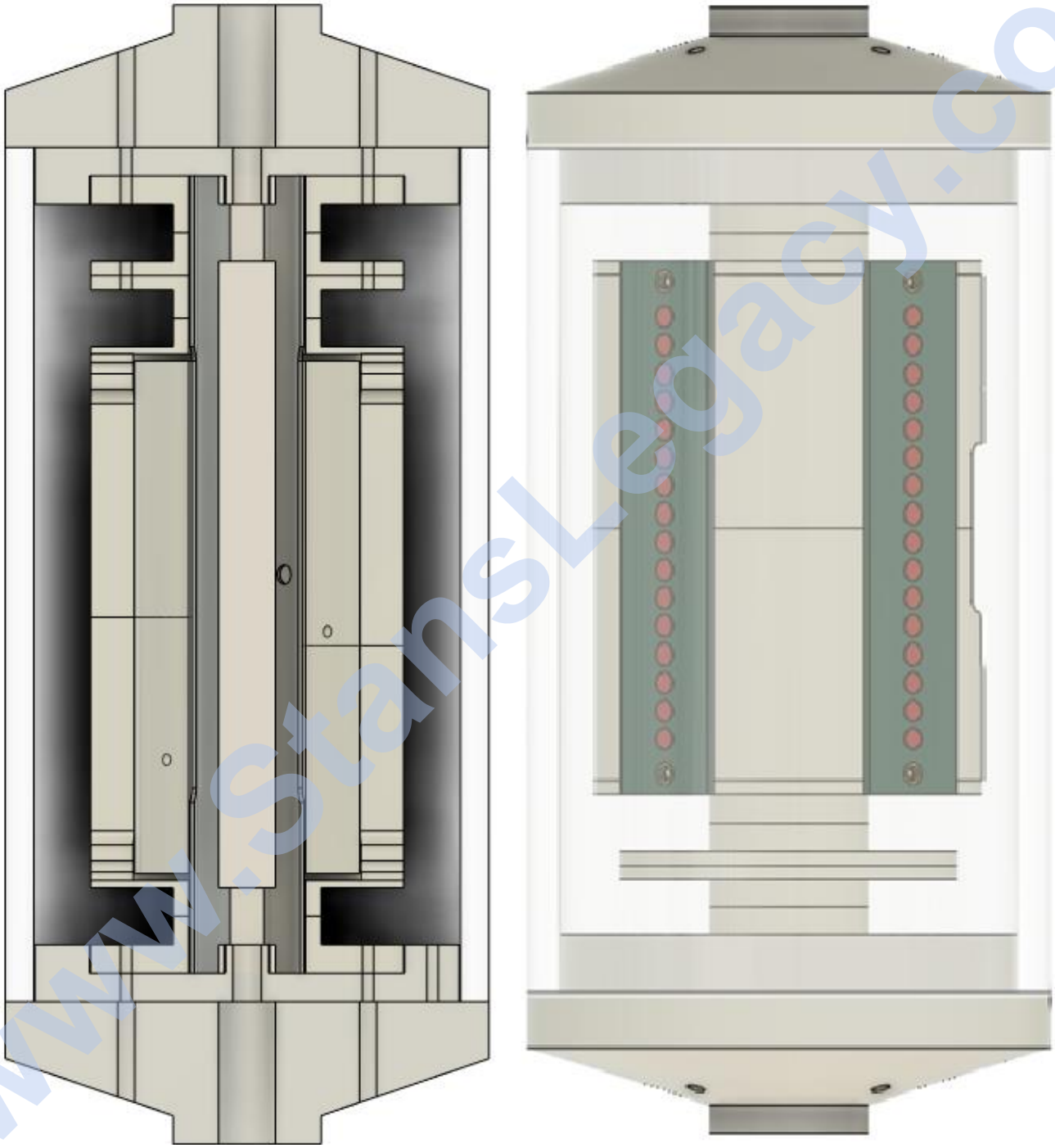

A CAD model of the complete system embodiment is shown below. For visibility purposes, VIC windings and terminal coverings were not included.

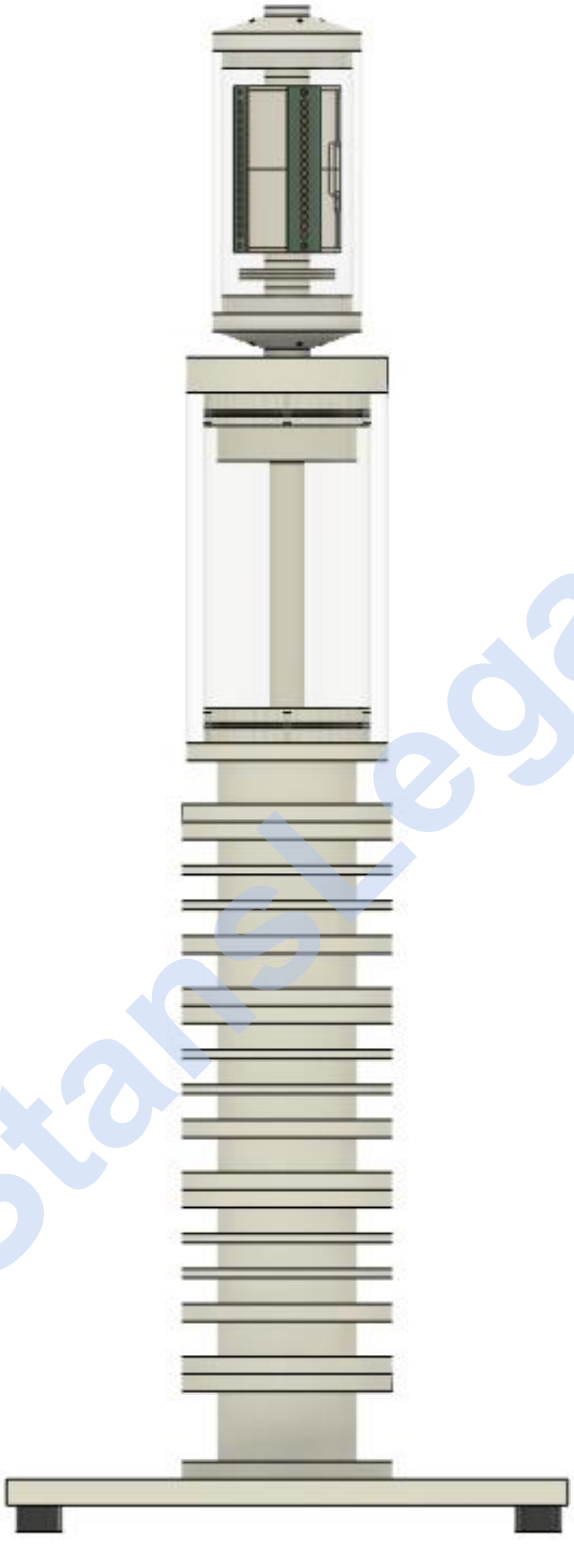

This concludes the system overview section. Subsequent sections will analyze the electronic circuitry.

Section Three: PC9XA – VIC Driver

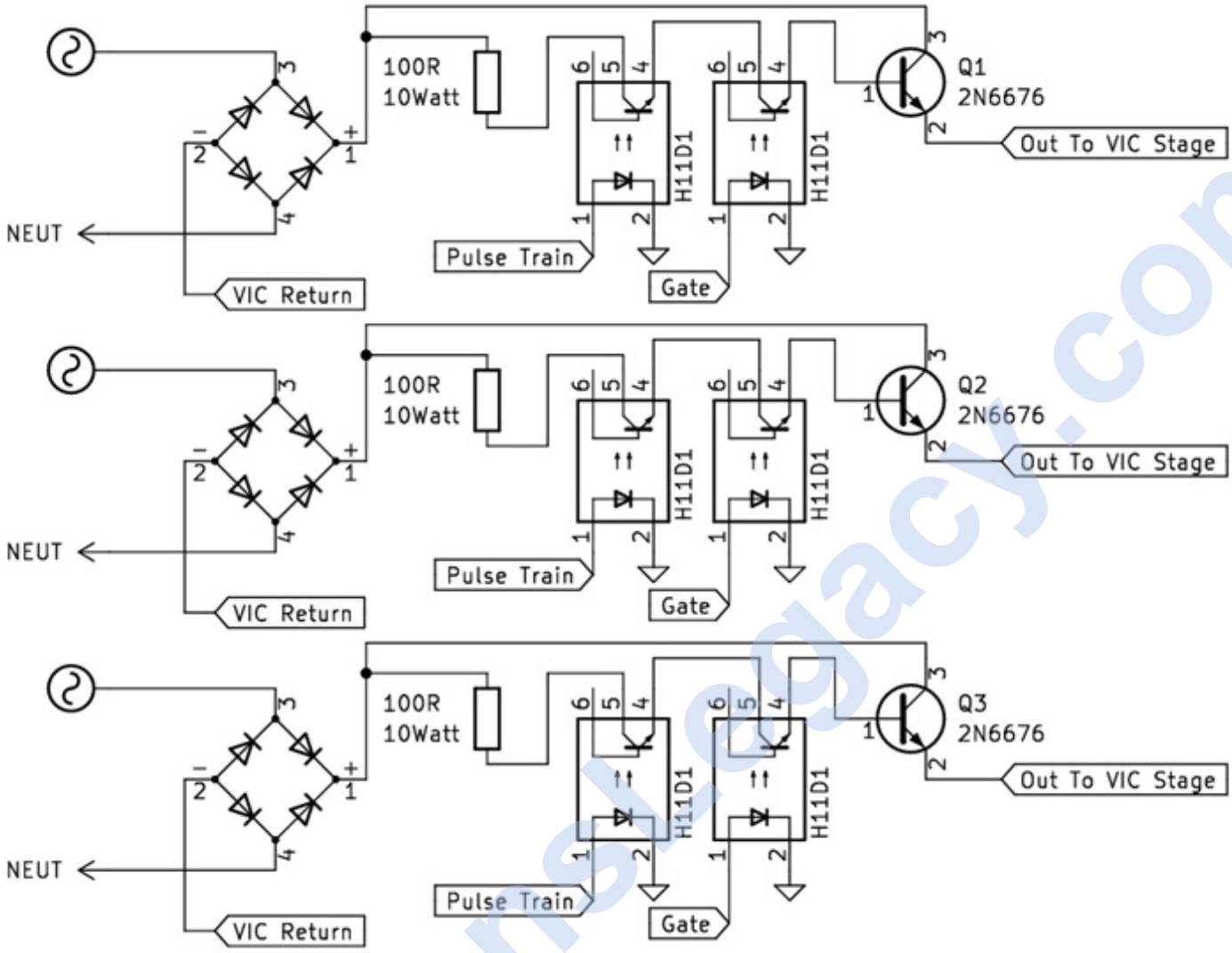

The circuit is composed of three independent power NPN-BJTs circuits. The 2N6676 was specified by Stan, however, any of appropriate rating or even modern N-Channel MOSFETs can be used. A rectifier stage produces a variable positive unipolar-pulsating waveform. Each circuit stage has a minimum of two optocouplers that provide electrical isolation between driver and waveform generation means. One provides a frequency pulse train ("Pulse Train"), the second one provides a gating frequency ("Gate") that controls how many frequency pulses are applied to the base of the driver component. A 100Ω/10W resistor provides a small resistance, as the required base current for the driver BJT is larger than a Darlington pair for example.

Majority of the current limiting is provided by optocoupler waveforms. Using N-Channel MOSFETs would provide additional isolation given the nature of their capacitance coupling. Greater signal clarity would also be afforded by using MOSFETs. Two interesting observations present themselves in regards to the above schematic. One, a smoothing capacitance is not explicitly shown. However, in order to produce specific waveforms for VIC operation, this would be a necessity. Second, the power BJT is an NPN type, which typically are used in low-side switching applications. The schematic illustrates a high-side switching mode.

Section Four: PC9XB - Variable Frequency Generator

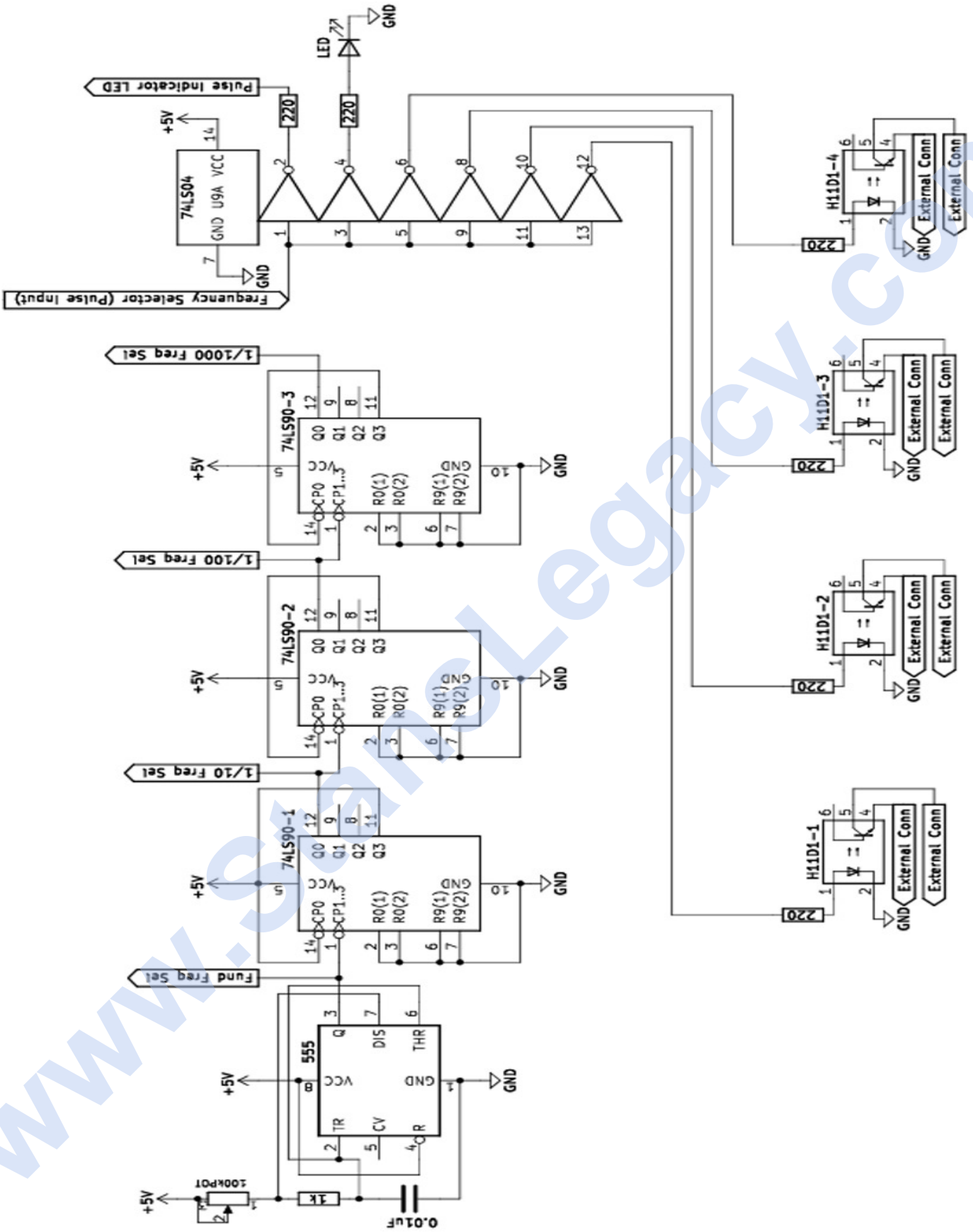

Replica Circuit Board:

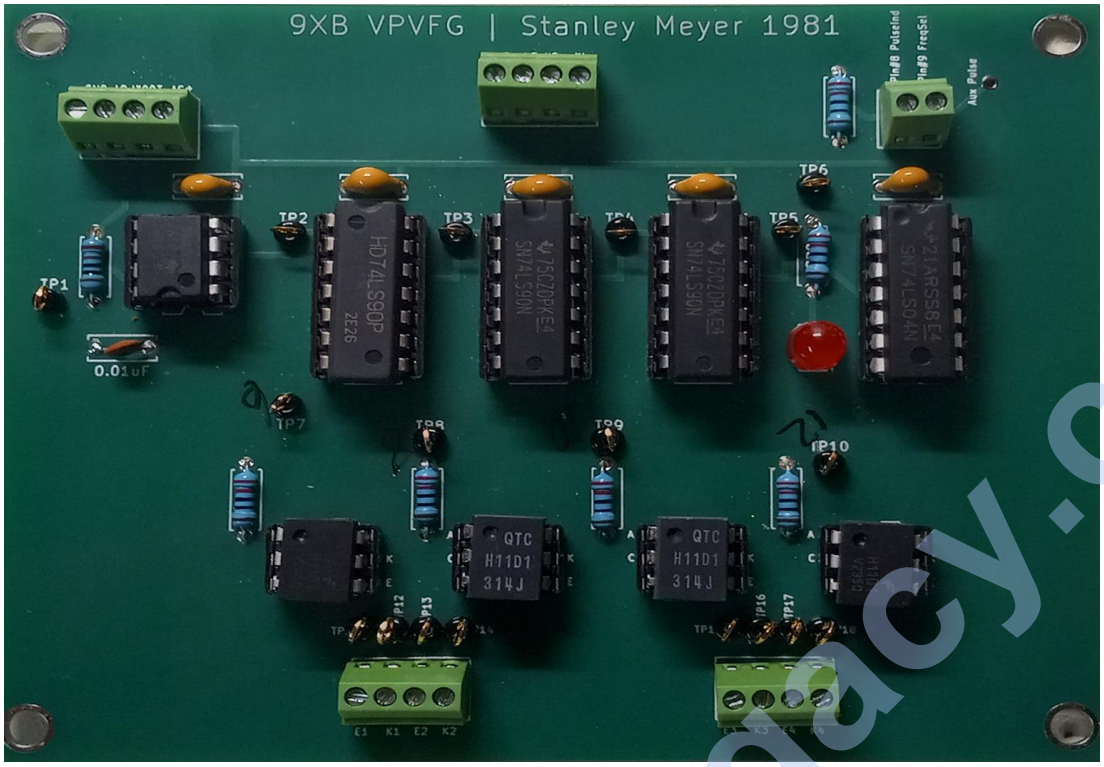

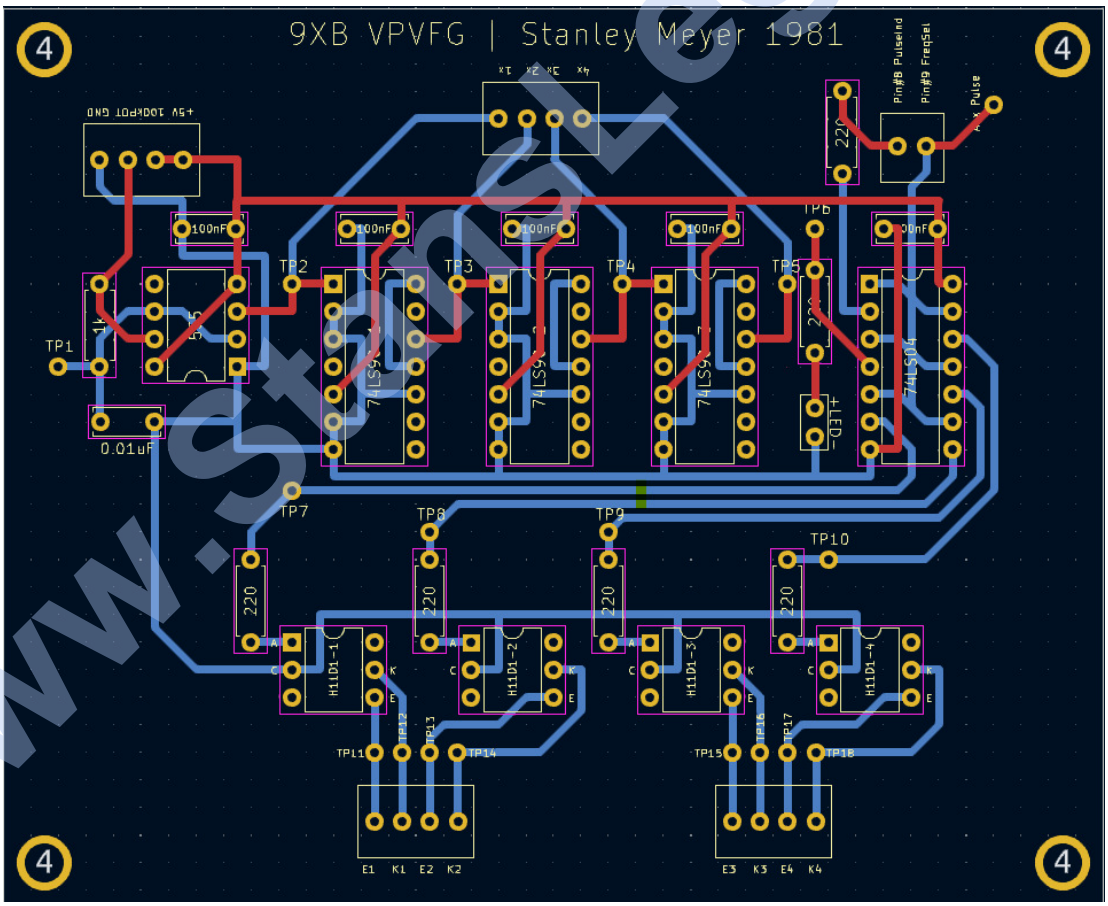

Stan's Original Explanation:

To avoid a constant voltage source to be applied to excitor array (voltage zones) while attenuating voltage amplitude for gas-rate control. (Note: Stan uses the word "attenuate" incorrectly. A more correct contextual word would be "modulate")

a.) The variable pulse voltage frequency is adjusted to keep amp flow to a minimum at a given voltage amplitude. The variable pulse voltage frequency amplitude is directly related to hydrogen gas production on demand.

Revised Explanation:

An adjustable frequency generator, with a fixed 50% duty cycle, that was utilized to produce a non-continuous application of source voltage. Paired with additional circuit stages that control the sequencing (PC9XE), gating of frequency pulse train (PC9XC) and providing a pulsating frequency for LED light applications.

Stan's Applications:

1.) **Hydrogen Fracturing Process:**
Frequency generator for VIC tuning, LED (photon injection) triggering, sequential selection of excitor pairs.

2.) **Electrical Particle Generator:**
Providing adjustable frequency generation means for triggering coil banks.

3.) **Gas Management System:**
Providing an adjustable master clock frequency for system processing.

4.) **8XA Circuit:**
Providing adjustable frequency for triggering of 120Hz rectified AC mains.

555 Operation:

The pulsing of the circuit is produced by the 555 in astable operation mode, shown in Figure 1 below. Frequency is determined by the RC time constant, produced from the values of the potentiometer (0Ω-100kΩ), R1(1kΩ) and C1(0.01uF = 10nF). As the potentiometer has its resistance varied from minimum (0Ω) to maximum (100kΩ) the time it takes to charge up C1 is varied proportionately.

Figure 1:

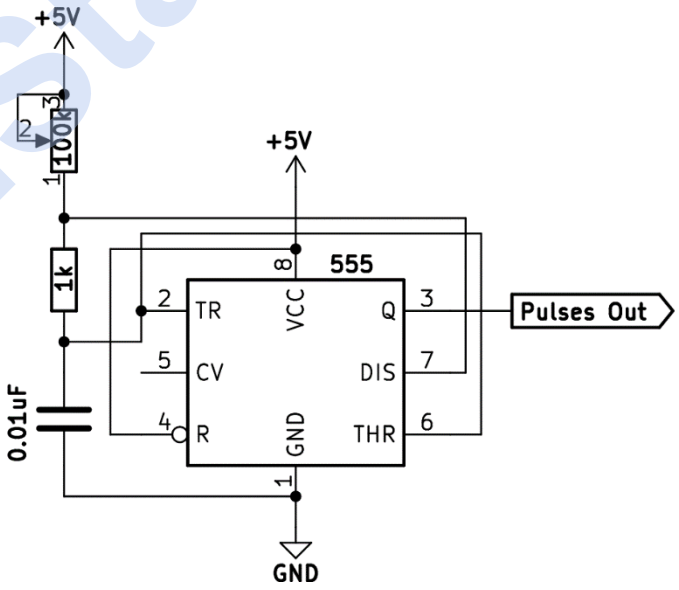

The frequency range for this arrangement can be calculated using the formula below:

$$F=\frac{1.44}{(R_1+2R_2)*C_1}$$

With the potentiometer resistance down to minimum value, 10Ω for example, this makes the maximum frequency of 71.79 kHz. With the potentiometer up to maximum value, 100kΩ, this makes the minimum frequency of 1.415 kHz.
To determine the on (HIGH) time and off (LOW) time, we can use the following formulas below:

$T_h = 0.693(R_1+R_2)*C_1$
$T_l = 0.693*R_2*C_1$

Duty Cycle may be calculated with the formula below:

$D=R_1/(R_1+R_2)$

For the maximum frequency 71.79 kHz, the high time: 6.99uS. The low time is: 6.93uS. Duty Cycle is: 50.25%
For the minimum frequency, 1.415 kHz, the high time is: 699uS. The low time is: 6.93uS. Duty Cycle is: 99.02%

From the above calculations, it can be seen that the duty cycle doesn't stay 50% throughout the frequency ranges. To accomplish this, the decade counters (74LS90) are used.

Decade Counter (74LS90) Operation:

The 7490, or 74LS90 contains a divide by 2 and divide by 5 stages. These two stages are connected to form a divide by 10. Internally, networks of rising edge triggered flip flops are shifting. Figure 2 below illustrates each 7490 connections to achieve divide-by-ten operations.

Figure 2:

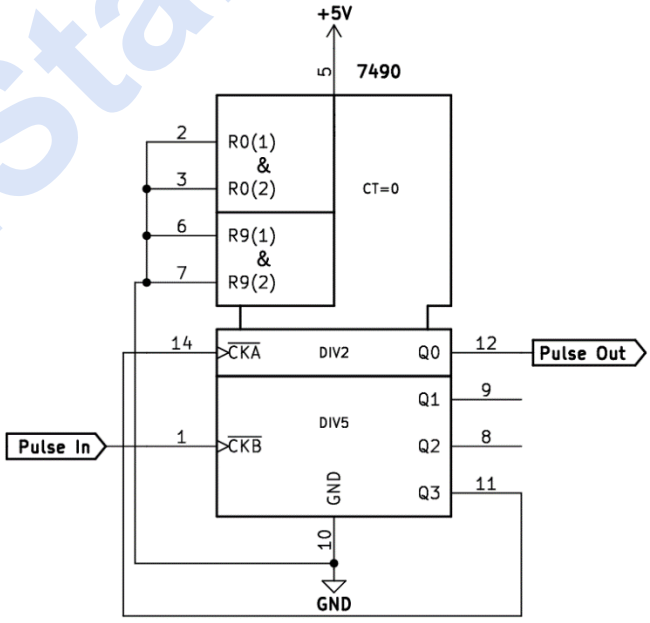

Oscilloscope Waveforms:

Pulse generation, supplied by the 555, produces a variable frequency output (pin #3). Given the circuit component values, varying the frequency also leads to a variance in duty cycle. Figure 3 below shows the measured duty cycle of ~1kHz. Scope measures 98.87% HIGH and 1.13% LOW.

Figure 3

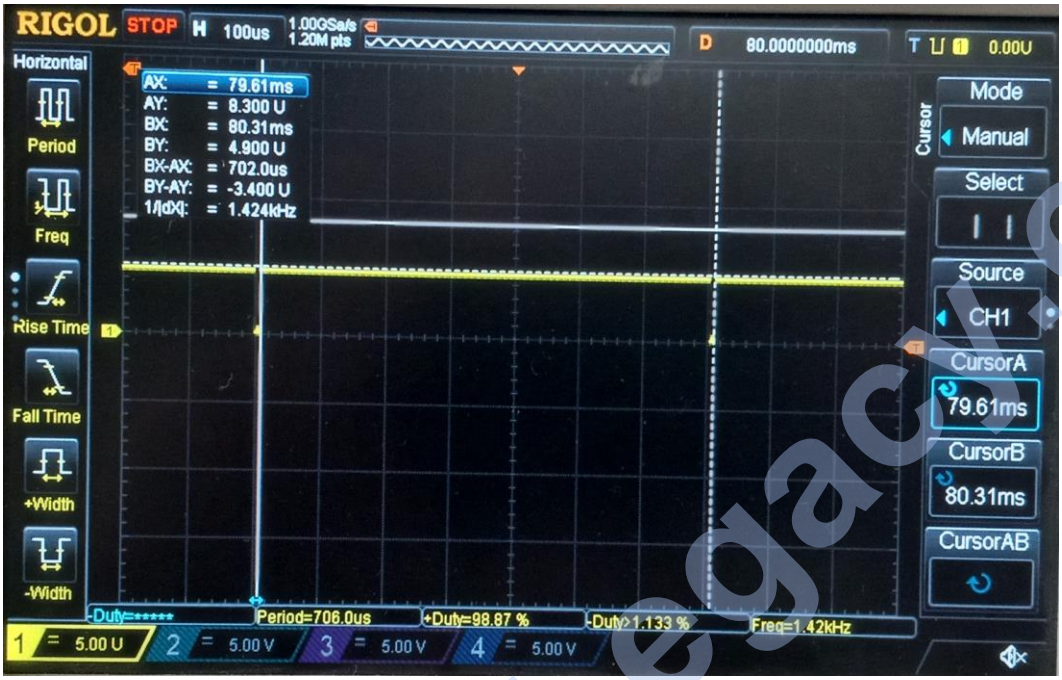

Figure 4 below shows the duty cycle measurement of the fundamental frequency adjusted to ~40kHz. Scope measures 68.70% HIGH and 31.30% LOW.

Figure 4:

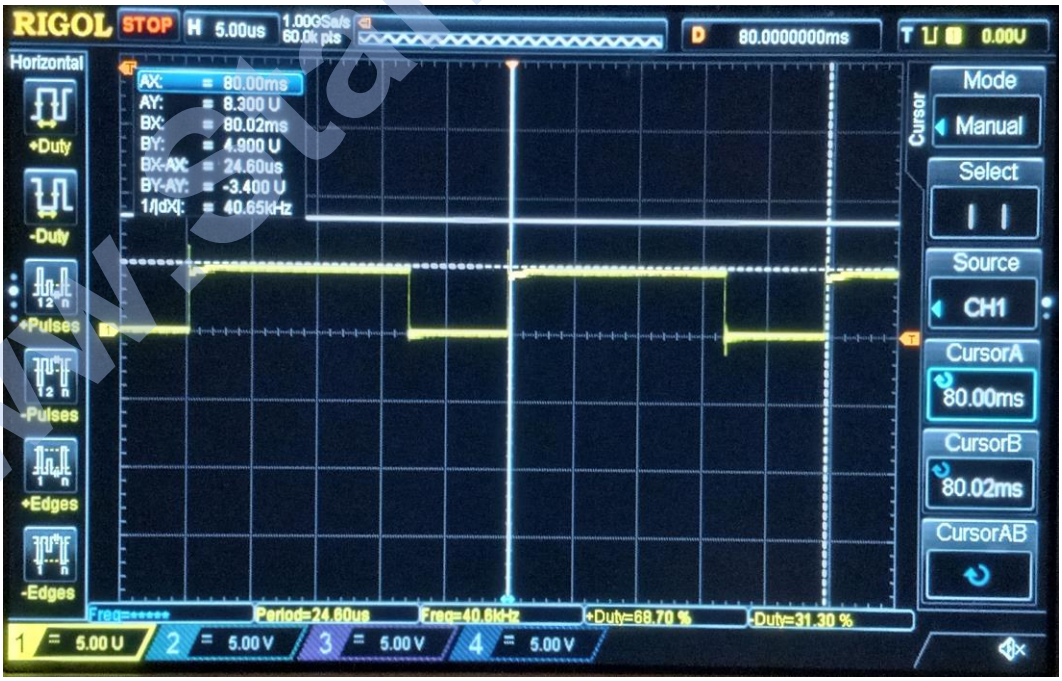

Frequency of the pulse is related to the period of the RC curve. Components of the RC curve (potentiometer and capacitor (0.01uF) determine this period. Figure 5 below demonstrates the longer period (800uS) for a lower frequency. In this capture, the frequency is 1.25kHz. To derive frequency from the period, the formula F = 1/T is utilized. Where 'T' is representative of the period time value. Therefore: F = 1 / 0.000800S, F = 1,250Hz.

Figure 5:

Figure 6 below demonstrates the RC curve for a higher frequency. In this capture, the frequency is ~20kHz. Higher frequencies have lower period time values. Notice that both scope shots are on the same time base, 200uS per division. This was intentionally done to show how the RC curve is occurring much faster compared to the 1.25kHz scope shot above. Comparing the two further demonstrates the linear relationship between RC charging time and frequency.

Figure 6:

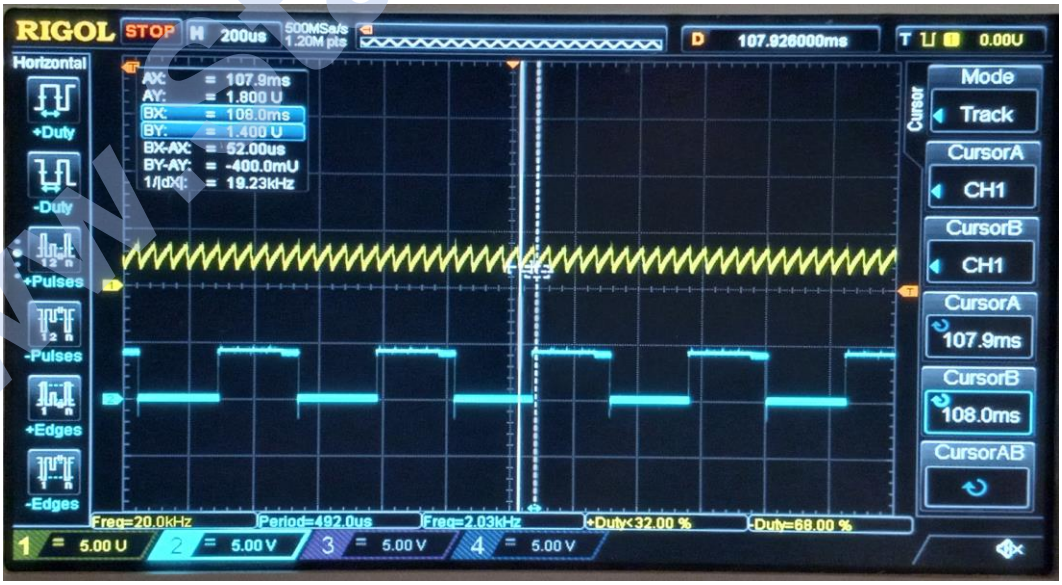

The 555 output (pin #3) frequency enters into the input (pin #1) of the first binary counter (74LS90-1), which is in a divide-by-ten arrangement. The counter begins the process of dividing the fundamental frequency by ten and conditioning the duty cycle to a fixed 50%. The output (pin #12), provides a frequency that is ten times less (1/10) that of the fundamental, and an external tap for selection of this frequency. Figure 7 below captures this first division. Channel one (yellow trace) shows the fundamental frequency as discussed earlier. Channel two (blue trace) shows the divided-by-ten frequency. Channel one has a measured frequency of 1.43kHz and a period of 700uS. Channel two has a measured frequency of 143Hz and period of 7mS. Finding the quotient between these two, the measurements are ten divisions between one another: 1,430Hz / 143Hz = 10; 7mS / 700uS = 10. This frequency output (143Hz) is connected with the input (pin #1) of the second divide-by-ten counter (74LS90-2).

Figure 7:

This second counter begins the process of dividing the fundamental frequency by one hundred. The output pin (#12), provides a frequency that is one hundred times (1/100) less than that of the fundamental. Another external tap is provided for selection of this frequency. As shown in Figure 8 below, channel one (yellow) represents the fundamental. Channel three (magenta) represents the division of one-one hundredth. The fundamental frequency is measured at 1.42kHz. The one-one hundredth division is measured at 14.20Hz.

Figure 8:

Figure 9 shows a comparison between the first division and the second division stage.

Figure 9:

This frequency output is connected with the input (pin #1) of the third divide-by-ten counter (74LS90-3). This third counter begins the process of dividing the frequency by ten again. The output pin (#12) provides a frequency that is one thousand times (1/1,000) less than that of the fundamental. Another external tap is provided for selection of this frequency at a fixed 50% duty cycle. As shown in Figure 10 below, the fundamental frequency (yellow trace) is 1.420kHz. Channel 4 (dark blue) is 1.42Hz, being one-one thousandth of the fundamental.

Figure 10:

Below, in Figure 11, a comparison between channel three (divide by one-one hundredth) and channel four (divide by one-one thousandth total) is provided.

Figure 11:

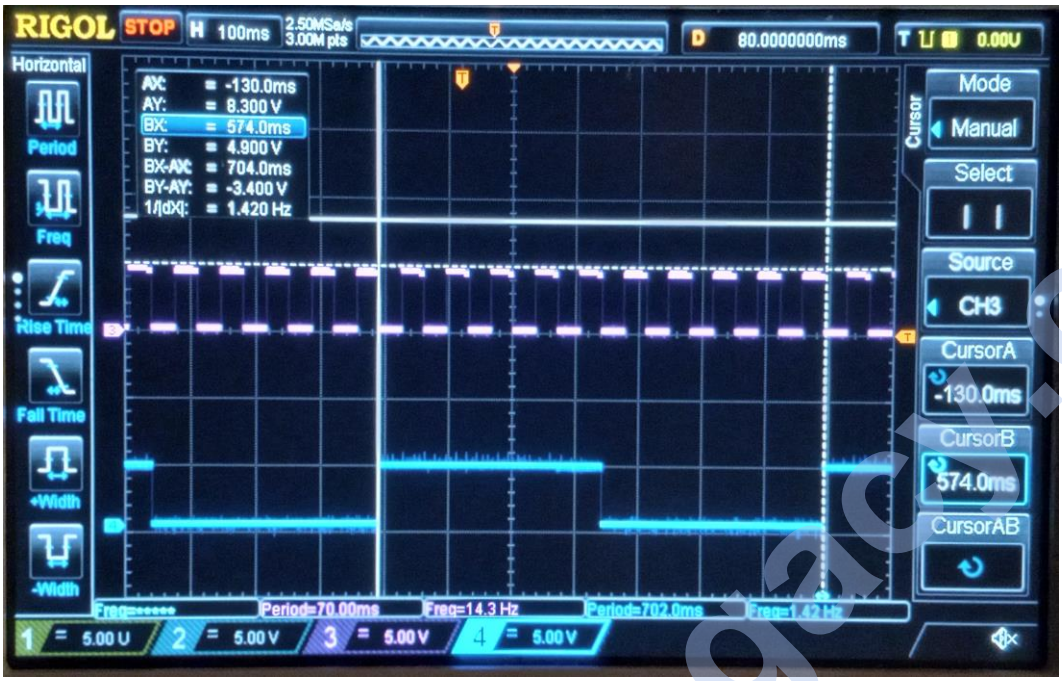

Below in Figure 12, is a scope shot showing a comparison between all four channels.

Figure 12:

A rotary switch provides the input, of whichever frequency is desired, into the inputs (pins #1, #3, #5, #9, #11, #13) of the hex inverter (74LS04). All of the inputs are connected together to synchronize the associated outputs. These outputs are logically inverted from the input pulse polarity as shown below in Figure 13. The input channel is represented by yellow trace. Other traces represent outputs to three of the four optocouplers.

Figure 13:

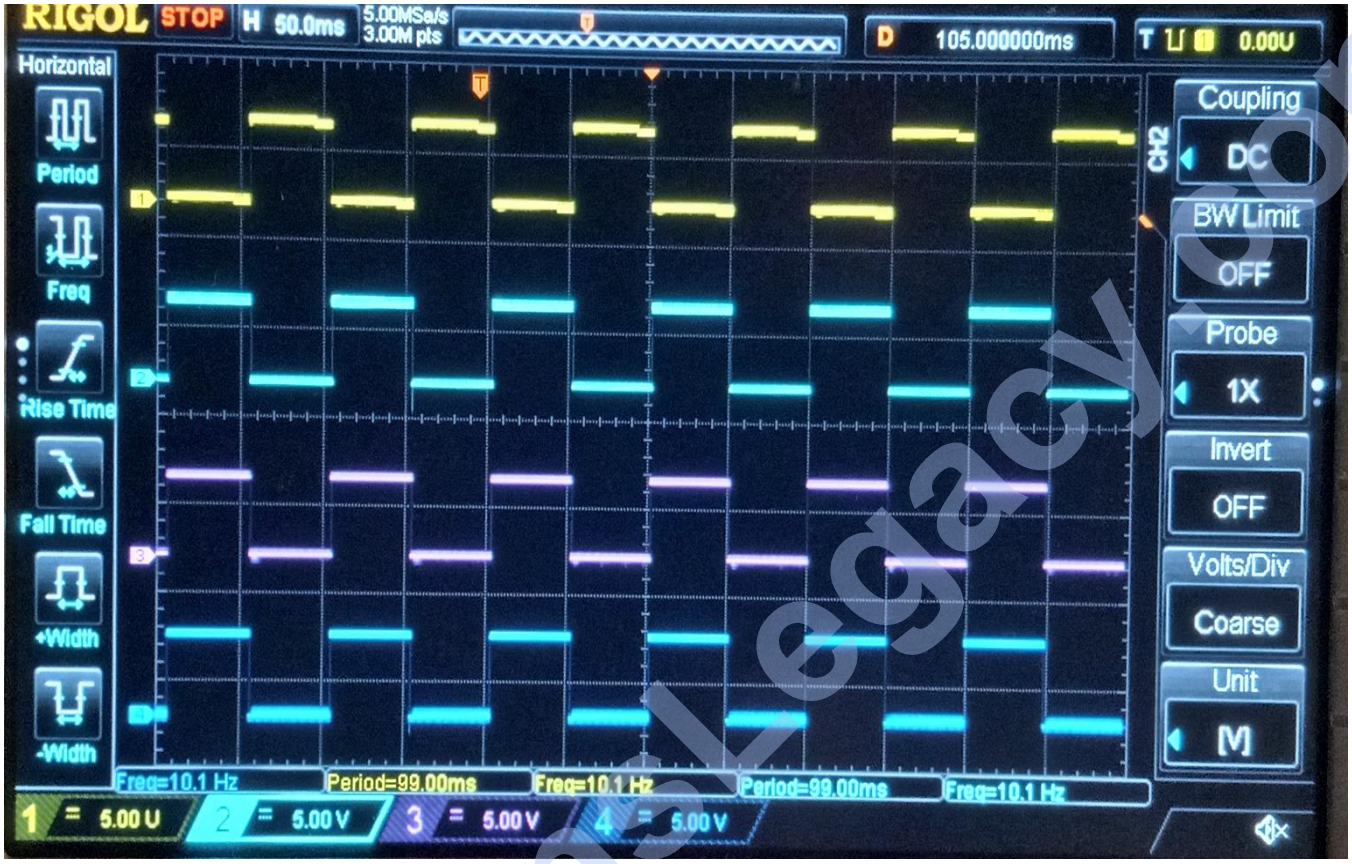

First output (pin #2) is connected to a series 200Ω, ¼ watt resistor which provides current limiting (20mA) to the cathode of an externally mounted LED. This external LED provides visual indication of the frequency received by the optocouplers. Second output (pin #4) is connected to a series 200Ω, ¼ watt resistor which provides current limiting (20mA) to the cathode of the PCB mounted LED. This LED provides visual indication of the frequency received by the optocouplers. Four other outputs (pins #6, #8, #10, #12) are connected to a series 200Ω, ¼ watt resistor which provides current limiting (20mA) to the anode of their respective optocouplers (H11D1-1, H11D1-2, H11D1-3, H11D1-4).

When the 74LS04 output logical states are HIGH (1), the associated optocoupler's internal LED turns on, which influences the base of the transistor, producing conduction on the output side. Conversely, when the 74LS04 output logical state are LOW (0), the associated optocoupler internal LED turns off, having been reversed biased. The optocouplers perform electrical isolation between the pulsing circuitry and their respective output terminals. The four optocouplers are used to provide pulsing for other circuitry that will be expanded upon in other sections. The schematic details which pin number is associated with the collector and emitter of the associated optocoupler.

Figure 14: Logical Flow – Phase 1:

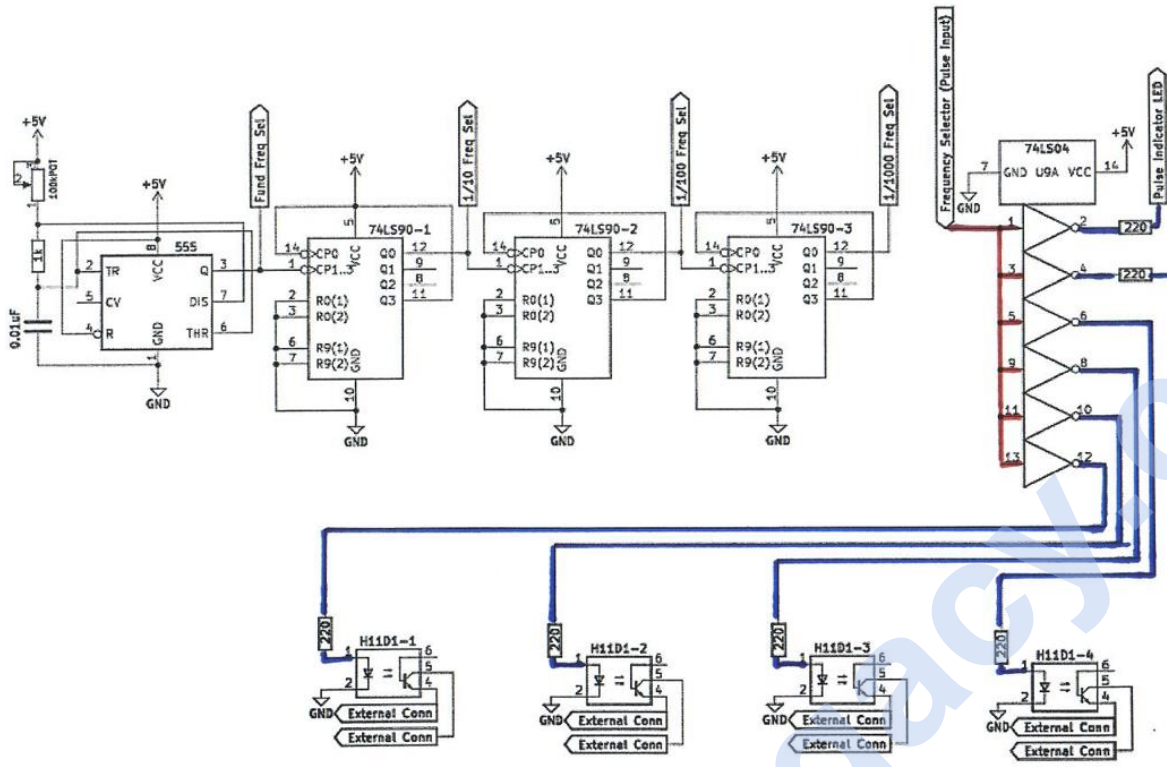

Figure 15: Logical Flow – Phase 2:

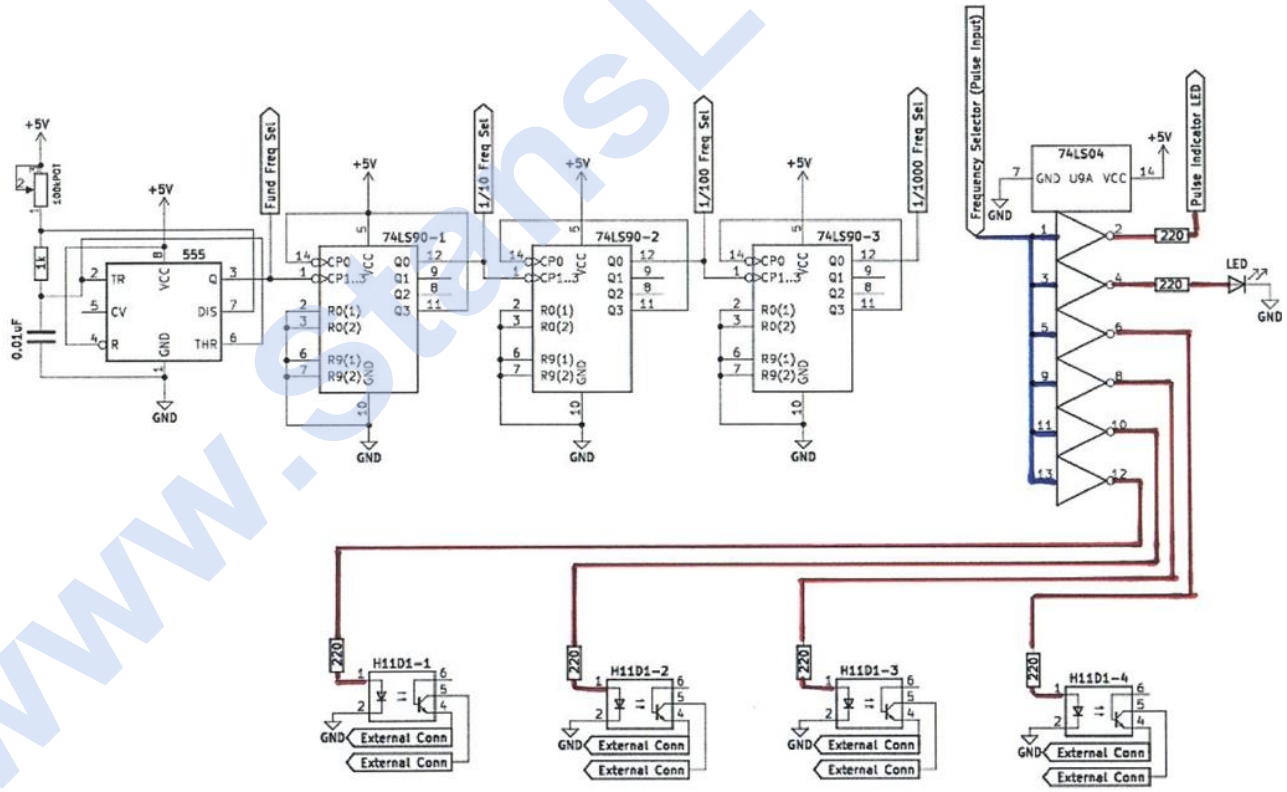

Section Five: PC9XC - Variable Gate

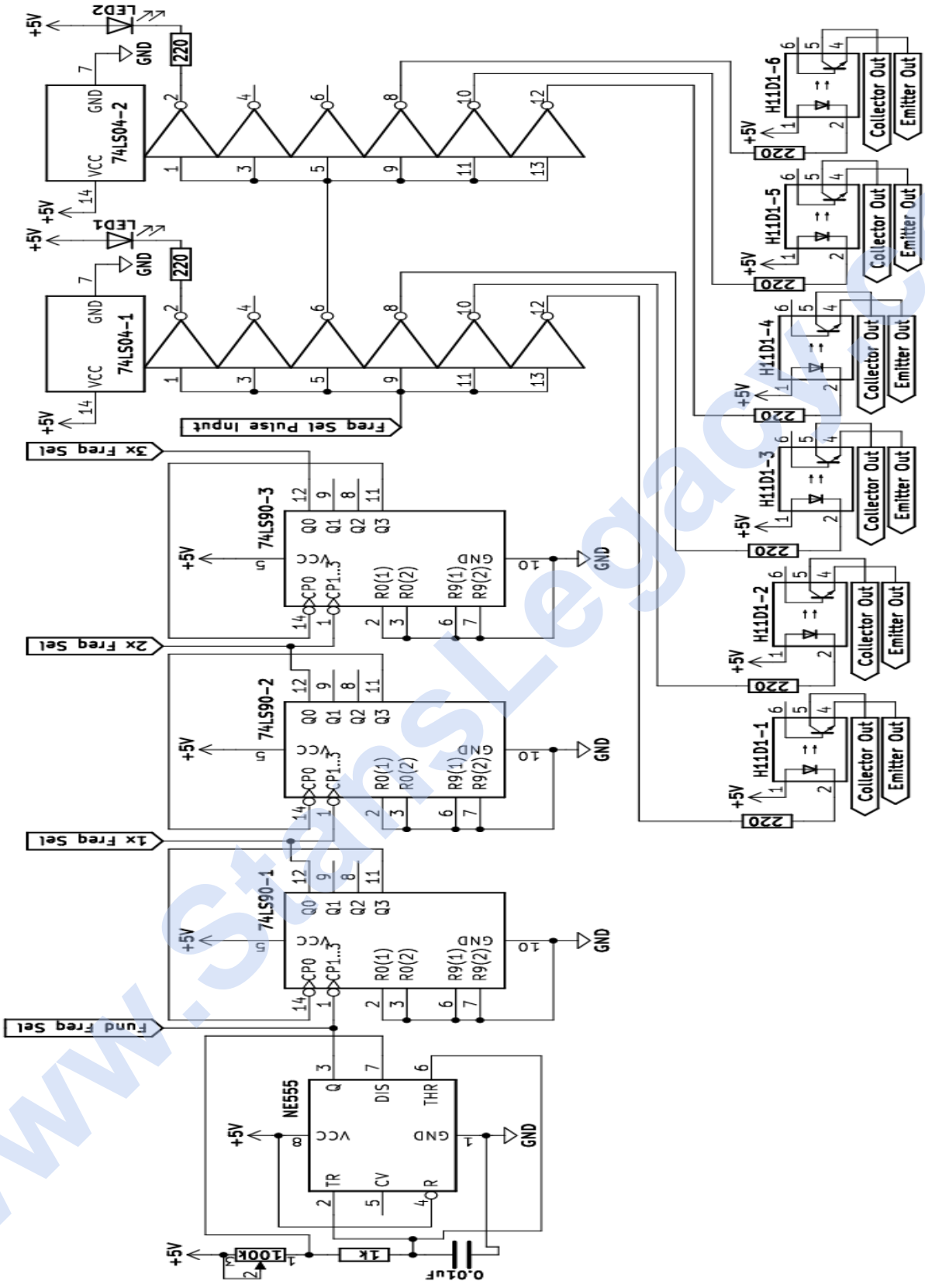

Replica Circuit Board:

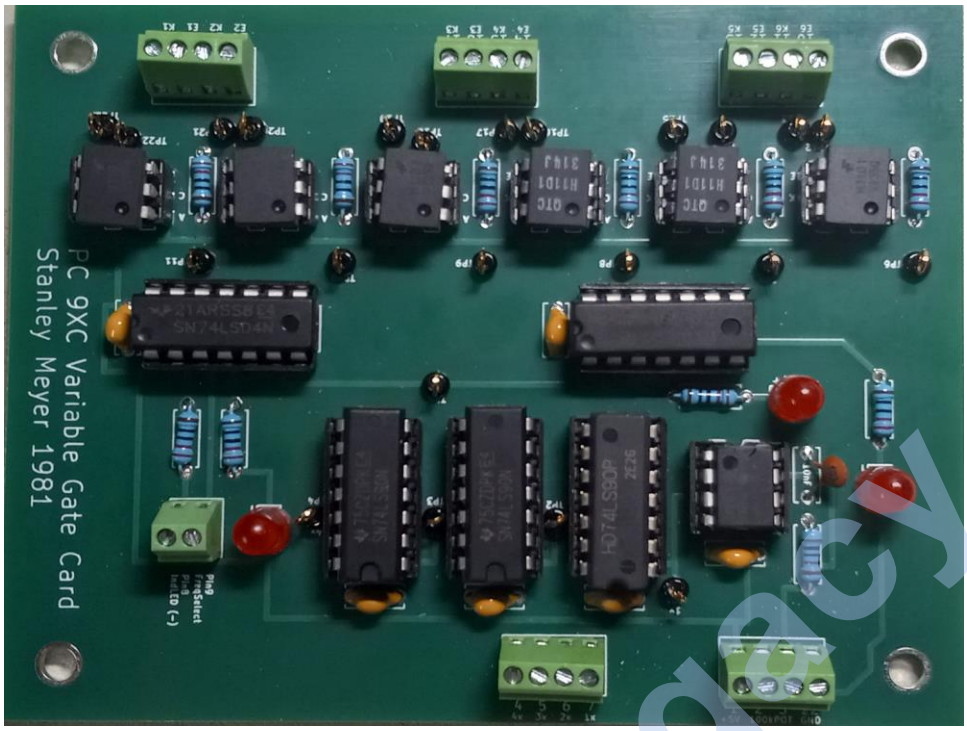

The decoupling capacitors were added across each IC for stability and noise reduction. LEDs visually indicate when the hex inverters (74LS04-1/74LS04-2) are in opposing polarity. Photos demonstrating this functionality are within this section. PCB trace layers are shown in the photo below.

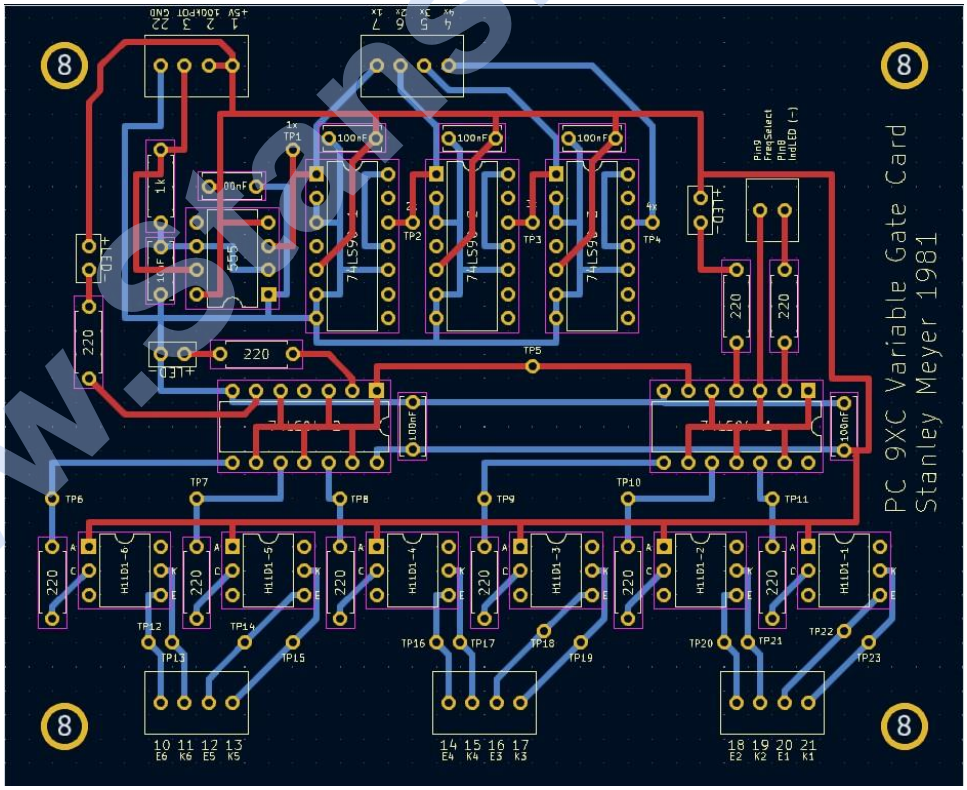

Stan's Original Explanation:

To switch off and on said generated pulse voltage frequency at a variable time rate while maintaining said voltage amplitude control.

a.) The adjustable pulse-train simply "concentrates" or time-regulates the applied pulse voltage frequency, allowing for higher voltage amplitude.

b.) The variable gated-pulse is now adjusted to reduce amp flow still further while allowing voltage amplitude and pulse voltage frequency to be adjusted to "tune-in" for higher gas-yields.

c.) Optocoupler is a photo-isolation switch that when triggered by variable gate circuit, a second variable triggering circuit, causes said pulse voltage frequency wave form to be altered. The gated pulse train is adjustable from 1% to 100% duty time. As on-time increases, off-time proportionately decreases, allowing more voltage pulses to be applied to said excitor's array.

Revised Explanation:

The circuit includes an integrated variable frequency generator, with a 50% duty cycle provided by three divide-by-ten counters (74LS90), the same circuit as the PC9XB. The pulse train is communicated to two hex inverter (74LS04-1 & 74LS04-2) stages that produce 180-degree phase shifted output pulses. Put more simply, this circuit performs a flip-flopping function. Optocouplers provide isolation between control circuitry and the switching applications that will be covered herein. Having two optocouplers in series, controlling PC9XA driver BJT, produces a two input "AND" gate.

The aforementioned description of duty cycle adjustment is slightly misleading. As the frequency is decreased, the number of pulses, delivered by the PC9XB, to the excitor array is increased. Conversely, as the frequency is increased, the number of pulses is decreased. In both cases, the off time is equal to the on time due to the fixed 50% duty cycle. A better understanding can be ascertained by viewing Stan's reference to "duty-cycle" variability within the scope of controlling the quantity of frequency pulses applied to the electrode pair.

Stan's Applications:

a.) Voltage Intensifier Circuit 9XA:
Adjusting the number of pulses applied to the power transistor driving the VIC coil. Can facilitate several different pulse applications including continuous, gated and sequenced.

b.) Dual Voltage Pulsing Circuit:
Adjusting the number of pulses applied to their associated power transistors driving the VIC coil. Providing two independently varied voltage pulse waveforms.

c.) Electron Extraction Circuit:
Providing alternating switching between applying step charging waveform to gas resonant cavity positive electrode and applying positive potential to resistive element to cause liberated electron flow.

d.) Steam Resonator Circuit:
Provide switching to associated power transistor to produce alternating application of positive polarity to electrodes.

Referencing Figure 16 below, optocoupler "H11D1-2" controls the number of pulses per unit of time from the frequency generator, PC9XB, to be applied to power transistor's base. Diagram 2 illustrates the waveform produced. While five pulses per half cycle are shown, both circuit's frequencies are independently adjusted, resulting in a lack of synchronization without precise adjustments. The period of the PC9XB optocoupler pulse train is represented by T_1, while T_2 represents the period of the PC9XC optocoupler pulse train. It can be seen that both are fifty percent. Voltage of the resultant waveform is independently adjustable via variable transformer.

Figure 16: Voltage Intensifier Circuit 9XA:

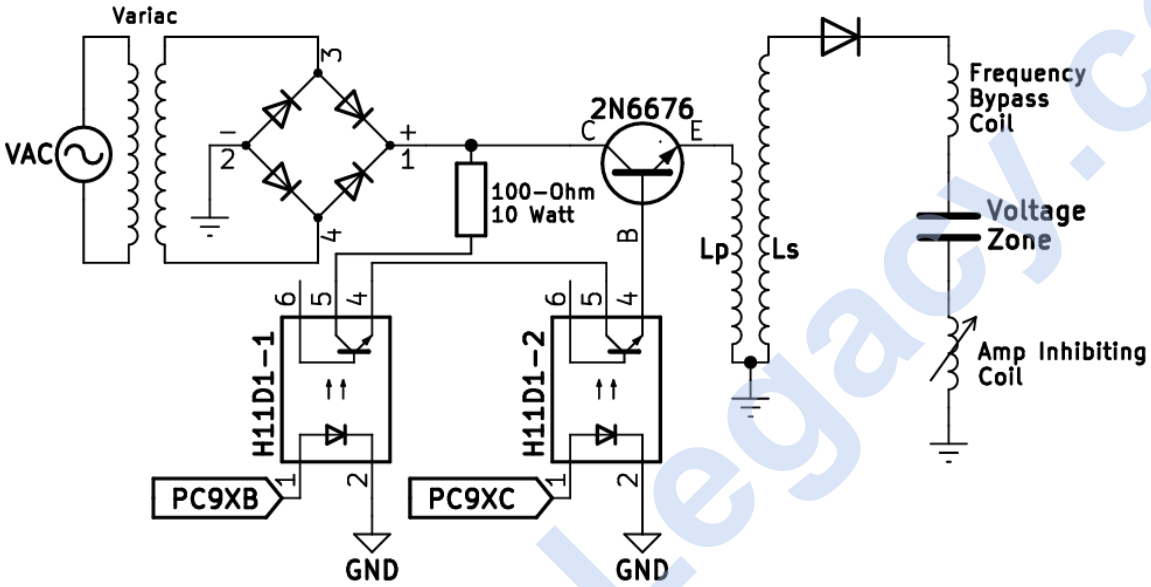

Diagram 2:

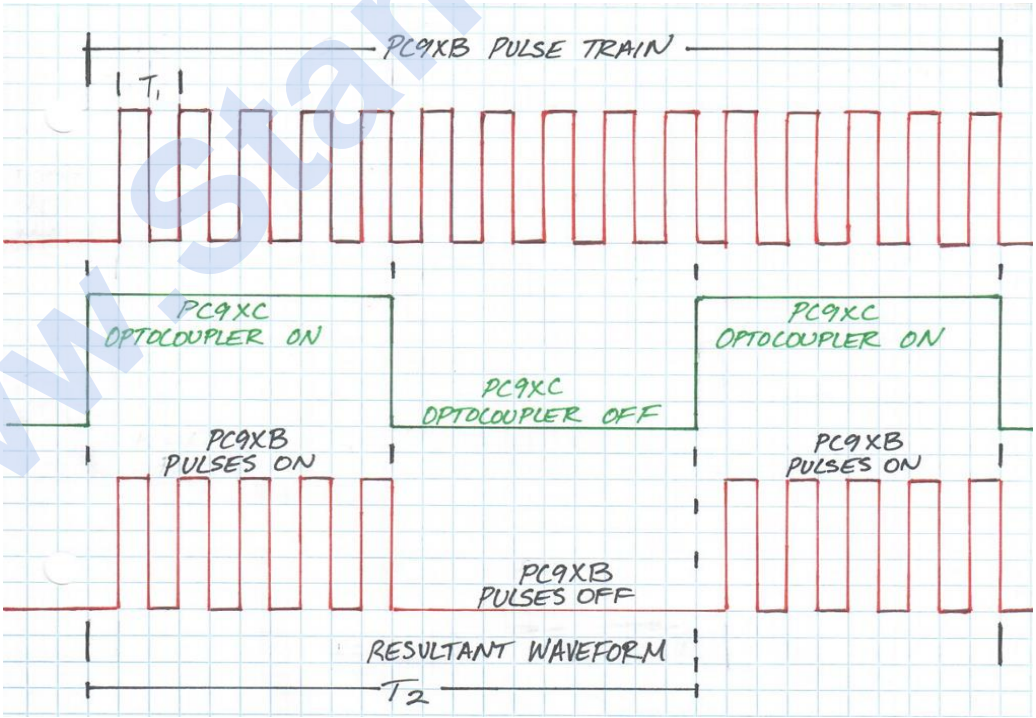

Figure 17 below, shows another embodiment. Four separate circuits, two PC9XB's and two PC9XC's are utilized to produce two independently adjustable voltage gated pulse trains that are applied to a resonant cavity of a spherical geometry. Diagram 3 illustrates the waveforms during circuit operation.

Figure 17: Dual Voltage Pulsing Circuit:

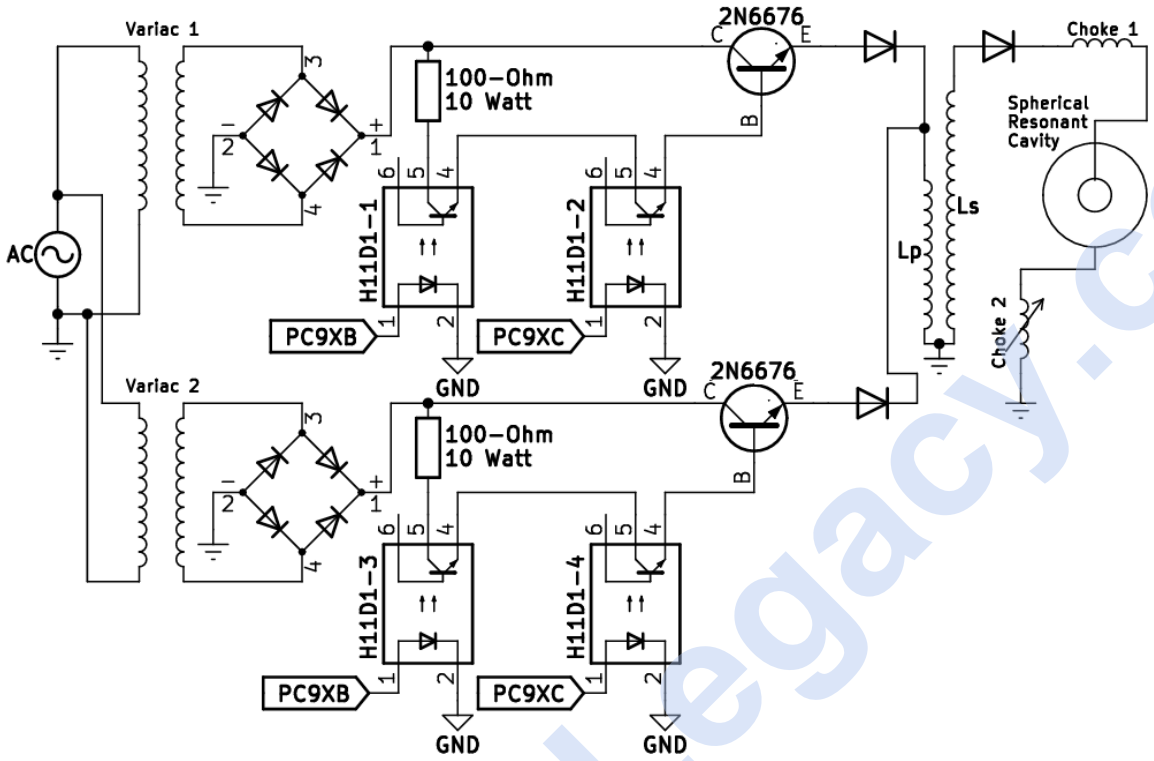

Diagram 3:

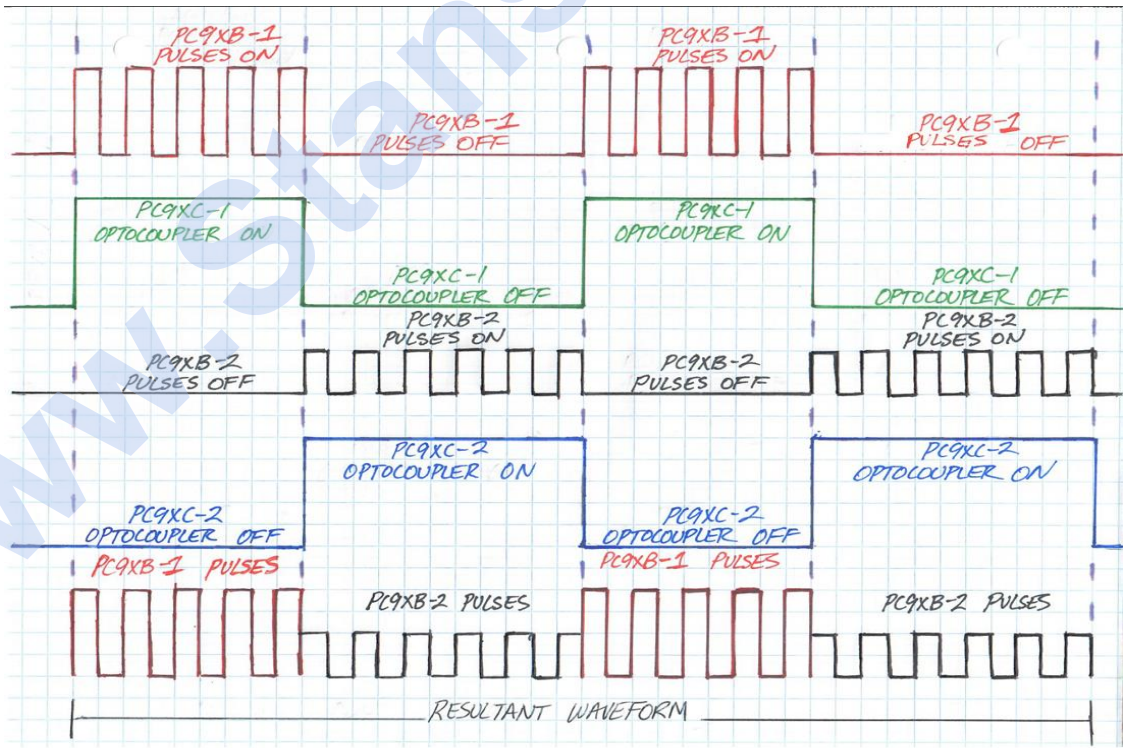

Figure 18 below illustrates the flip-flop switching application that facilitates electron extraction. Rectified mains supply provides a unipolar DC waveform that energizes the step-down transformer to produce a low voltage at a fixed frequency of 120Hz. Conversely, a filtering capacitance can allow a wider range of frequencies. Secondary coil taps in conjunction with switch-selected optocoupler triggered SCRs controls the voltage applied to the primary coil of the VIC step up stage (see page 79 for circuit board). The 120Hz has a superimposed gate signal via optocoupler "H11D1-5", which is triggered via a PC9XC circuit. This optocoupler controls the number of pulses applied to the base of the power NPN. Diagram 4 details the waveform of this flip-flopping behavior.

The optocoupler "H11D1-6" is triggered 180º out of phase with respect to H11D1-5. During this time, positive potential is applied to one side of the electron consuming device. This causes liberated electrons within gas resonant cavity (see Gas Resonant Cavity / Hydrogen Gas Gun section for further details) to be attracted to this positive potential which leads to flow into electron consuming device.

Figure 18: Electron Extraction Circuit:

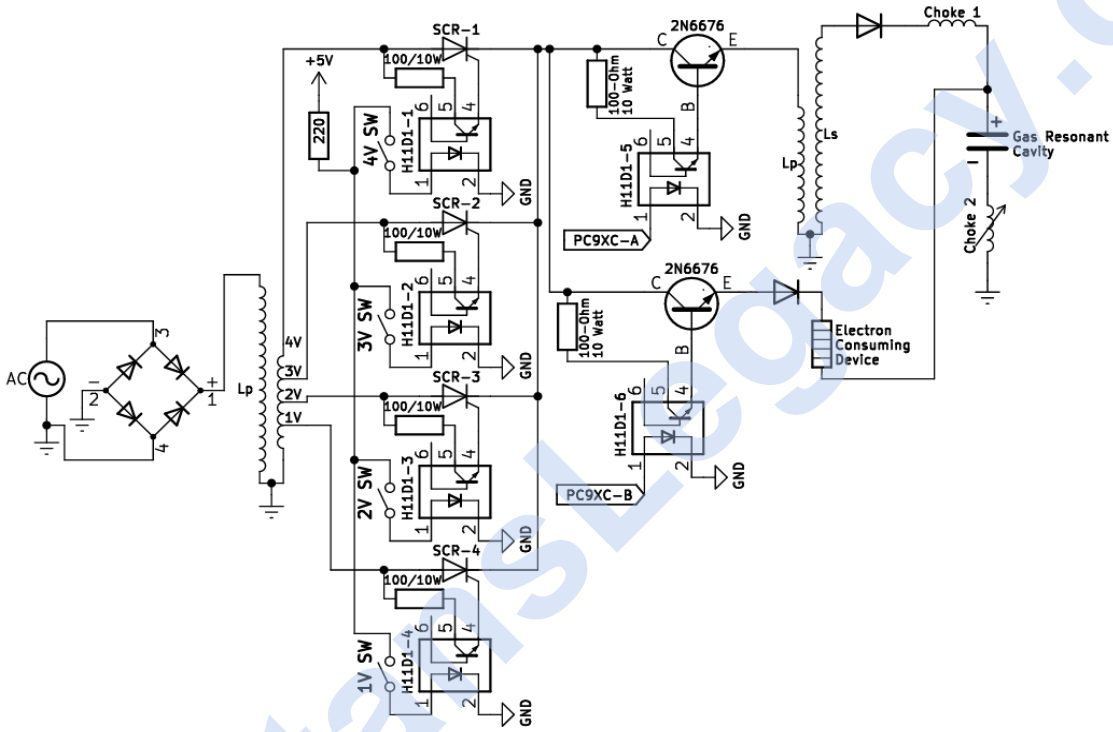

Diagram 4:

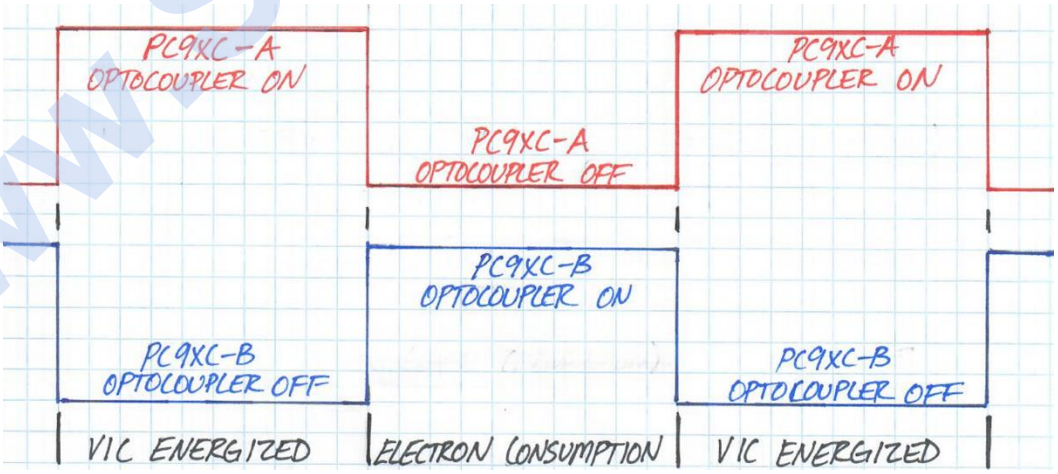

Figure 19: Electron Extraction Logical Flow – Phase 1:

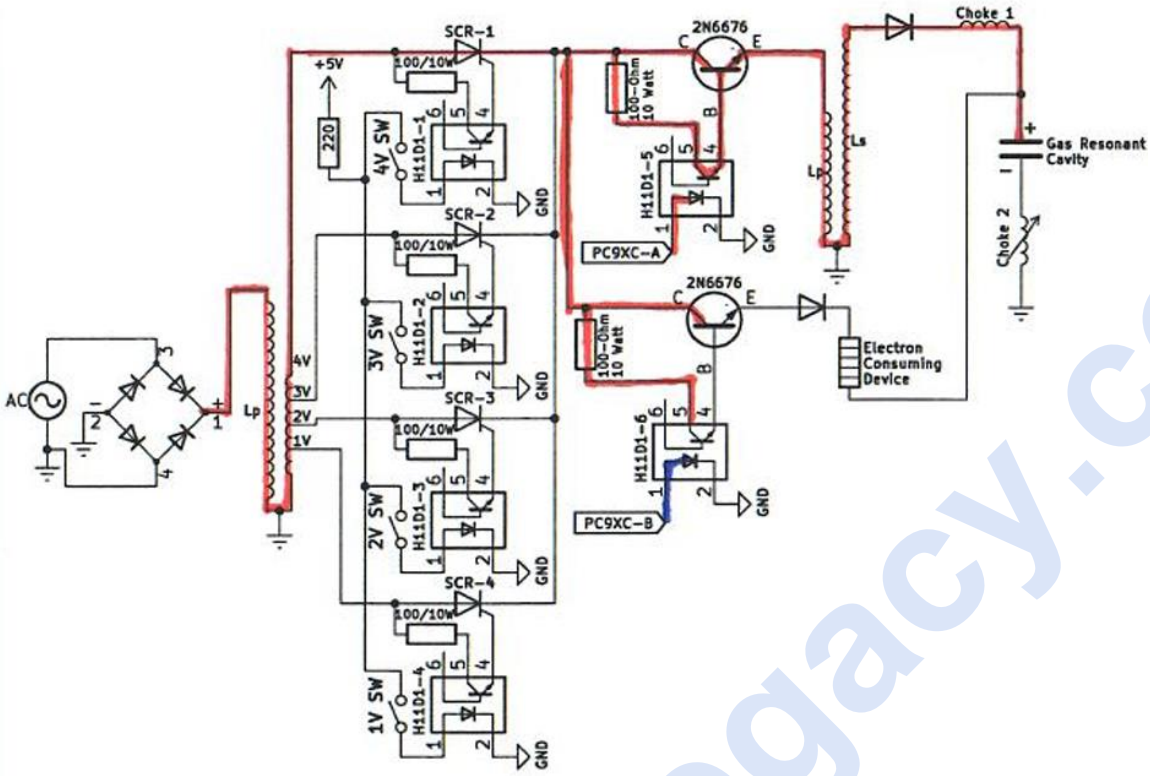

Figure 20: Electron Extraction Logical Flow – Phase 2:

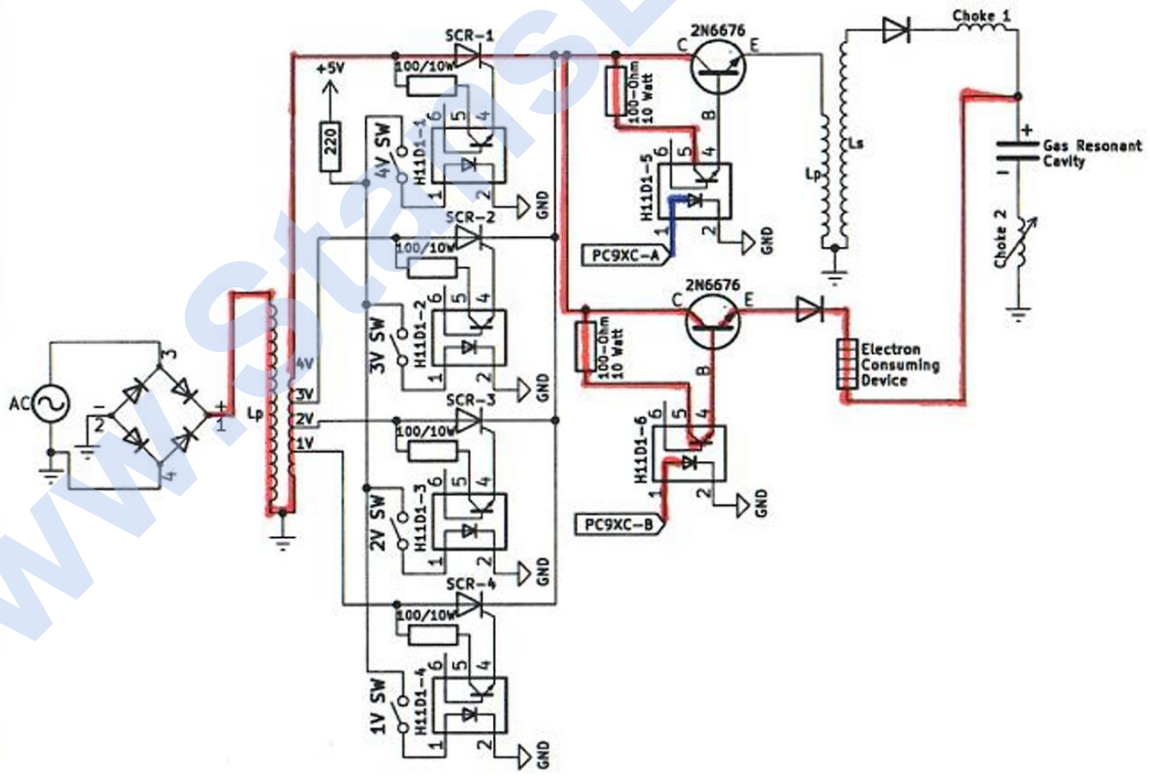

With reference to Figure 21 below, another application utilizing the flip-flopping action is illustrated for operation of the steam resonator. As shown in the aforementioned Diagram 4, the optocoupler signals, PC9XC-A and PC9XC-B are 180º out of phase with respect to one another. An adjustable rectified DC voltage is supplied, via the variable transformer, having a fixed frequency of 120Hz. During PC9XC-A triggering of the first power transistor, a unipolar rippling DC waveform is applied to the first primary coil, causing a high positive potential – via step-up transformer – to be applied to the first resonant charging choke coil, by forward biasing the series diode, onto the top plate of the resonant cavity structure. The bottom primary/secondary pair is opposite in polarity, reverse biasing the series diode, not permitting any potential to be applied to the second plate.

During PC9XC-B triggering of the second transistor, a unipolar rippling DC waveform is applied to the second primary coil, causing a higher positive potential – via step-up transformer - to be applied to the second resonant charging choke coil, by forward biasing the series diode, onto the bottom plate of the resonant cavity structure. At this time, the top primary/secondary pair is opposite in polarity, reverse biasing the series diode, not permitting any potential to be applied to the top plate.

It should be apparent, that applying a differential polarity is avoided. Only positive polarity is utilized in this arrangement, as only one pair of electrodes are present. This flip-flopping positive polarity influences the oxygen and hydrogen atoms, causing atomic/molecular flexing which produces heat energy.

Figure 21 Steam Resonator Circuit:

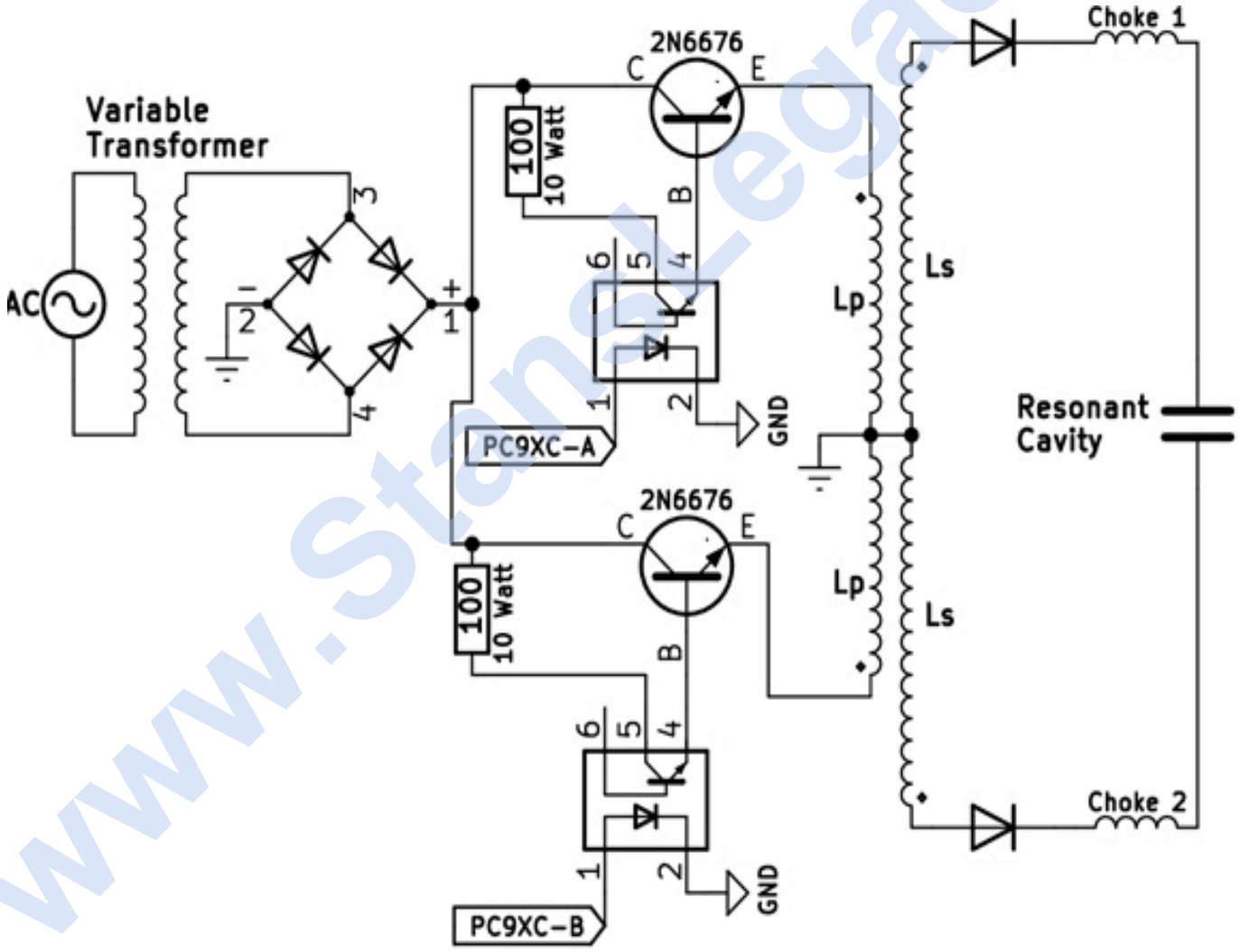

Figure 22: Steam Resonator Logical Flow – Phase 1:

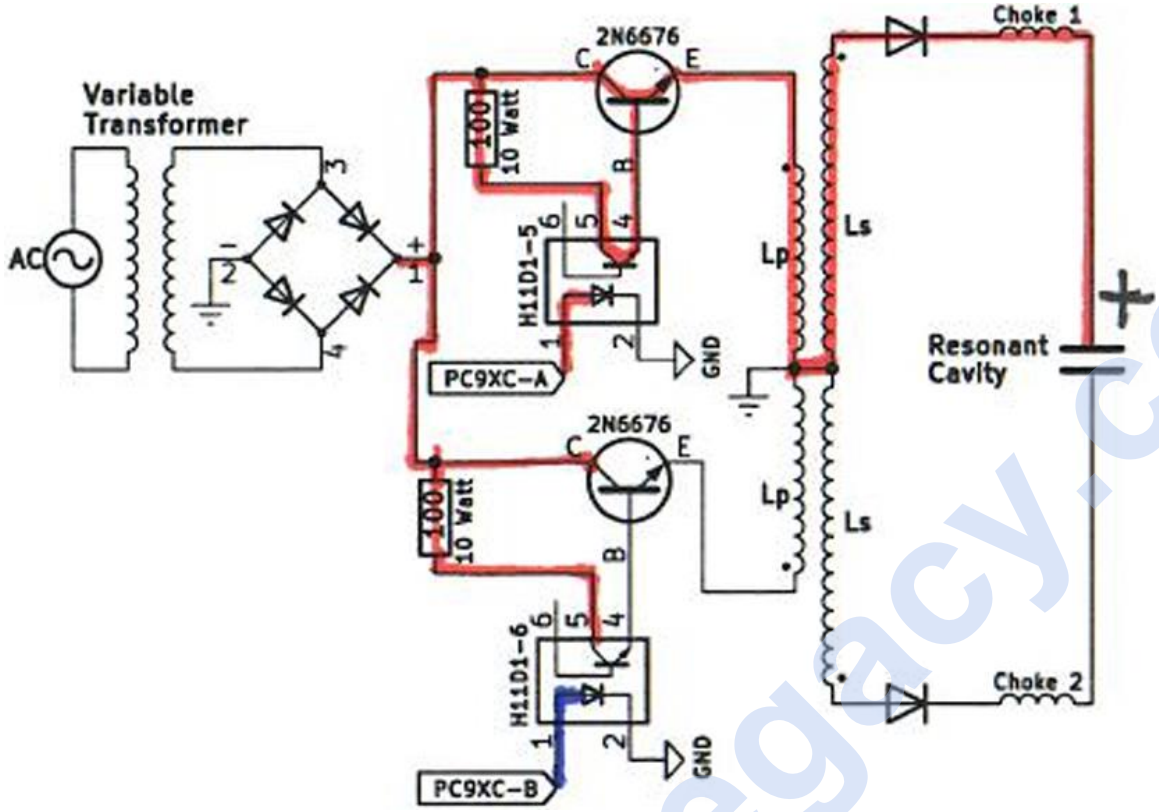

Figure 23: Steam Resonator Logical Flow – Phase 2:

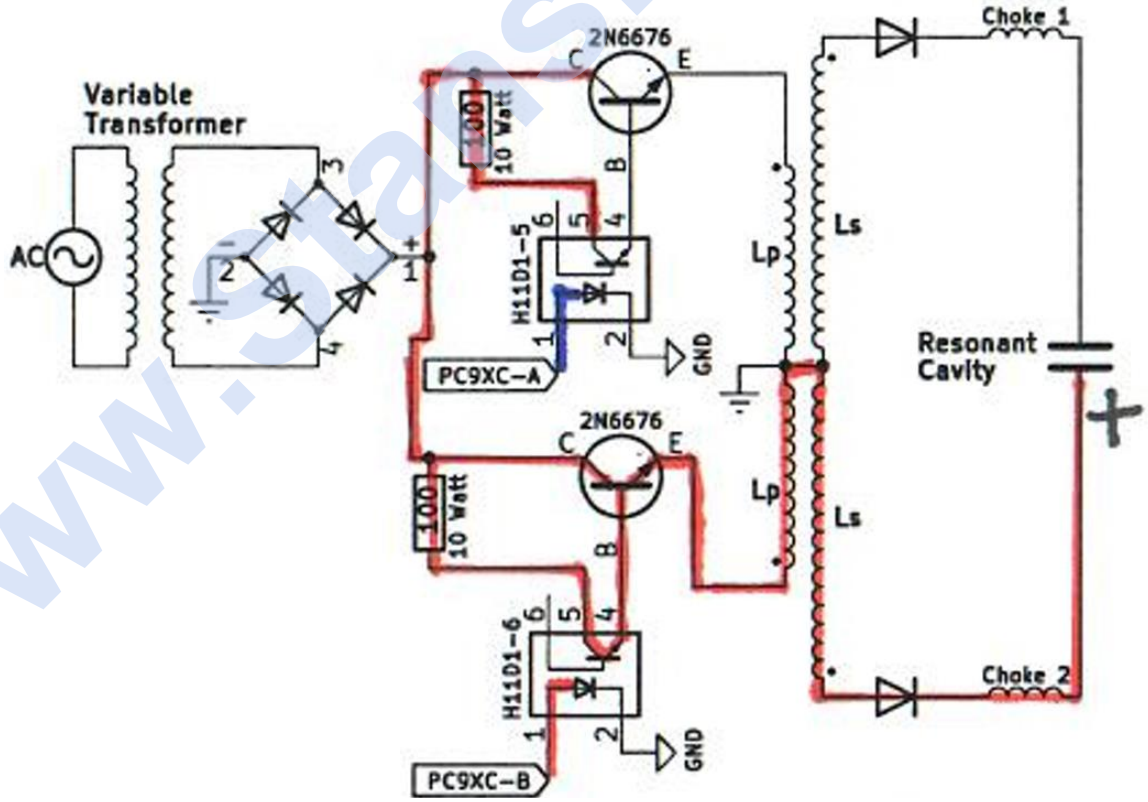

Frequency is supplied by a PC9XB arrangement (see PC9XB analysis section for refresher) where an initial frequency is divided by multiples of ten and conditioned to have a 50% duty cycle. This circuit incorporates a frequency selection capability that is provided by a rotary switch, having the pole terminal interconnected to inputs 1,3,5,9,11,13 of the first hex inverter IC (74LS04-1). The input waveform polarity is inverted 180^{o} as shown in Figure 24 below. Channel one (yellow) is representative of the pulse frequency into input pins. Channels 2, 3 and 4 (teal, magenta, dark blue) are representative of the three channels going out to optocoupler sets associated with this first hex inverter.

Figure 24:

74LS04-1 output pin #2 has a 220Ω, ¼ watt resistor wired in series which triggers an externally mounted LED, indicating the inverter's LOW logic level. 74LS04-2 output pin #2 has a 220Ω, ¼ watt resistor wired in series to provide a visual indication during the opposing logic state of the 74LS04-1. Output pins #8, #10, #12 of each inverter are connected to their respective optocouplers, each having a series 220Ω, ¼ watt cathode resistor to limit the current to 20mA. Optocouplers (H11D1-1, H11D1-2, H11D1-3) are all turned ON at the same time when 74LS04-1 is in a LOW logic state. During a HIGH logic state, these optocouplers are all turned OFF.

74LS04-1 output pin #6 is connected to the input pins #1, #3, #5, #9, #11, and #13 of the second hex inverter IC (74LS04-2). This produces a logical state that is inverse relative to 74LS04-1 but non-inverted relative to pulse frequency polarity (see logic chart below). Optocouplers (H11D1-4, H11D1-5, H11D1-6) are all triggered at the same time when 74LS04-2 is in a LOW logic state. During a HIGH logic state, these optocouplers are all turned OFF. Logic is summarized below in Table 1.

Table 1:

74LS04-1 Inputs State From Freq Gen	74LS04-1 Outputs State	H11D1-1 H11D1-2 H11D1-3 State	74LS04-2 Inputs State From Pin#6 74LS04-1	74LS04-2 Outputs State	H11D1-4 H11D1-5 H11D1-6 State
HIGH	LOW	ON	LOW	HIGH	OFF
LOW	HIGH	OFF	HIGH	LOW	ON

The photo below shows three LEDs. The applied pulse frequency LED (outlined in yellow) provides a visual indication that pulses are being applied. When 74LS04-1's LED (outlined in green) is illuminated, the first bank of optocouplers (H11D1-1, H11D1-2 and H11D1-3) are being triggered.

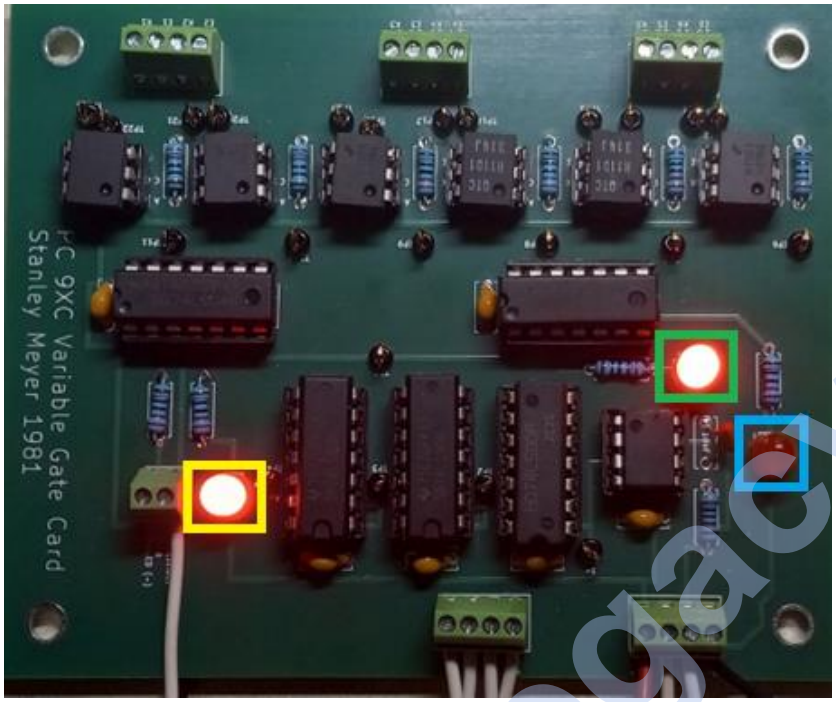

When 74LS04-2's LED (outlined in blue) is illuminated, the second bank of optocouplers (H11D1-4, H11D1-5 and H11D1-6) are being triggered.

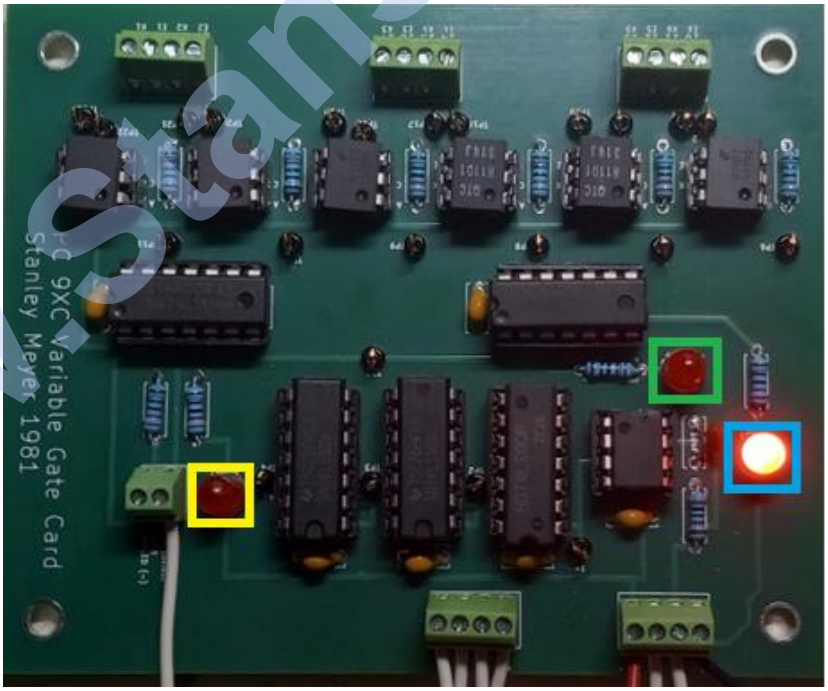

It can be seen from above that this circuit provides a method for alternate switching that has isolation protection. Additionally, for higher frequency switching applications, the 74HC04 model is preferred.

Figure 25: Logical Flow – Phase 1:

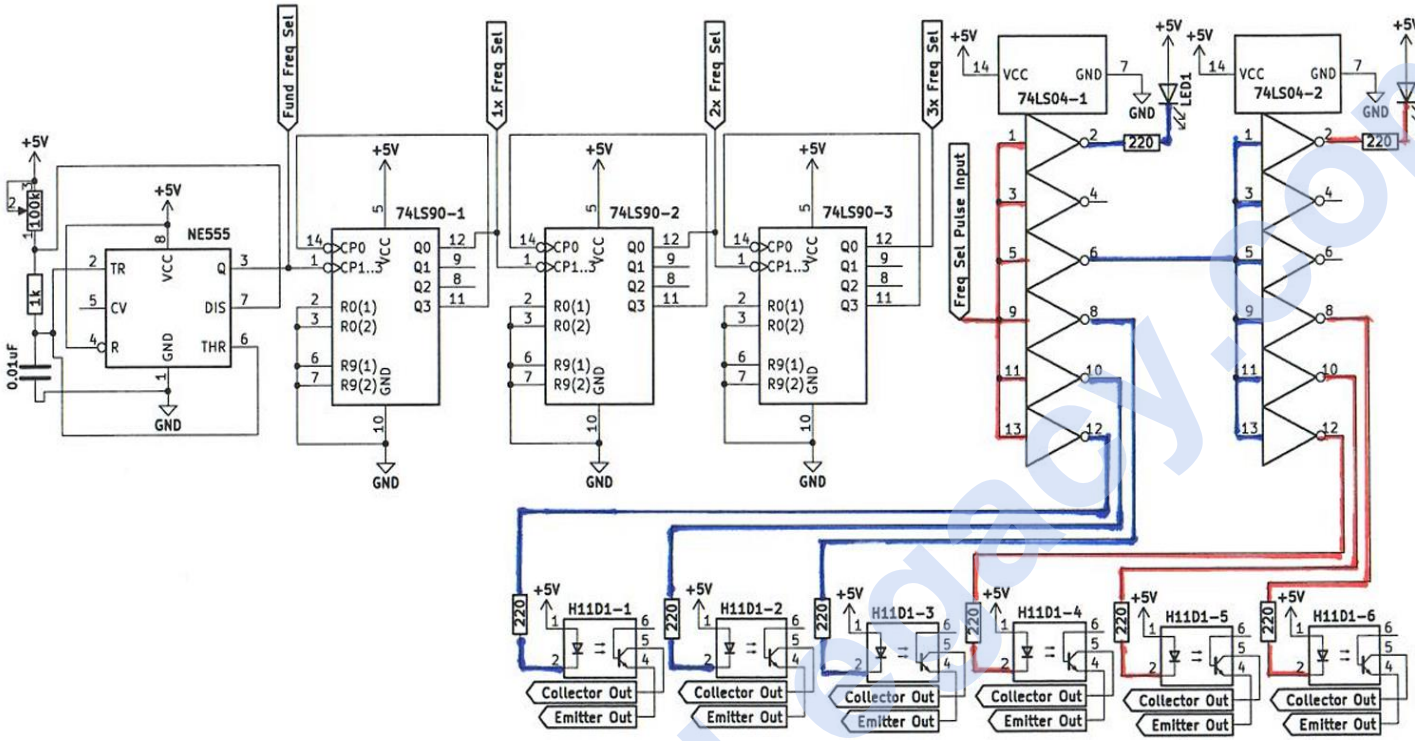

Figure 26: Logical Flow – Phase 2:

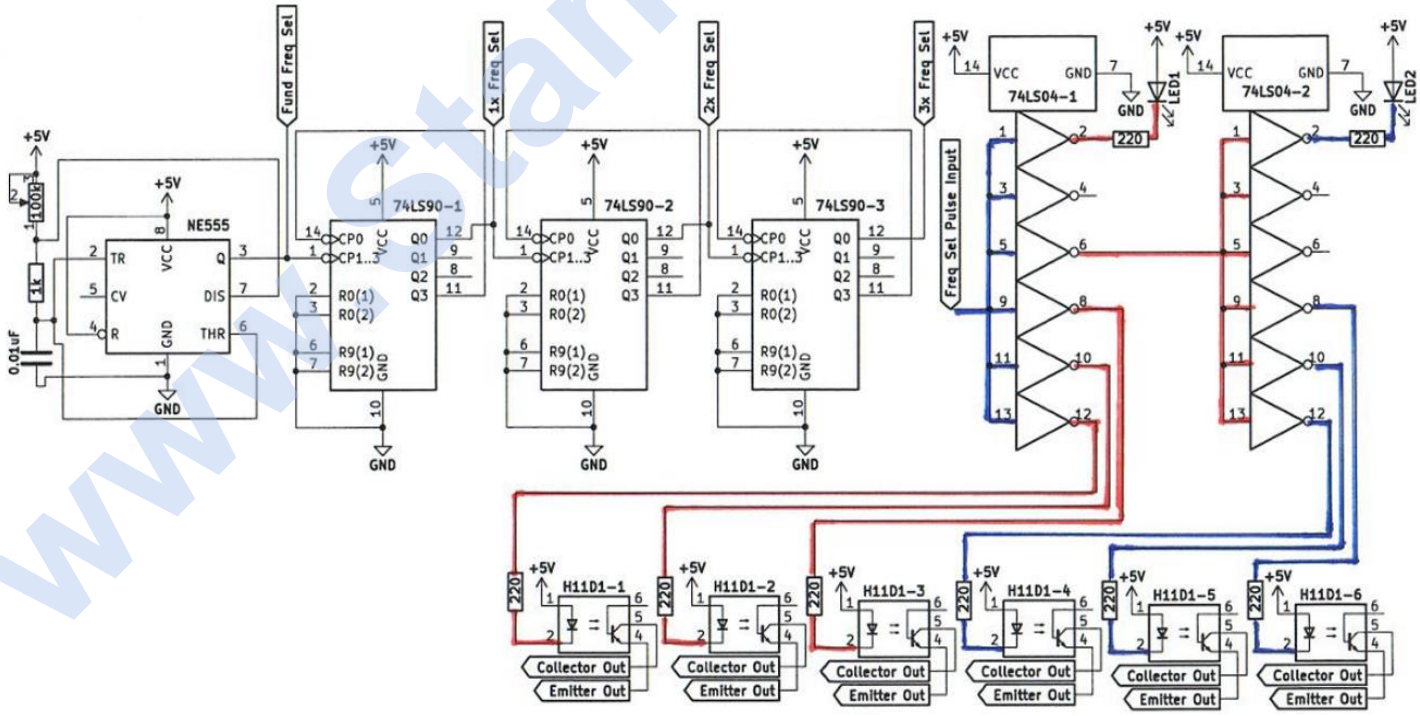

Section Six: PC9XD – Regulated Voltage Supply

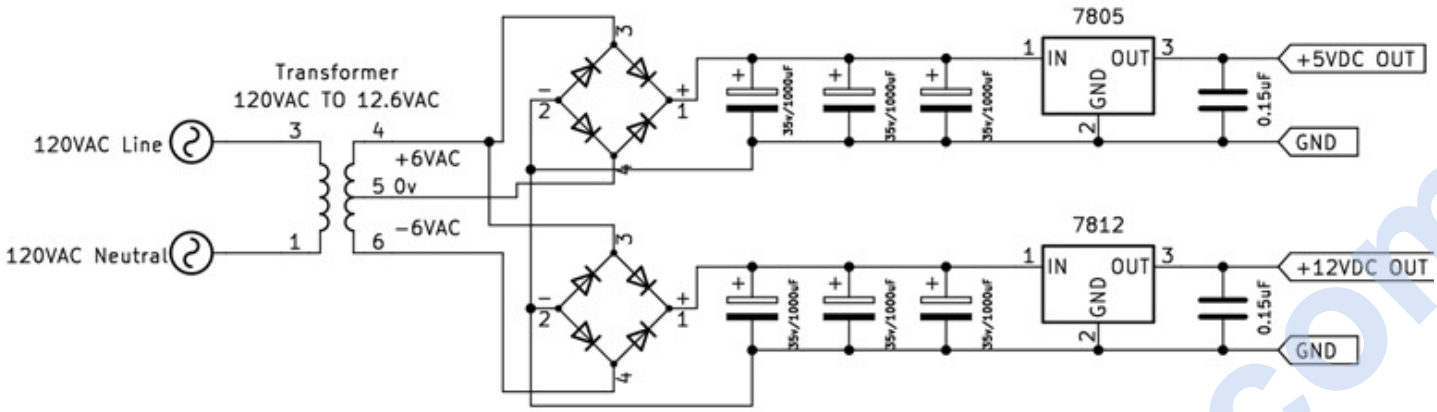

Throughout Stan's early technological developments, this regulated power supply was utilized to provide 5v and 12v DC. Both the 7805 & 7812 regulators are rated for a maximum of one amp. The 5v supply was used to power TTL era electronics. The 12v supply could've been used for CMOS electronics in later developments, panel indicators, etc. A 120VAC supply is applied to a step-down transformer with a center tap. This provides 12VAC across the entire secondary, while across the center tap, 6VAC is provided. Reduced voltages are rectified, producing 120HZ fixed frequency and rippling DC waveforms. The lower frequency rippling is removed via the banks of 1000uF electrolytic capacitors in parallel, producing a total filter capacitance of 3000uF. Additional filtering capacitors are placed across voltage regulator outputs.

Replica Circuit Board:

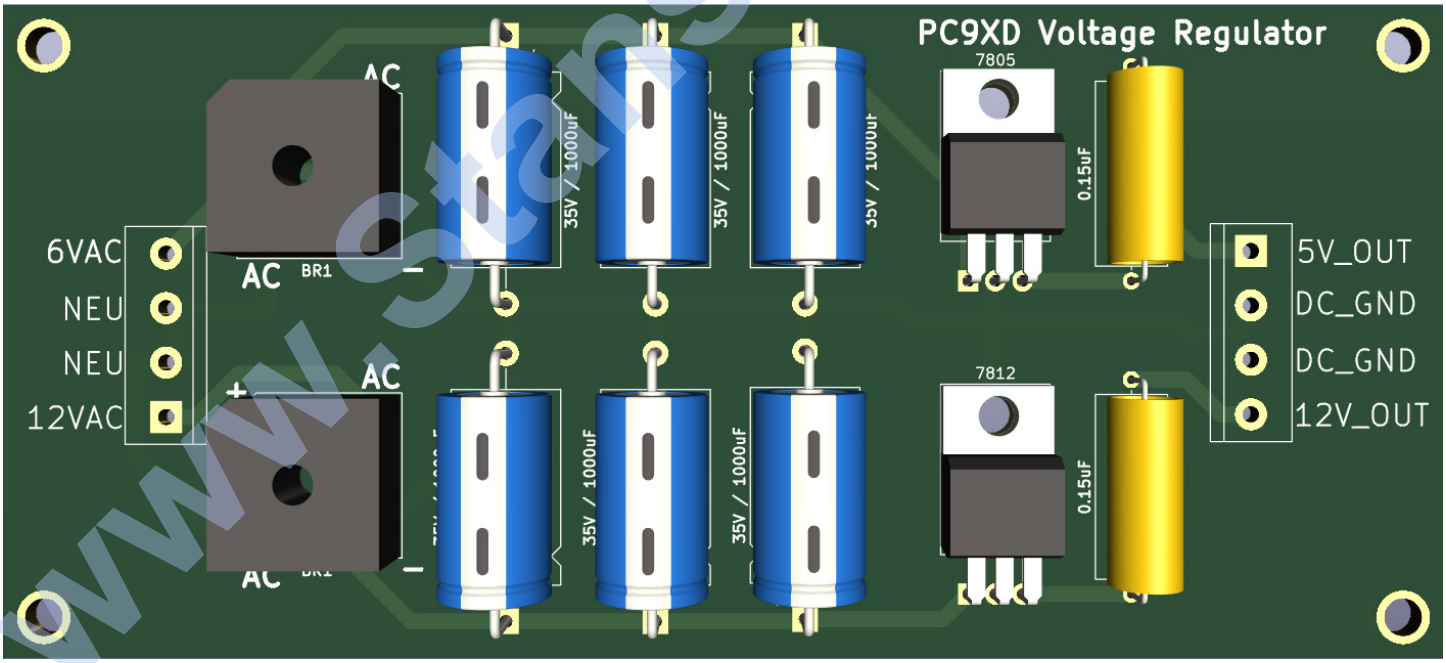

Section Seven: PC9XE – Sequential Gate Circuit

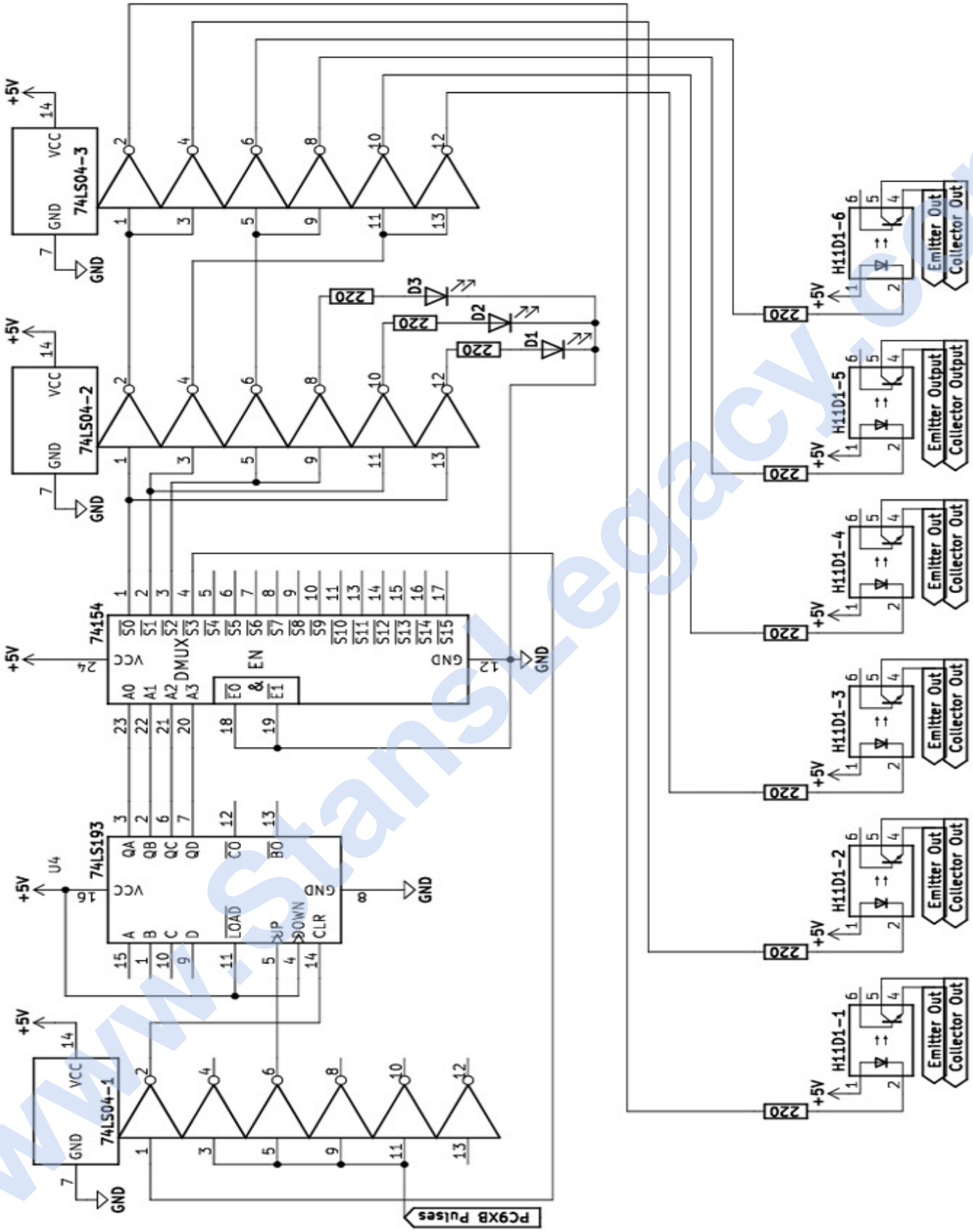

Replica Circuit Board:

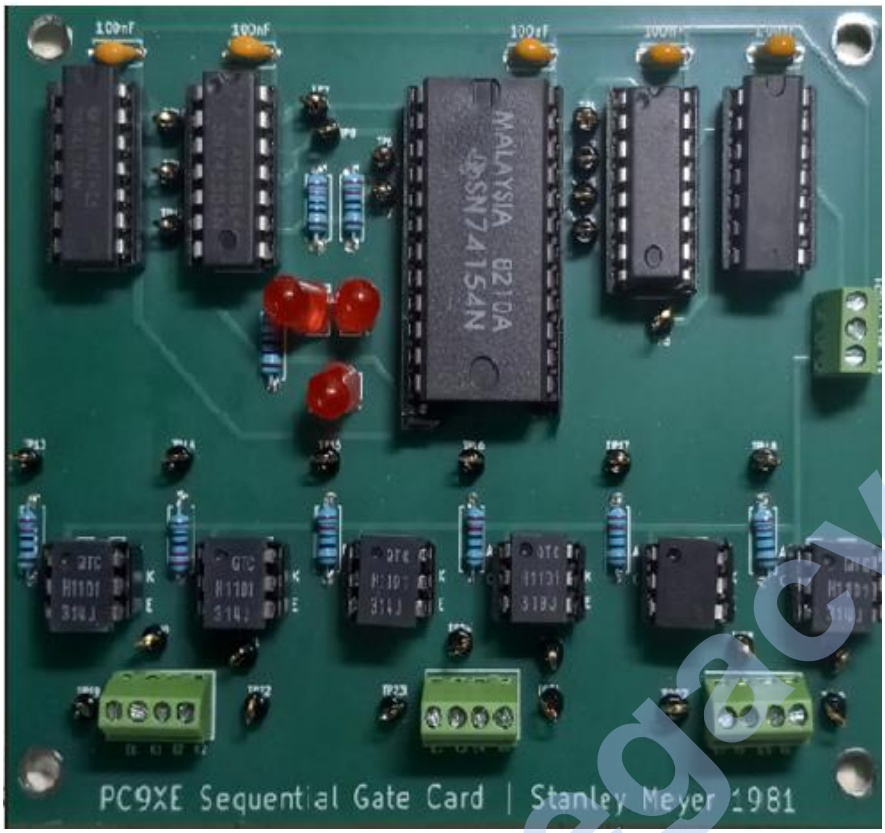

NOTE: Decoupling capacitors (100nF) were added to the replica board to increase noise immunity. Their presence does not affect circuit operation.

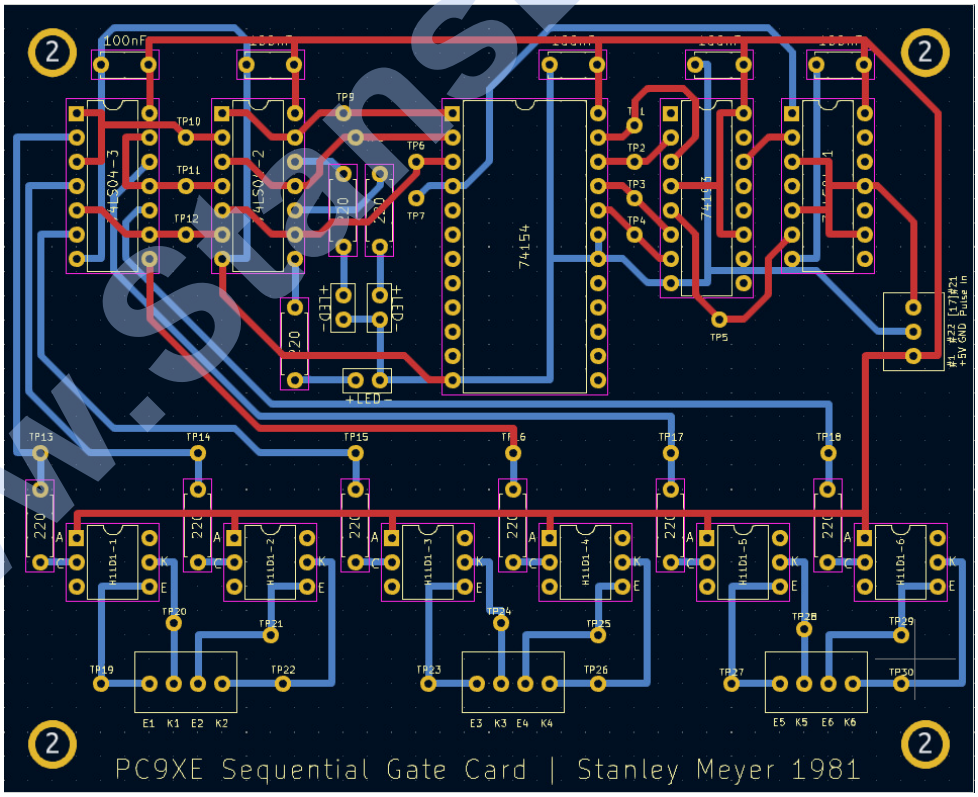

Stan's Original Explanation:

To increase gas production beyond voltage attenuation while keeping power loss to a minimum.

a.) Said sequential gate control circuit is
b.) variable to control gas production beyond said voltage attenuation controls (seventh-stage to voltage attenuation).
c.) Said variable pulsing circuit remains the same when adding additional excitor-arrays as herein described. In other words, power loss or drainage is held to a minimum (ninth-stage to amp restriction).

Note Stan utilizes the word "attenuation", which is incorrect within the scope of circuit operations he describes. The author believes the word "modulation" is more appropriate.

Revised Explanation:

The circuit allows sequential selection of multiple circuit channels through opto-coupler isolation. The principle involves selecting and isolating a single pair of electrodes to avoid continuous application of power. Selection is possible between one to sixteen separate channels.

Stan's Applications:

1.) Sequential selection of individual electrode pairs to prevent accumulated voltage leaking by applying VIC to all simultaneously when sharing a common water containing vessel.
2.) Gas accelerator tube, using sequentially triggered electrodes for acceleration of gas atoms. See Figure 35.
3.) 10 coil – EPG linear pump assembly. Note, no literature or photographic evidence supports this application, this is speculative given the electronics in Stan's era. Schematic below illustrates one possible method.

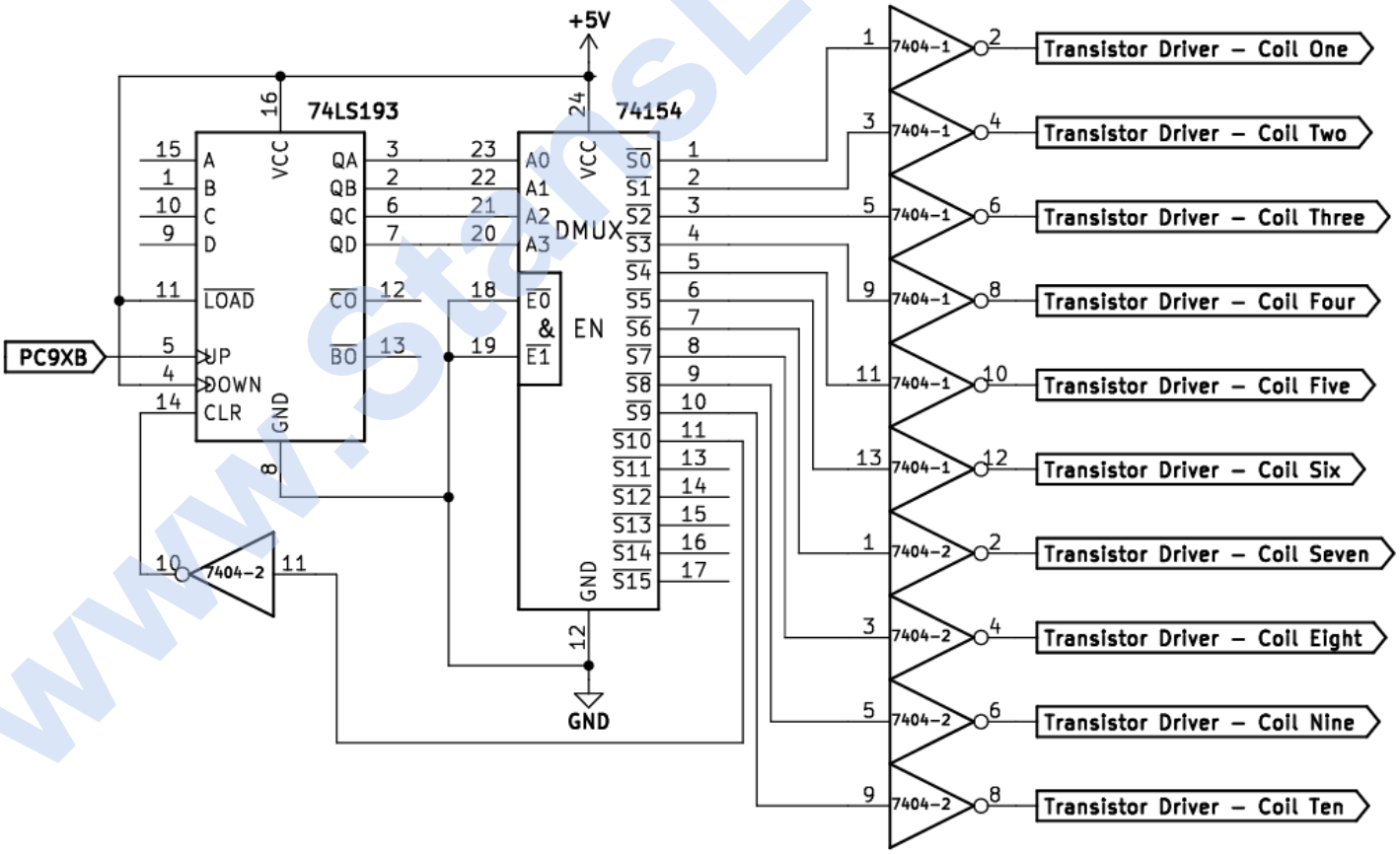

Figure 27:

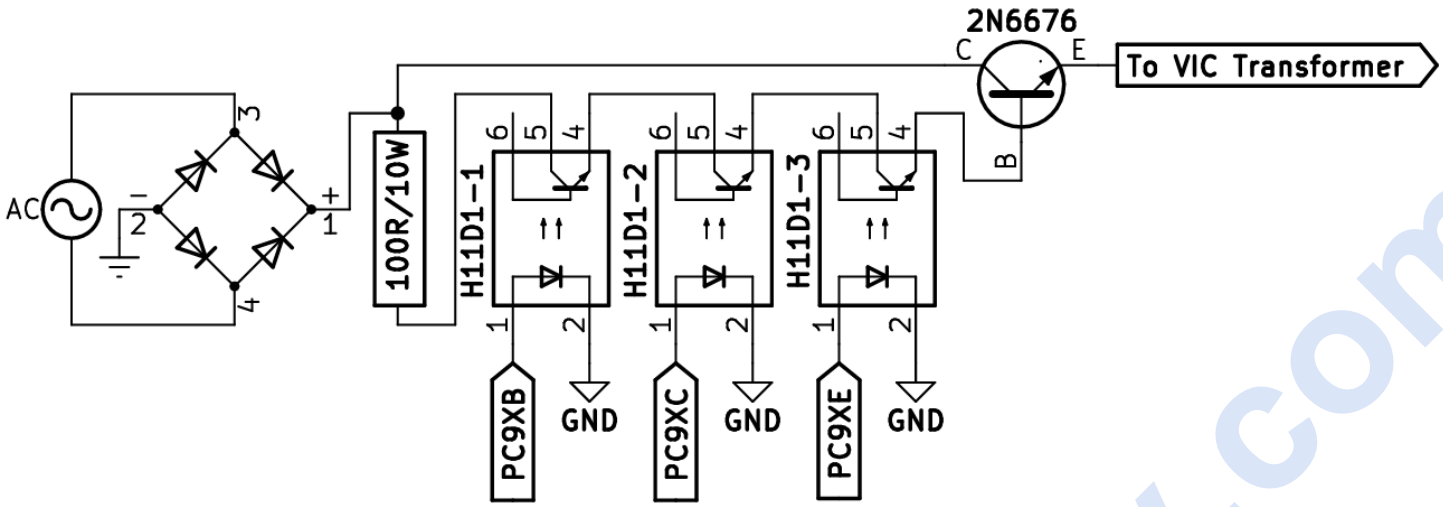

From Figure 27 above, the "optocoupler network" forms a triple AND circuit. First, the PC9XB frequency generator provides a 50% duty cycle square wave of a desired frequency to obtain resonance. Second, the PC9XC variable gate (with a fixed 50% duty cycle frequency) provides a gating function that performs, variability of how many pulses are permitted to be applied to transistor base. Third, the PC9XE sequentially completes the circuit, behaving as a solid-state switch to permit gated waveform to be applied to power transistor base. The power transistor is an NPN type, in a high side switching arrangement. Two models are referenced: 2N6676: 300v @ 15A / 2N6496: 110v @ 15A. Given the voltage ratings, input voltage could range from 110v to 240v.

PC9XE (Sequential Gate Circuit) - Circuit Analysis

The goal of this circuit is to provide a sequenced pattern of two optocoupler pairs. The two main components producing this effect are the 74193 Binary Counter in conjunction with the 74154 Demultiplexer. To facilitate the understanding of each IC's operation, dedicated overviews follow below.

Binary Counter Operation (74LS193):

The 4-bit binary counter, shown in Figure 28, can perform counting-up (pin #5) and counting-down (pin #4) functions. Counting up/down is accomplished when LOW to HIGH pulse edge is applied to the respective pin. The direction of count (up/down) is determined by which count input is pulsed while the other is held HIGH. In Stan's application, a counting-up arrangement was used. Figure 28 shows the DOWN (pin #4) attached to the voltage supply (pin #16) to maintain a constant HIGH state for counting-up operation. LOAD (pin #11) is attached to voltage supply to inhibit this function, as no loading of inputs is performed during circuit operation.

CLEAR (pin #14) is utilized to force all the four outputs to a LOW logic state when a HIGH logic state is applied. Clearing is independent of the count and load inputs. This means that at any point in counting, if the CLEAR function is triggered, the outputs will be reset to all LOW (0) and counting will start at the beginning (0000). Each count-up pulse applied will cause the four binary outputs (QA, QB, QC, QD) to increment in an increasing binary count order. Counting will increment from 0 to 15 (1-16 in decimal). When exceeding 15 ("F") occurs, the CARRY OVER (pin #12) produces a pulse equal in width to the count pulse. In certain applications, this pulse can be used to return the counter back to starting at 0. Table 2 provides a functional overview of the binary counter operation.

Figure 28 – 74193:

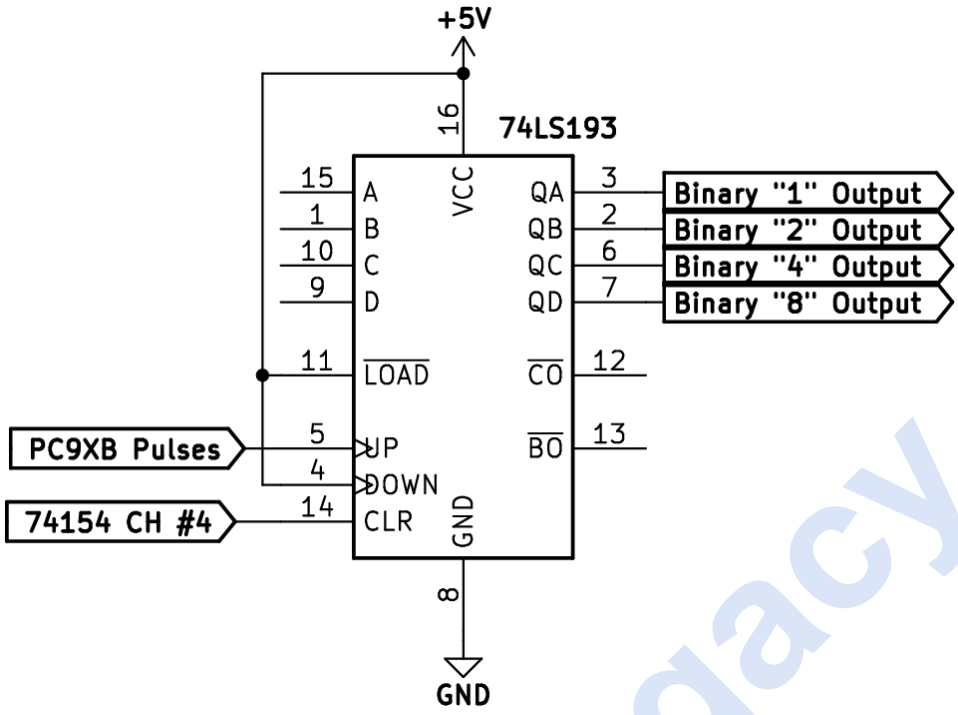

Table 2 - 74193 Functional Operation:

Pulse Number	QD (8)	QC (4)	QB (2)	QA (1)	Binary Number	Decimal Number
0	0	0	0	0	0	1
1	0	0	0	1	1	2
2	0	0	1	0	2	3
3	0	0	1	1	3	4
4	0	1	0	0	4	5
5	0	1	0	1	5	6
6	0	1	1	0	6	7
7	0	1	1	1	7	8
8	1	0	0	0	8	9
9	1	0	0	1	9	10
10	1	0	1	0	A	11
11	1	0	1	1	B	12
12	1	1	0	0	C	13
13	1	1	0	1	D	14
14	1	1	1	0	E	15
15	1	1	1	1	F	16

Demultiplexer (74154) Operation:

In simple terms, this model of demultiplexer (DMUX), as shown in Figure 29 below, is an integrated circuit capable of up to 16 channel selections through what is known as decoding. Channel selections only occur one at a time. The channel selected is dependent upon the binary values at the four inputs (pins #23, #22, #21, #20). All output channels are at a resting logic state of HIGH (1). When a channel is selected, the logic state changes to LOW (0). Two enable pins (pins #18, #19) must be kept at a LOW logic level in order for chip to operate. This will be understood shortly. The frequency of binary value inputs determines how fast the output channels are selected.

Figure 29:

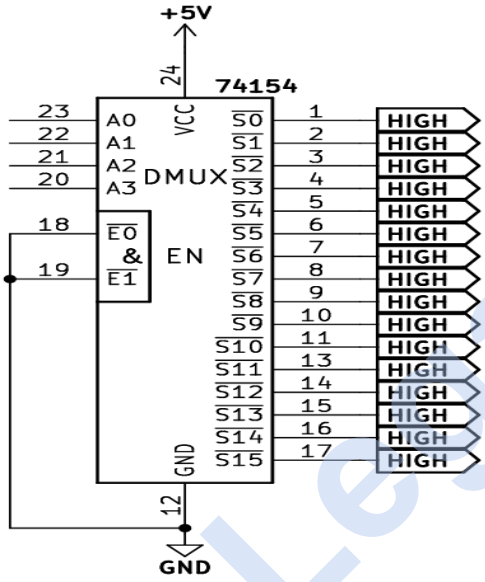

Shown in Table 3 below, the function table showing the correlation between the binary input values (A=#23, B=#22, C=#21, D=#20). A logical state of LOW (0) is represented by "L". A logical state of HIGH (1) is represented by "H". It can be seen that the two enable pins (G1, G2) are kept LOW through the channel selection process.

Table 3: Demultiplexer Operation

G1	G2	D	C	B	A	0	1	2	3	4	5	6	7	8	9	10	11	12	13	14	15
L	L	L	L	L	L	L	H	H	H	H	H	H	H	H	H	H	H	H	H	H	H
L	L	L	L	L	H	H	L	H	H	H	H	H	H	H	H	H	H	H	H	H	H
L	L	L	L	H	L	H	H	L	H	H	H	H	H	H	H	H	H	H	H	H	H
L	L	L	L	H	H	H	H	H	L	H	H	H	H	H	H	H	H	H	H	H	H
L	L	L	H	L	L	H	H	H	H	L	H	H	H	H	H	H	H	H	H	H	H
L	L	L	H	L	H	H	H	H	H	H	L	H	H	H	H	H	H	H	H	H	H
L	L	L	H	H	L	H	H	H	H	H	H	L	H	H	H	H	H	H	H	H	H
L	L	L	H	H	H	H	H	H	H	H	H	H	L	H	H	H	H	H	H	H	H
L	L	H	L	L	L	H	H	H	H	H	H	H	H	L	H	H	H	H	H	H	H
L	L	H	L	L	H	H	H	H	H	H	H	H	H	H	L	H	H	H	H	H	H
L	L	H	L	H	L	H	H	H	H	H	H	H	H	H	H	L	H	H	H	H	H
L	L	H	L	H	H	H	H	H	H	H	H	H	H	H	H	H	L	H	H	H	H
L	L	H	H	L	L	H	H	H	H	H	H	H	H	H	H	H	H	L	H	H	H
L	L	H	H	L	H	H	H	H	H	H	H	H	H	H	H	H	H	H	L	H	H
L	L	H	H	H	L	H	H	H	H	H	H	H	H	H	H	H	H	H	H	L	H
L	L	H	H	H	H	H	H	H	H	H	H	H	H	H	H	H	H	H	H	H	L
L	H	X	X	X	X	H	H	H	H	H	H	H	H	H	H	H	H	H	H	H	H
H	L	X	X	X	X	H	H	H	H	H	H	H	H	H	H	H	H	H	H	H	H
H	H	X	X	X	X	H	H	H	H	H	H	H	H	H	H	H	H	H	H	H	H

74154 Waveform Analysis:

Diagram 5 below illustrates a representation of what a digital analysis would show for all sixteen channels during operation. Binary value at the input pins is located at the far left, with corresponding channel selection. The last channel could be used to trigger the clear pin on the driving binary counter for certain applications.

Diagram 5:

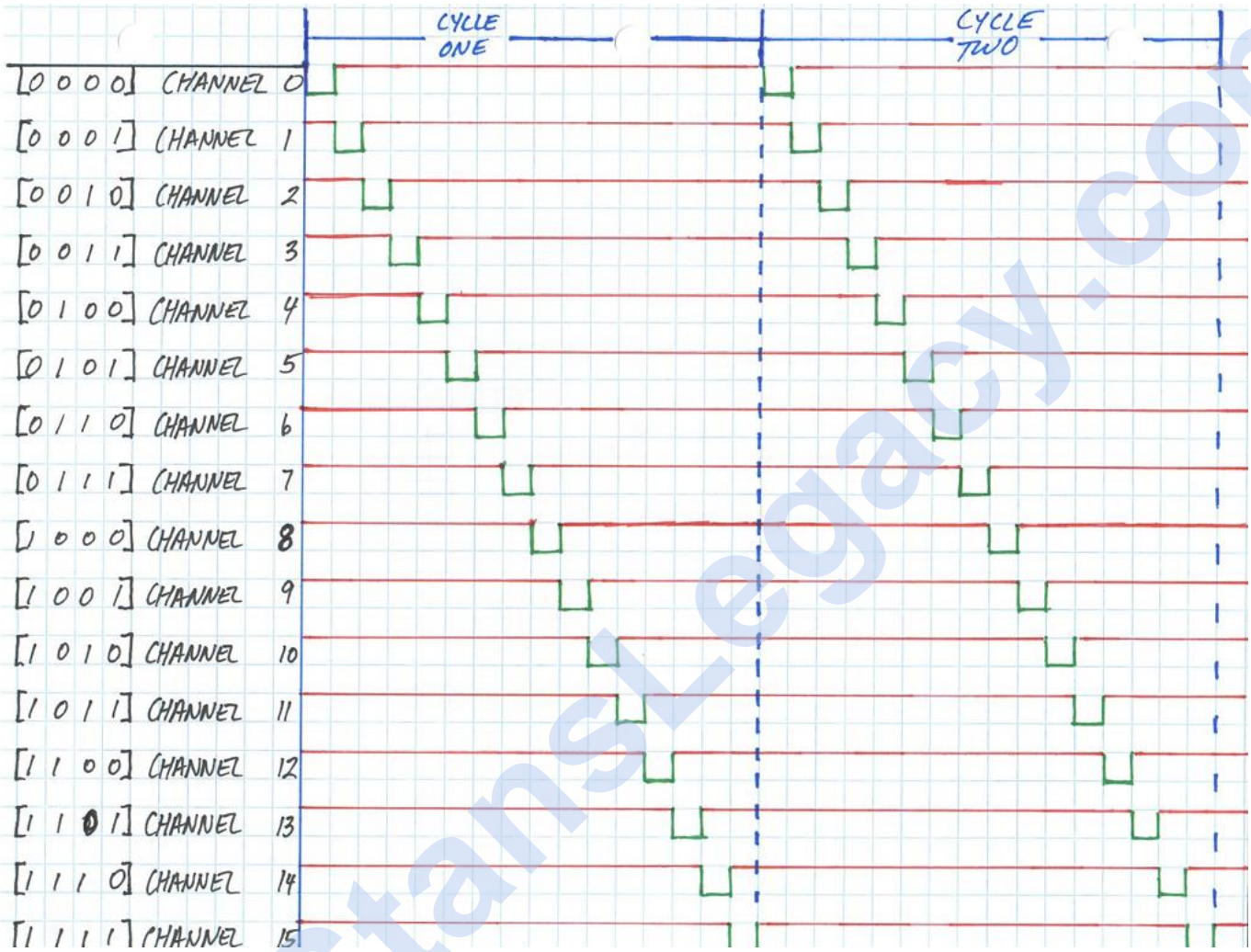

74154 Internal Operation:

Internally, the 74154 is composed of two stages of four inverters at the binary inputs. The first stage changes the LOW (0) logic into HIGH (1) logic. Second stage of inverters re-invert the HIGH (1) logic back to LOW (0) logic states. These work in conjunction with a network of NAND logic gates to control the selection of each output channel. Both enable inputs (G1/G2) are connected to ground (0V), being inverted before entering their associated AND logic gate. This arrangement produces a constant HIGH logic state to one input of each of the sixteen NAND gates (as seen by the red lines). None of the channels are available for selection without G1 and G2 being maintained LOW.

Within the next sixteen pages (46-61), the internal operations for each channel selection are provided. The red lines are indicative of the circuits associated HIGH (1) logic states. The blue lines are indicative of the circuits associated with LOW (0) logic states.

Sequence One:

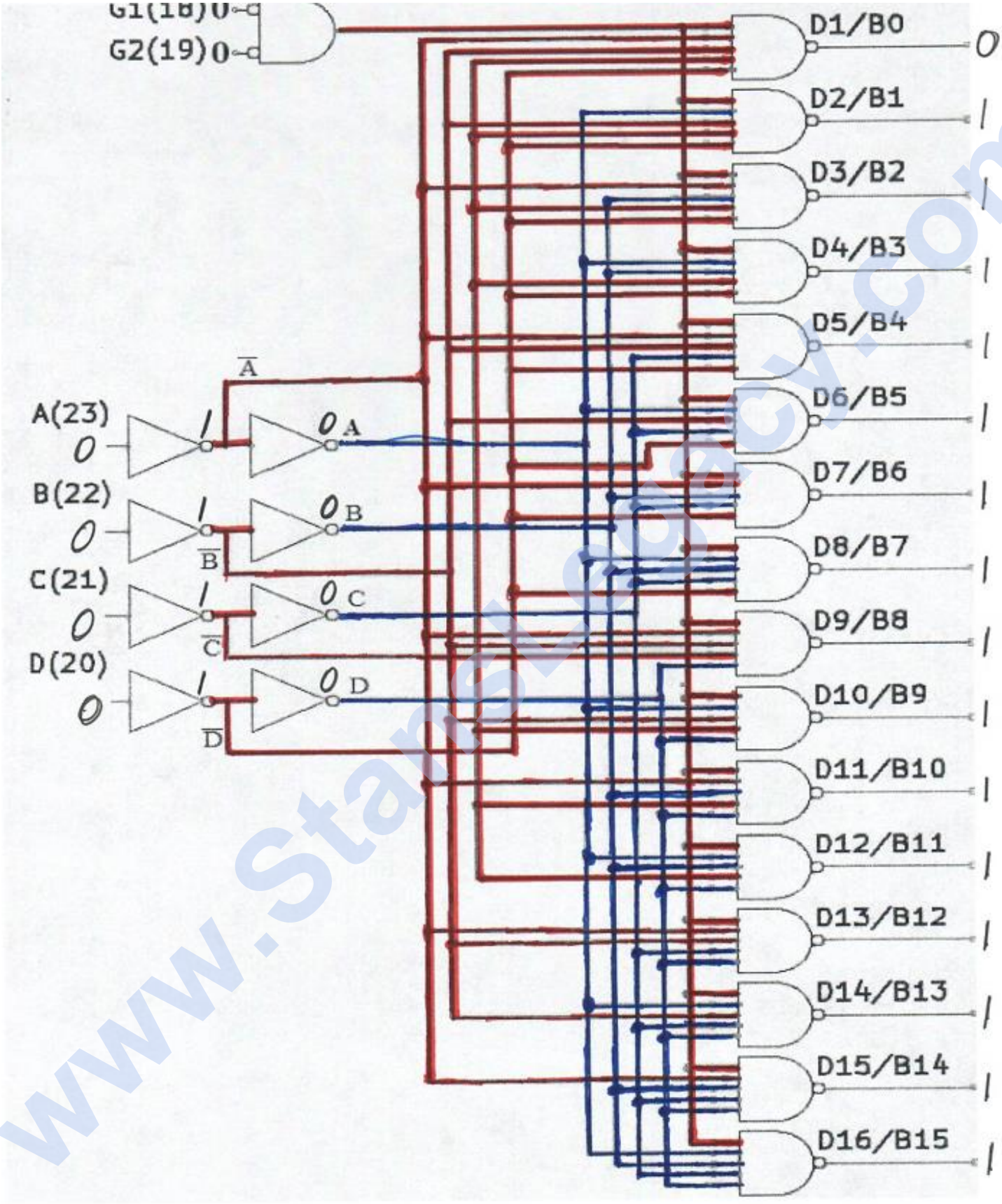

Sequence Two:

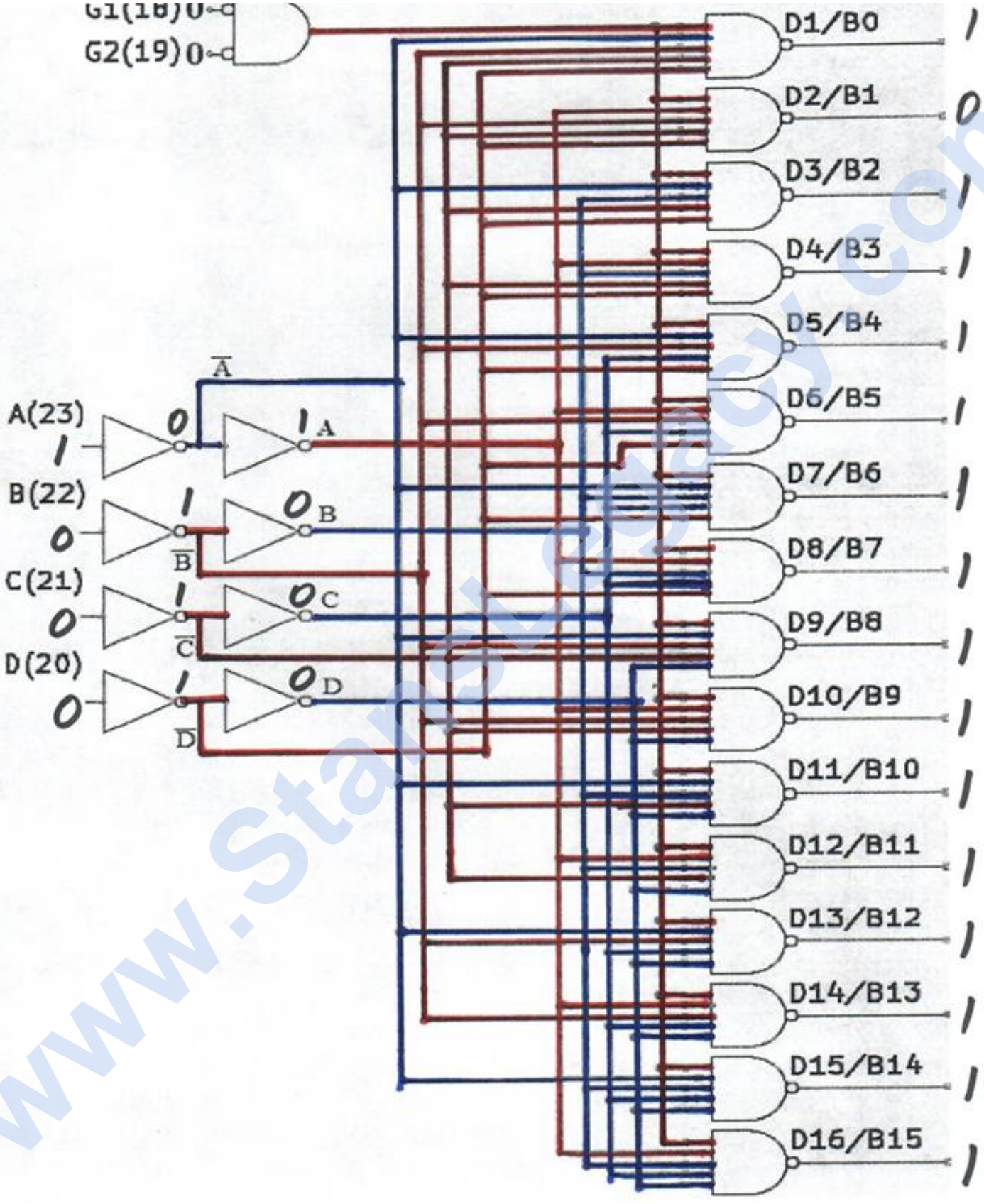

Sequence Three:

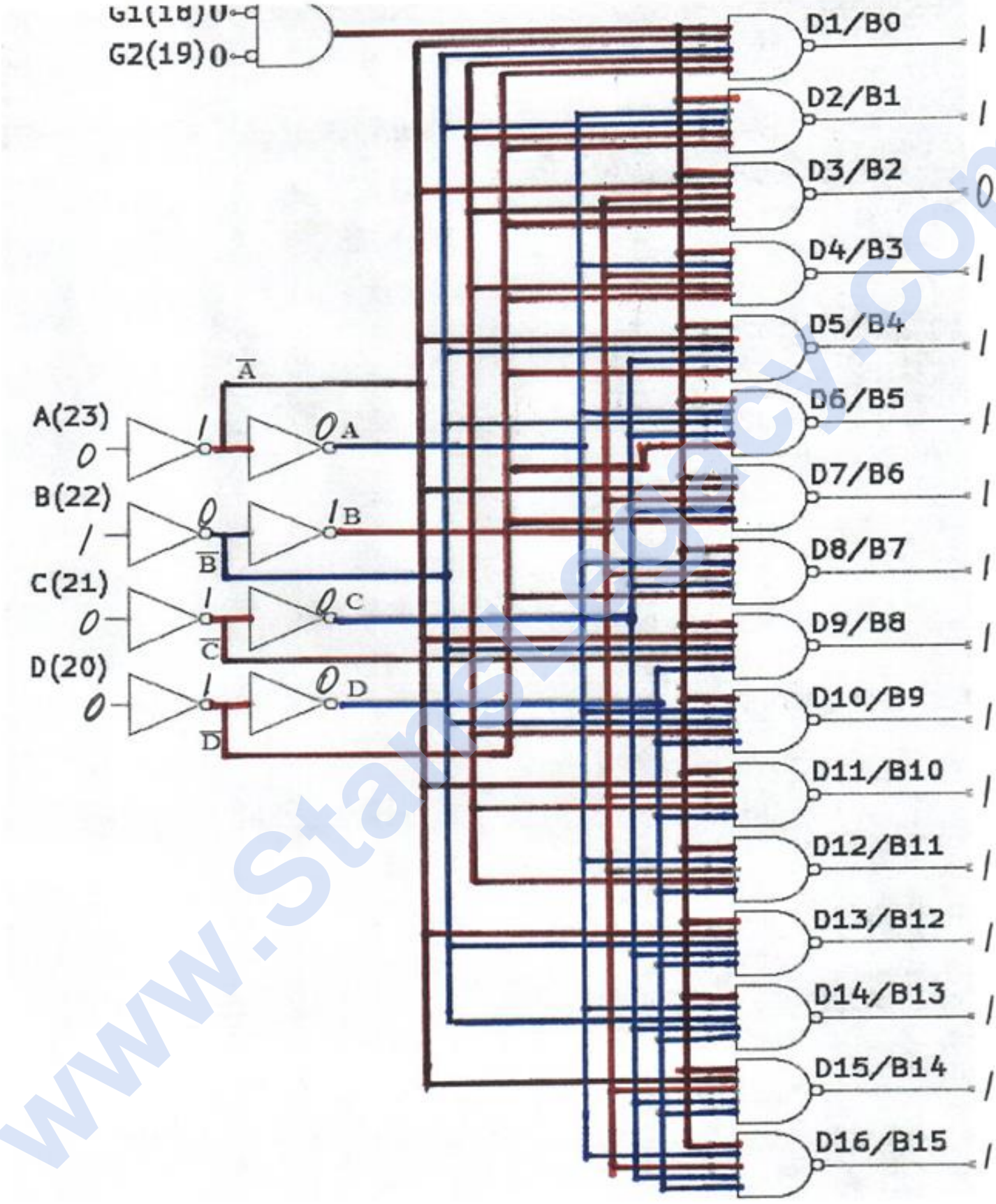

Sequence Four:

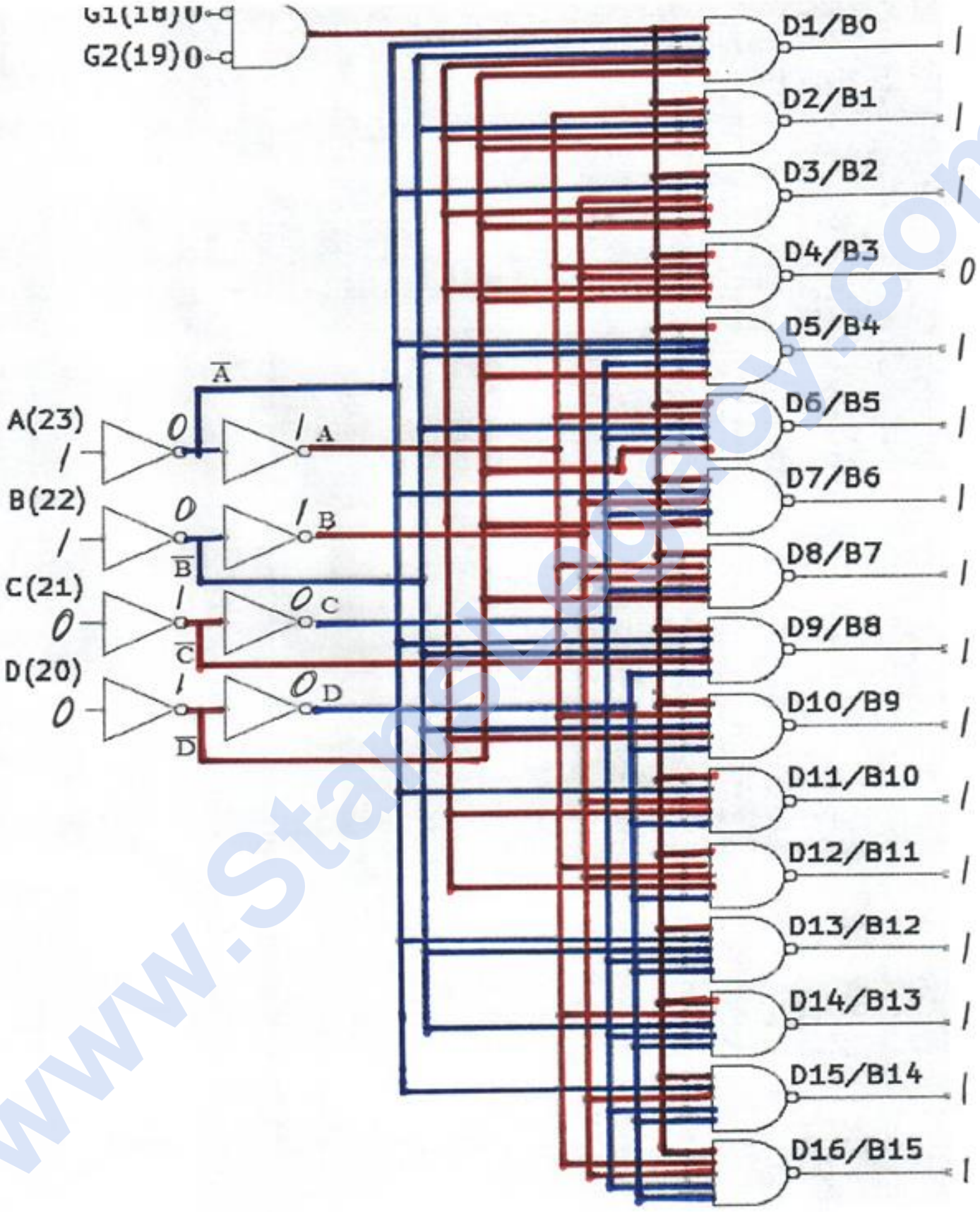

Sequence Five:

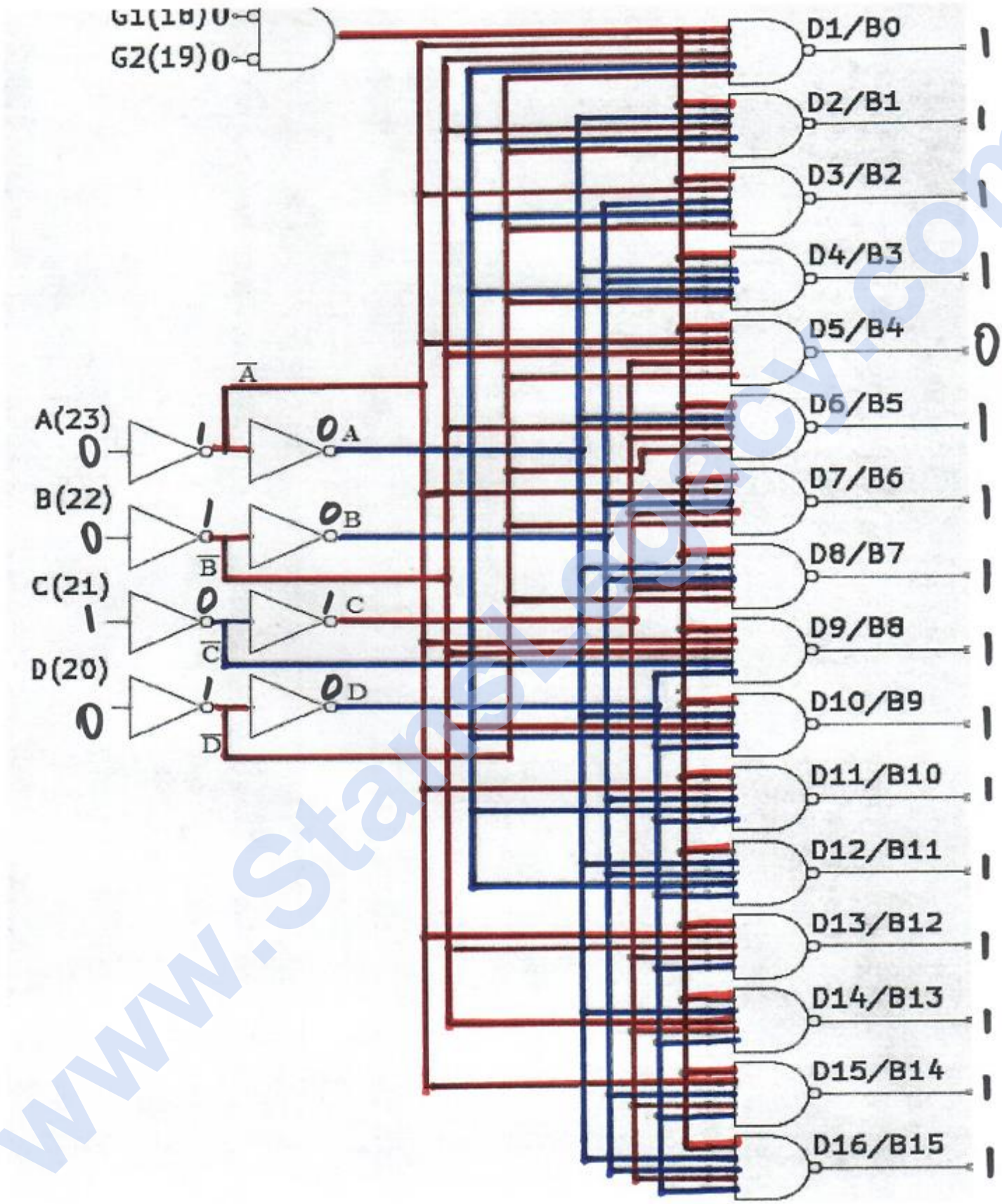

Sequence Six:

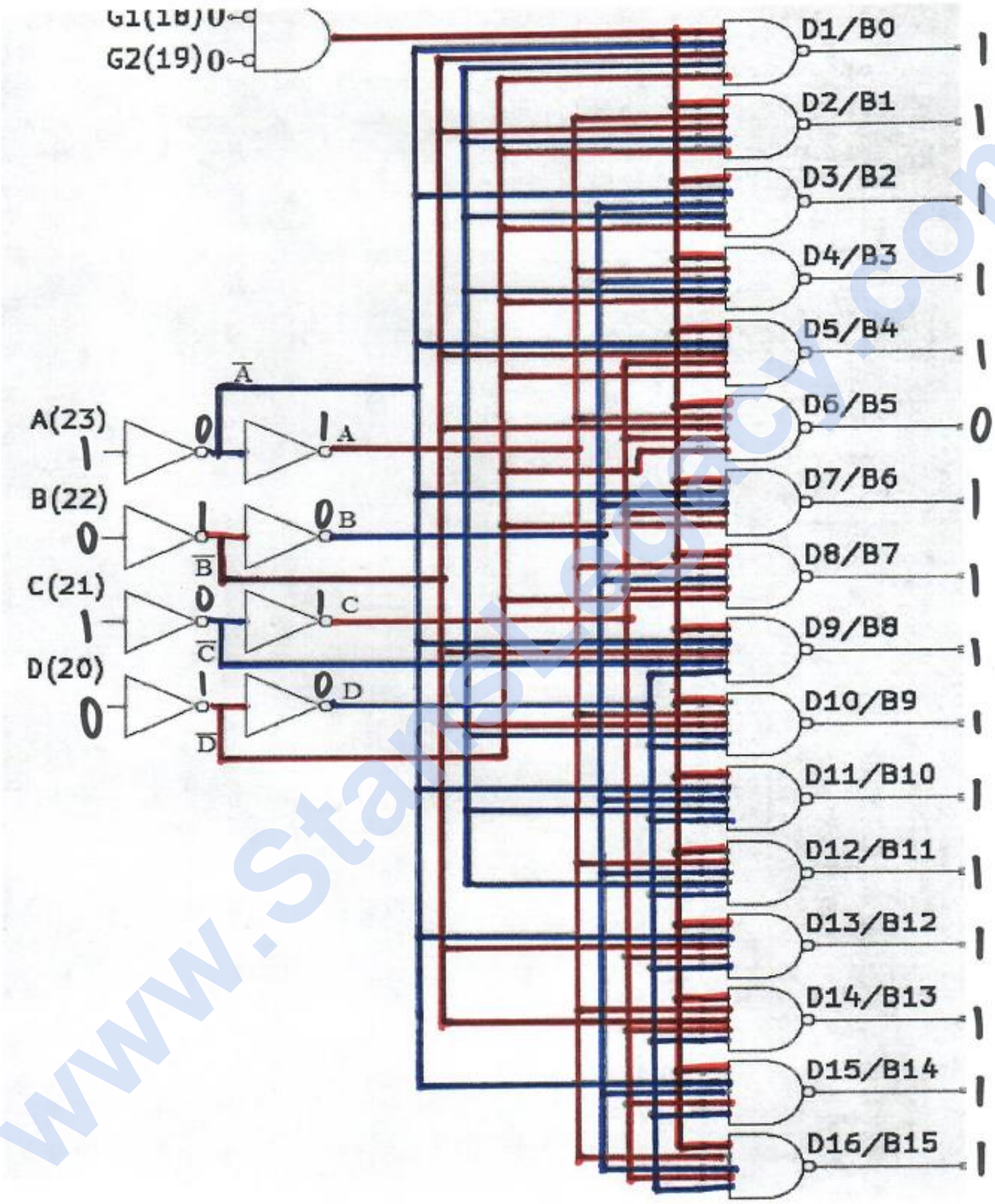

Sequence Seven:

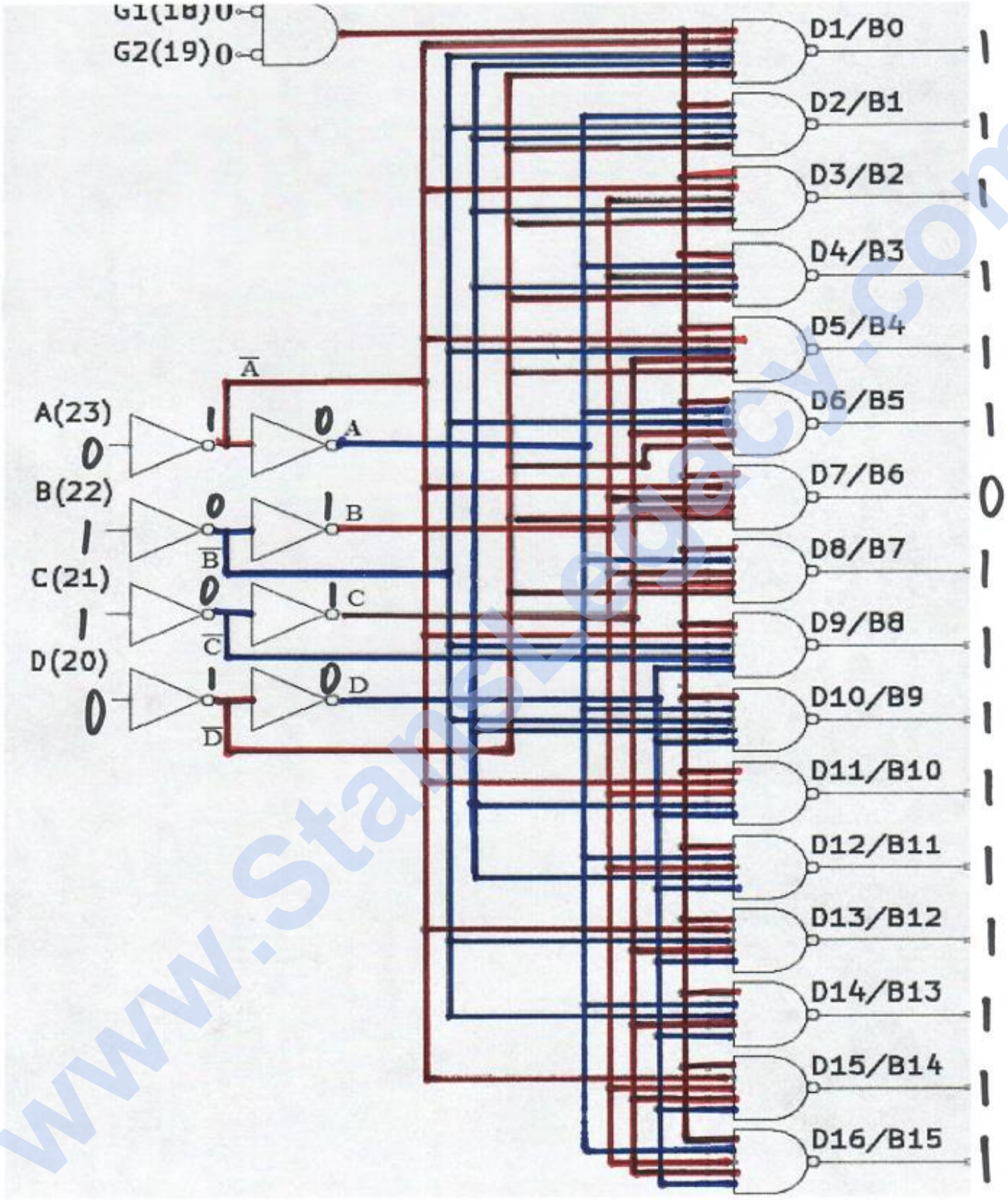

Sequence Eight:

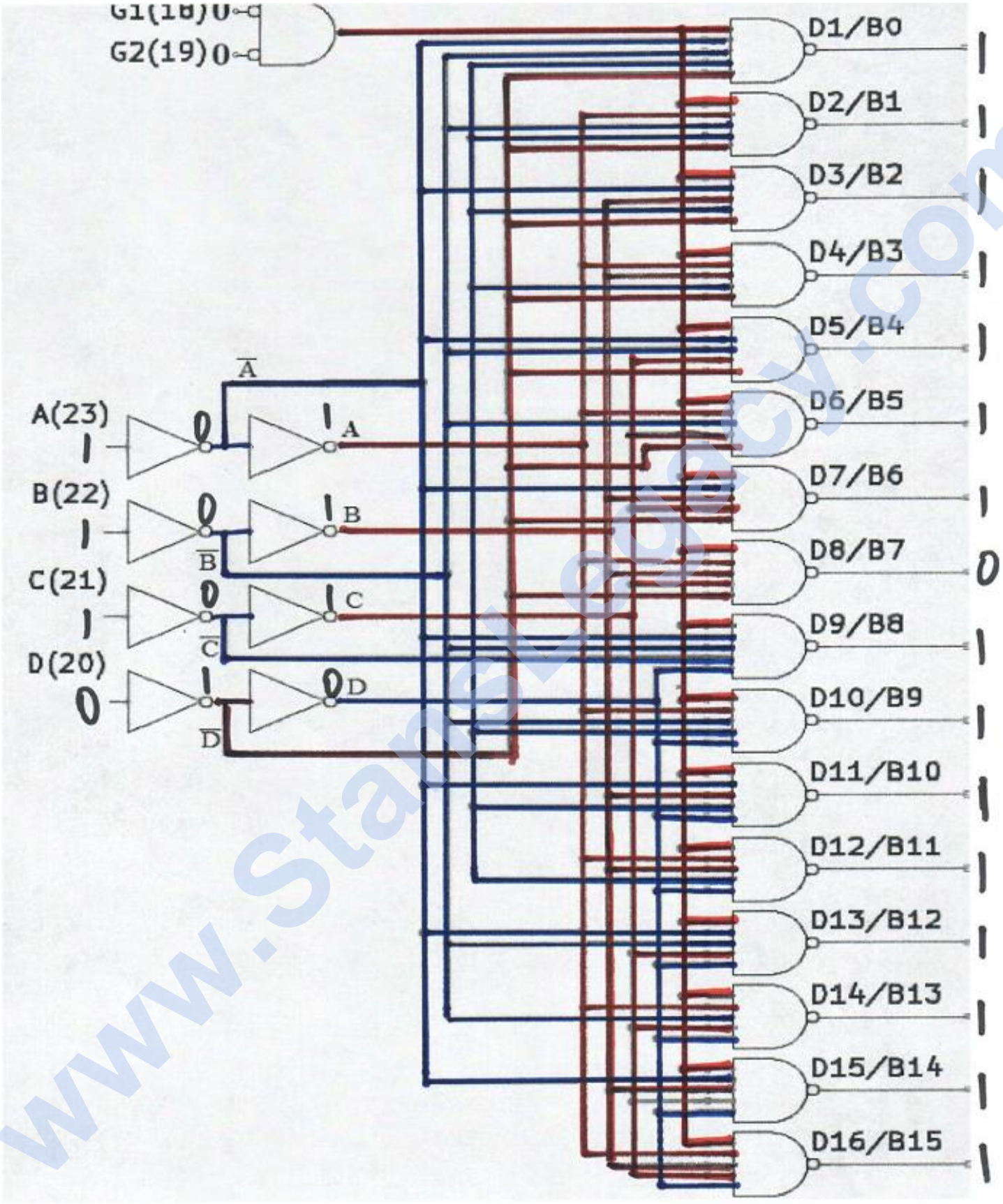

Sequence Nine:

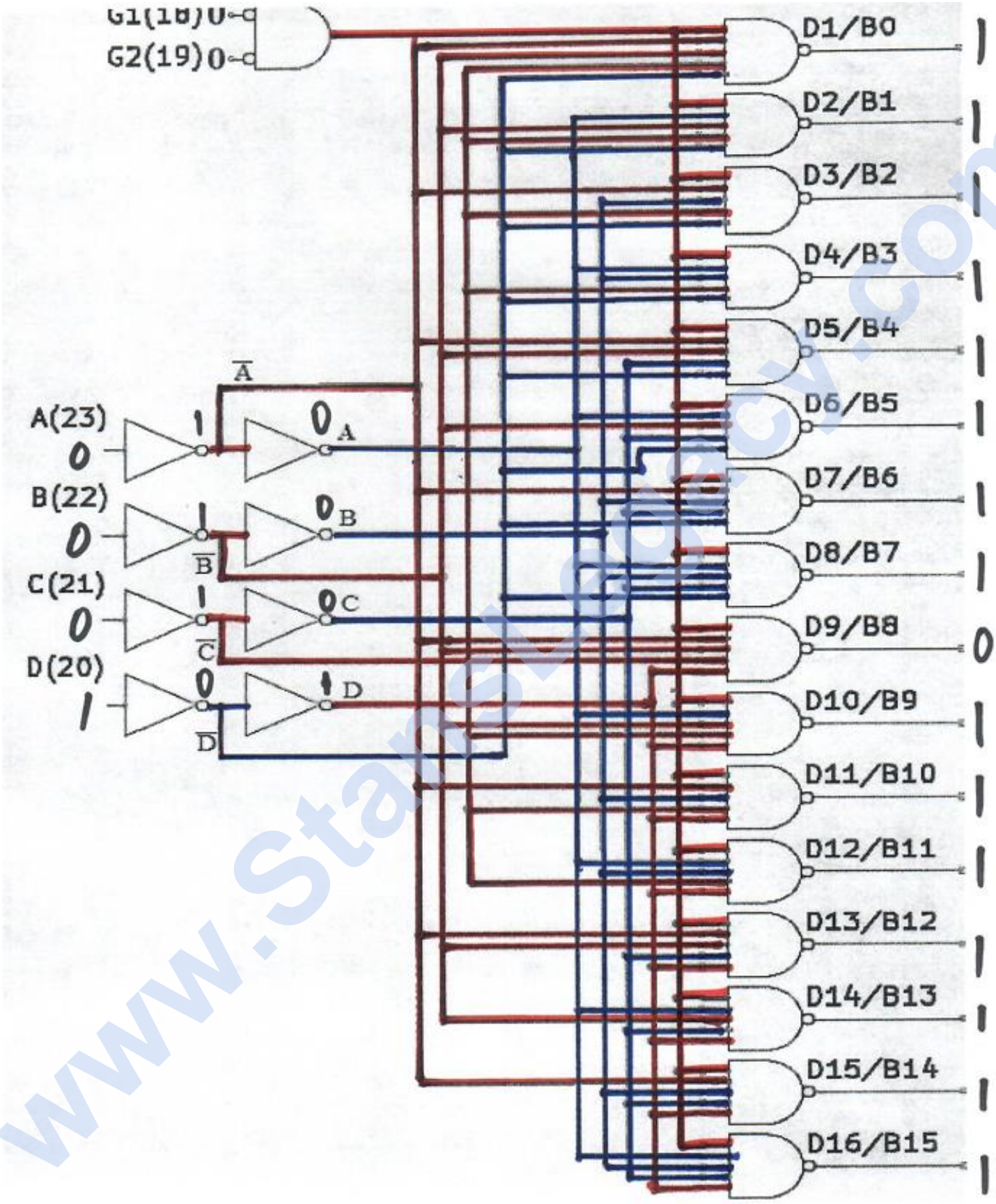

Sequence Ten:

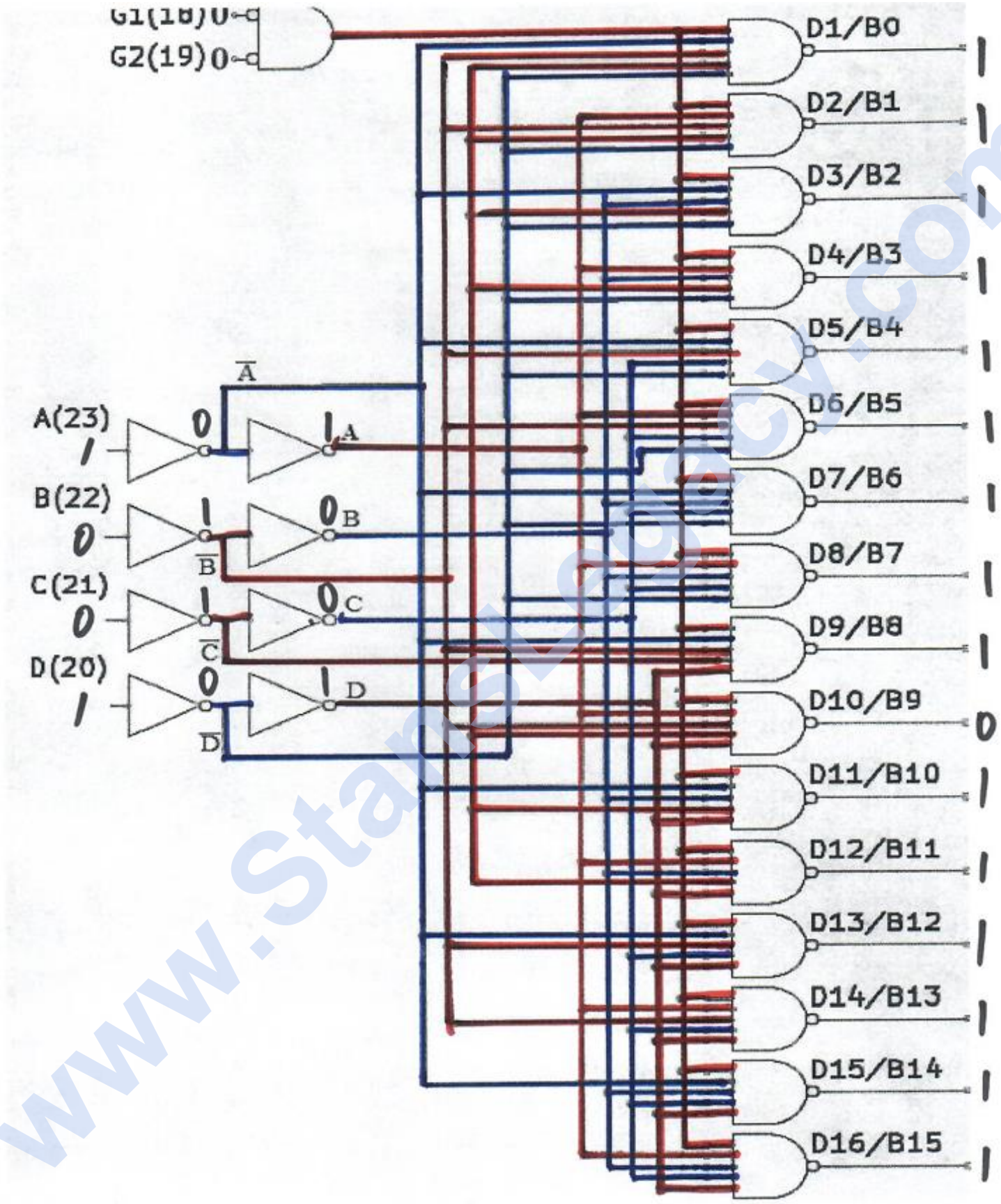

Sequence Eleven:

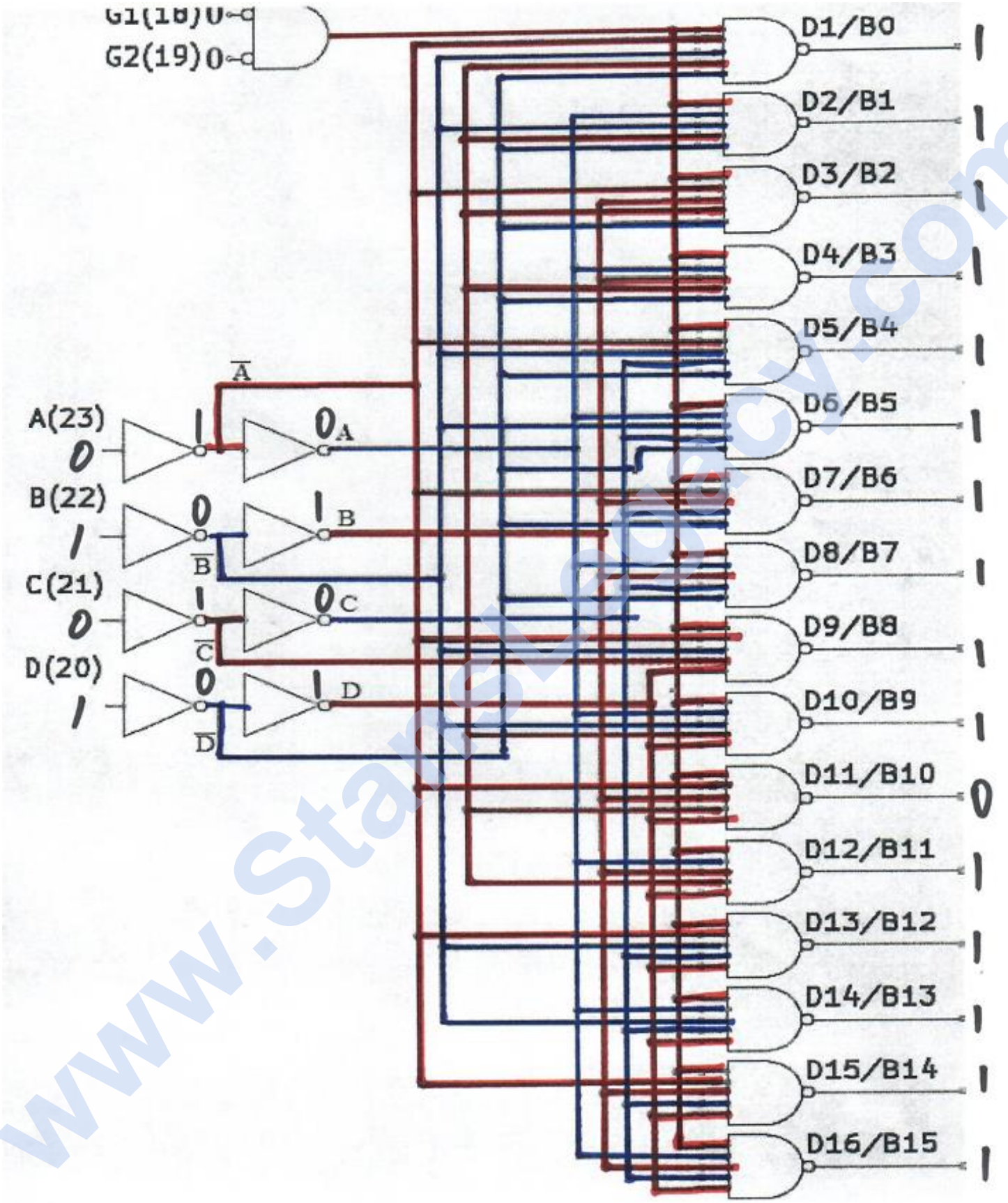

Sequence Twelve:

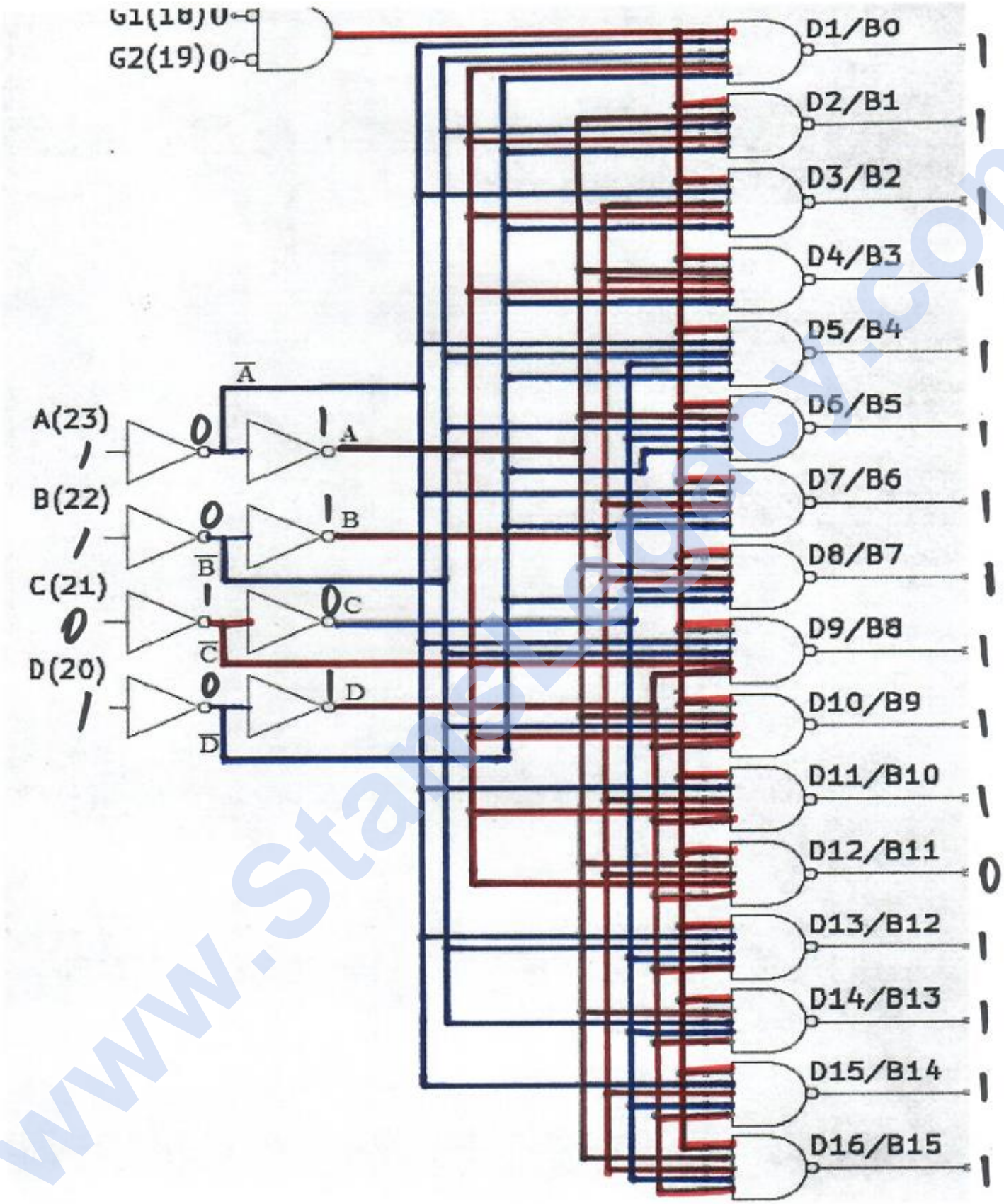

Sequence Thirteen:

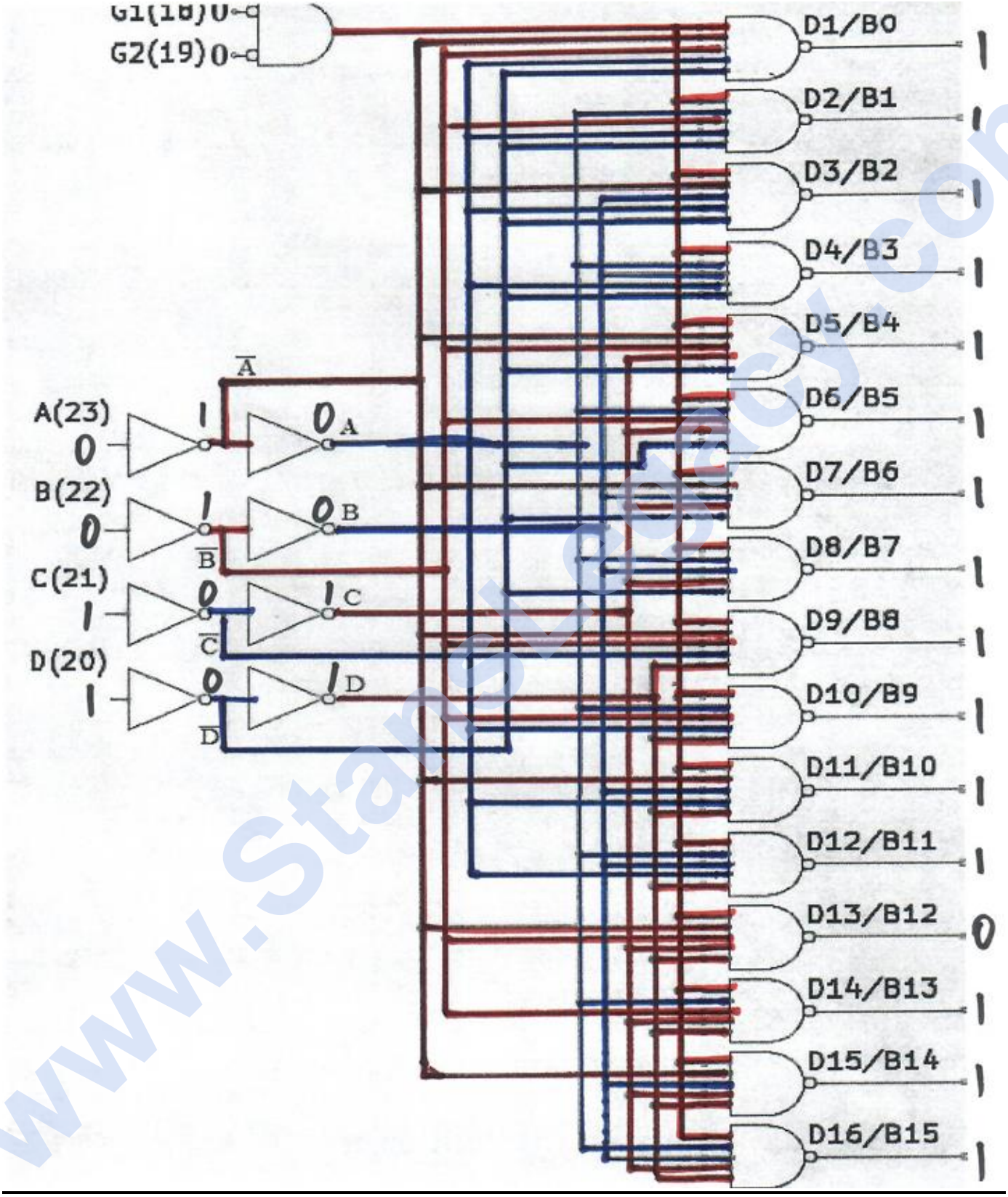

Sequence Fourteen:

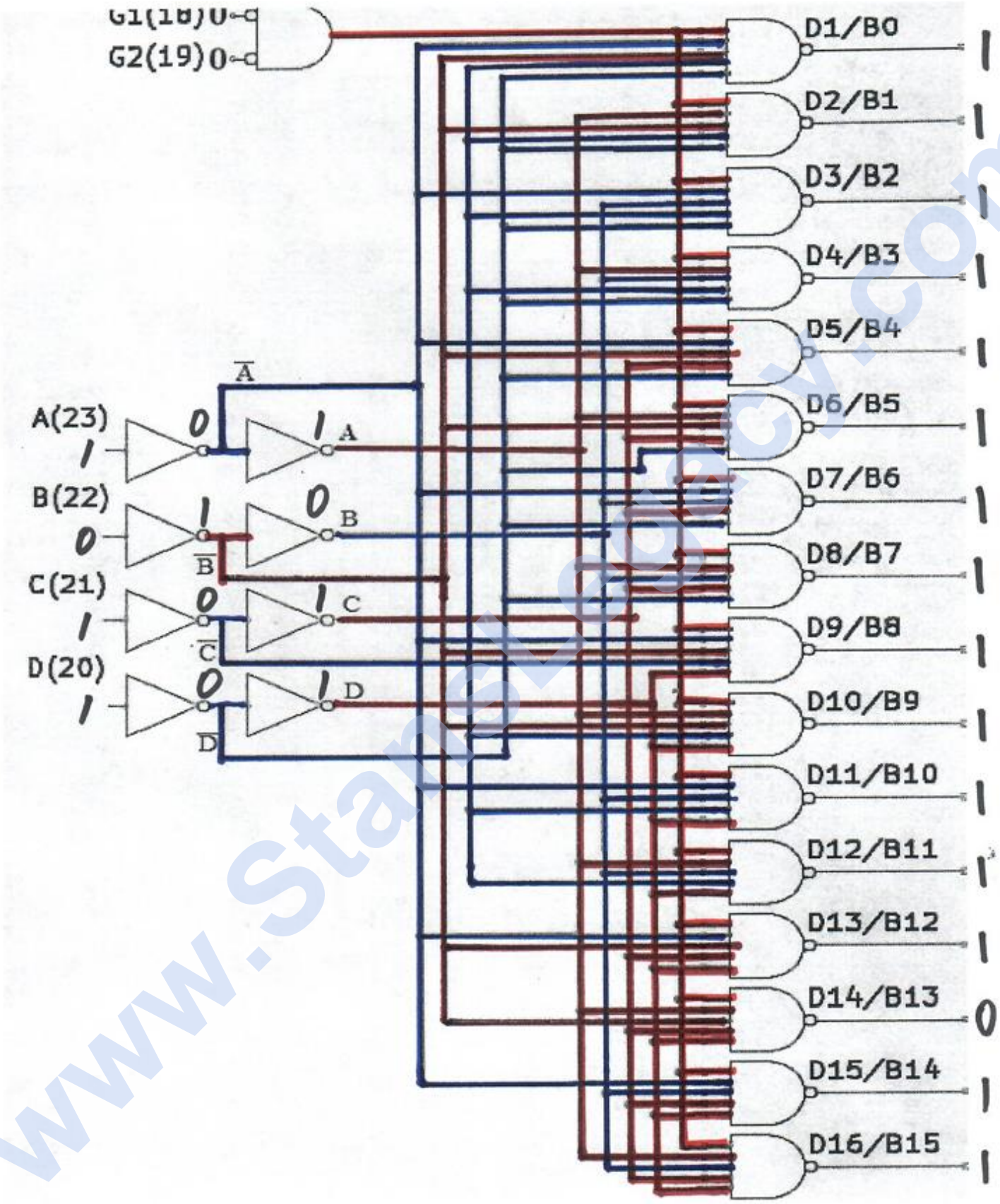

Sequence Fifteen:

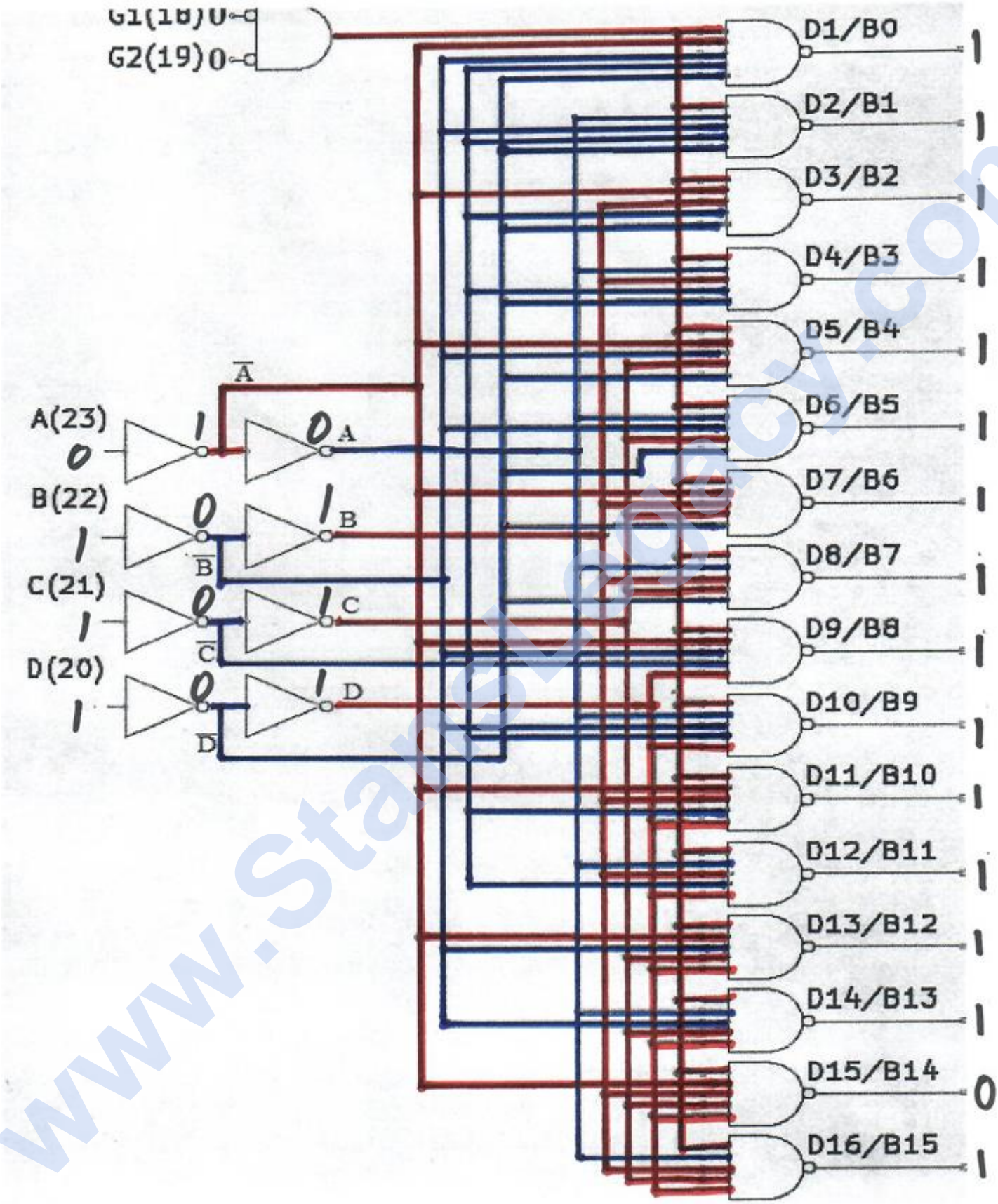

Sequence Sixteen:

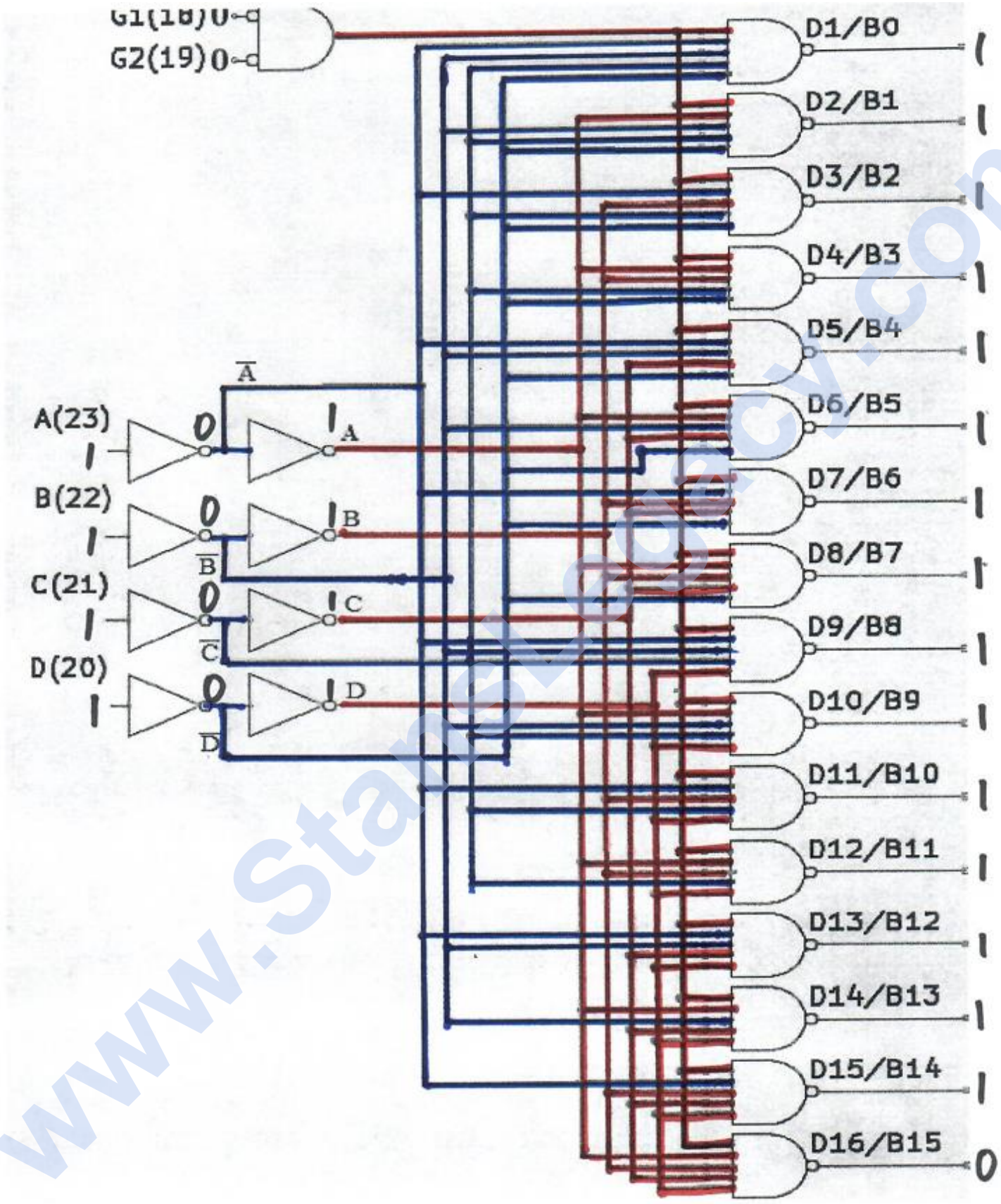

Stan's Application (Triple Stacked Resonant Cavities):

Stan utilized only three channels of the 74154 to sequence through the triple stack resonant cavity assemblies shown below in Figure 30. Figure 31 illustrates this schematically.

Figure 30:

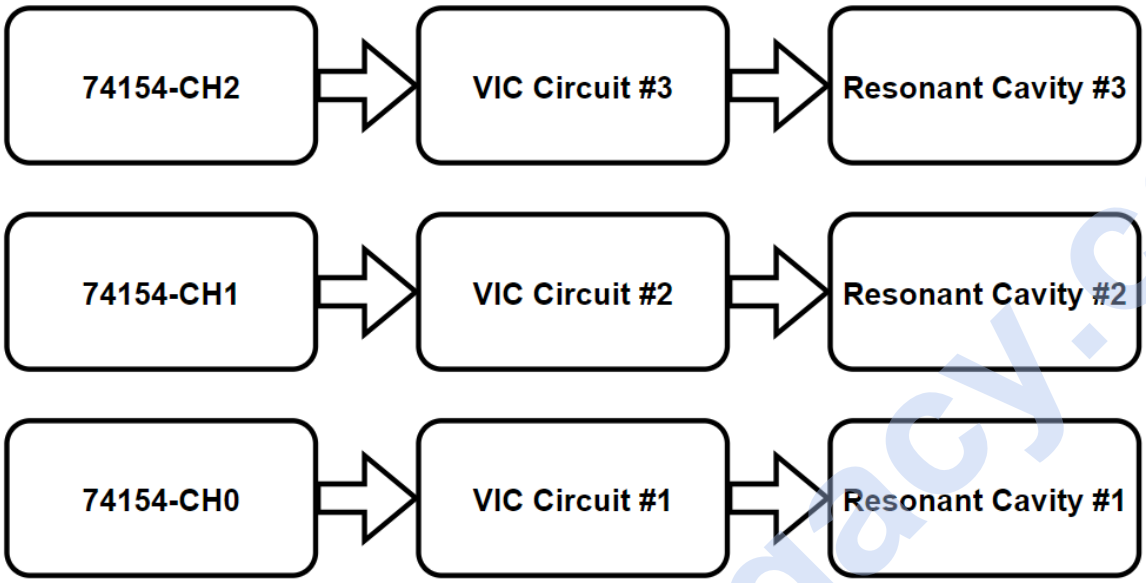

Figure 31:

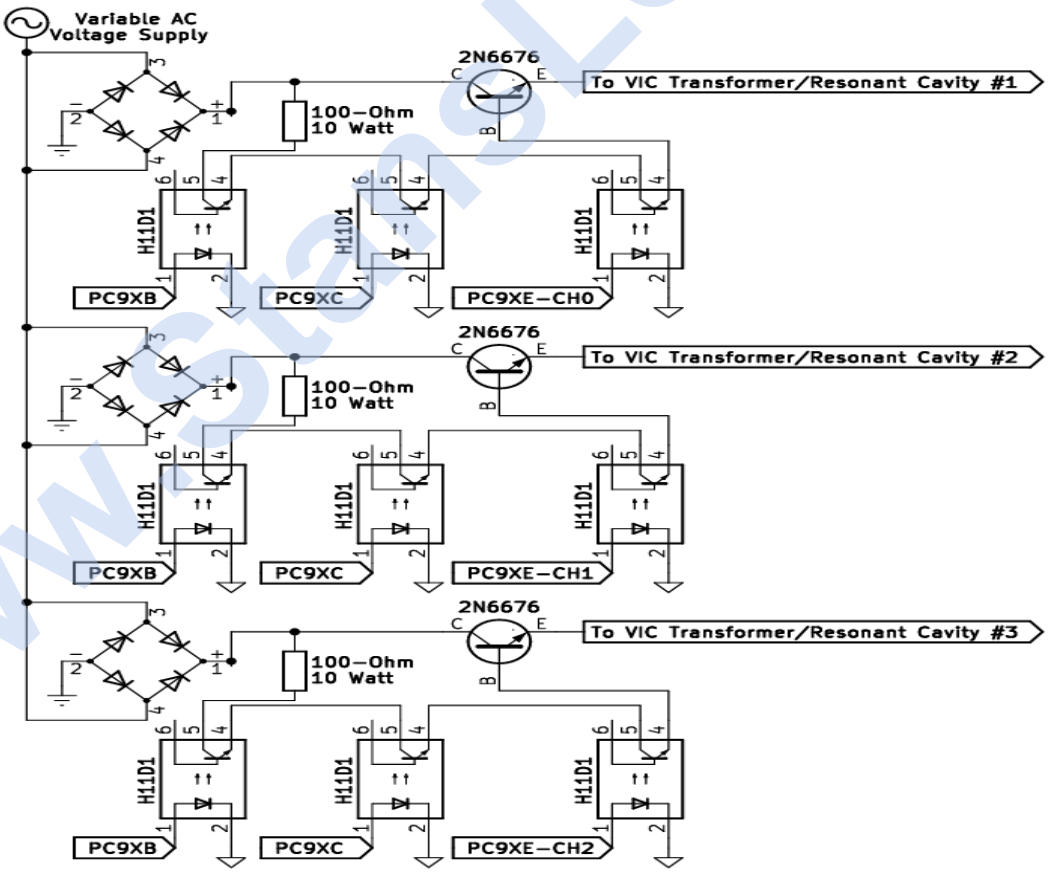

One of the more exotic applications for the PC9XE, shown below in Figure 32, was a method to accelerate hydrogen and oxygen gases. Comparable to modern particle accelerator chambers, unipolar voltage pulses would've propelled hydrogen and oxygen gases to high velocities. In other literary references, Stan describes particle impact being related to "resonant action". This tube may have been and early adaption related to this process. Within his literature, specific design details were not disclosed. Due to an absence of any photographic evidence, a cut-away CAD model is provided below for a visual aid.

Figure 32: Gas Accelerator Tube:

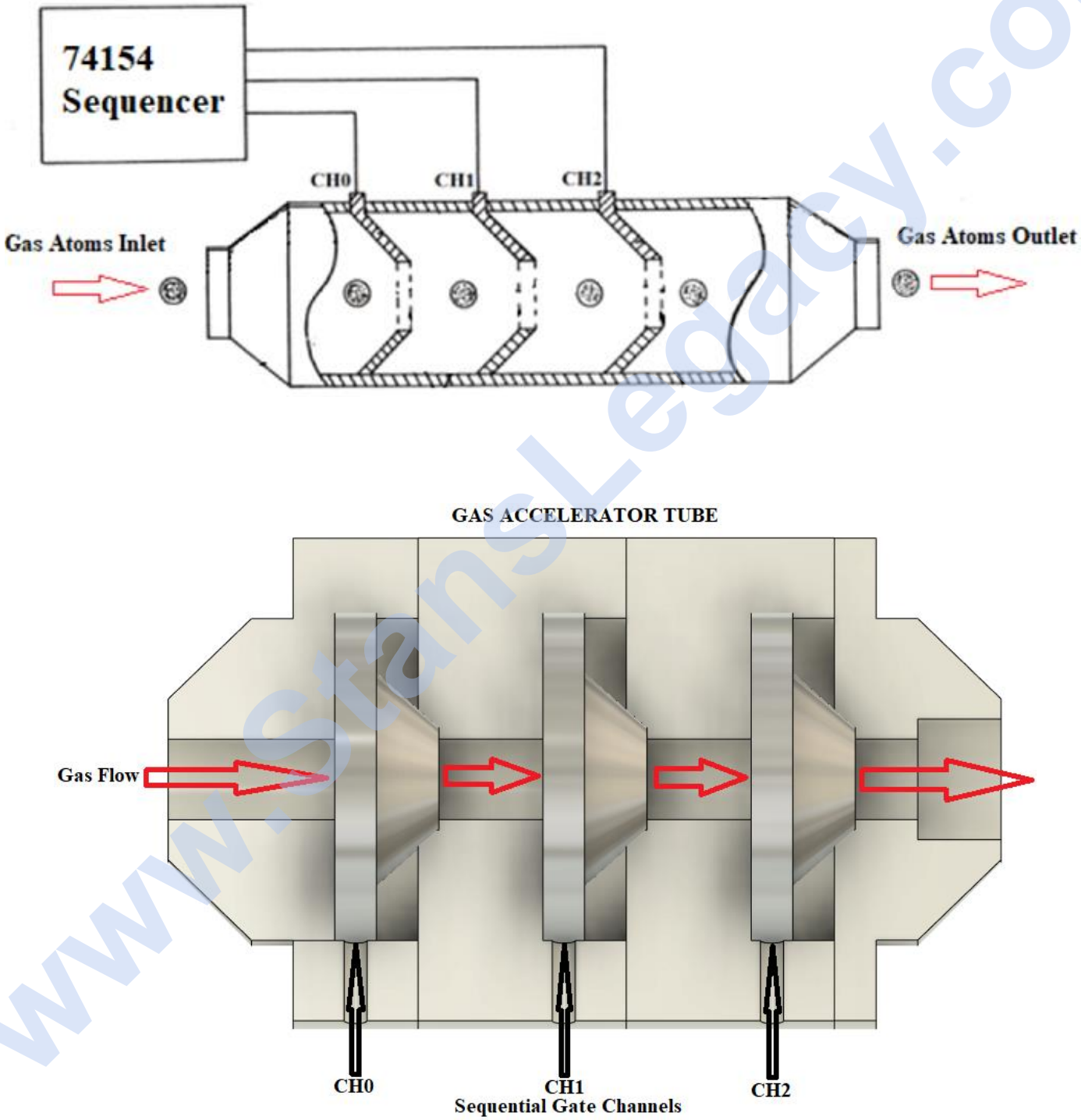

Stan's Three Sequence Overview:

As the binary counter increments, corresponding binary values are sent over the four lines as shown below. Initial state of 0000, after clear has been triggered, causing the 74154's S0 (Channel "1") to change from a HIGH state to LOW state as shown below in Figure 33.

Figure 33:

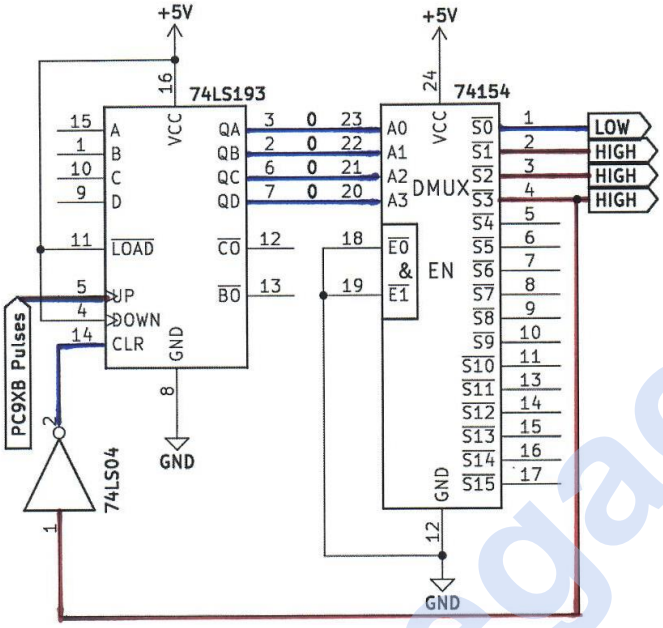

A LOW to HIGH pulse (Pulse #1) received from the 9XB, incrementing the 74193 to a binary value of "1" (0001). This output state causes the 74154's S1 (Channel "2") to change from a HIGH to LOW state. Previous S0 (Channel "1") returns back to HIGH state as shown below in Figure 34.

Figure 34:

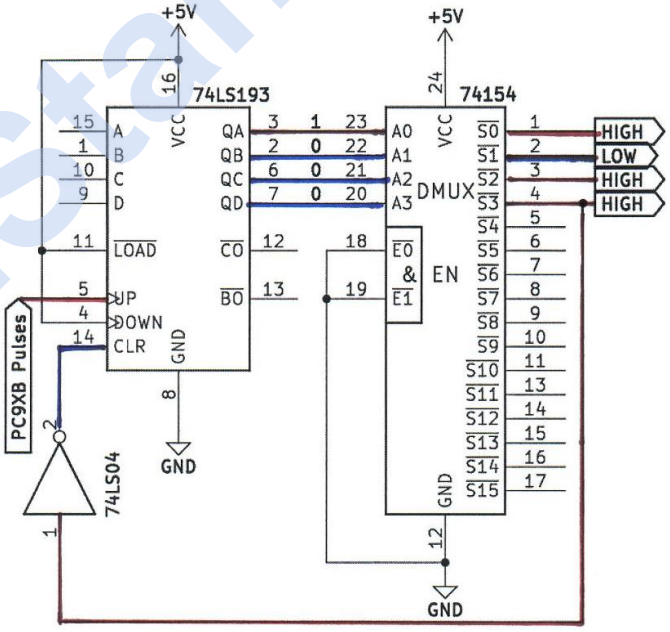

Another LOW to HIGH pulse (Pulse #2) is received from the 9XB, incrementing the 74193 to a binary value of "2" (0010). This causes the DMUX's output S2 (Channel "3") to change from a resting HIGH state to LOW state. Previous S1 (Channel "2") changes back to HIGH from triggered LOW state as shown below in Figure 35.

Figure 35:

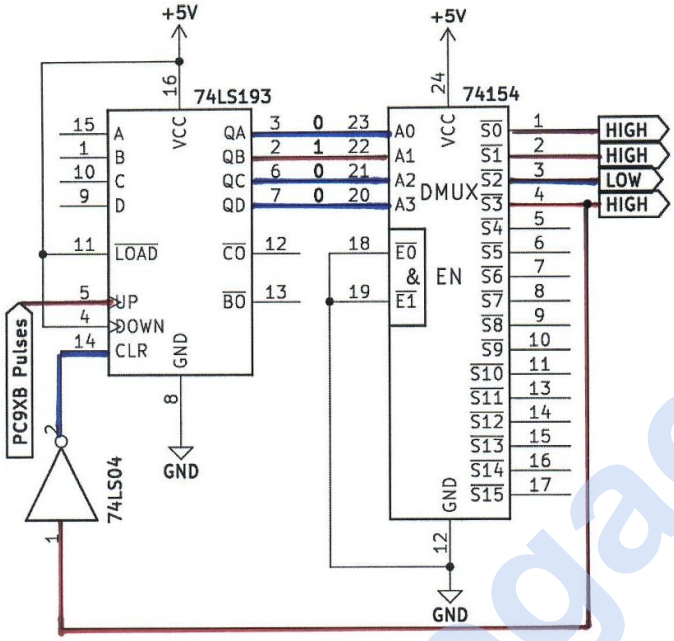

Finally, a LOW to HIGH pulse (Pulse #3) is received from the 9XB, Incrementing the 74193 to a binary value of "3" (0011). This causes DMUX's S3 (Channel "4") to change from resting HIGH state to LOW state. Previous S2 (Channel "3") returns to HIGH state from triggered LOW state as shown below in Figure 36.

Figure 36:

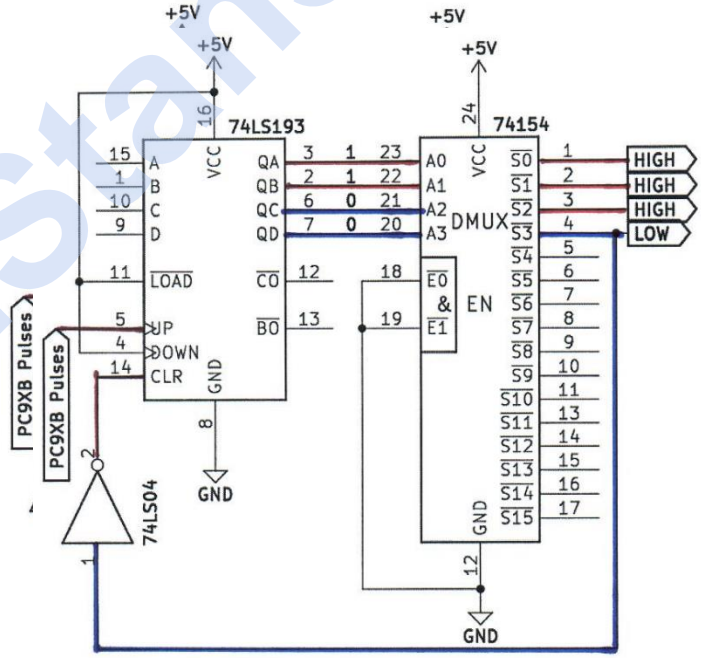

Referencing Figure 37 below, this S2 (channel "4") is routed back to the first 74LS04 hex inverter (input pin #1). Blue is representative of LOW logic level. When the LOW (0) logic state is inputted into the inverter, the output (pin #2) produces the complement, which is HIGH (1). Red is representative of HIGH logic level. It should be remembered from the above overview, that when the CLEAR pin receives a HIGH (1) logic level, the binary counter's outputs are reset and counting begins starting at zero once again. This concludes the sequencing amount used by Stan. One through three, then reset on four.

Figure 37:

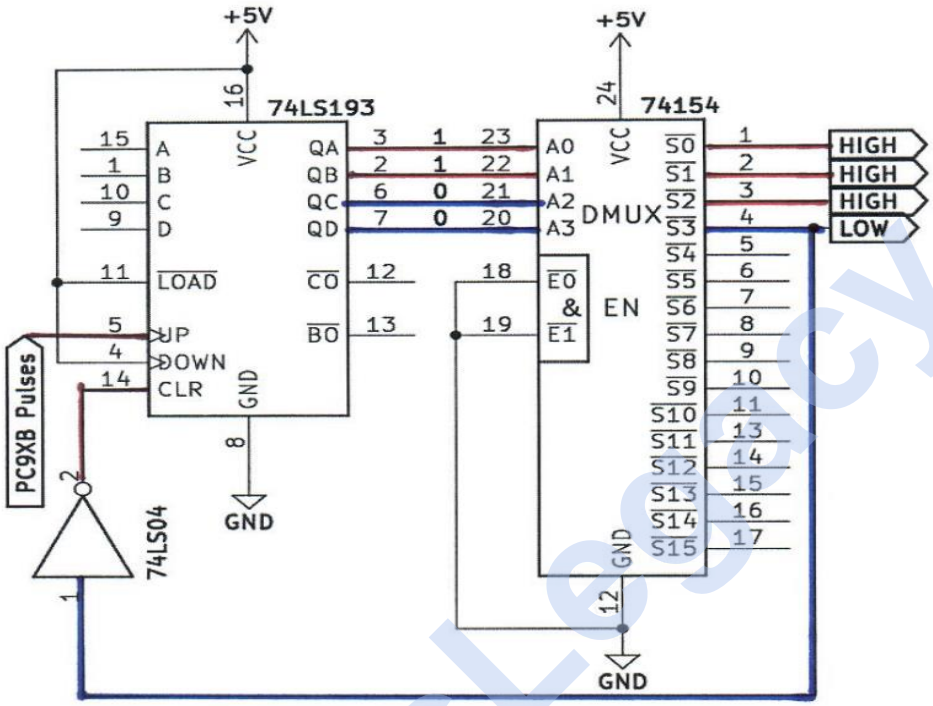

Oscilloscope Waveform Analysis:

While diagrammatical representations can effectively describe circuit operation, a better understanding comes from visually captured waveforms during each stage. Subsequent oscilloscope analysis details the following circuit stages:

- Figure 38 - PC9XB waveform entering 7404-1 hex inverter IC
- Figure 39 - Incrementation of 74193
- Figure 40 - 74193 output channels counting sequence
- Figure 41 - 74154 output channels
- Figure 42 - 74154 output channels through 7404-2 hex inverter IC, triggering LEDs
- Figure 43 - First LED illuminated
- Figure 44 - Second LED illuminated
- Figure 45 - Third LED illuminated
- Figure 46 - 74154 output channels through 7404-3 hex inverter IC, triggering optocouplers

Pulse train (from PC9XB) is applied into the first hex inverter (74LS04-1) input pins #3, #5, #9, and #11. Duty cycle is a fixed at 50%. Figure 38 below is provided to demonstrate the relationship between the input pulse train (Yellow), inverter input (pin #11 - Blue) and inverter output (pin #6 - Magenta).

Figure 38:

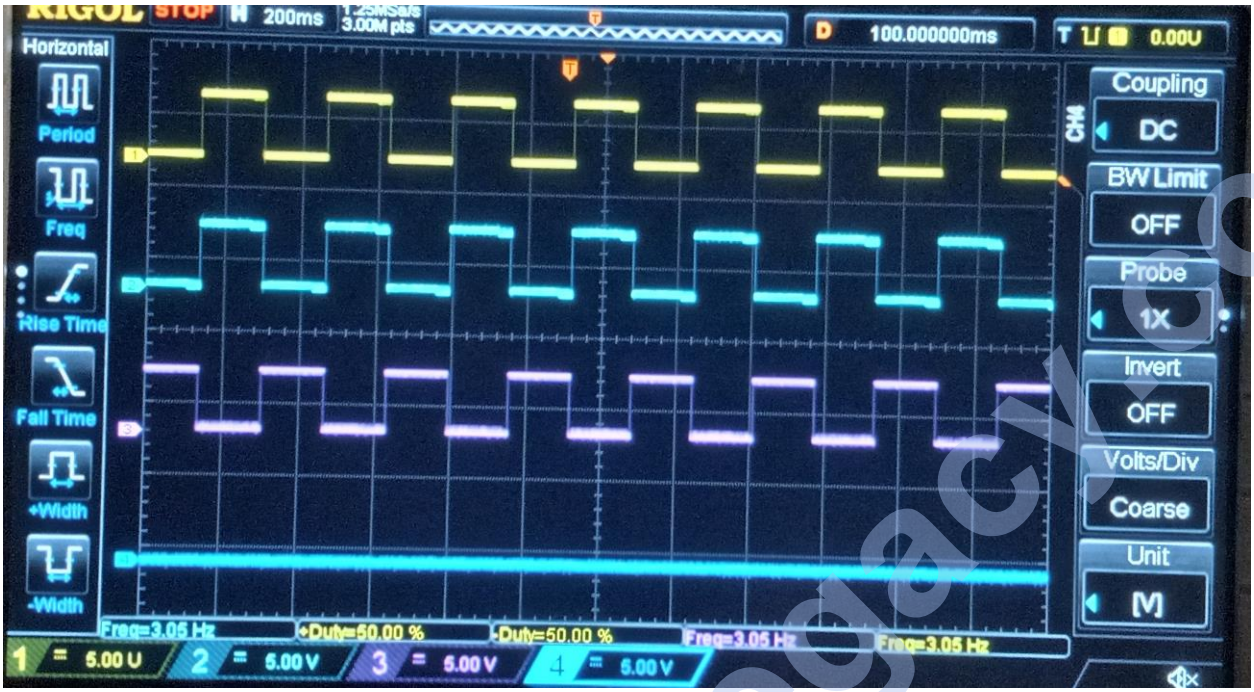

Output pin #6 increments the COUNT UP (pin #5) of binary counter (74LS193) by providing a HIGH logic state from the pulse frequency during its LOW logic state. Figure 39 below shows the clock pulse applied to pin #5.

Figure 39:

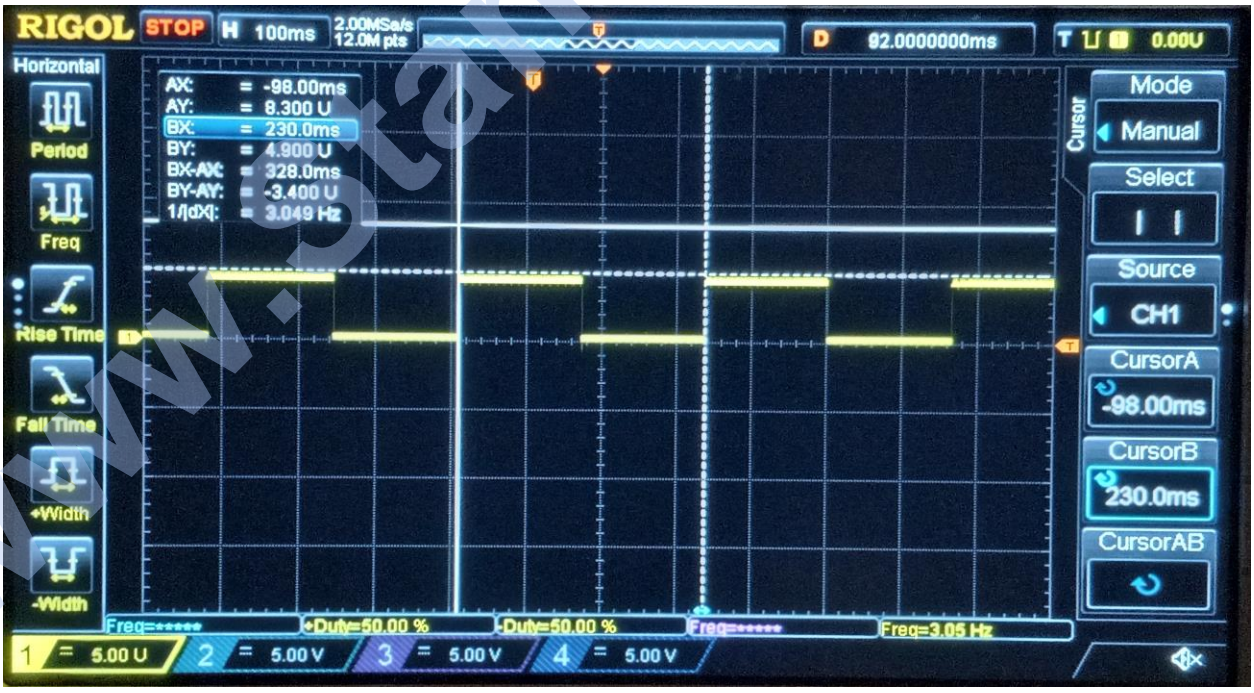

Pins #4, #11 on the 74193 are connected to V_{cc} (pin #16) to maintain a HIGH logic state. Due to LOAD and COUNT DOWN not being used, a HIGH logic state is maintained for operation. Binary output pins (#3[QA], #2[QB], #6[QC], and #7[QD]) count through a 4-bit binary sequence (0-3) for every low to rising edge of clock. In Figure 40 below, the counting sequence is shown. Count values are divided by the white vertical lines. The counter is only counting to binary 2 (decimal "3") with a reset on binary 3 (decimal "4"). Therefore, only two channels are utilized. Binary output [QA] is represented by the blue trace. Output [QB] is represented by the magenta trace.

Figure 40:

Outputs from the binary counter are communicated to the inputs of the DMUX (pin #23[A0], #22[A1], #21[A2] and #20[A3]). These cause the DMUX to select corresponding channels (pin #0[CH1], #1[CH2], and #2[CH3], #3[CH4]). When a corresponding channel is triggered, its logical state changes from a resting HIGH to LOW. Four outputs are selected in a sequential fashion. Figure 41 below, illustrates the sequential manner of each channel. The first channel is represented by the yellow trace. The second channel is represented by the blue trace. The third channel is represented by the magenta trace. Finally, the fourth channel is represented by the dark blue trace, which is LOW due to being reset signal for binary counter.

Figure 41:

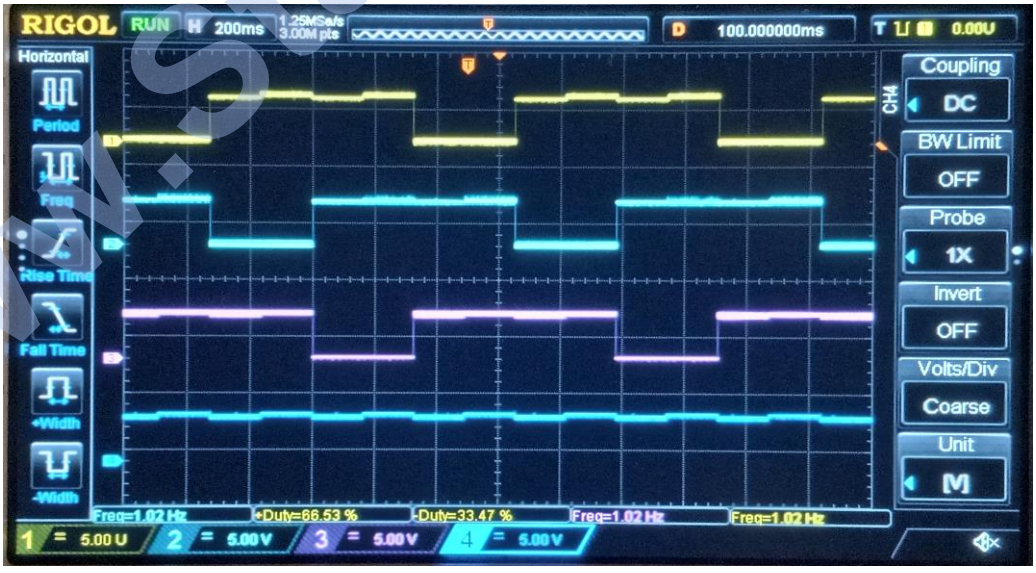

Figure 42 below, shows the inversion of each 74154 channel, after passing through the second hex inverter (74LS04-2). Channel 1 is connected to input pins #1 and #13. Channel 2 is connected to input pins #3 and #11. Channel 3 is connected to input pins #5 and #9. All inputs are at a LOW logic state. Output pins #8, #10 and #12 are connected to the anode of an LED through a series resistor of 220Ω. These LEDs provide visual indication of what channel is currently on when corresponding output is in a HIGH logic state. Each LED has a 20mA current through it [5v / 220Ω = 0.020A (20mA)].

Figure 42:

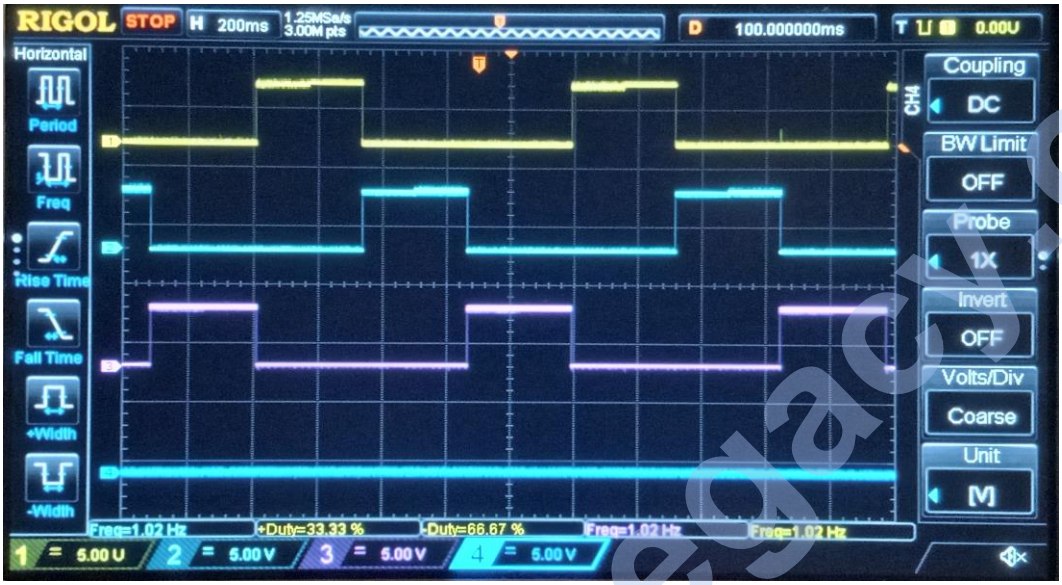

Figure 43 below shows the first LED illuminated, which represents output “0” (Pin #1) of the DMUX.

Figure 43:

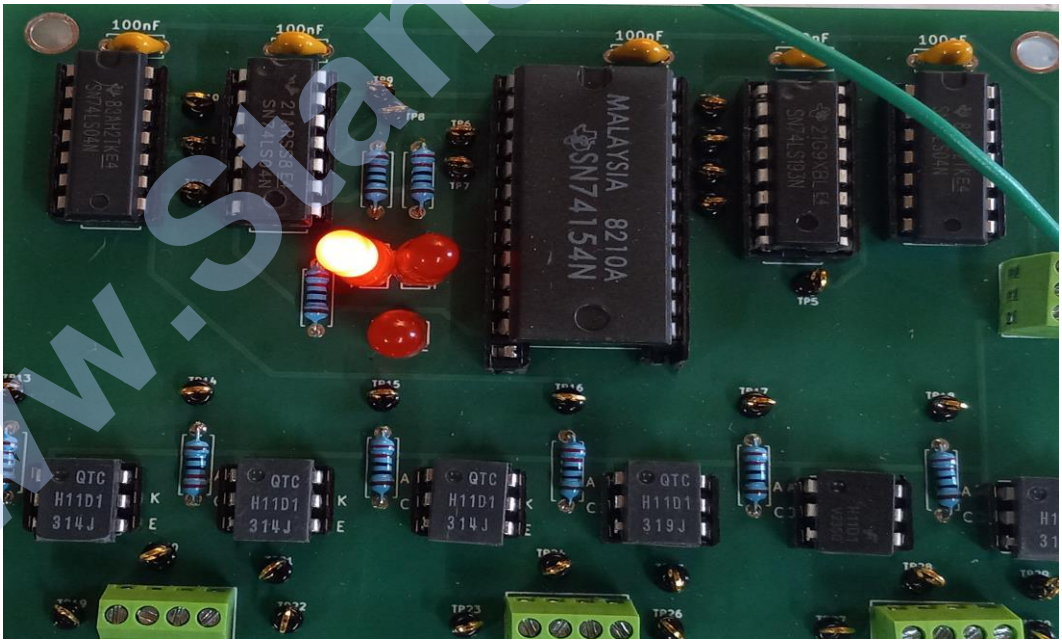

Figure 44 below shows the second LED illuminated, which represents output “1” (Pin #2) of the DMUX.

Figure 44:

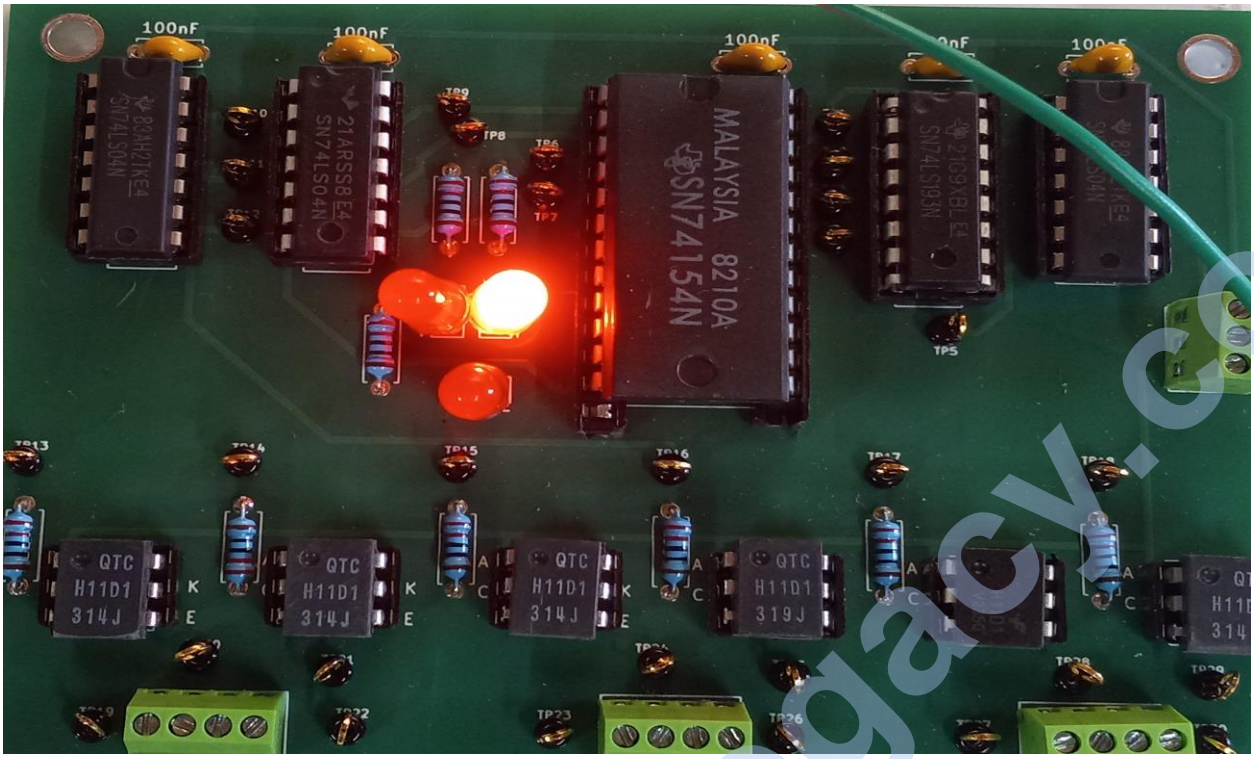

Figure 45 below shows the third LED illuminated, which represents output “2” (Pin #3) of the DMUX.

Figure 45:

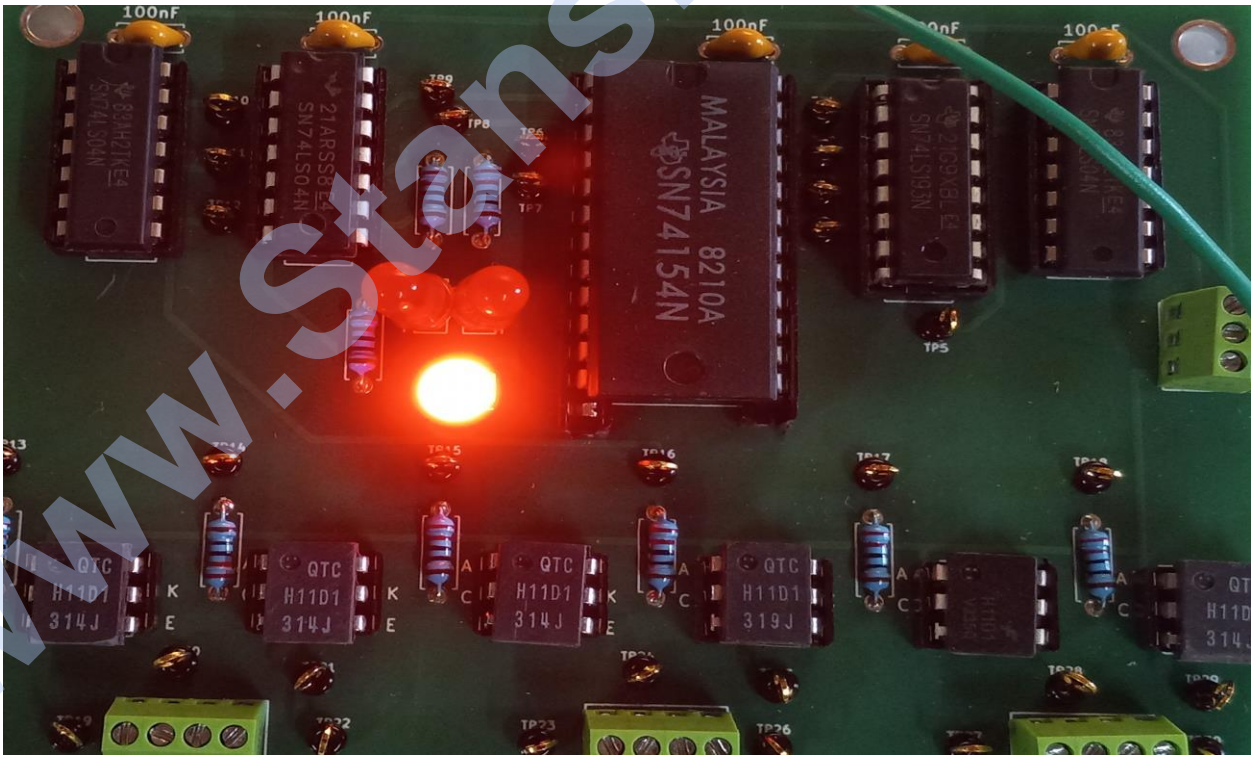

The second hex inverter, 74LS04-2, output pins: #2, #4, and #6 are connected to paired inputs on the third hex inverter 74LS04-3. Figure 46 below shows the waveforms communicated to each pair of H11D1 associated with outputs from this third hex inverter. Yellow trace shows sequence 1 (binary S0) which triggers H11D1-1 and H11D1-2 via 74LS04-3 output pins #2 and #4. Teal trace shows sequence 2 (binary S1) which triggers H11D1-3 and H11D1-4 via 74LS04-3 output pins #10 and #12. Magenta trace shows sequence 3 (binary S2) which triggers H11D1-5 and H11D1-6 via 74LS04-3 pins #6 and #8. A sequential order has been maintained.

Figure 46:

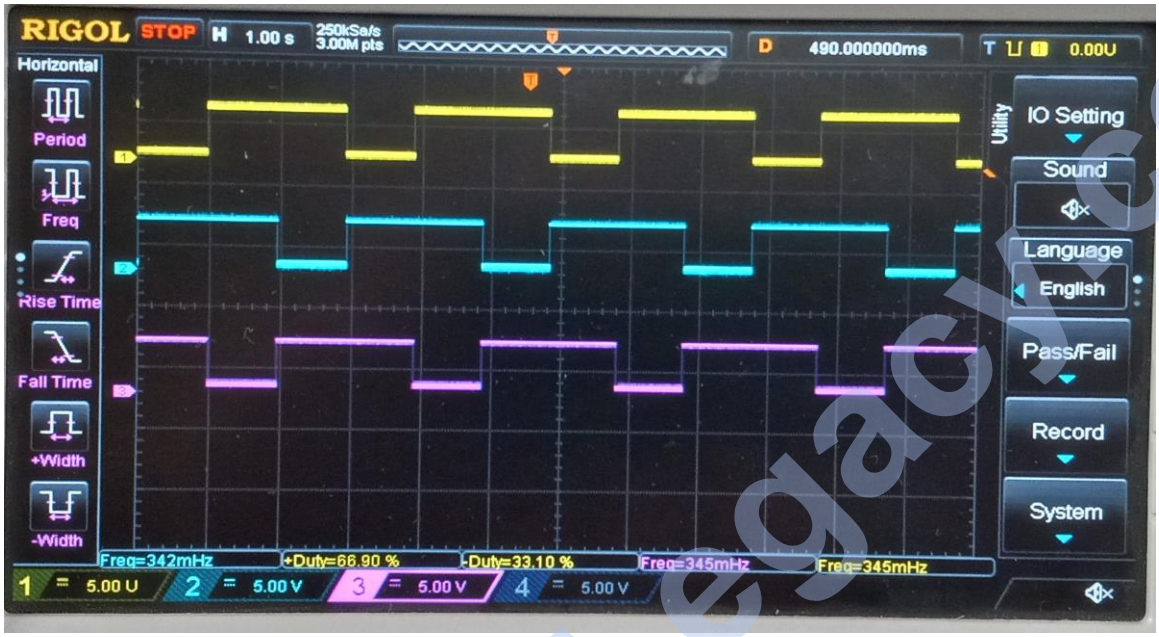

The output pins produce a LOW logic state. This LOW logic pulls down on the optocoupler cathode, turning on the internal LED. When outputs are in a HIGH logic state, the internal LED becomes reversed bias, thus keeping the LED off. The use of optocouplers provides isolation between the control circuitry and the optocoupler outputs. In simple terms, an optocoupler is a light triggered bipolar junction transistor (BJT). When the LED is turned on, the light sensitive base of the BJT causes the Collector/Emitter to come into conduction, performing the function of a switch. The amount of current conducted is related to the Current Transfer Ratio (CTR) of the optocoupler. This is similar to the gain of a regular BJT but measured as a ratio of the output current to the input current. For the H11D1, this is 20% on average. The collector and emitter of each optocoupler are connected to individual pins to allow external circuit connections. Table 4 below details the logic continuity from the DMUX, through the hex inverters, to the optocouplers:

Table 4:

DMUX Outputs	74LS04-2 Inputs	74LS04-2 Outputs	74LS04-3 Inputs	74LS04-3 Outputs	Optocouplers
CH1 - HIGH	#1 / #13 - HIGH	#2 / #12 - LOW	#1 / #3 - LOW	#2 / #4 - HIGH	H11D1-1 / H11D1-2 (OFF)
CH1 - LOW	#1 / #13 - LOW	#2 / #12 - HIGH	#1 / #3 - HIGH	#2 / #4 - LOW	H11D1-1 / H11D1-2 (ON)
CH2 - HIGH	#3 / #11 - HIGH	#4 / #10 - LOW	#11 / #13 - LOW	#10 / #12 - HIGH	H11D1-3 / H11D1-4 (OFF)
CH2 - LOW	#3 / #11 - LOW	#4 / #10 - HIGH	#11 / #13 - HIGH	#10 / #12 - LOW	H11D1-3 / H11D1-4 (ON)
CH3 - HIGH	#5 / #9 - HIGH	#6 / #8 - LOW	#5 / #9 - LOW	#6 / #8 - HIGH	H11D1-5 / H11D1-6 (OFF)
CH3 - LOW	#5 / #9 - LOW	#6 / #8 - HIGH	#5 / #9 - HIGH	#6 / #8 - LOW	H11D1-5 / H11D1-6 (ON)

Figure 47: (Logical Flow Phase 1):

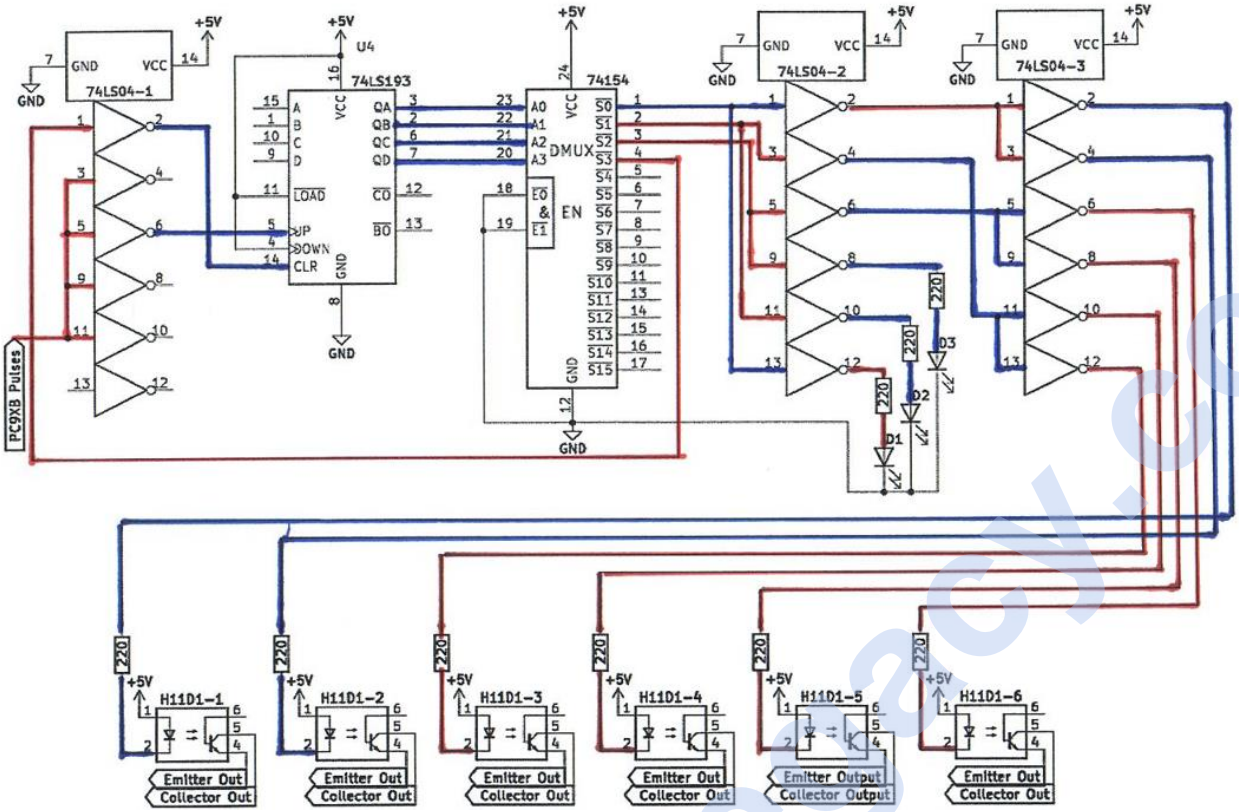

Figure 48: (Logical Flow – Phase 2):

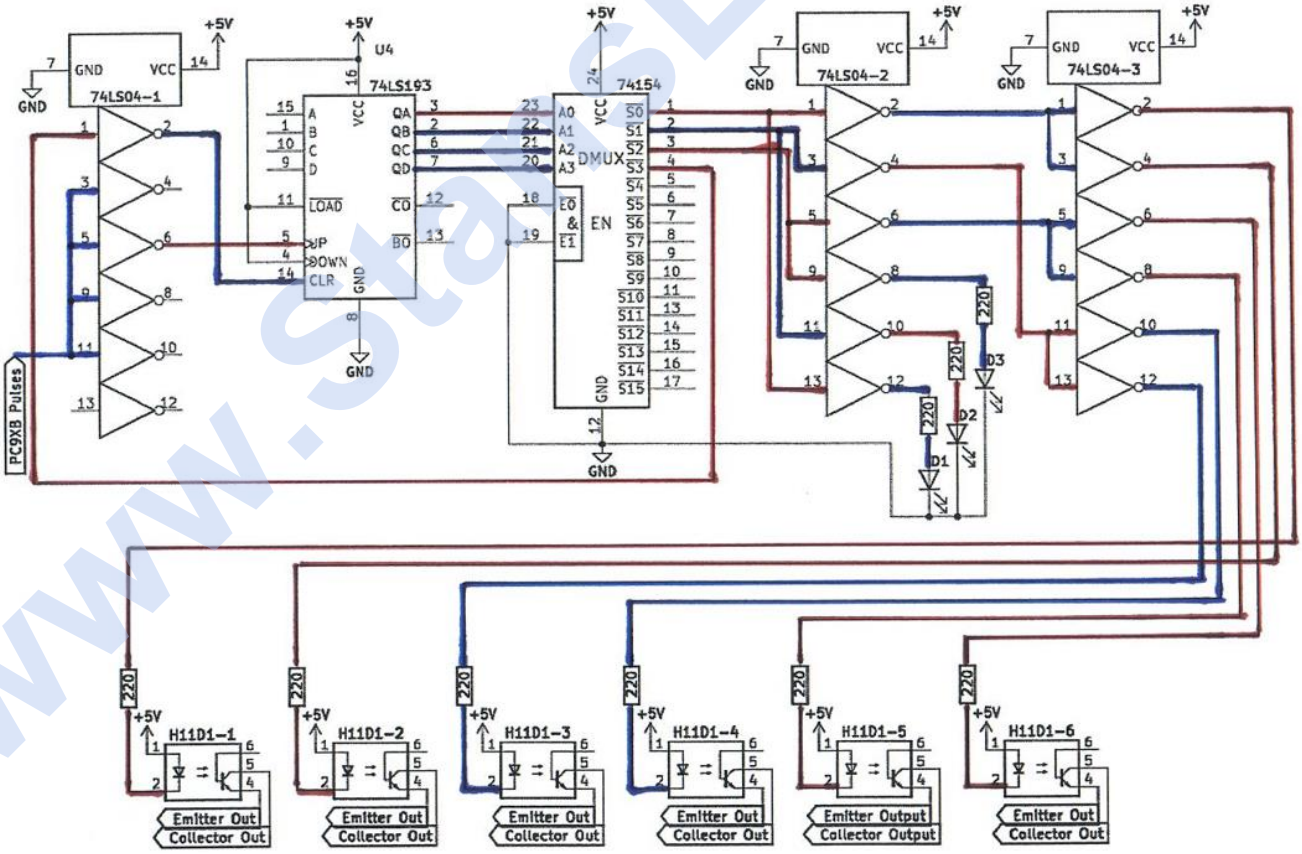

Figure 49: (Logical Flow – Phase 3):

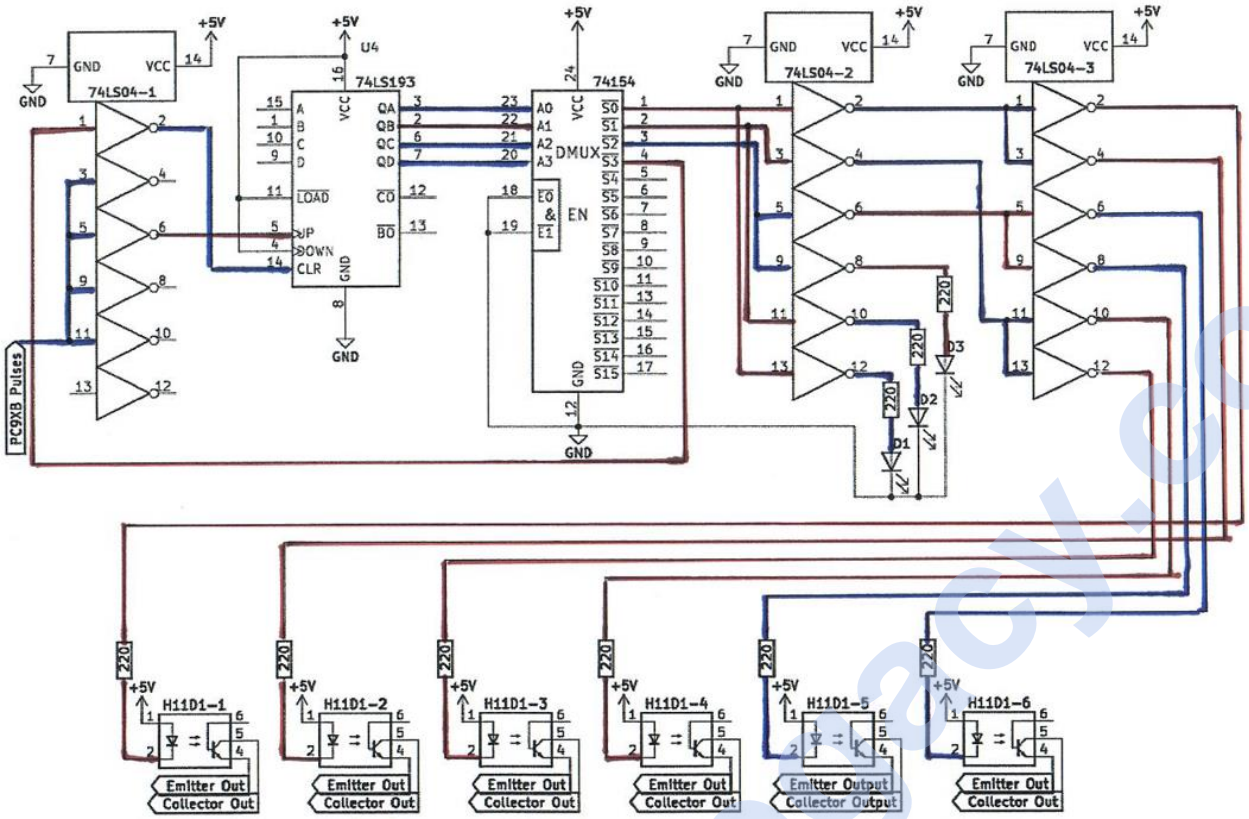

Figure 50: (Logical Flow – Phase 4):

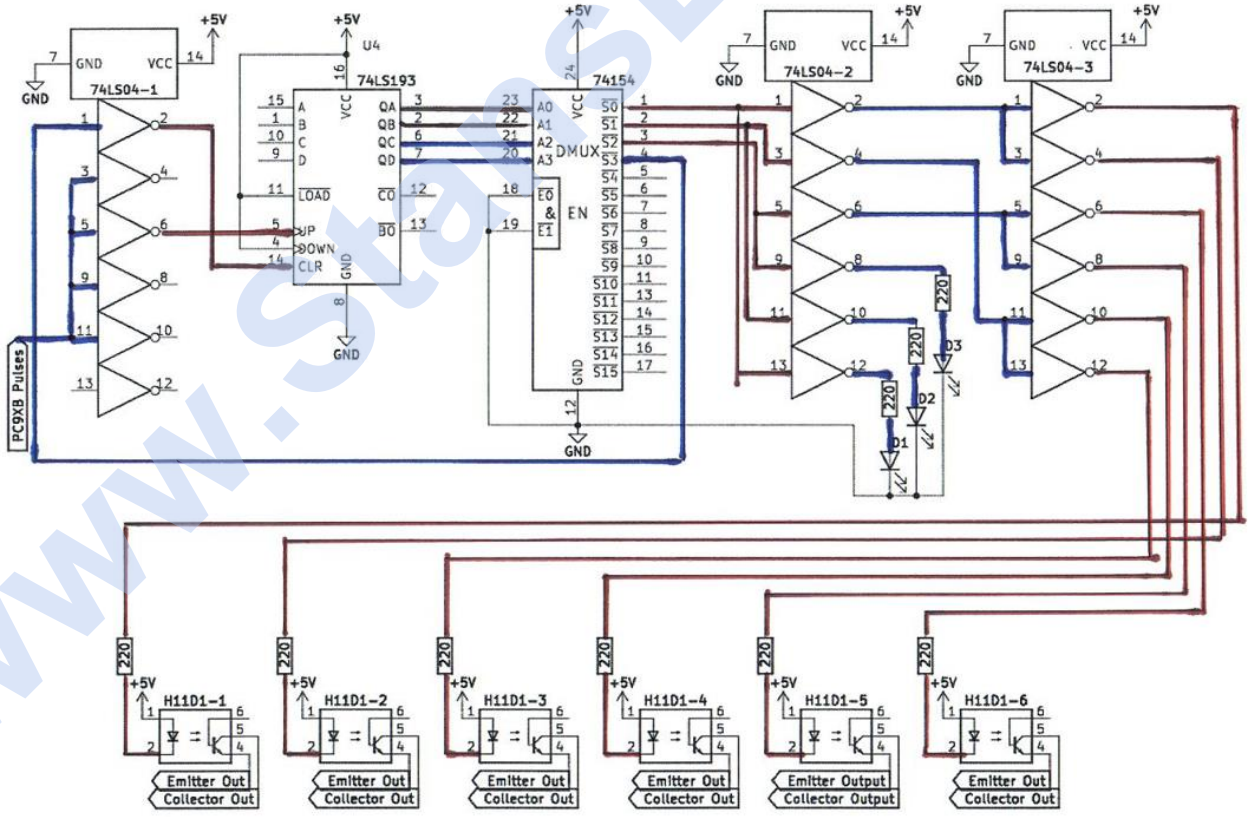

Section Eight: 20YJJ2 - Light Injector Module

The light injector module was a circular PCB composed of forty-one 5mm LEDs with 220Ω-1/4watt current limiting resistors. During Stan's era of development, LEDs had colored lenses which provided a diffused form of light. In the early 1980s, the colors available were red, amber and limited versions of green. Blue LEDs weren't available until late the 1980s. Throughout his technology, only red colored LEDs are referenced.

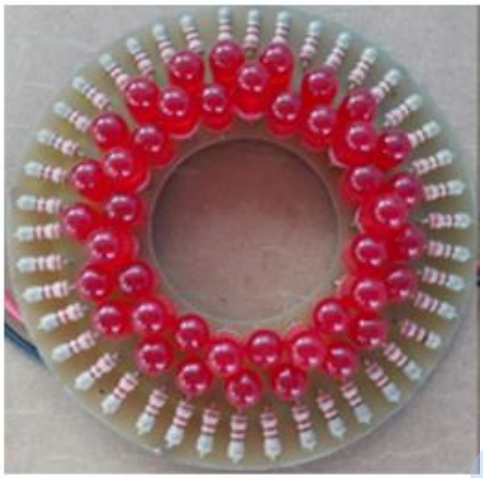

Transferring light energy was accomplished via a clear acrylic lens piece. The CAD model below outlines the various sections. Being recessed inside each resonant cavity, exposed to water continuously, O-rings are provided for sealing. This protects the PCB from short circuiting. A recession is provided for both a lens of a desired color and the LED PCB. Machining tolerances are such that the outer electrode, which extends through the center, are pressed-fit to ensure stability. Connection to the outer electrode is provided via the terminal through-hole. Stan's literature does not reference any machining that would've provided focusing capability of the diffused light into individual coherent beams.

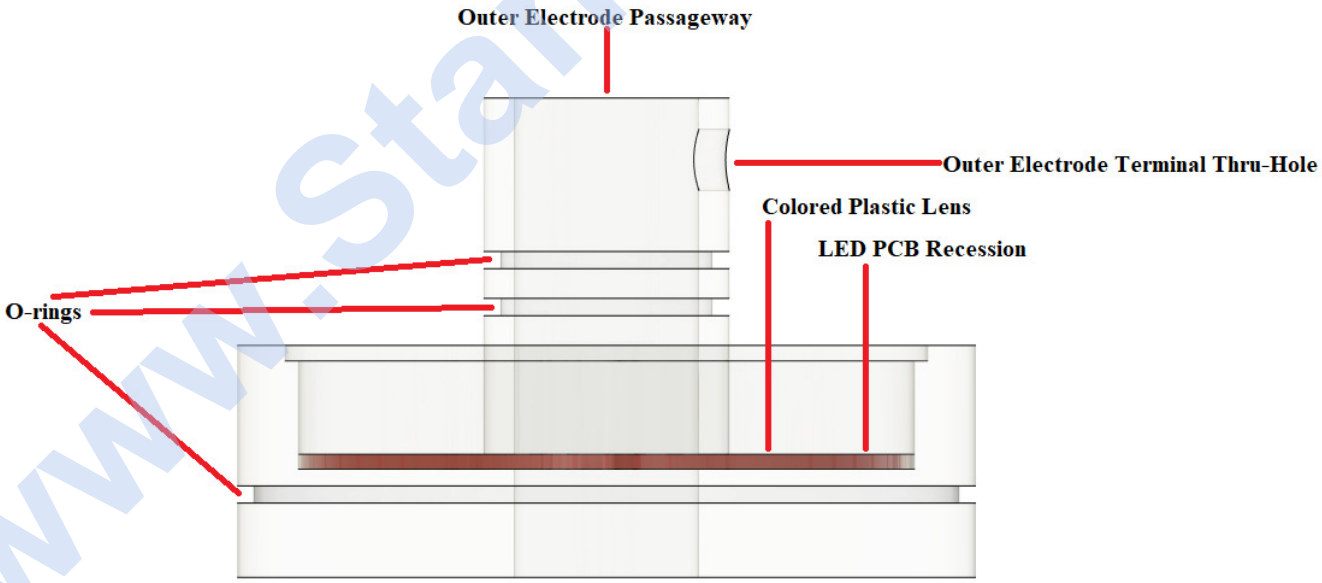

Red LEDs had a forward voltage of 1.7v with a maximum current rating of 20mA (0.020A). With forty-one LEDs, all in parallel, the total current draw would be 820mA (0.820A). The original schematic, shown below, shows a power NPN-BJT driving multiple module boards from a rectified step-down supply. Utilizing a step-down provides a train of unipolar-positive pulses with a fixed frequency of 120Hz. The optocoupler provides a gating frequency, determined by the frequency of pulses fed to it. An N-channel MOSFET could replace the BJT. This circuit could've also driven the LEDs mounted on the Gas Resonant Cavity (Hydrogen Gas Gun).

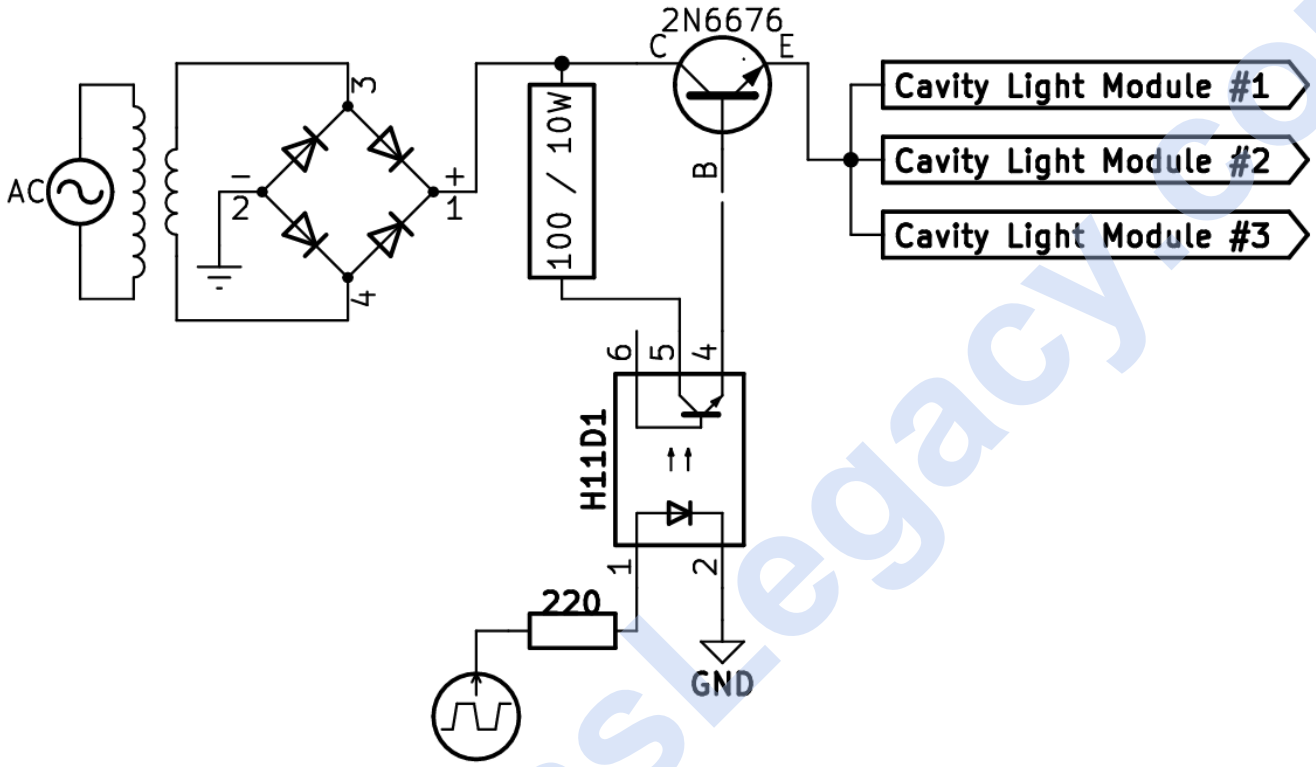

Intensity of the light was dictated by the amount of current supplied to the LEDs. The formula within the Birth of New Technology, (Memo WFC 420, page 1-9) provides the relationship between current and duty cycle time of pulses:

$$Le\sqrt{\frac{(I_{on})^2\,T_1}{T_1+T_2}}$$

Where:

L_e is the light intensity in watt

T_1 is duty-cycle (current) ON-time

T_2 is duty-cycle (current) OFF-time

I_{on} is RMS value of load current during ON-time period

Section Nine: 20JX - Gas Resonant Cavity

(Source: photo courtesy Don Gabel)

Objective:

To stimulate combustible gases into critical-state prior to gas thermal ignition.

Source of Combustible Gases:

Combustible gases expelled from the fuel cell, enter into and pass through a gas resonant cavity. The combustible gas mixture is composed of hydrogen, oxygen and ambient air gases. The hydrogen gas provides the thermal explosive force (gtnt), the oxygen retards the gas thermal ignition process to a controllable state.

Voltage Stimulation Process:

Opposite electrical voltage zones form on either side of the moving combustible gas mixture as it travels through the tubular structure (20JX). When exposed to a pulsating voltage that increases via VIC, the gas atoms become ionized (gain or lose electrons), altering their electrical and mass balance. Gases that don't ionize may capture free electrons when exposed to light or photon stimulation. The VIC limits current flow, preventing electron replacement and pushing the gas ions towards a critical state. The repetitive voltage pulse train keeps the gas ions in a critical state by continually attracting more negatively charged electrons to the positive electrode, while the positively charged nuclei of the gas atoms move toward the negative electrode.

Photon Injection:

As gas atoms are elongated by electron removal, laser light of a specific frequency is introduced into the gas ionization process. This laser energy destabilizes the gas ions further by increasing the energy of the gas nuclei, causing electrons to move to higher energy levels and aiding in their ejection. The laser pulsing circuit (LEDs on the Hydrogen Gas Gun) channels light energy through an optical lens into the voltage chamber. This process of injecting laser energy into the gas ionization is known as "The Atomic Polarization Process."

Triggering Atomic Yield of Water:

Charged and laser-excited combustible gas ions from the Gas Resonant Cavity (20JX) enter a quenching disc assembly and are pressurized during spark ignition. The unstable hydrogen and oxygen atoms release excess thermal energy. Ambient air assists this explosive reaction under controlled conditions. Atomic energy is maximized when an electron-deficient oxygen atom captures an electron from a hydrogen atom before or during the combustion process.

Electron Extraction:

To enhance the capture of liberated electrons during hydrogen fracturing, an electron extractor grid is placed above the gas resonant cavity. This grid is connected to an electrical circuit that directs the electrons to a load, such as a light bulb, when a positive voltage is applied. When the positive voltage is switched on or pulsed, the freed electrons are pulled from the gas cavity into the light bulb. The electrons flow through the bulb, causing it to consume current and produce heat through energy transformation.

To prevent electron oscillation or deflection during hydrogen fracturing, the electrical circuit is connected directly to the positive electrode. The positive waveform, synchronized with the pulse train via a blocking diode and alternating gate circuit (see PC9XC section), directs electron flow to the electrical load. The resistive element wire helps prevent voltage leakage while the circuit is on. The electron extraction process is maintained by adjusting the trigger pulse in proportion to the applied voltage, accommodating varying gas flow rates. This process also prevents spark ignition of combustible gases in the gas resonant cavity by preventing electron buildup.

Voltage Level Switching:

To vary or change applied voltage level to the gas resonant cavity assembly by means of solid-state switching, a toroidal pulsing transformer is used in place of variable isolation transformer - adding more secondary pickup windings to provide a greater SCR switching range - reference back to Figure () schematic. In the PCB shown below, as the circuit details, the SCR selection is isolated via the H11D1 optocouplers. The 2N6403 SCRs are rated 800V/16A.

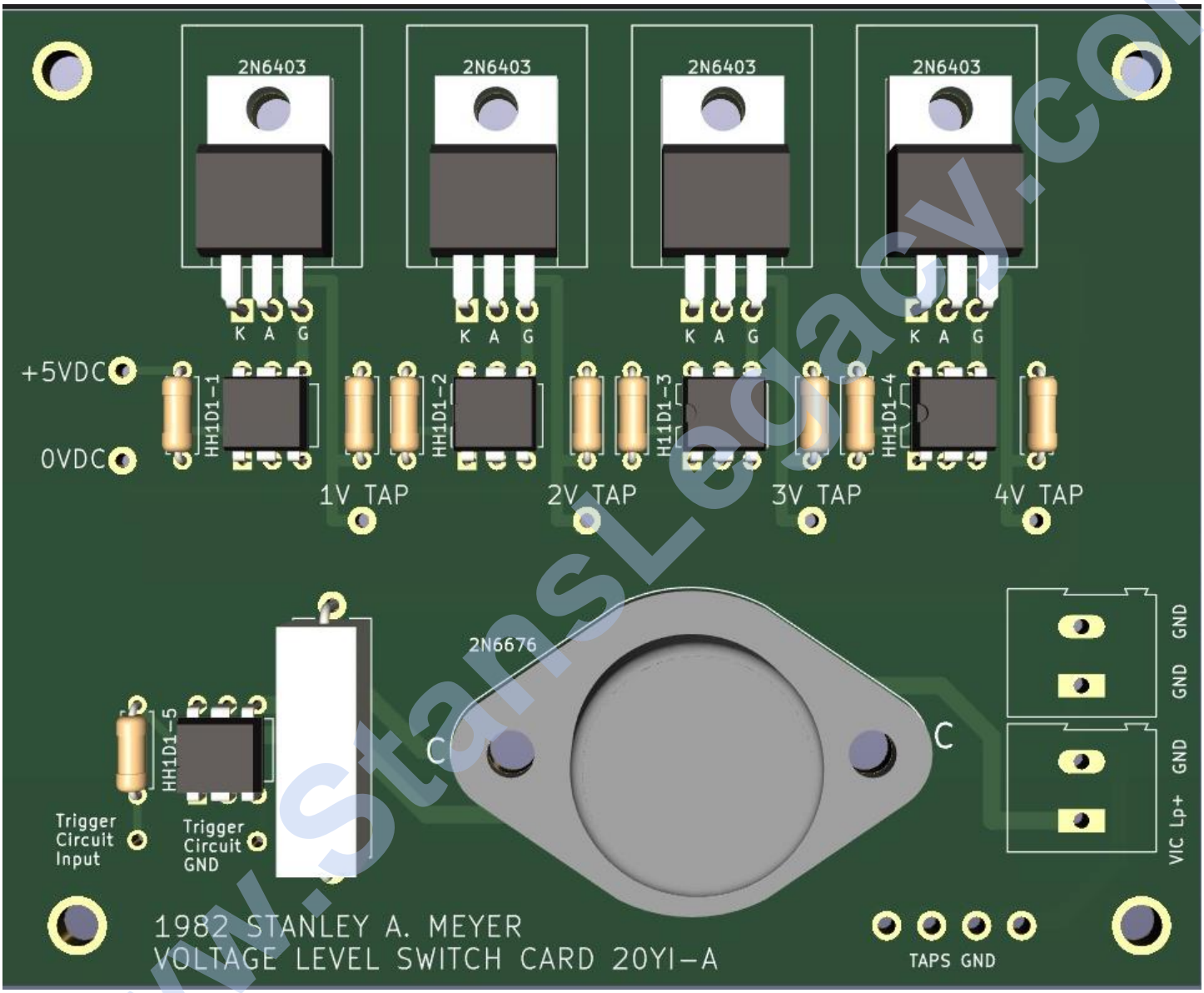

Section Ten: Water Tank

The water tank simply provides a reservoir of water that utilizes gravity to replenish resonant cavities during operation. The CAD model below details the operation.

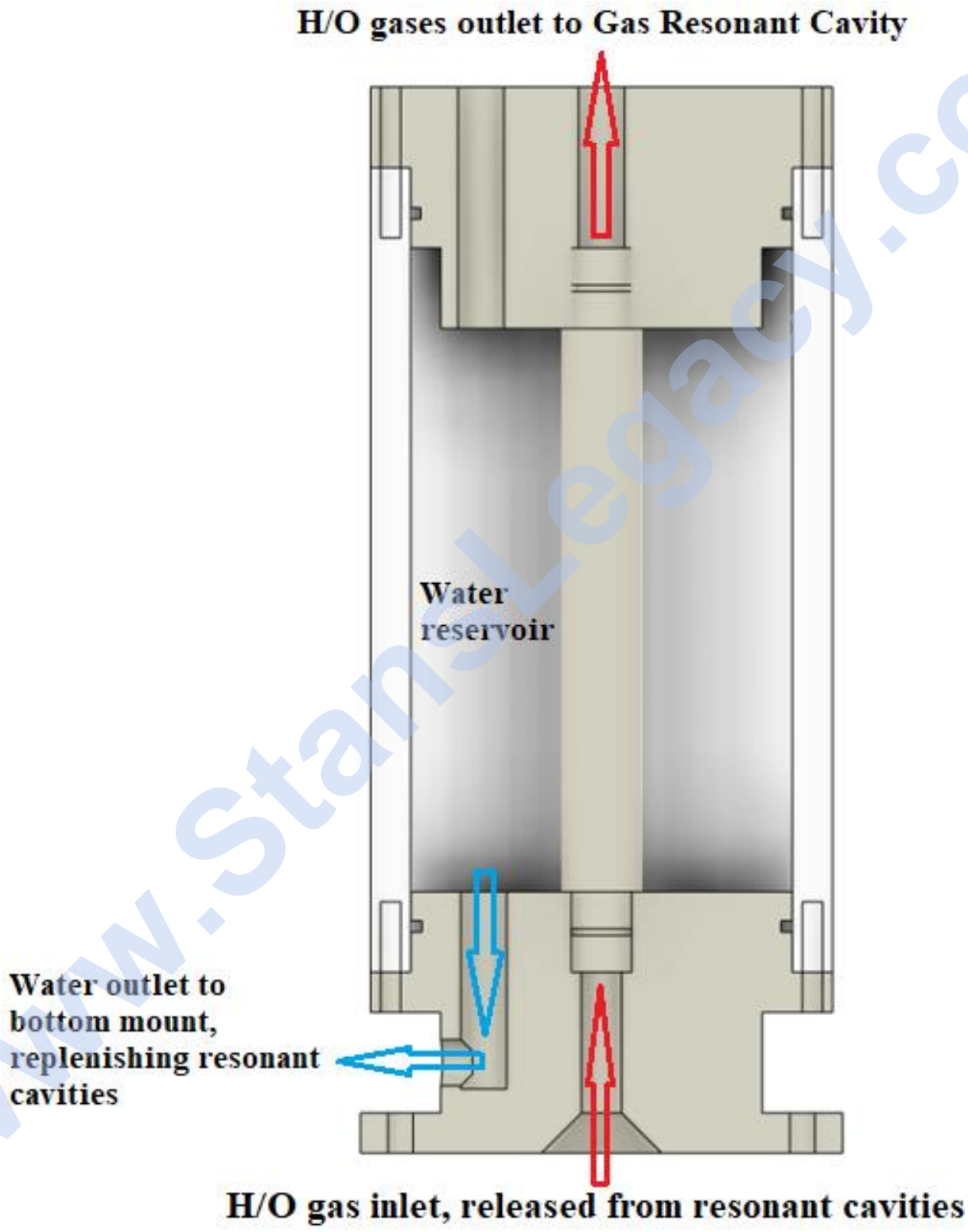

APPENDIX A: Gas Resonant Cavity Dimensions

VIC Bobbin Part A:

Half of VIC bobbin, measuring 0.25” in thickness.

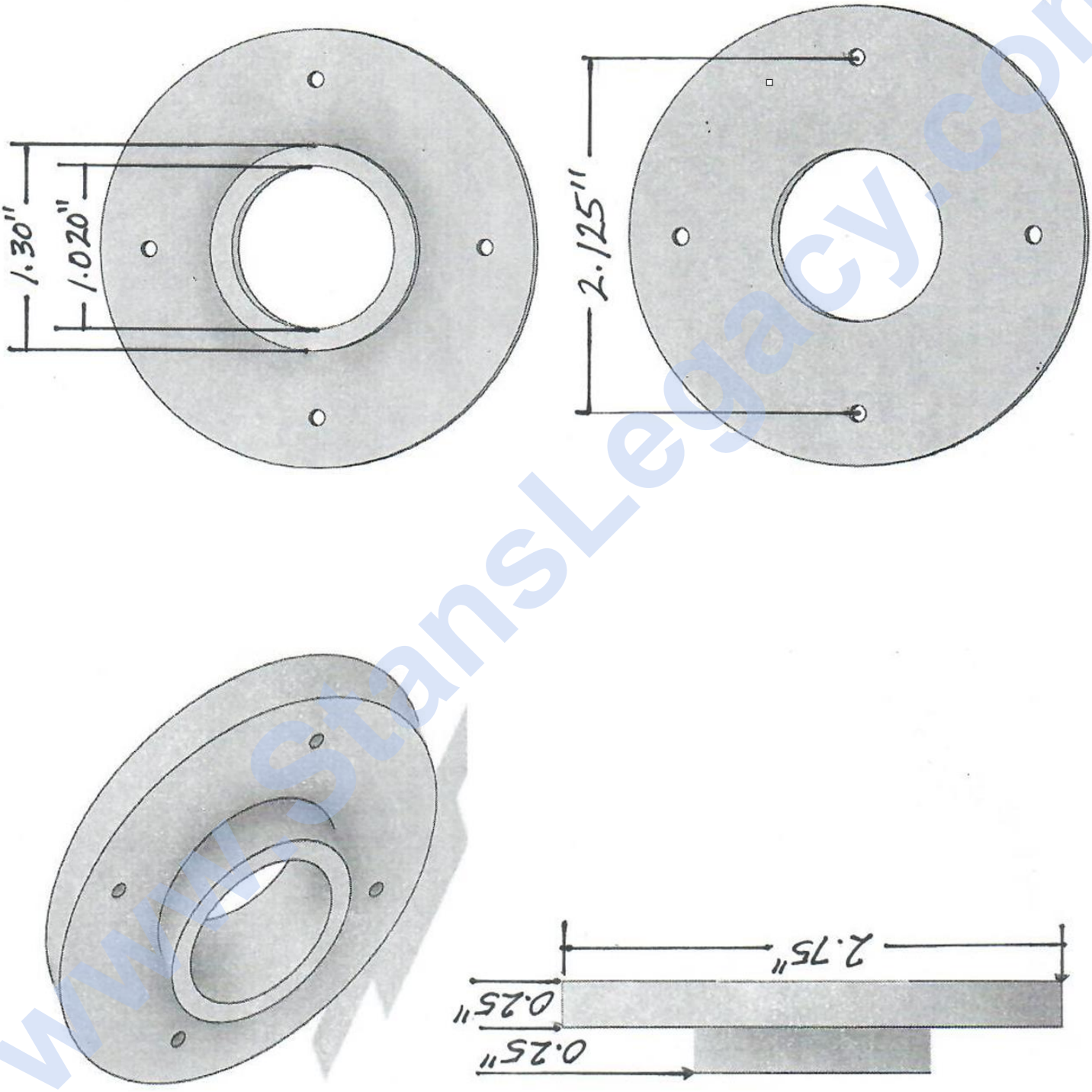

VIC Bobbin Part B:

Half of VIC bobbin, measuring 0.125” in thickness.

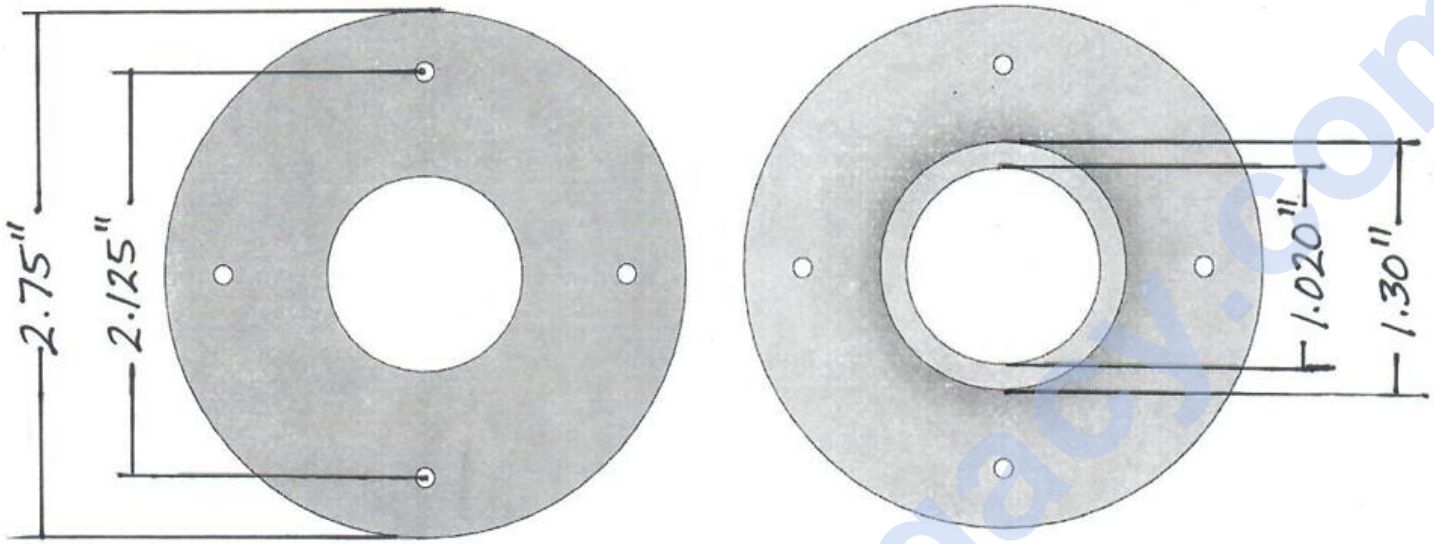

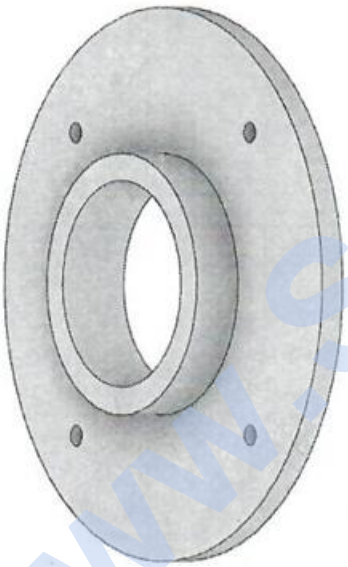

VIC Bobbin Part C:

Half of VIC bobbin, measuring 0.0625” in thickness. Attaches to LED body piece.

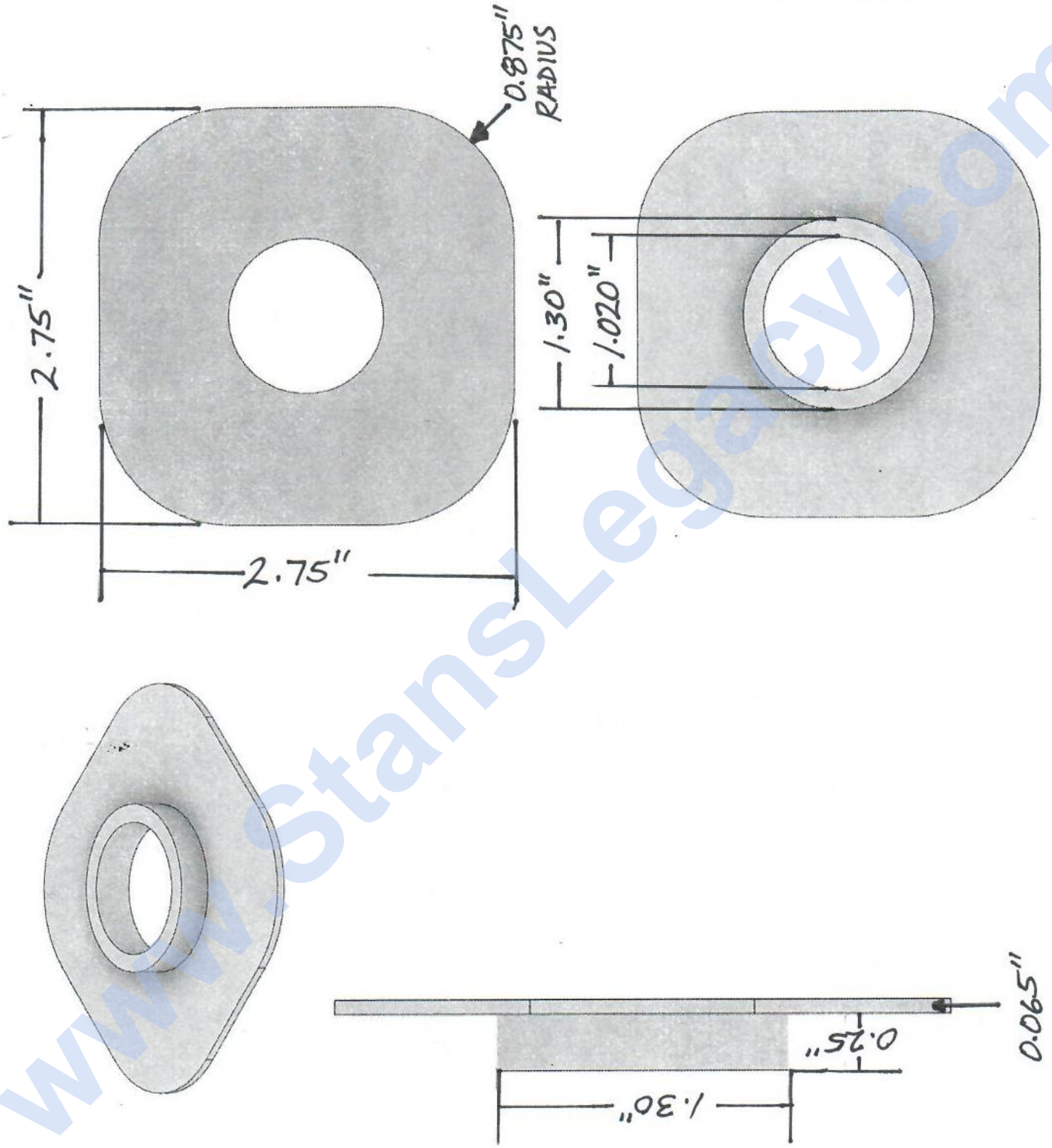

16 LED PCB:

Mounts to LED Body inside the 0.25” grooves.

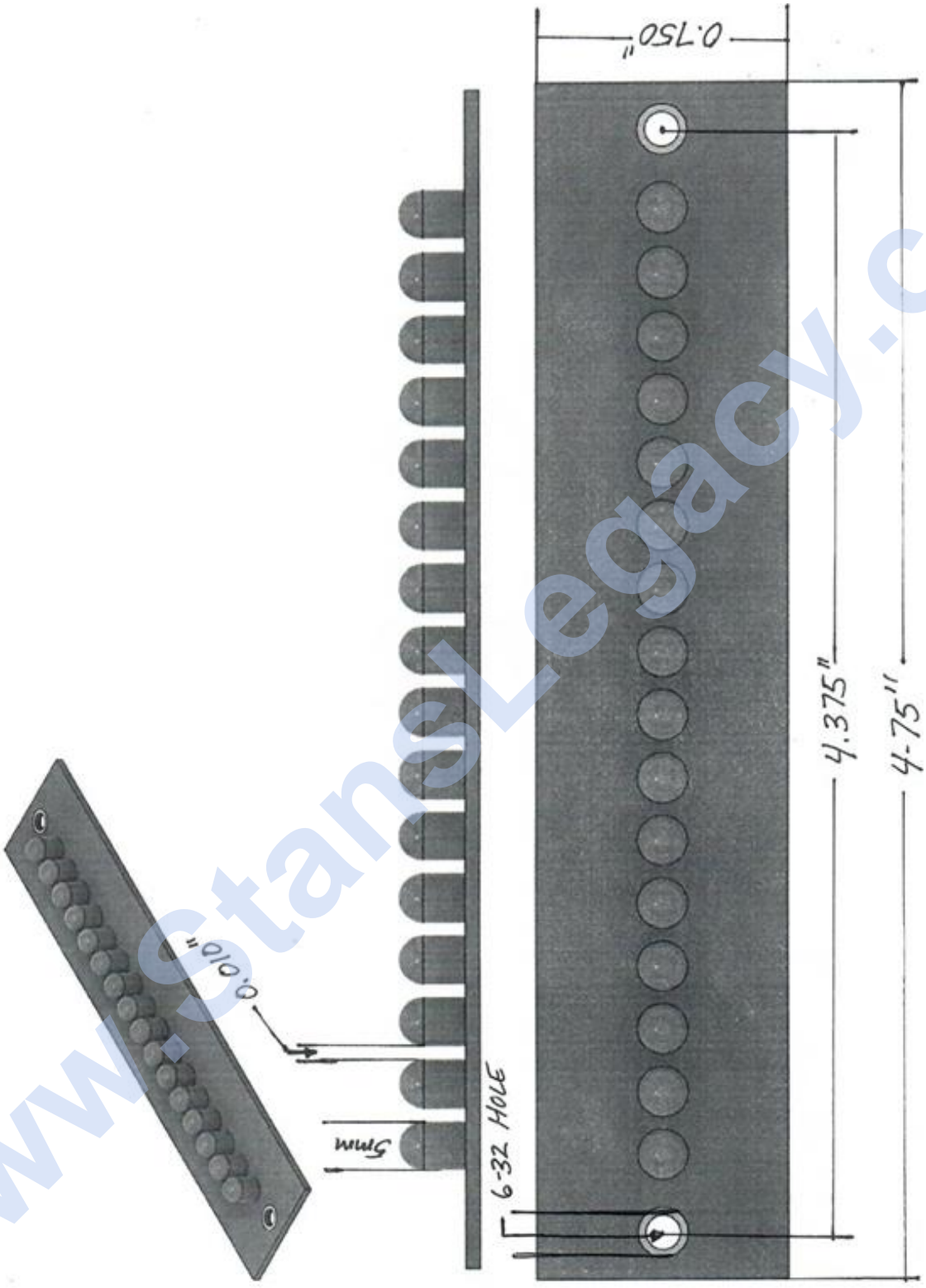

Acrylic Lens:

Clear acrylic cylinder that acts a lens to transfer the LED light to the space between the inner and outer electrodes. For economy, a rubber mold may be made and liquid acrylic casting produced.

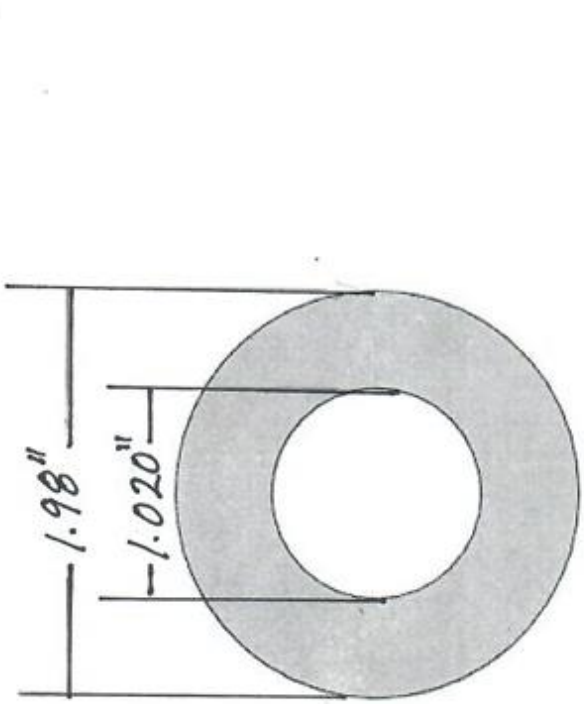

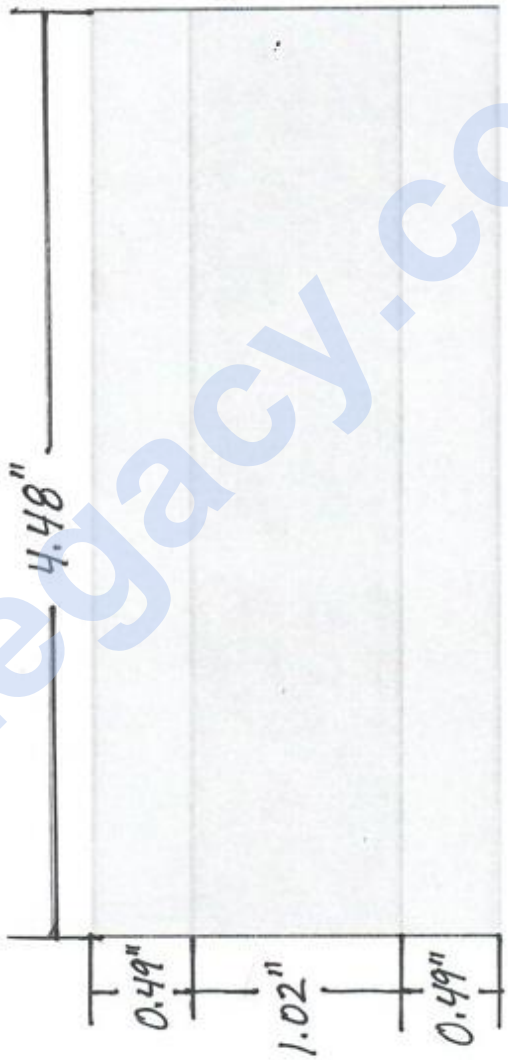

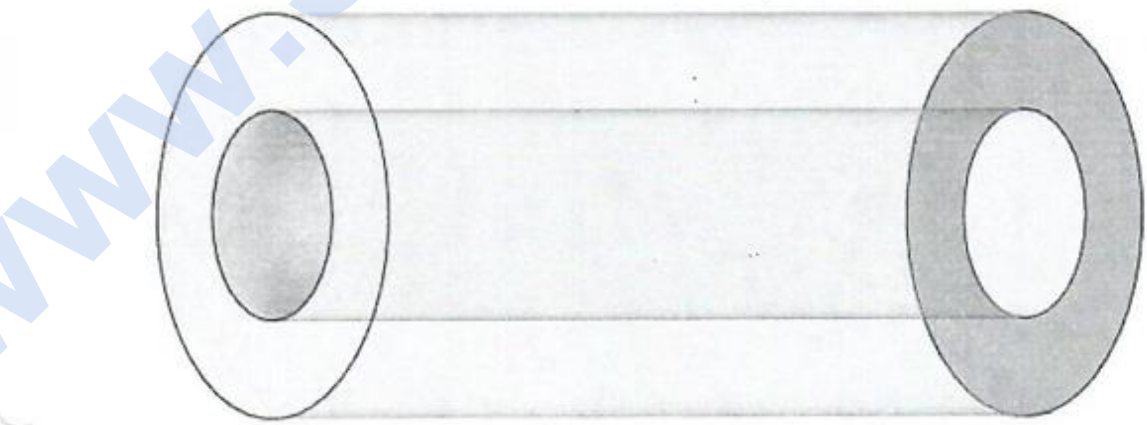

LED Body Part A – View 1:

Top part of LED body.

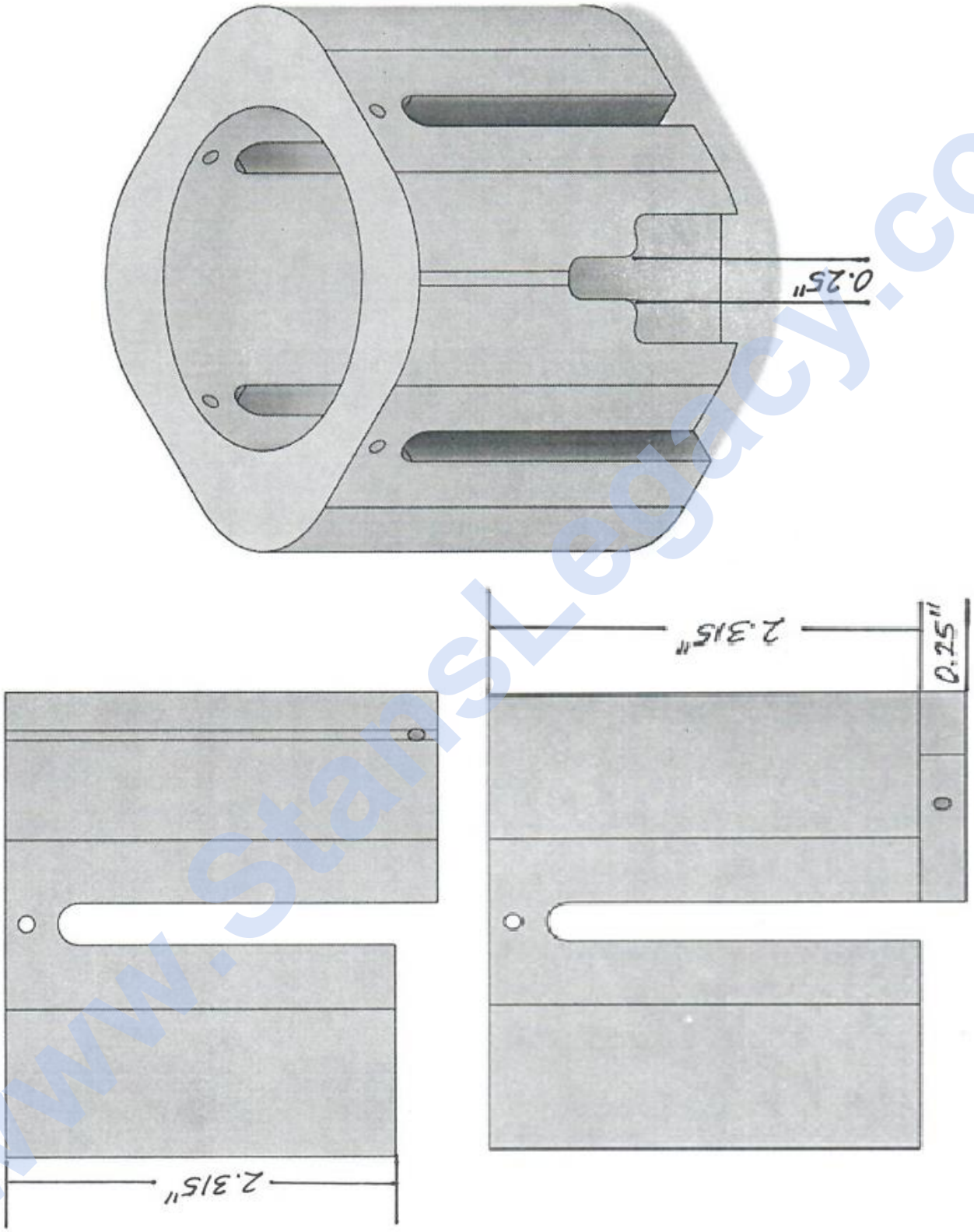

LED Body Part A – View 2:

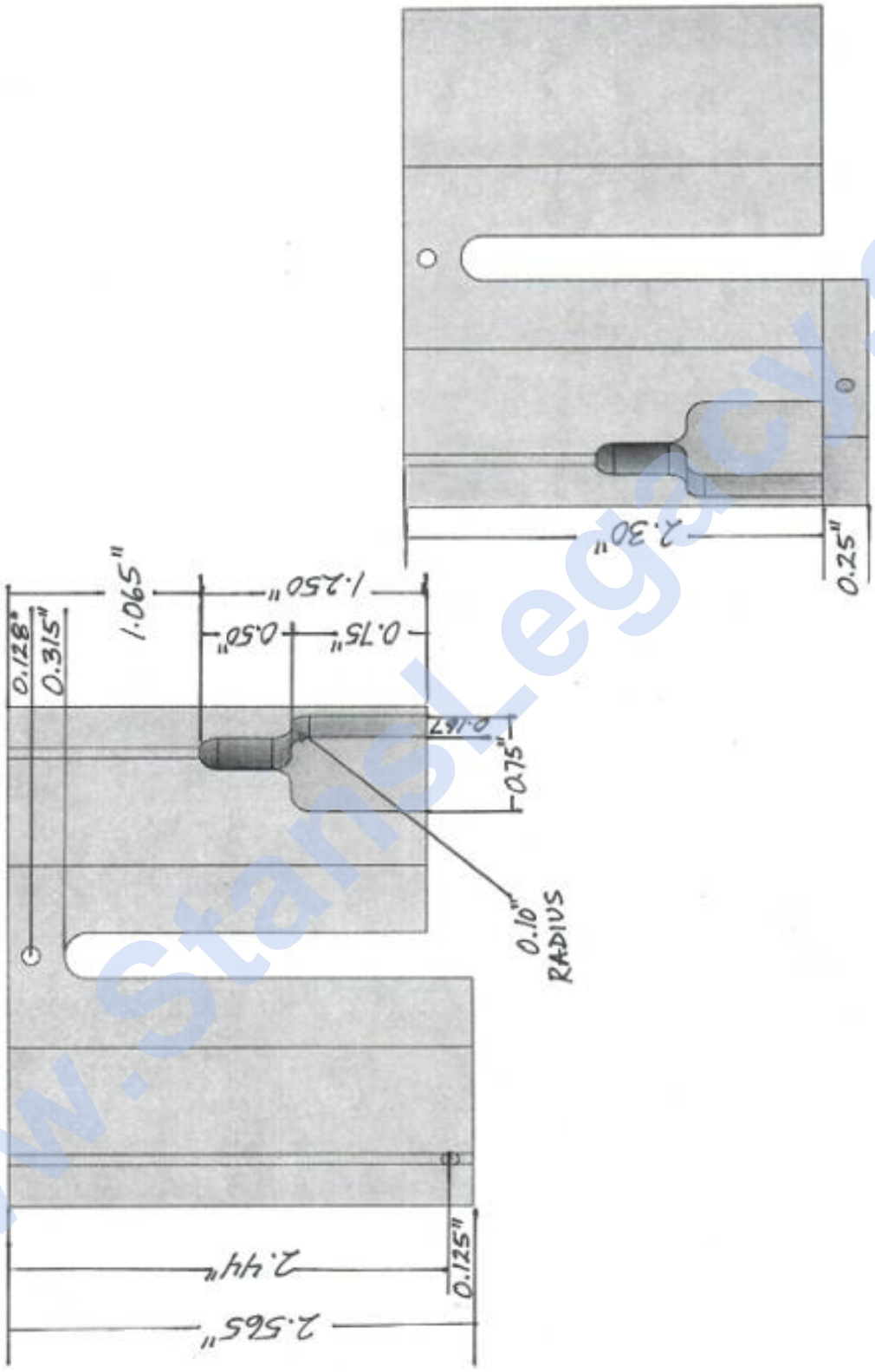

LED Body Part A – View 3:

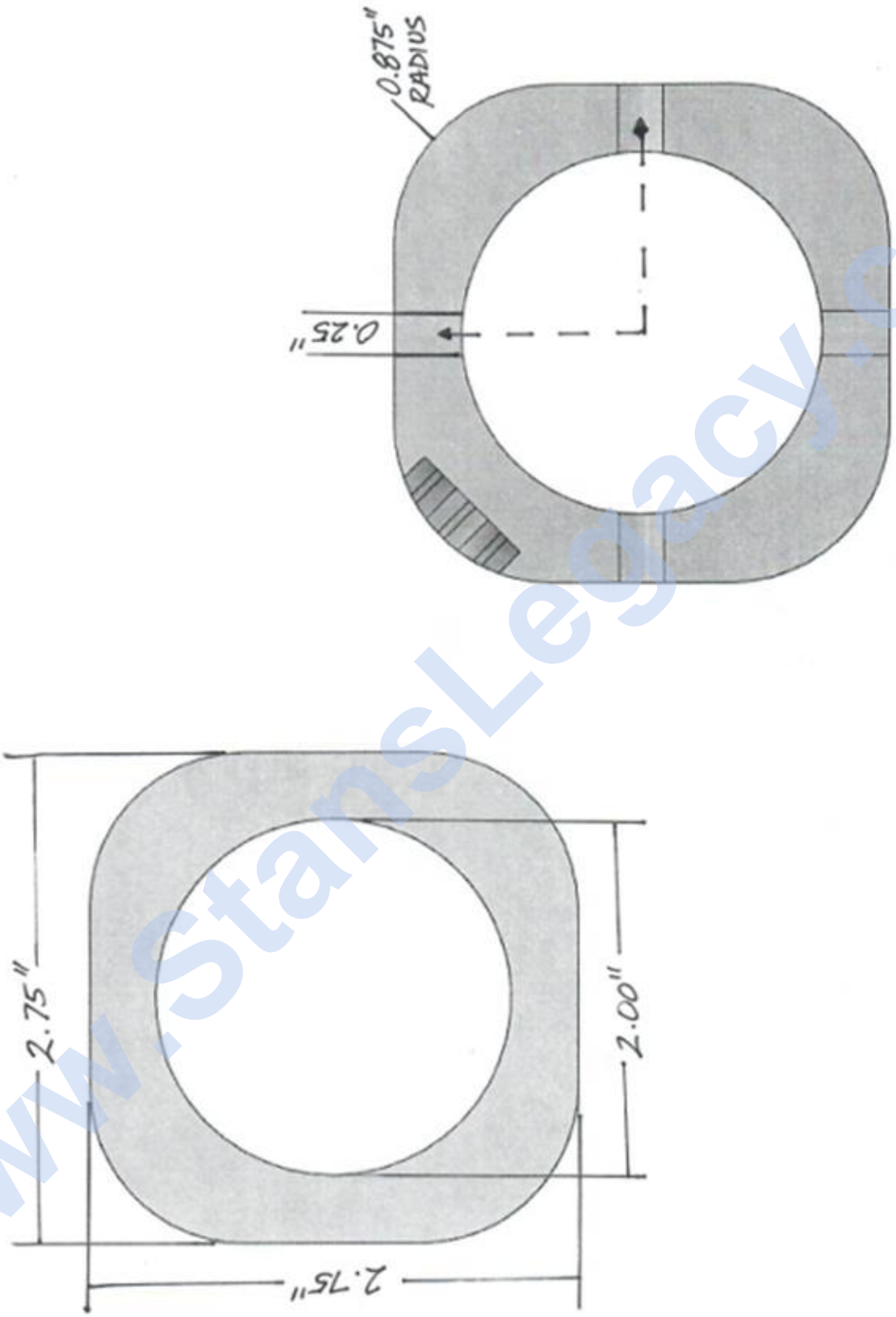

LED Body Part B – View 1:

Bottom part of LED body.

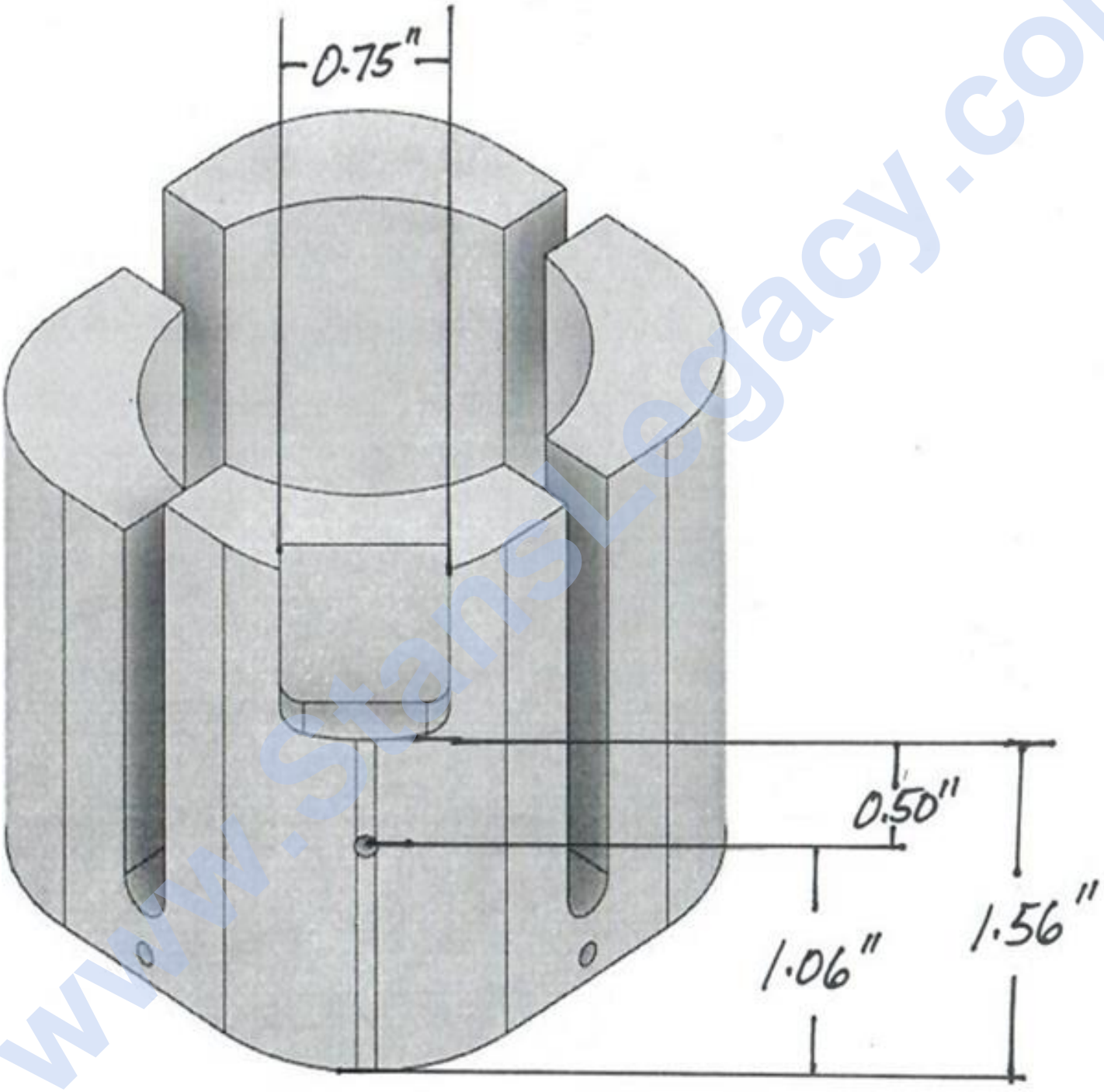

LED Body Part B – View 2:

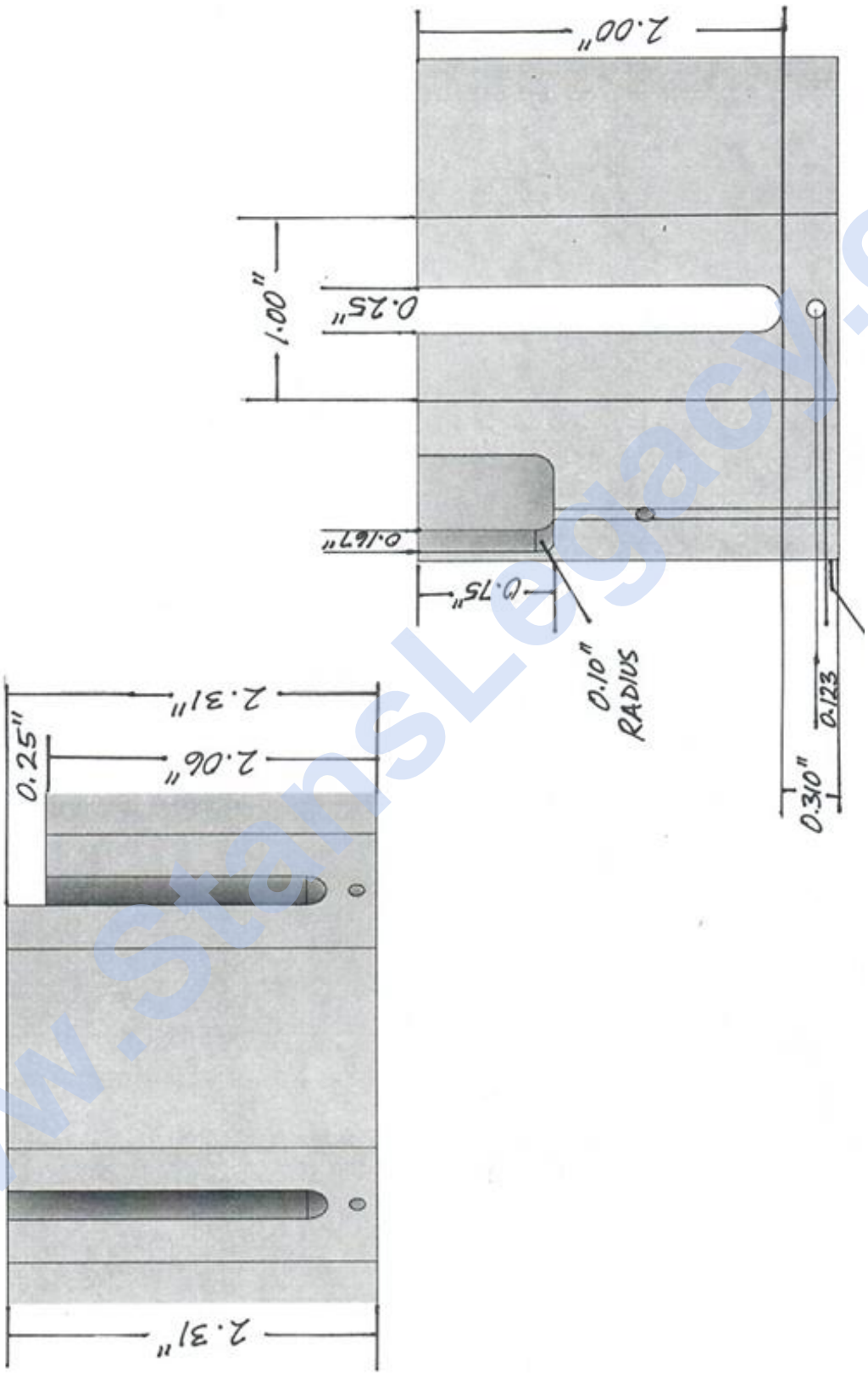

LED Body Part B – View 3:

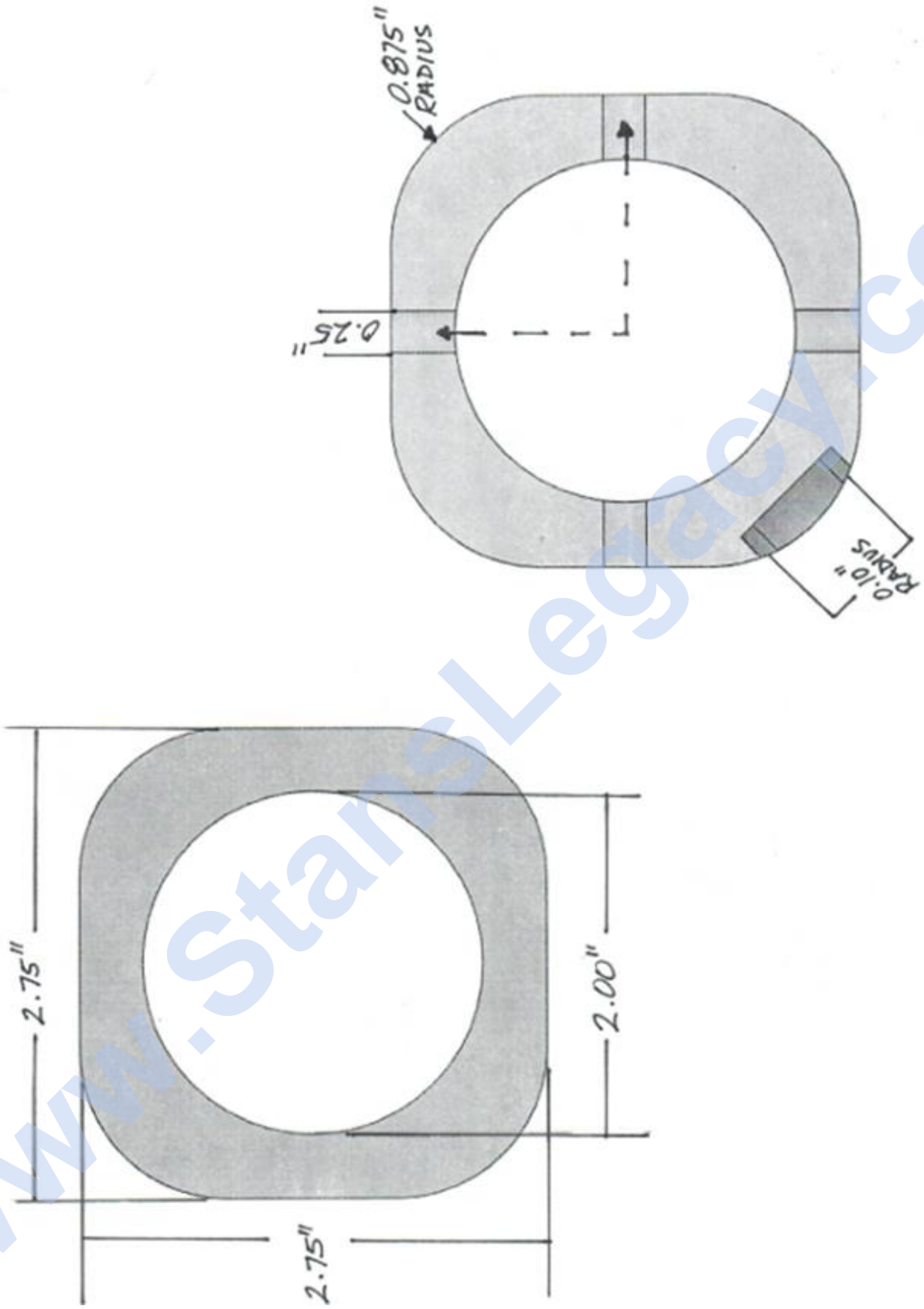

Inside Bottom Cap – View 1:

Bottom of inside cap

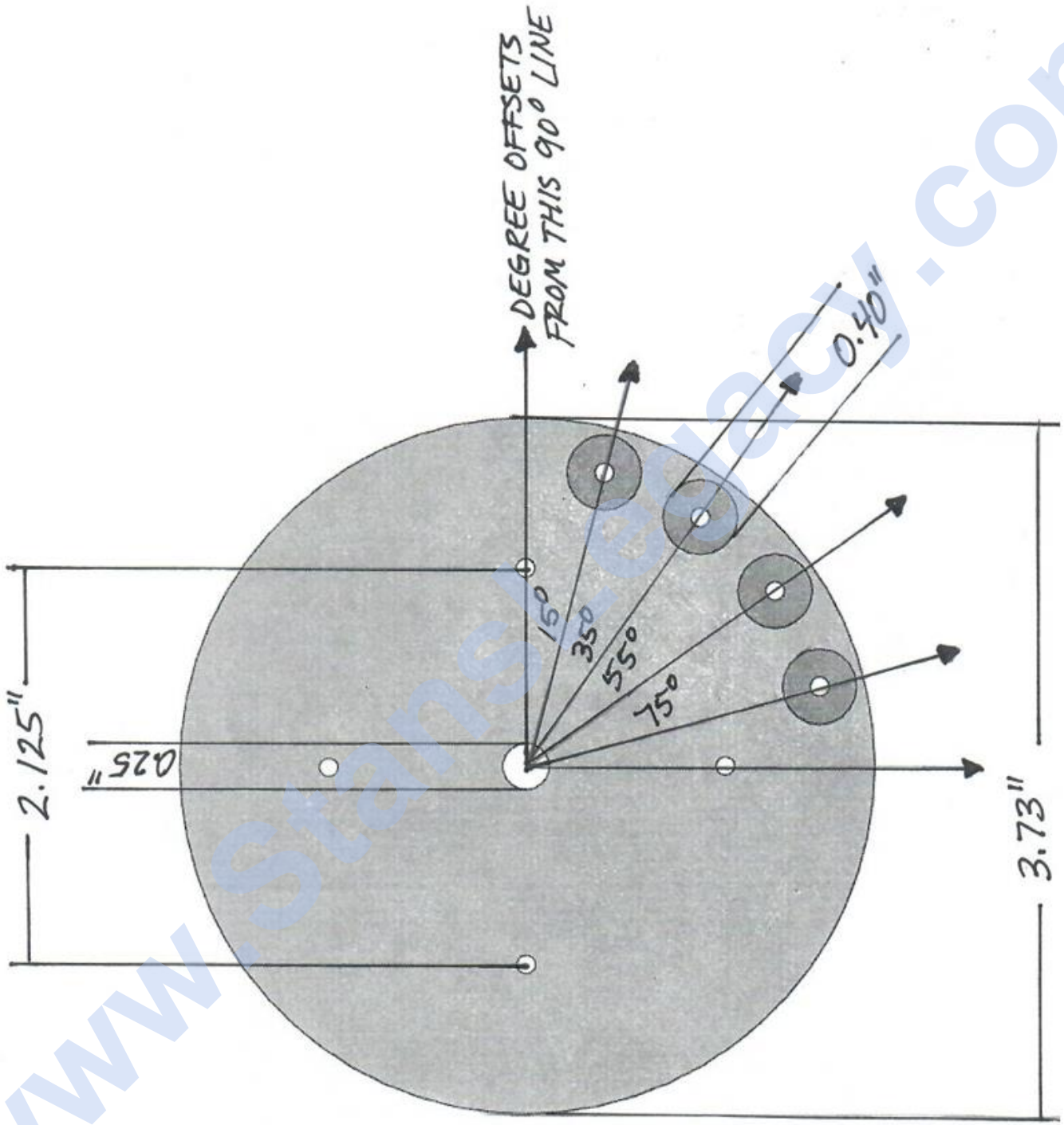

Inside Bottom Cap – View 2:

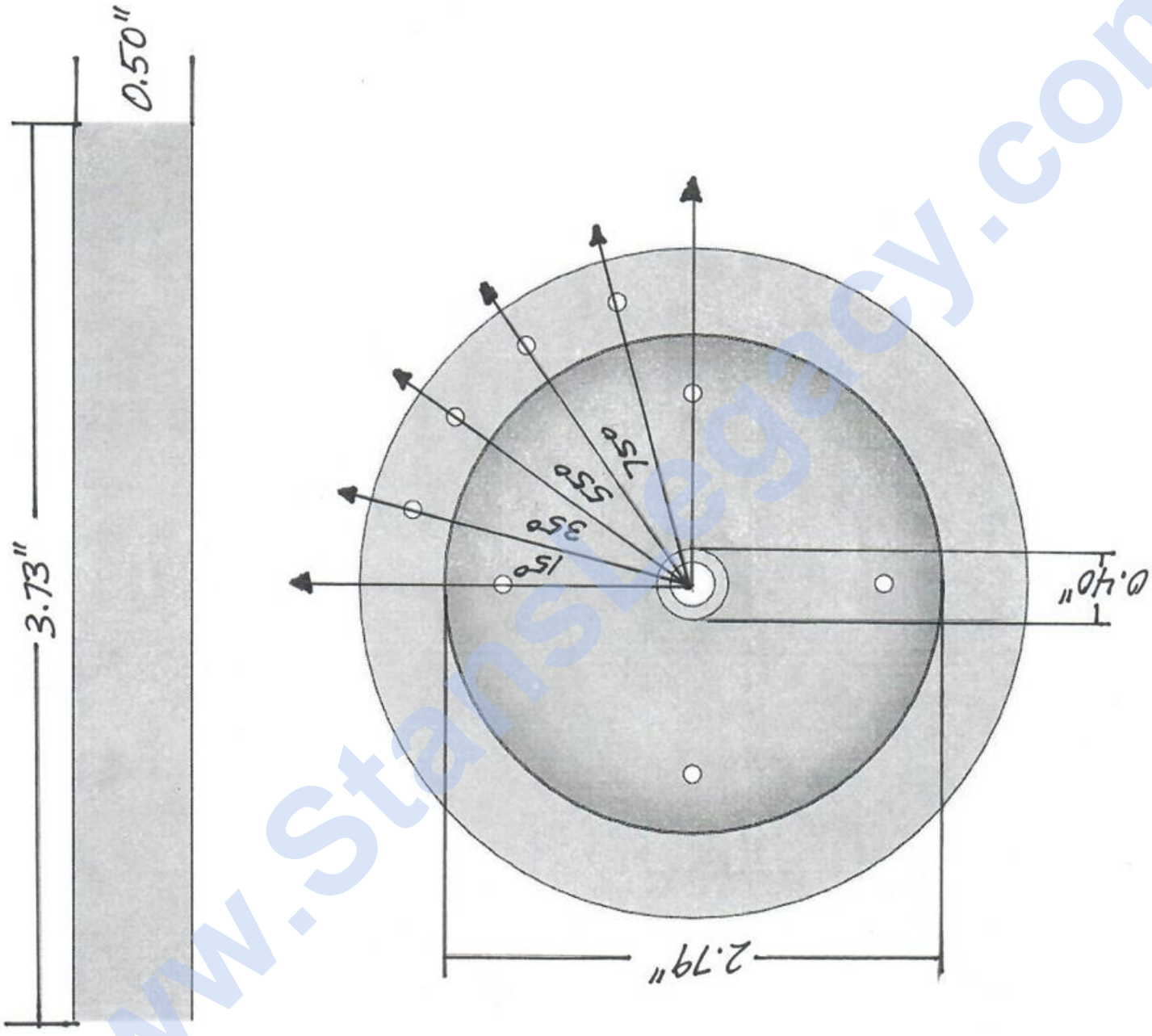

Outside Bottom Cap – View 1:

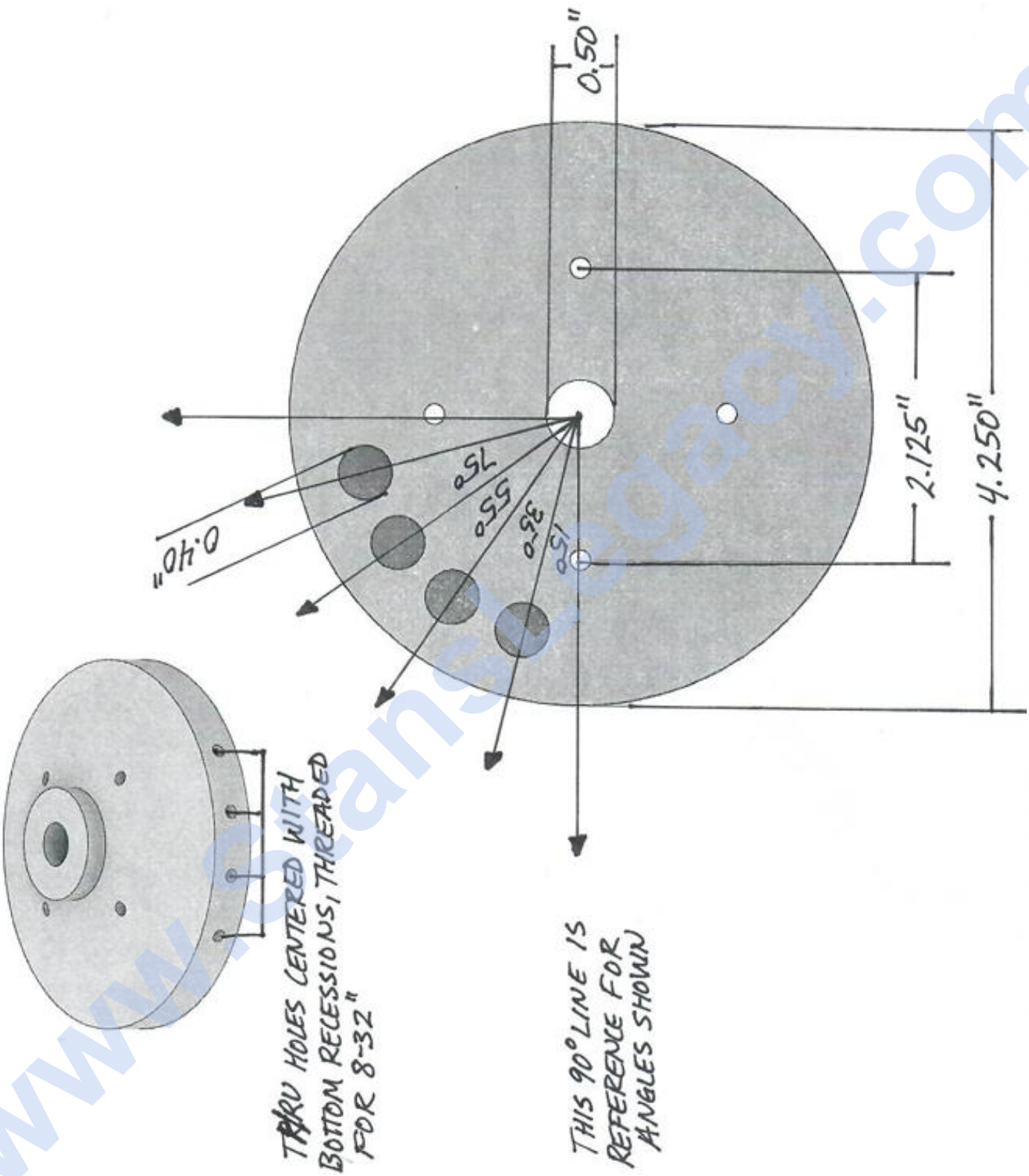

Outside Bottom Cap – View 2:

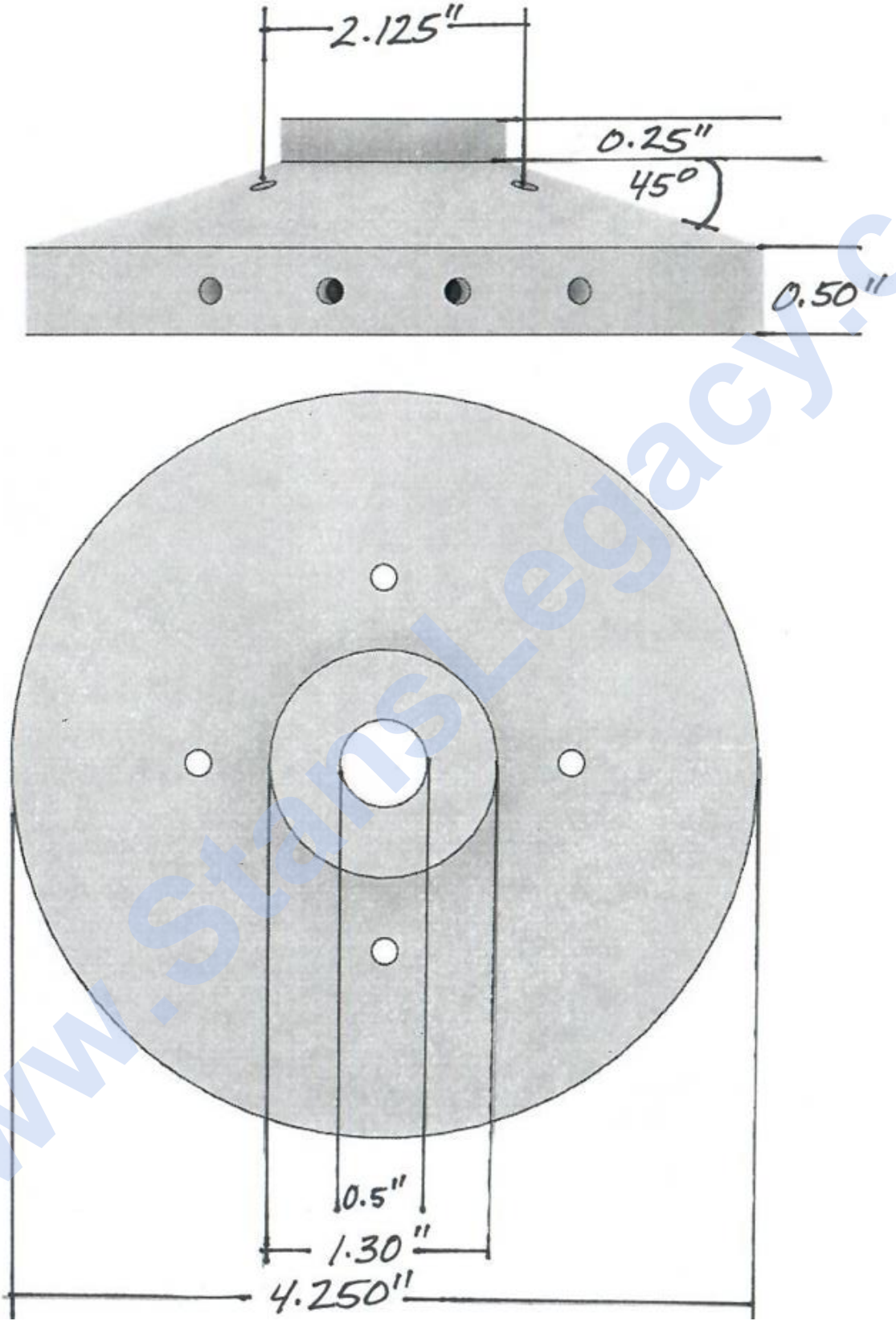

Inner Electrode:

T-304 Stainless Steel

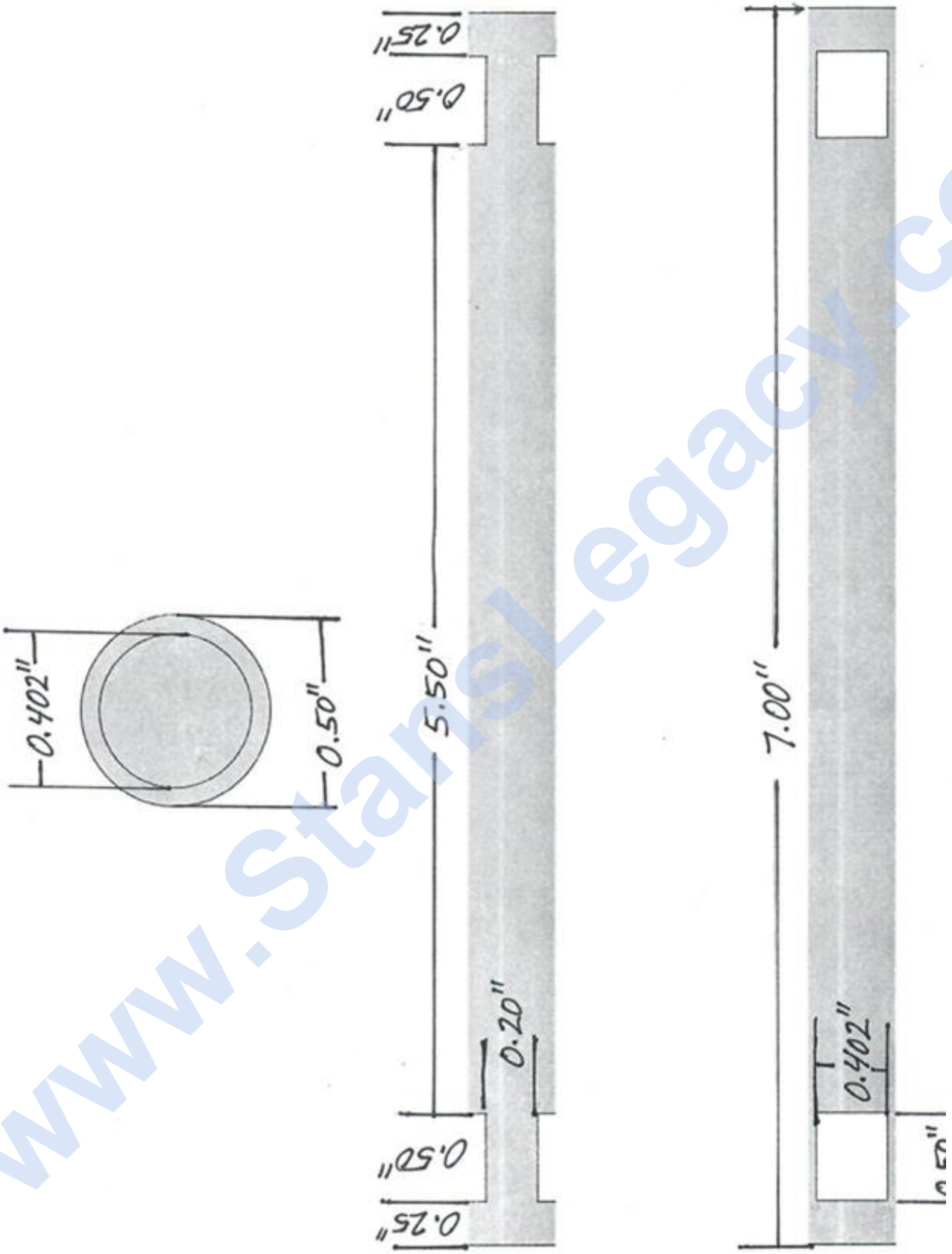

Outer Electrode (Cathode):

T-304 Stainless Steel

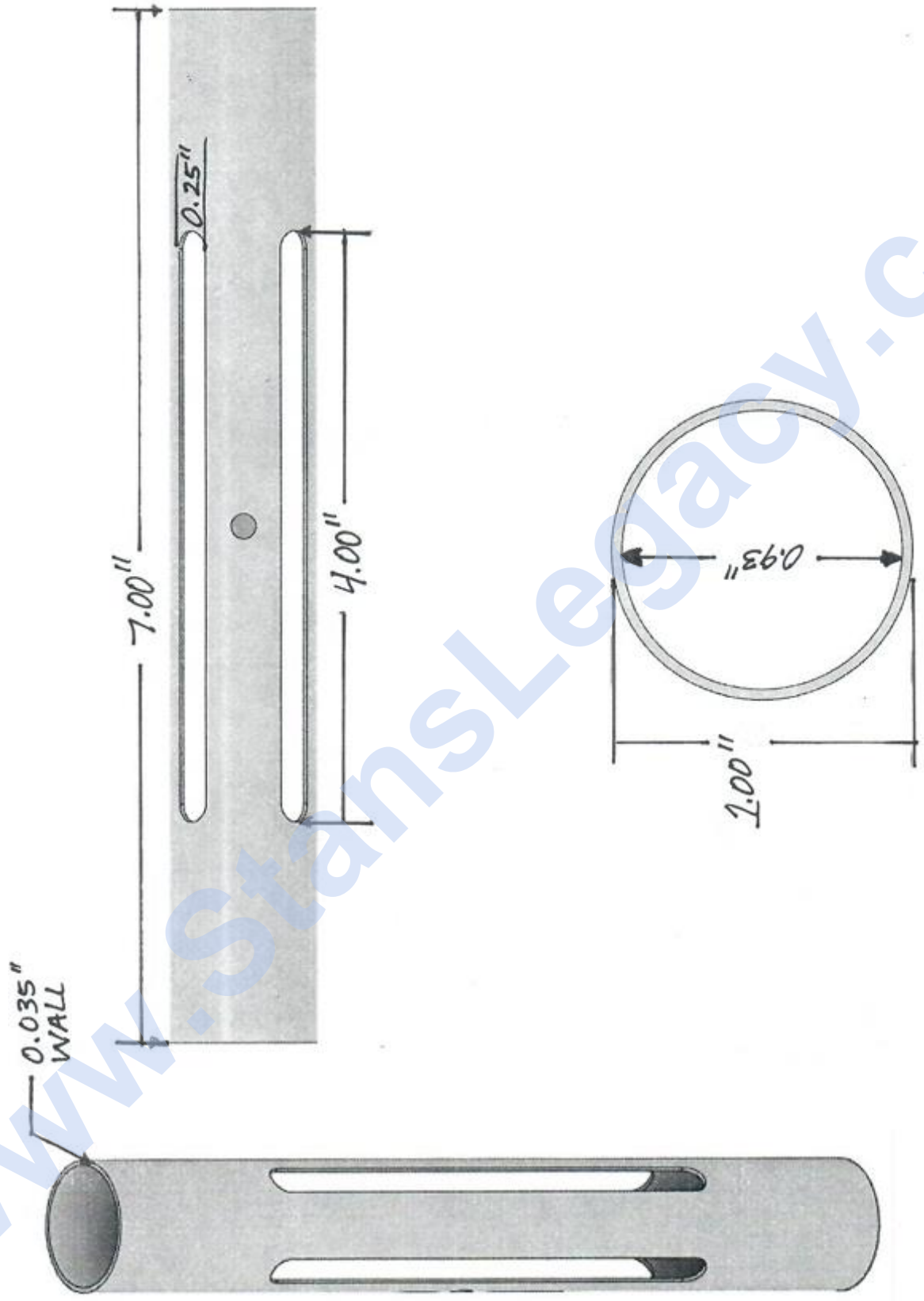

Outer Electrode Groove Stencil Part A:

3D printable stencil to help layout where LED grooves are to be milled on outer electrode.

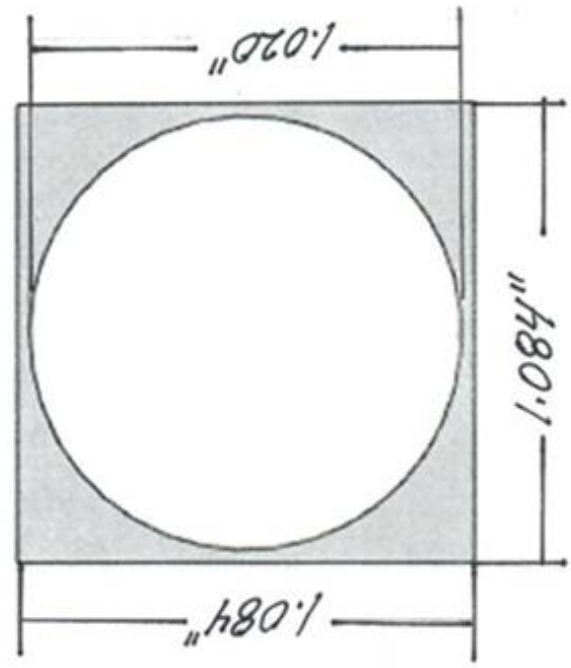

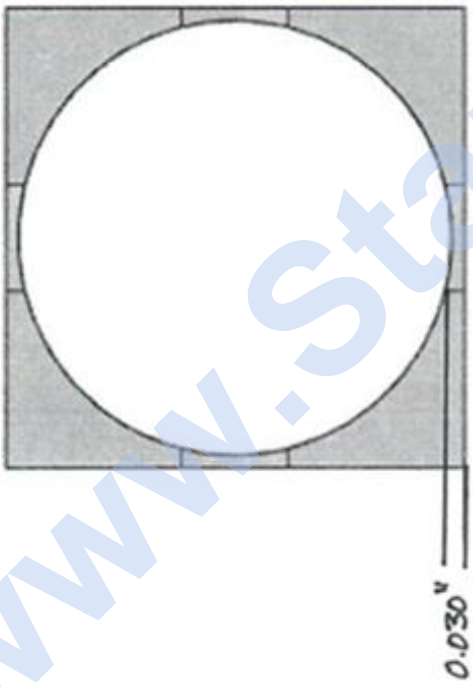

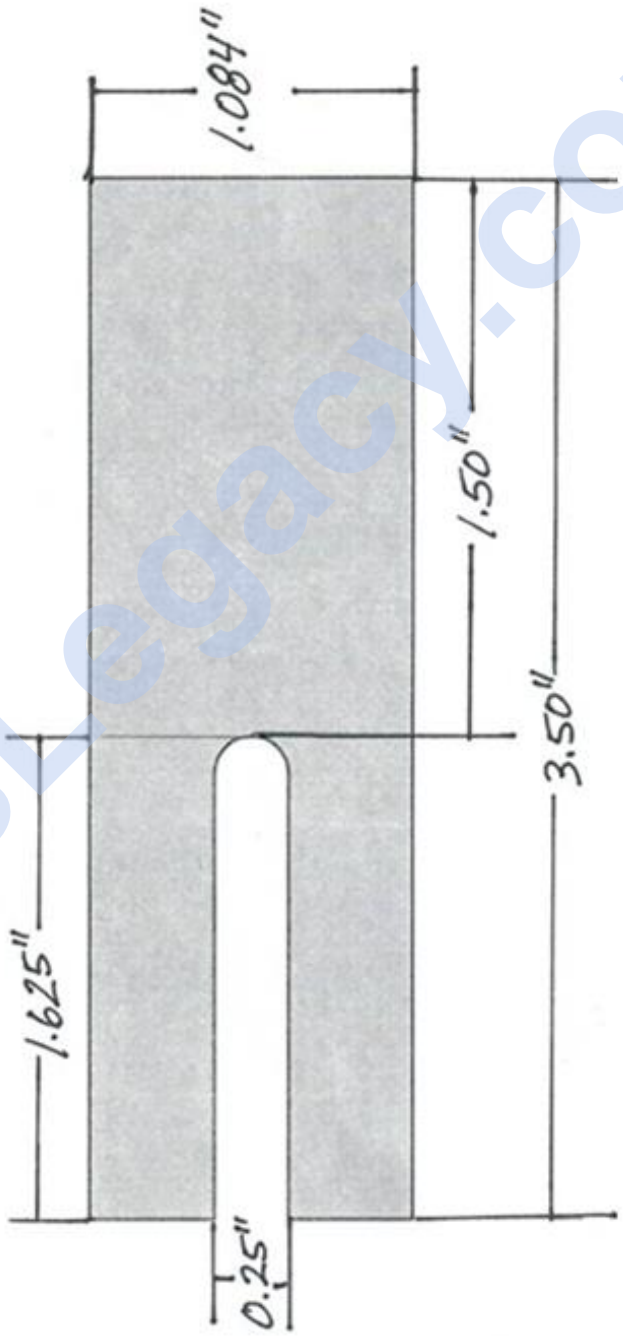

Outer Electrode Groove Stencil Part B:

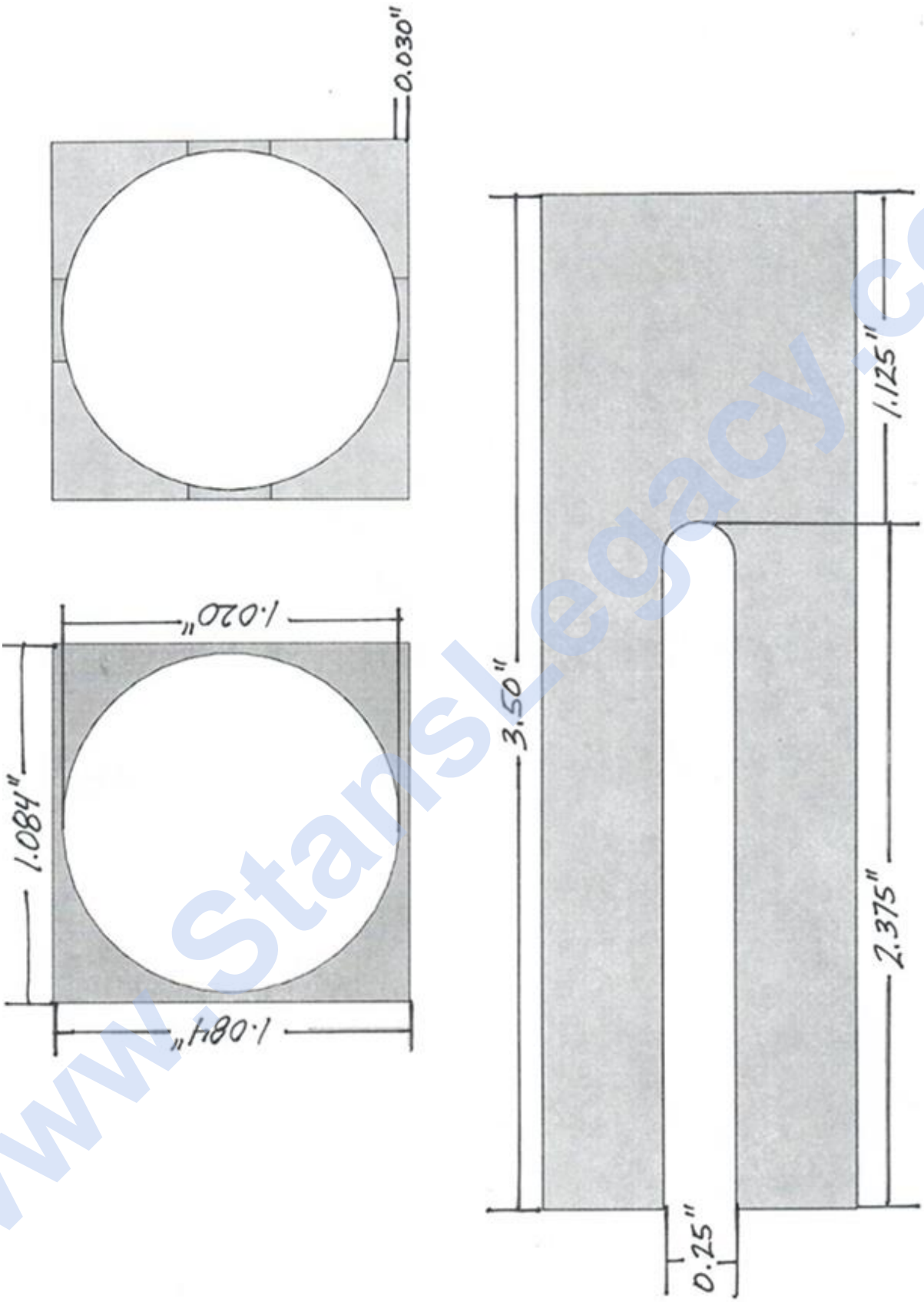

Inside Top Cap – View 1:

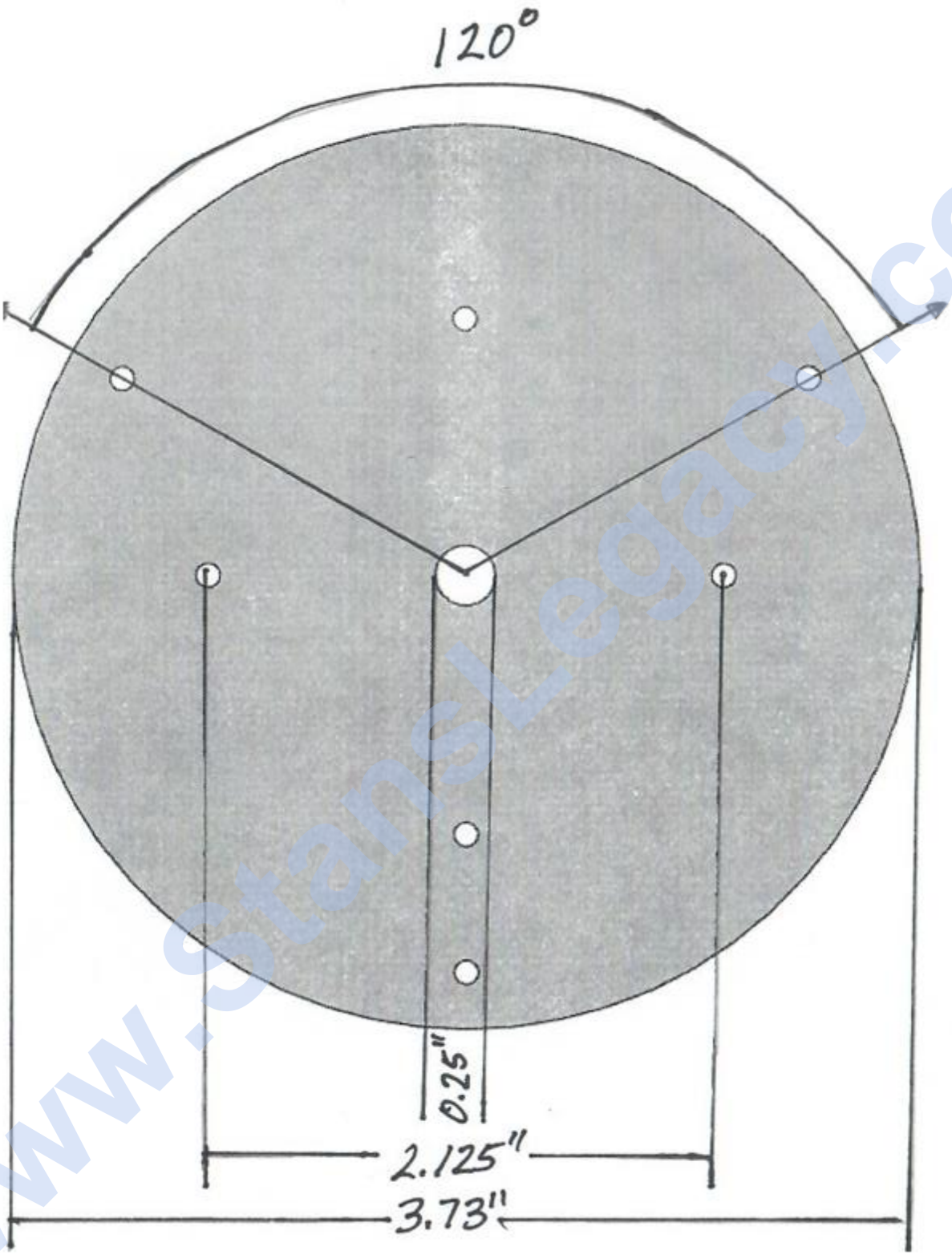

Inside Top Cap – View 2:

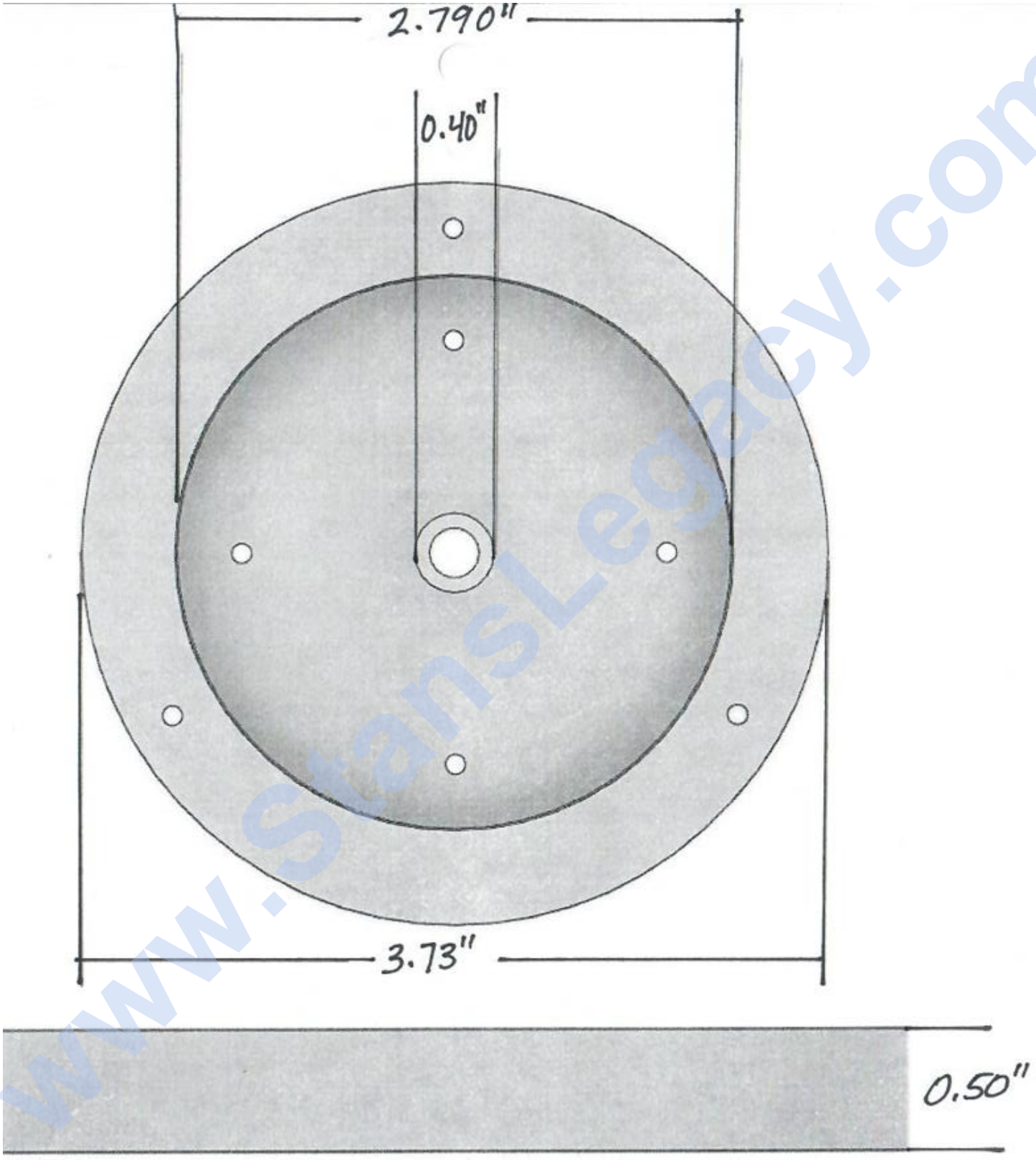

Outside Top Cap – View 1:

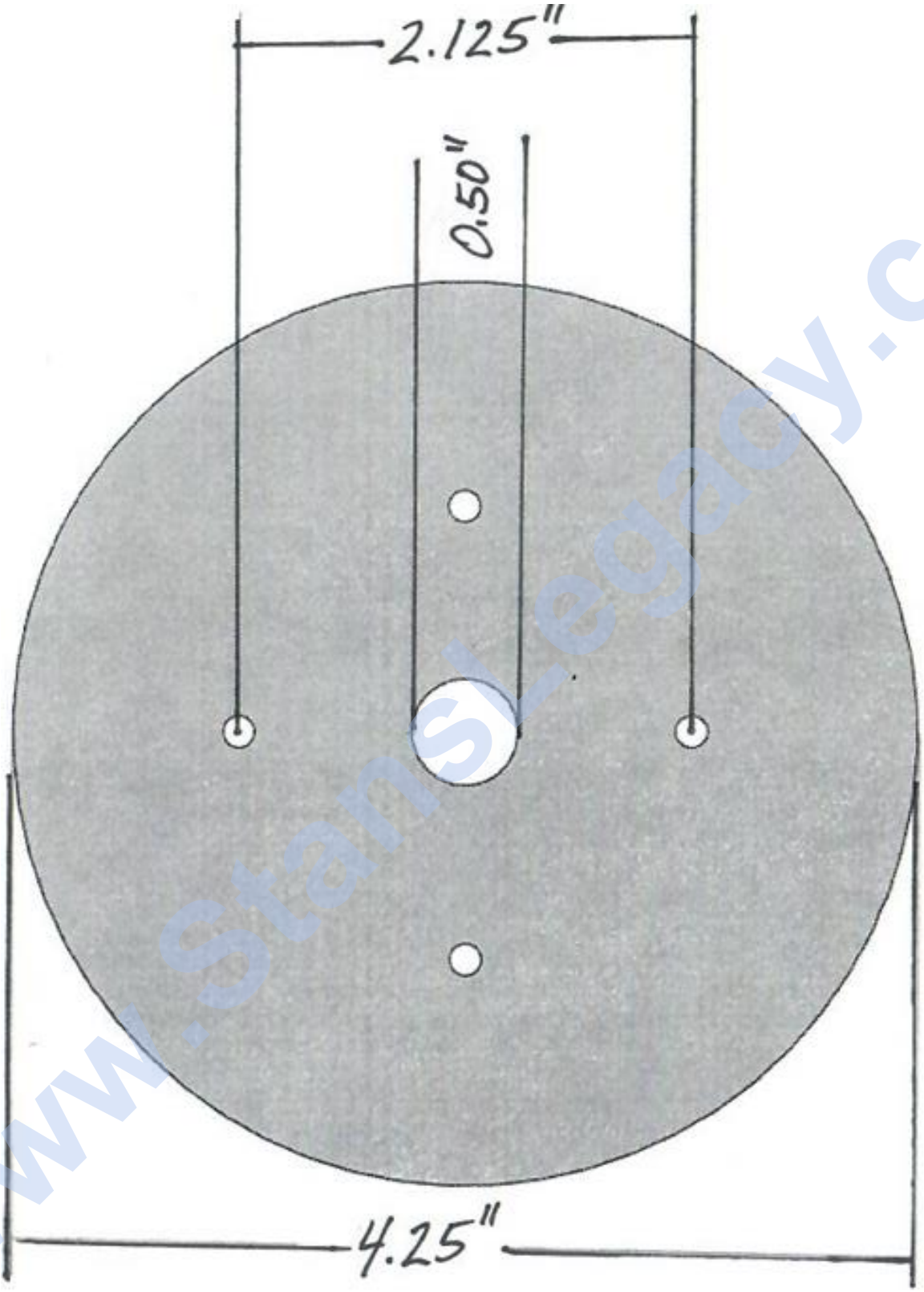

Outside Top Cap – View 2:

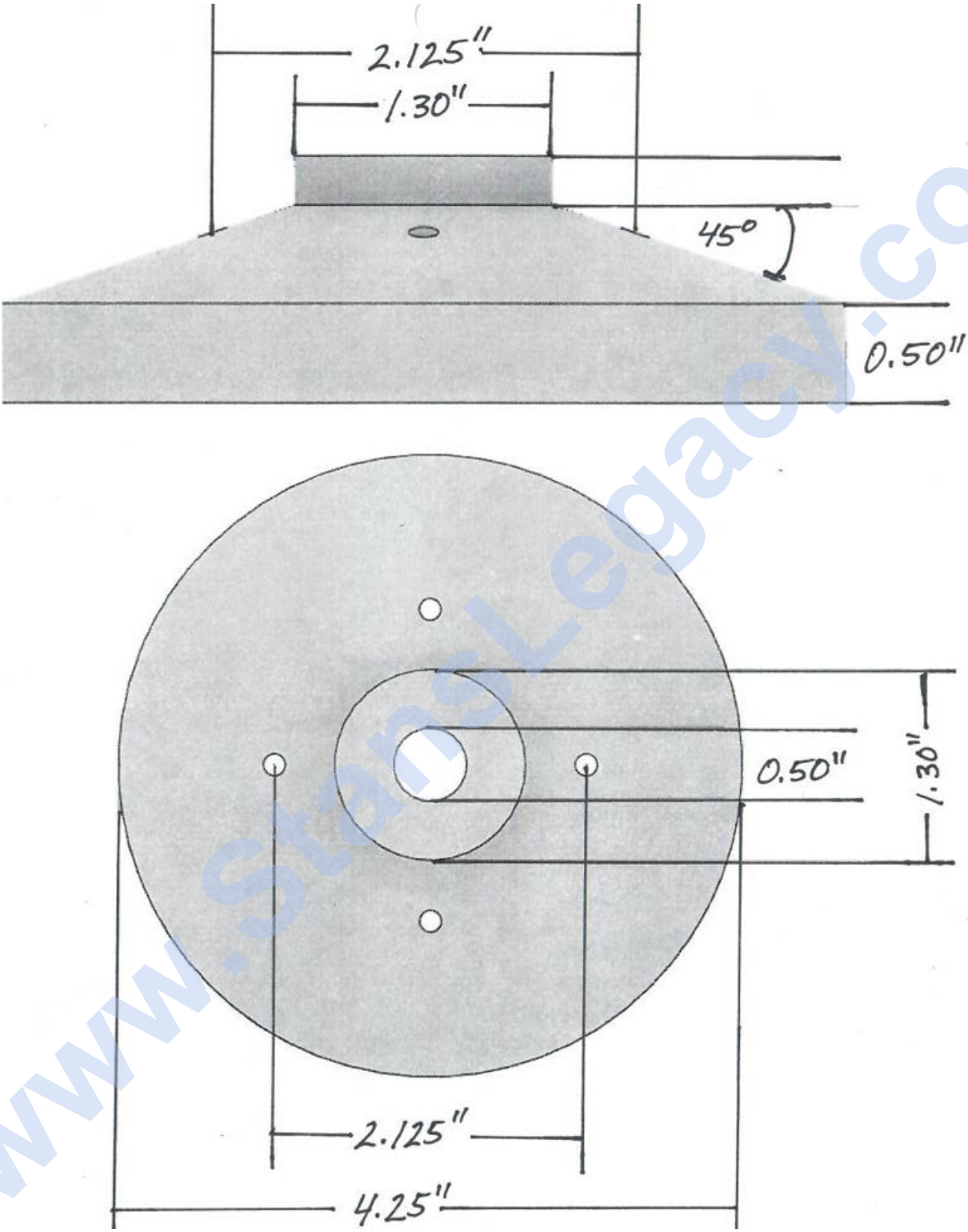

APPENDIX B: Resonant Cavity Dimensions

Cutaway View

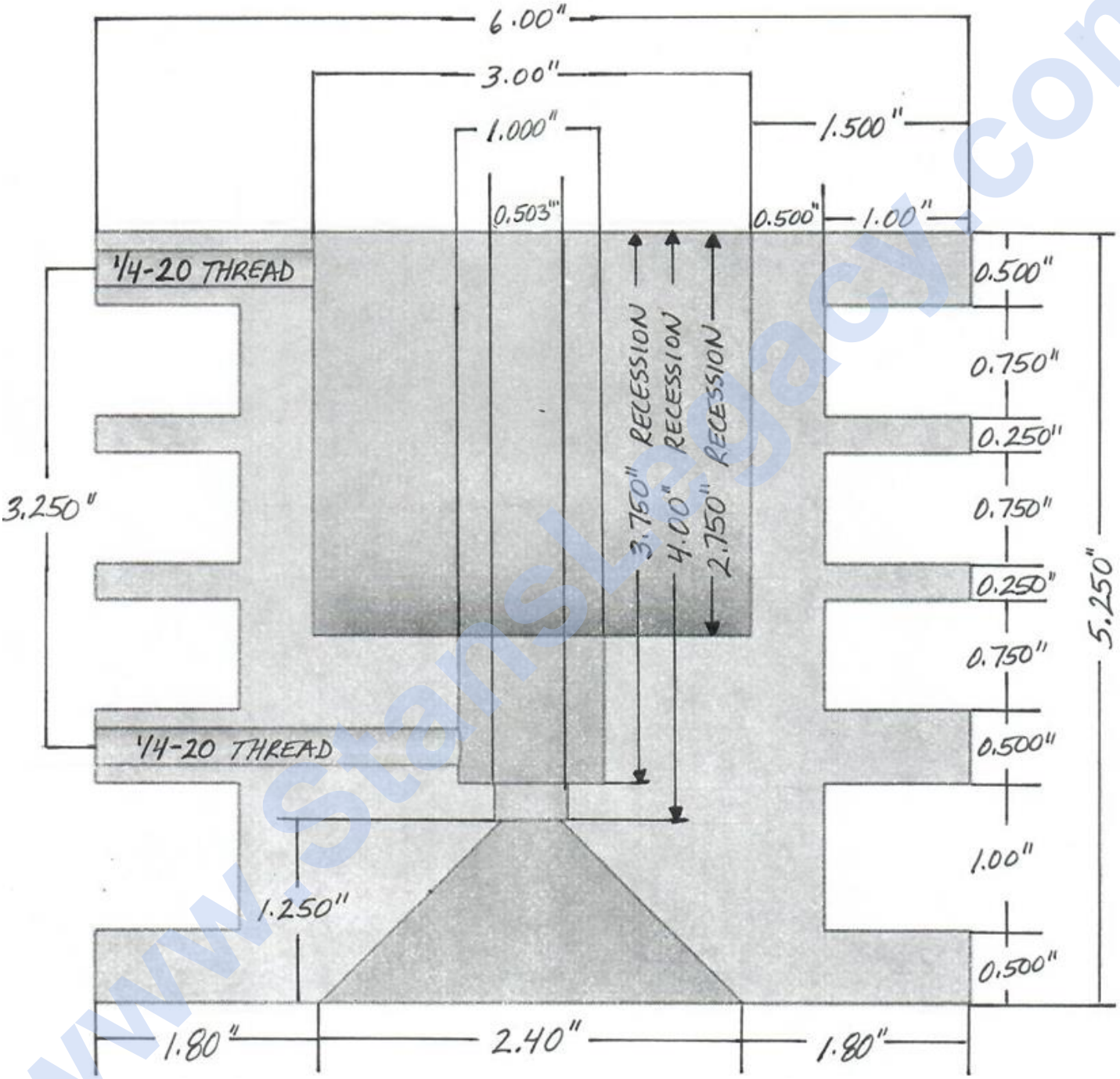

Top View

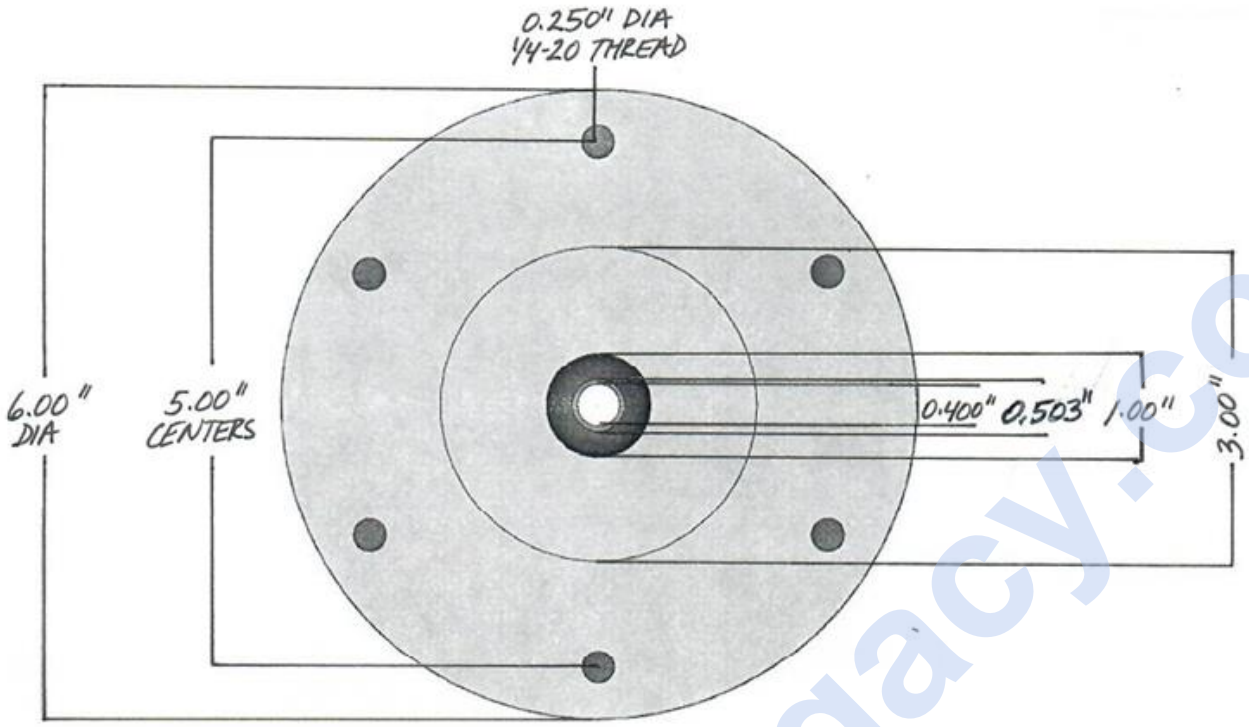

Bottom View

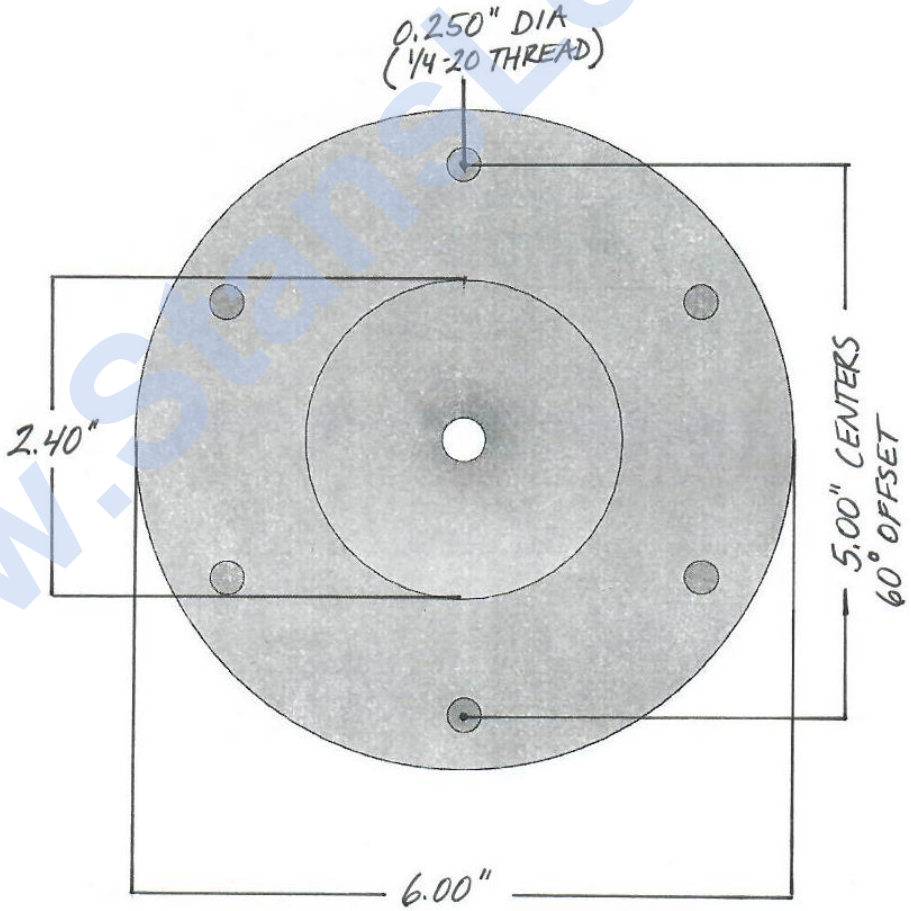

Outer Electrode

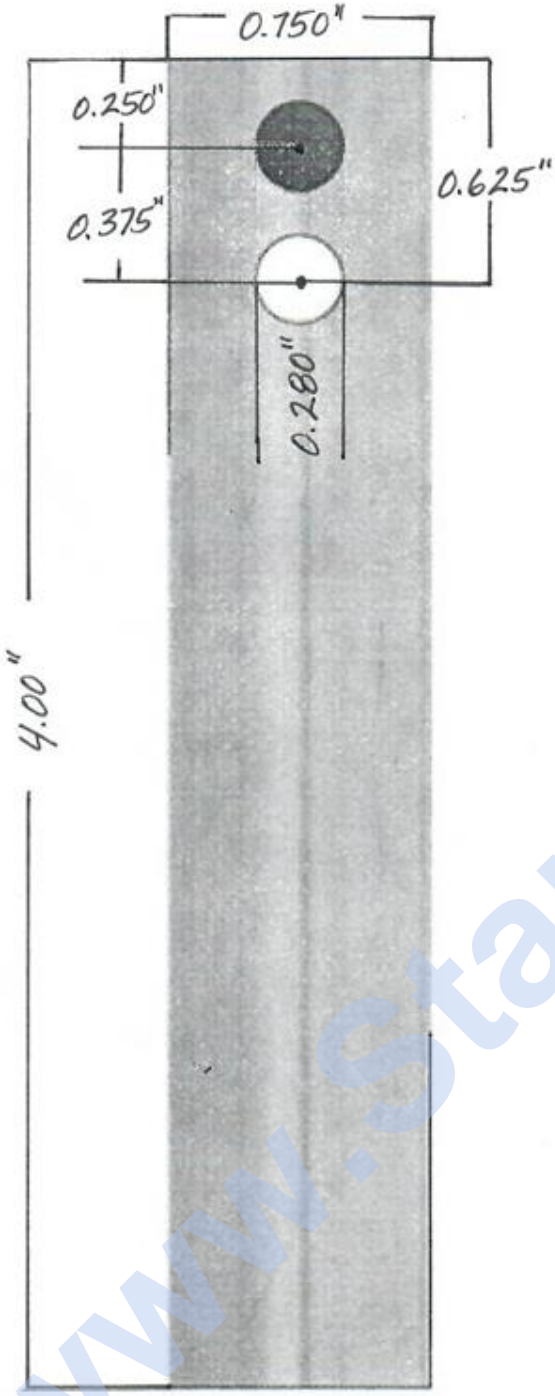

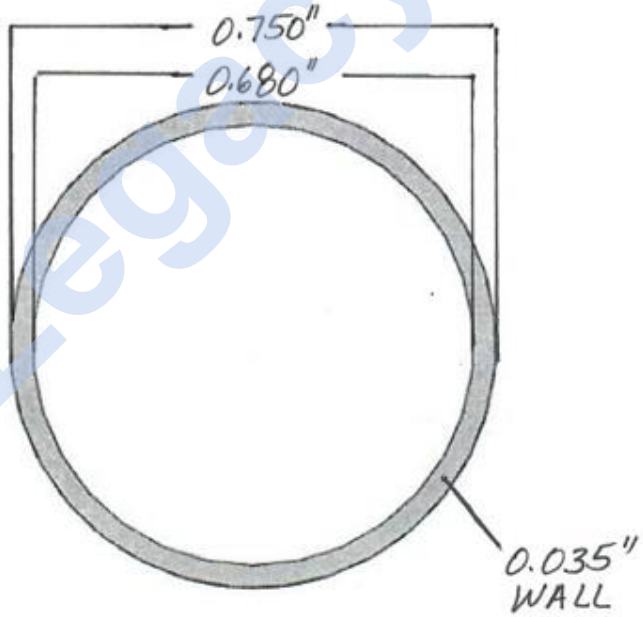

Inner Electrode

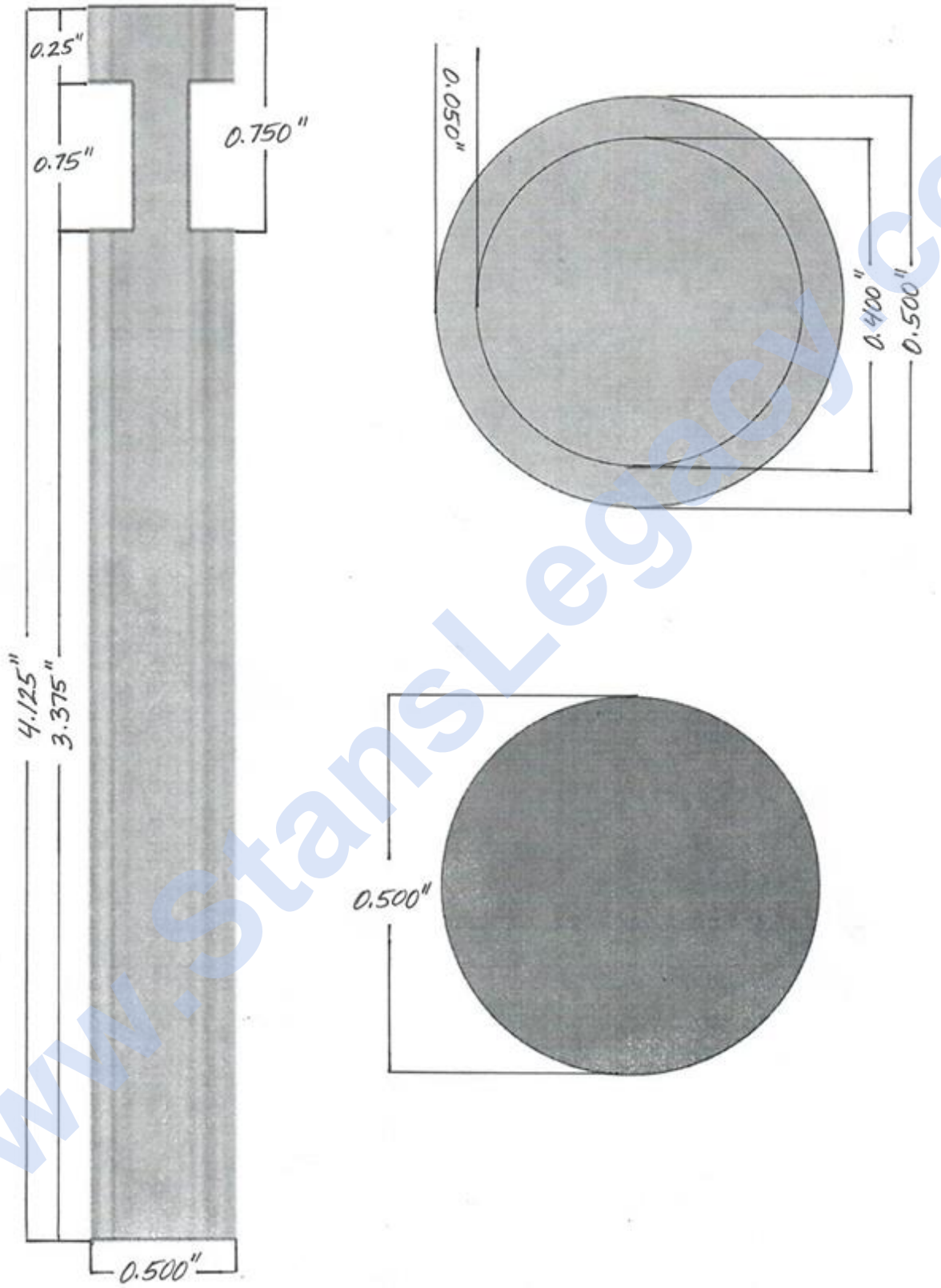

Electrode Cap – Cutaway & Side Views

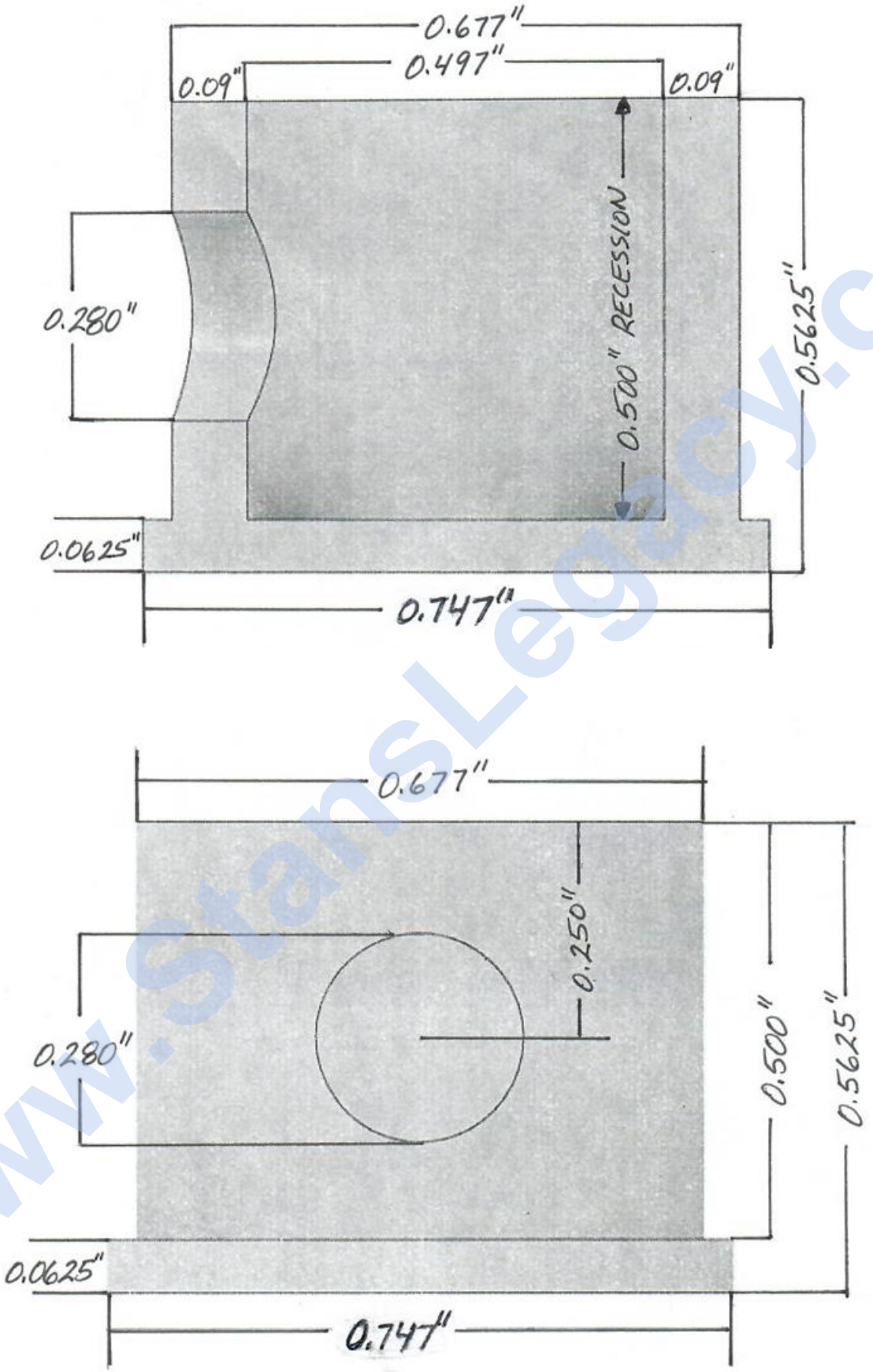

APPENDIX C: Bottom Mount Dimensions

Cutaway View

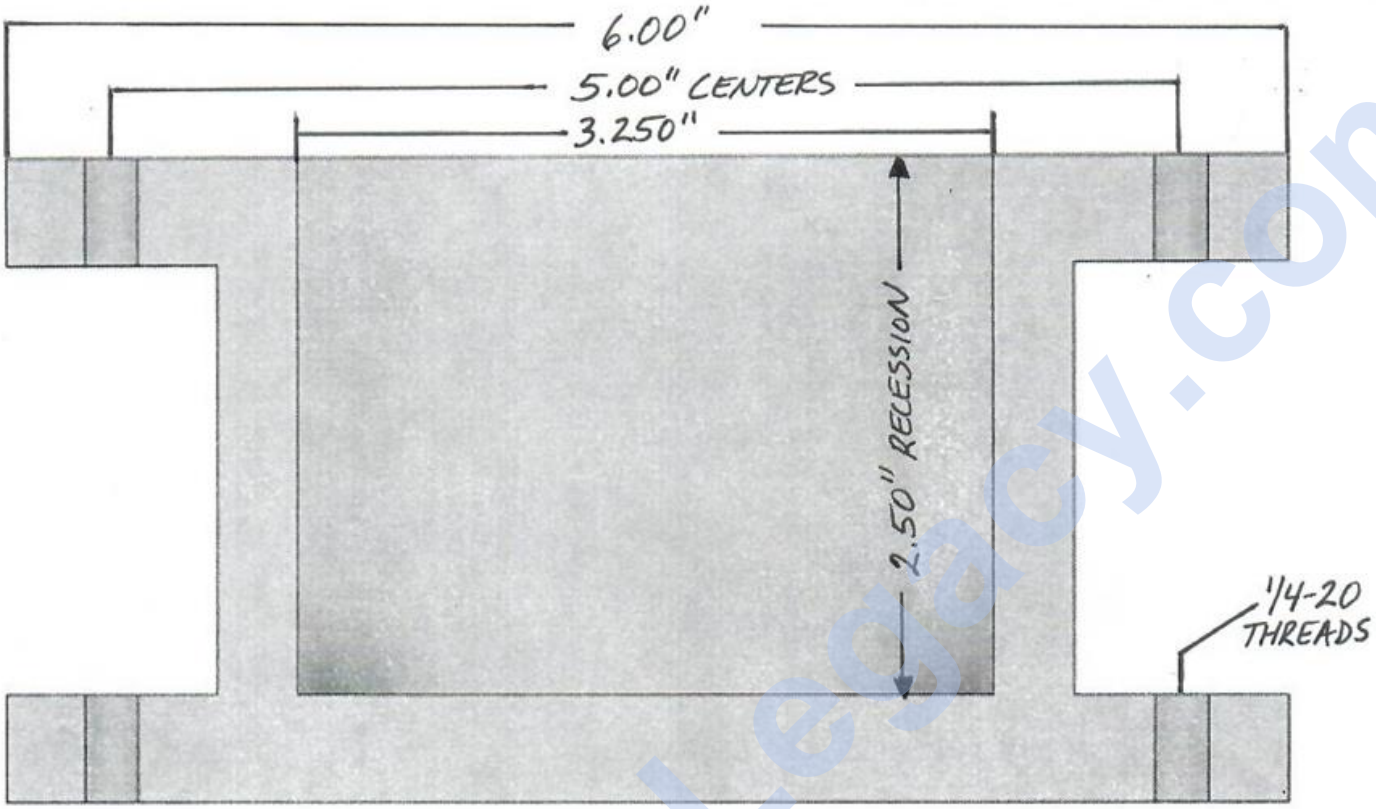

Side View

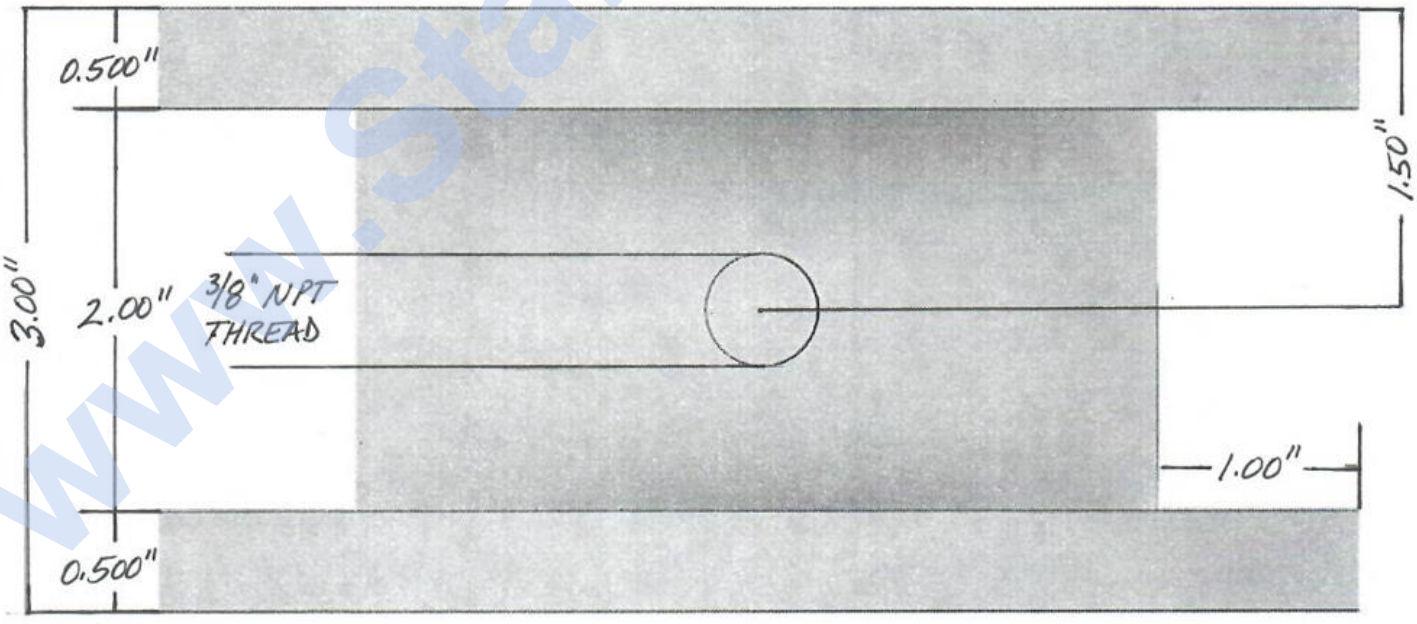

Top View

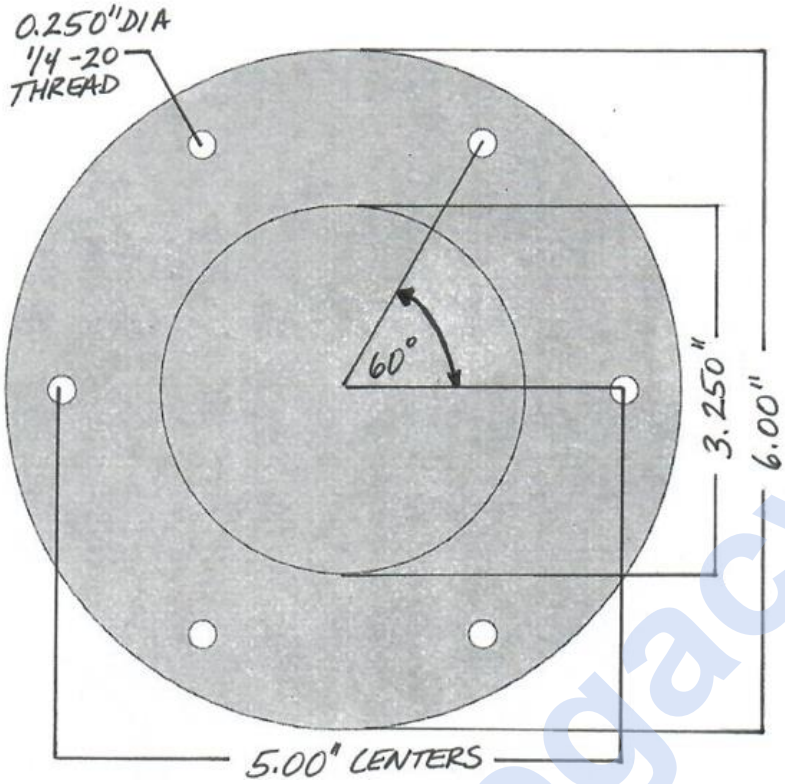

Bottom View

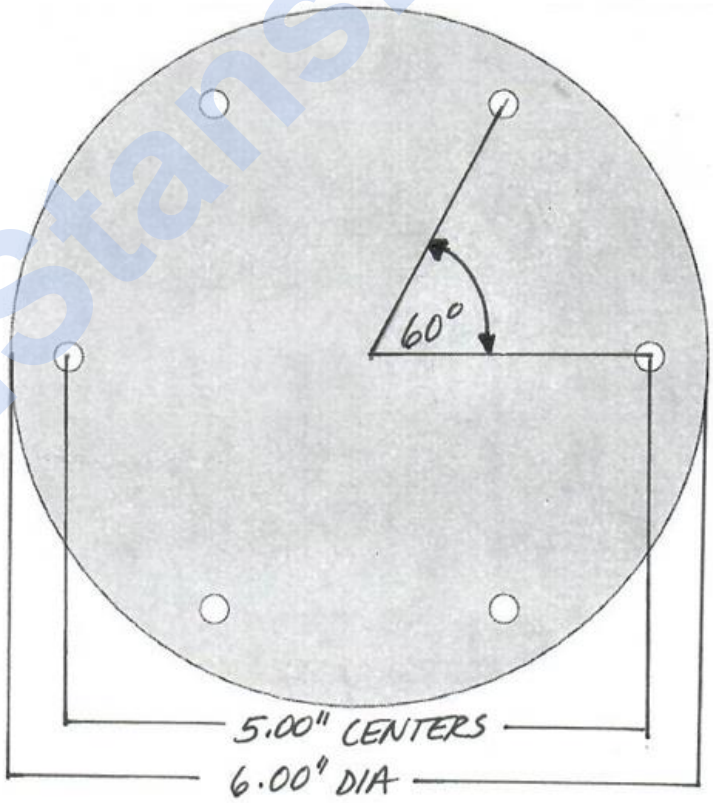

APPENDIX D: Acrylic Lens

Side View

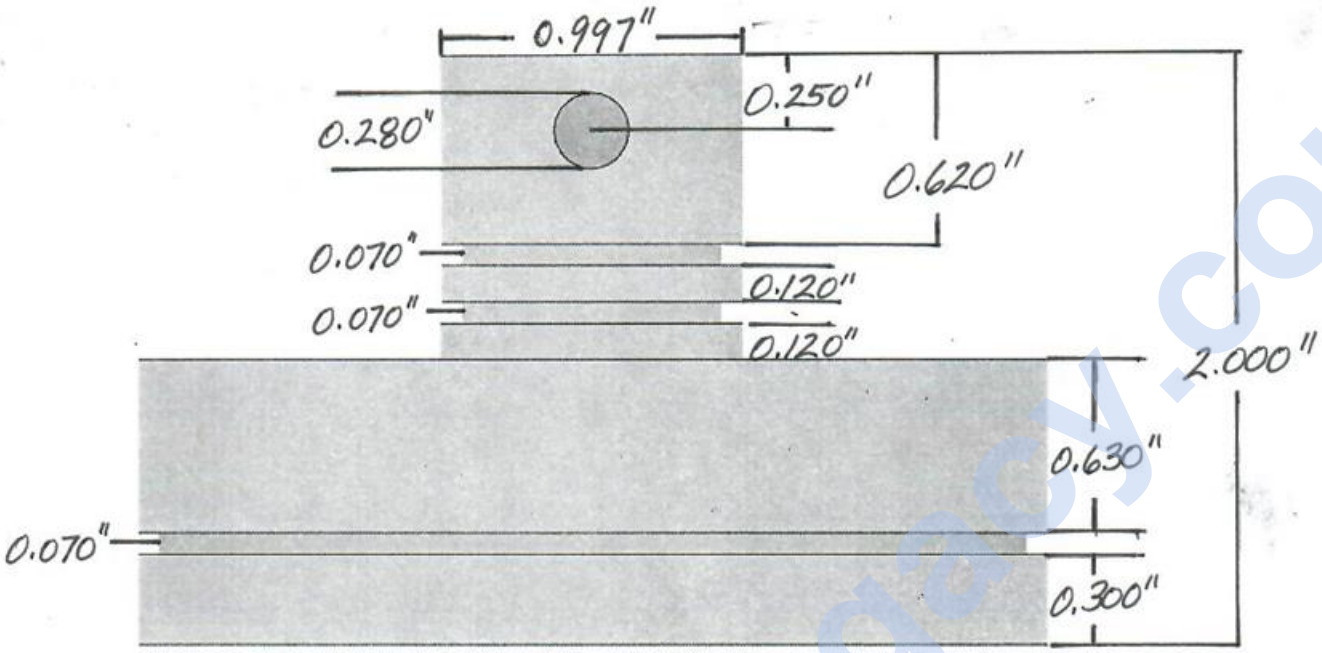

Cutaway View

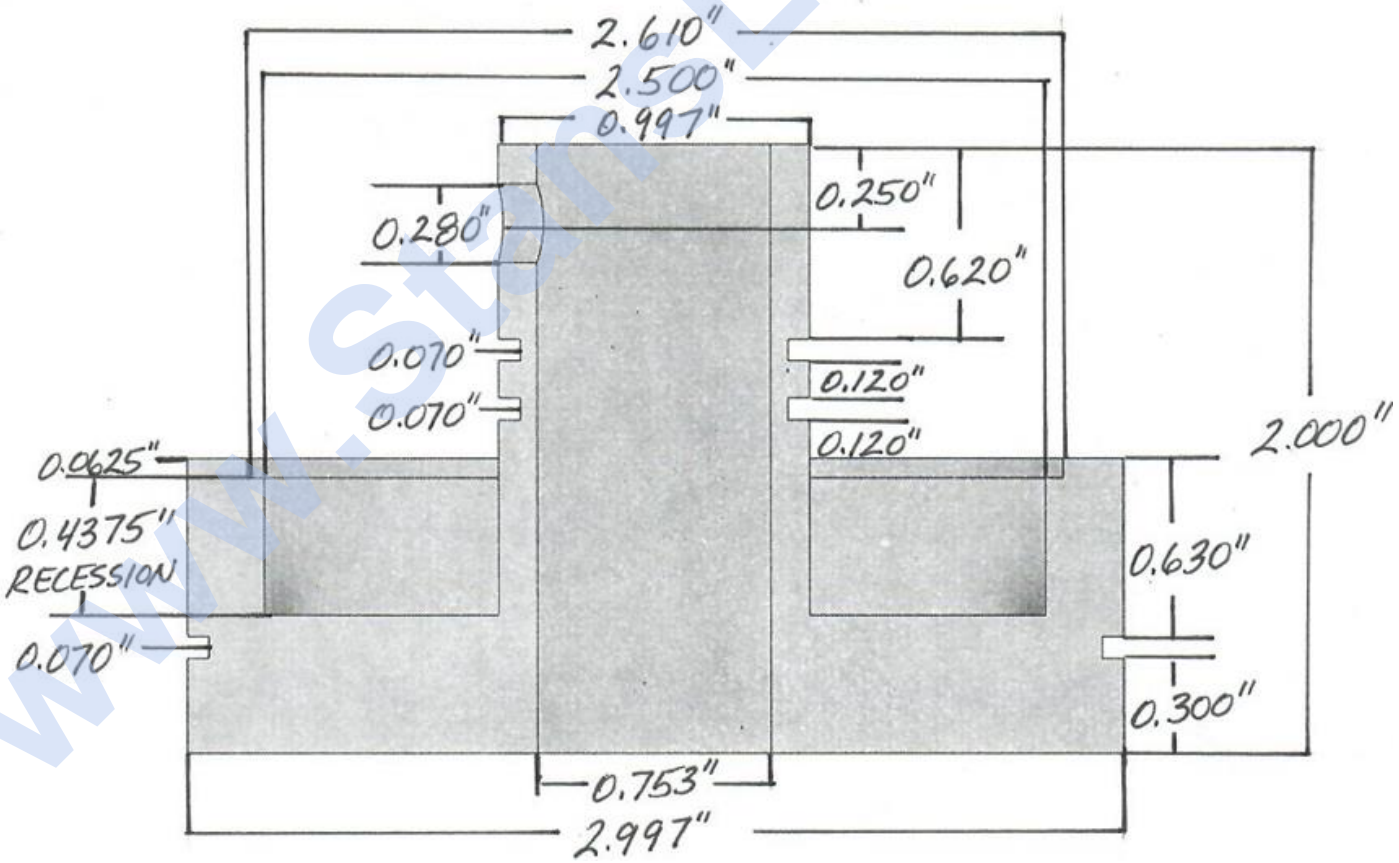

Bottom View

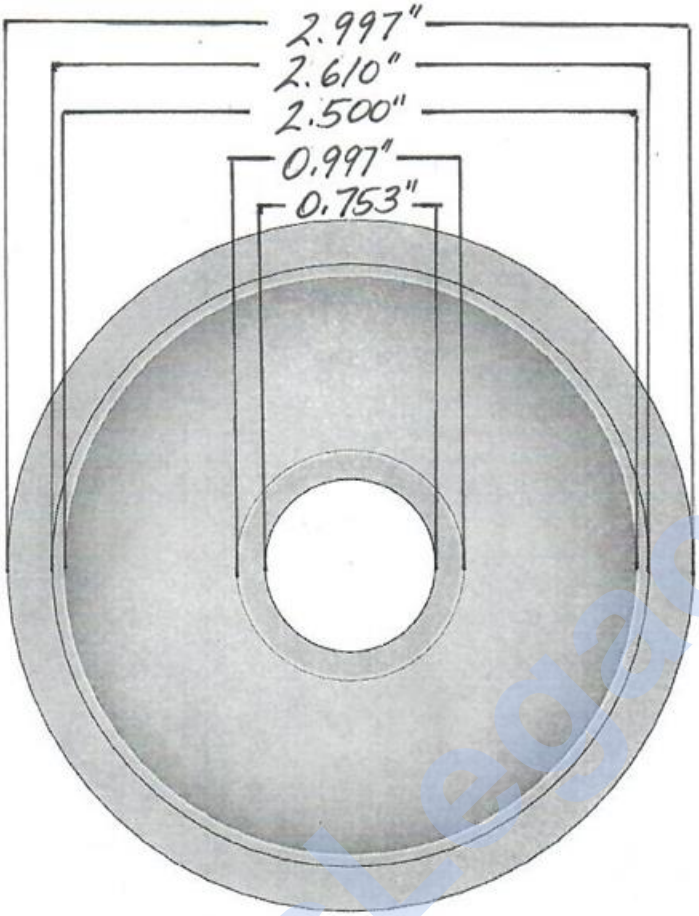

Top View

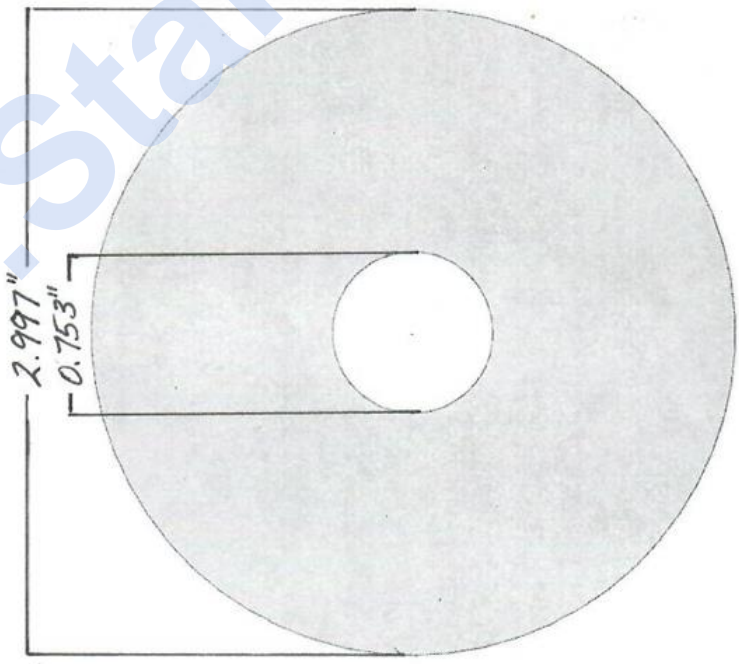

O-rings

(Thickness – 0.070”)

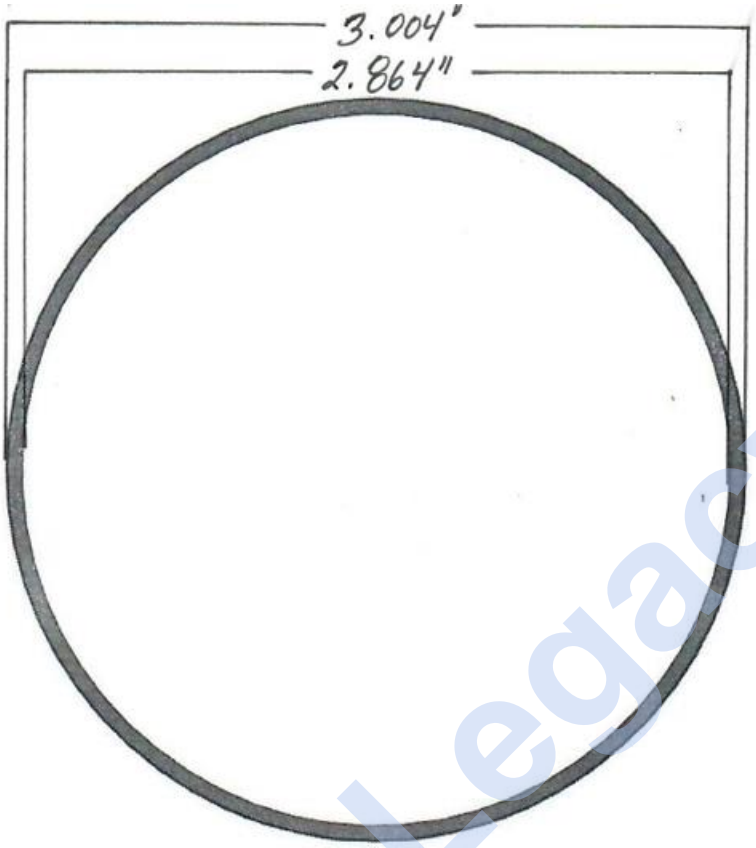

(Thickness – 0.070”)

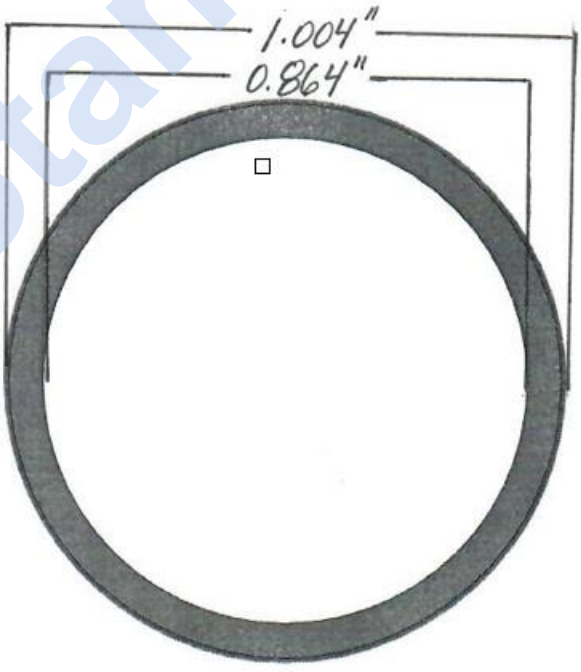

APPENDIX E: Colored Lens

Top/Bottom View

(Thickness – 0.0625”)

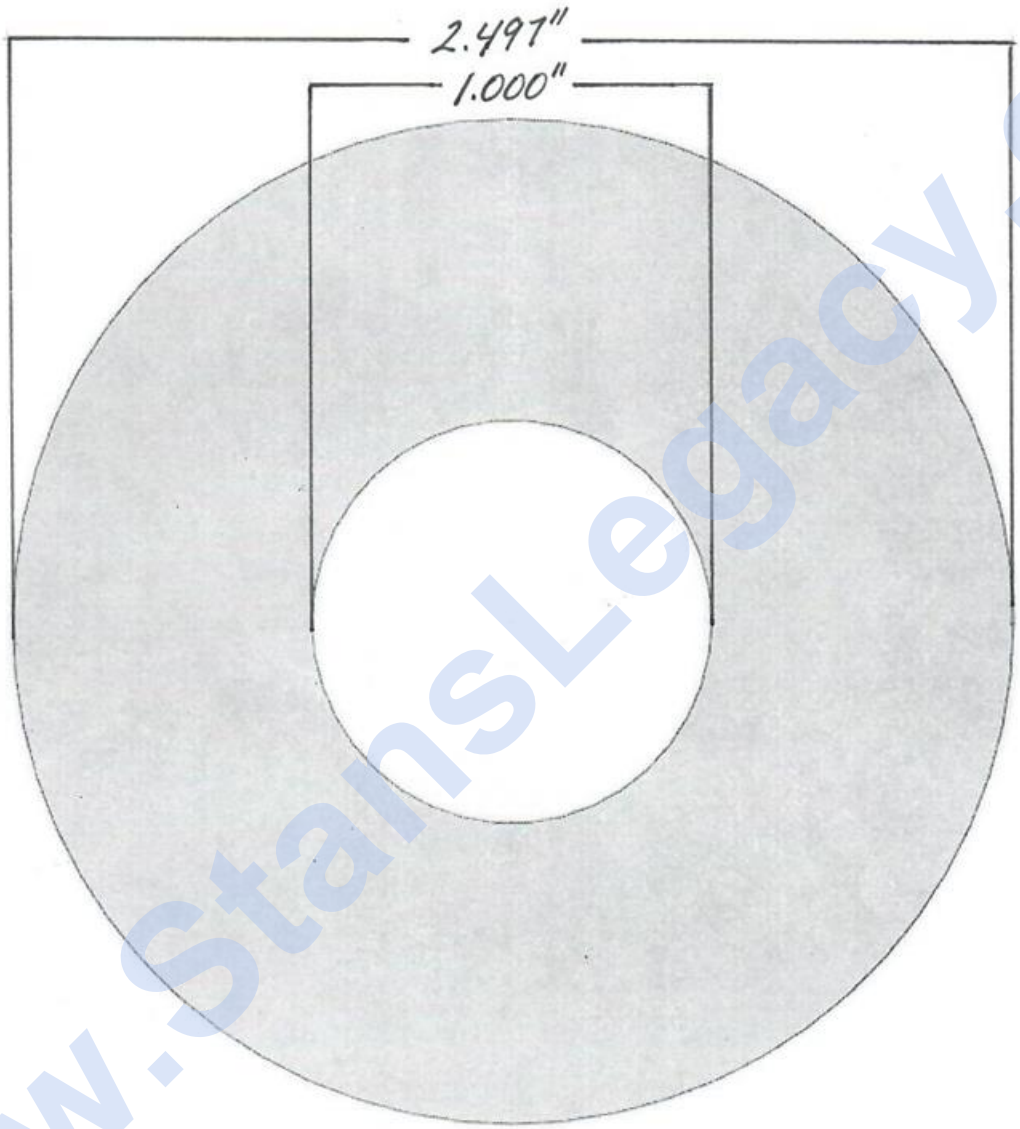

APPENDIX F: Base Board & Rubber Feet

Top View

(Thickness – 0.75")

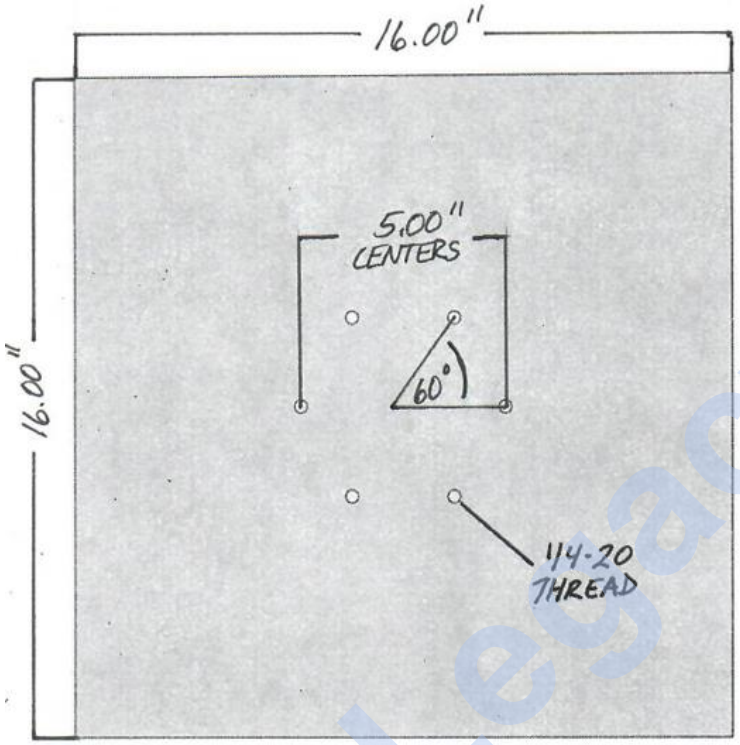

Bottom View

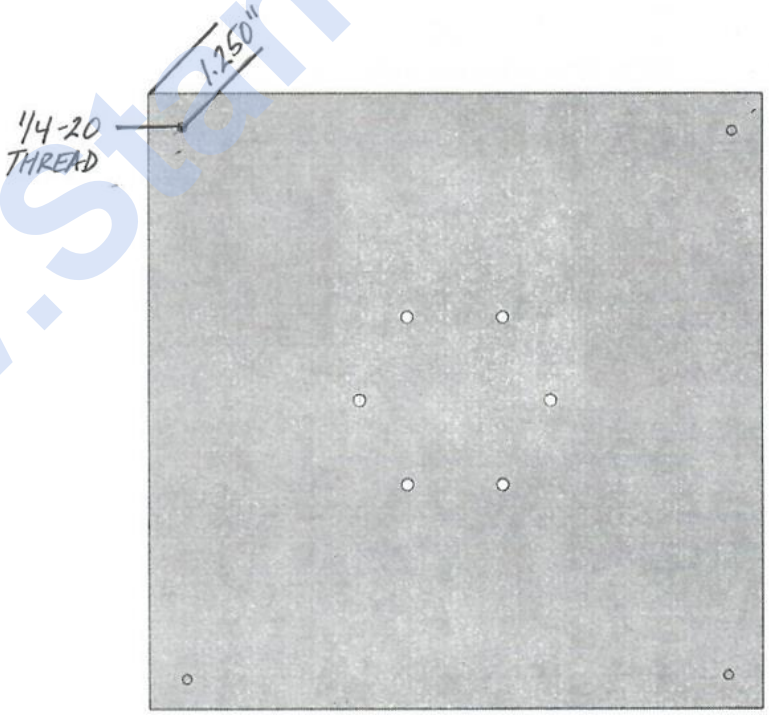

Rubber Feet – Top / Side / Bottom Views

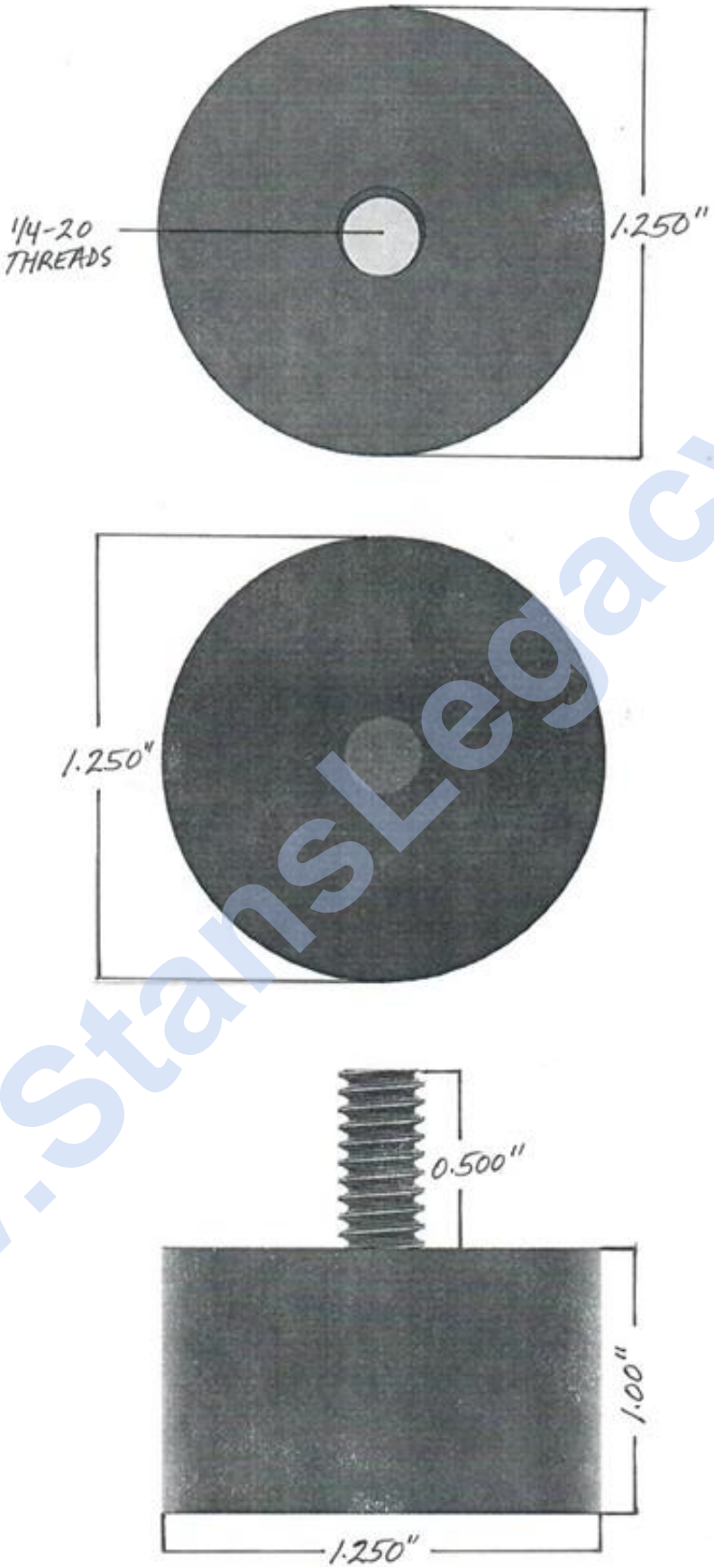

APPENDIX G: Insulative Cone

Cutaway View

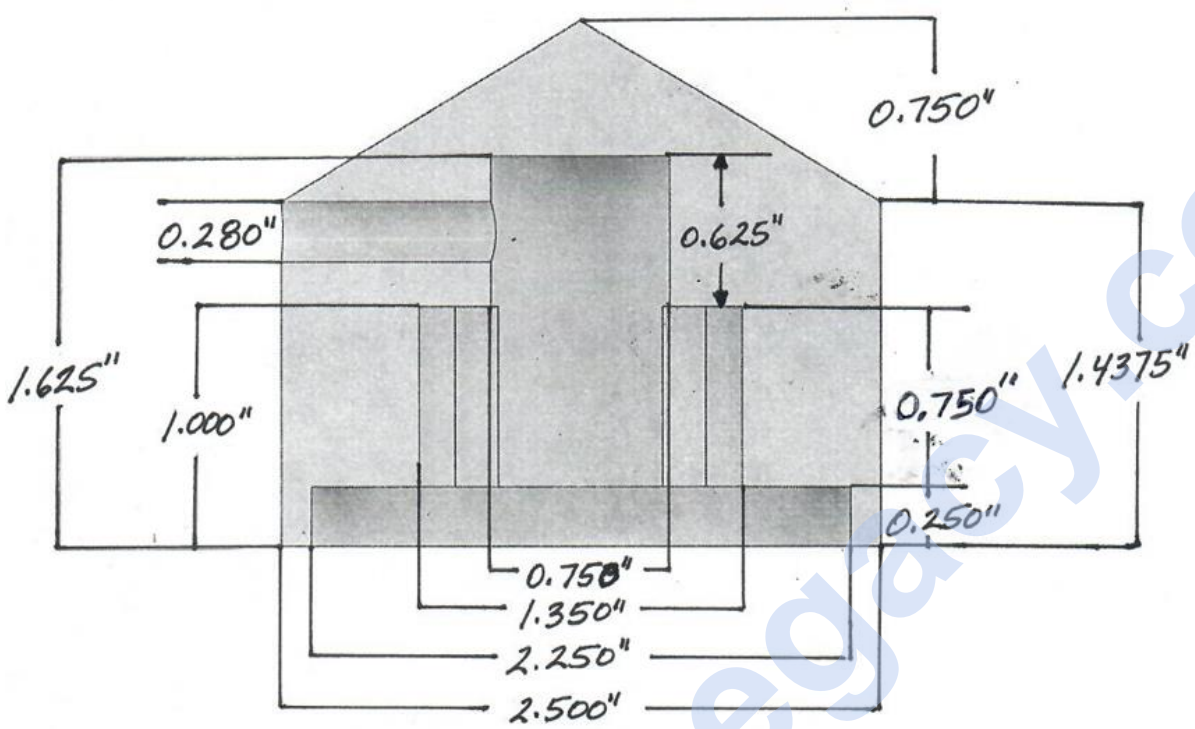

Side View

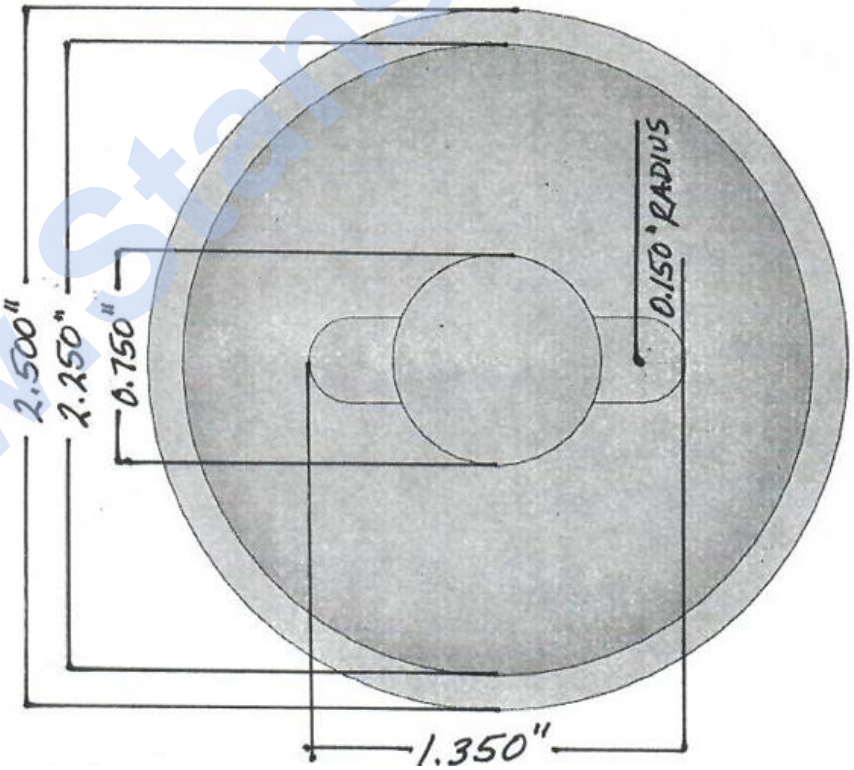

APPENDIX H: Water Tank

Side View

Top View:

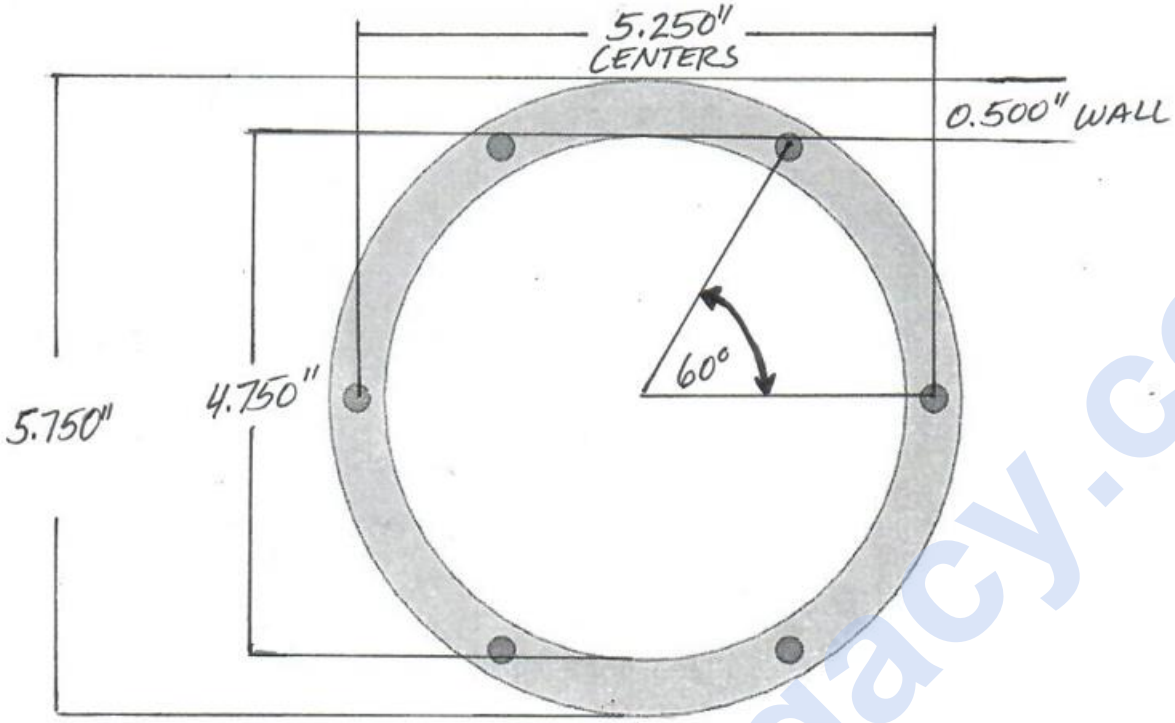

Bottom View:

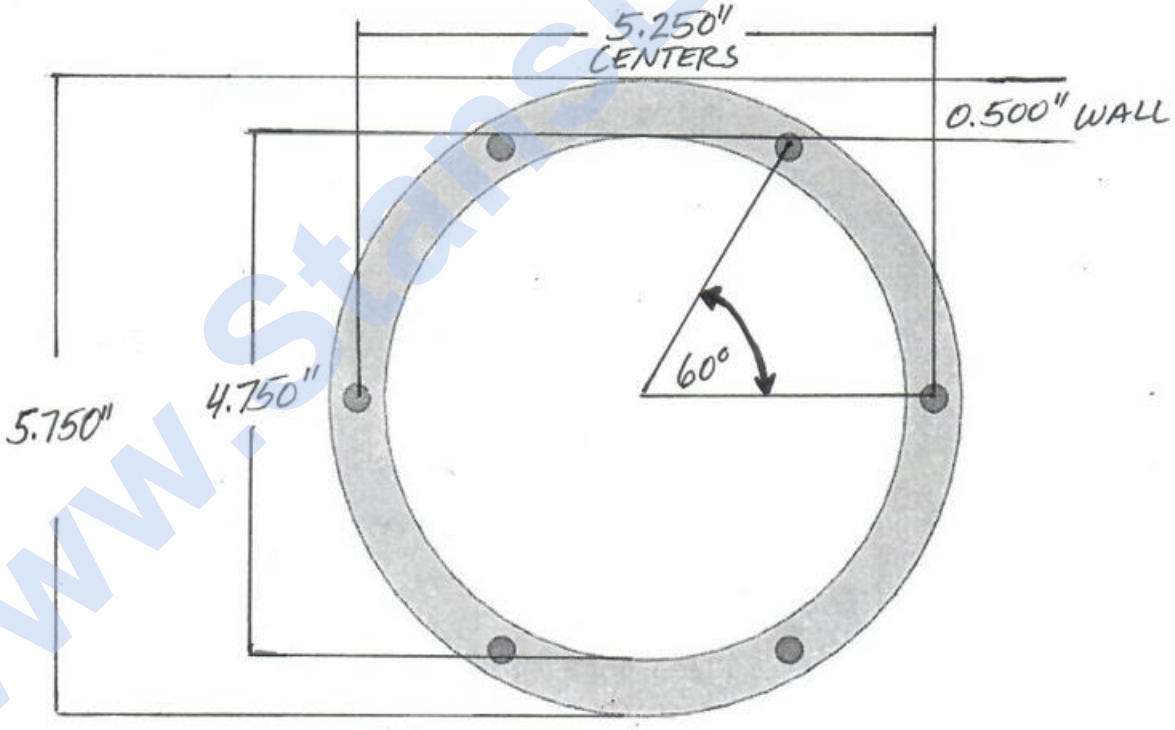

Top Cap – Cutaway View

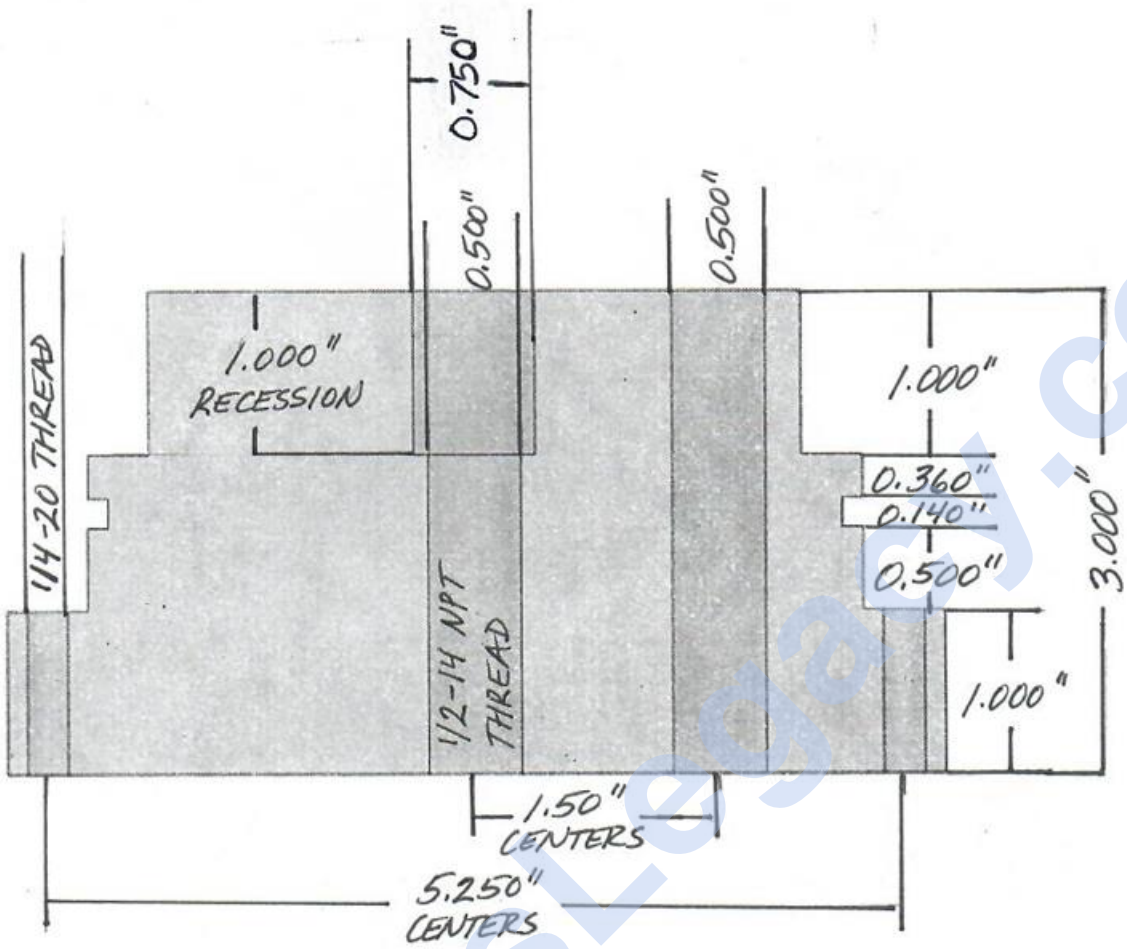

Top Cap – Side View

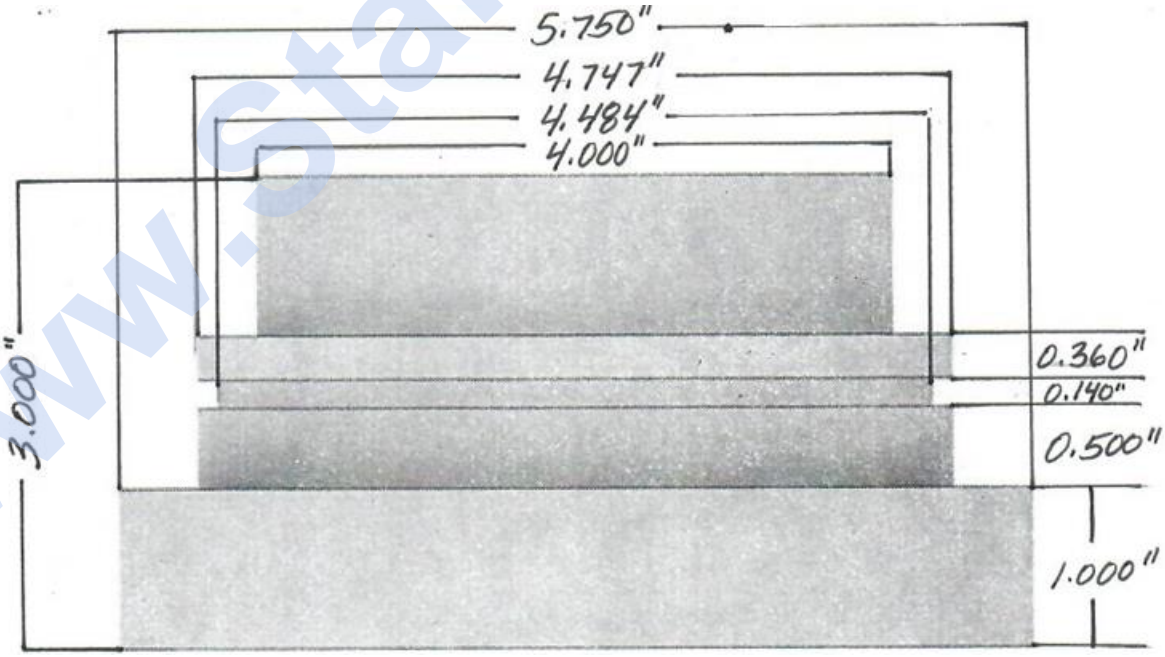

Top Cap – Top View

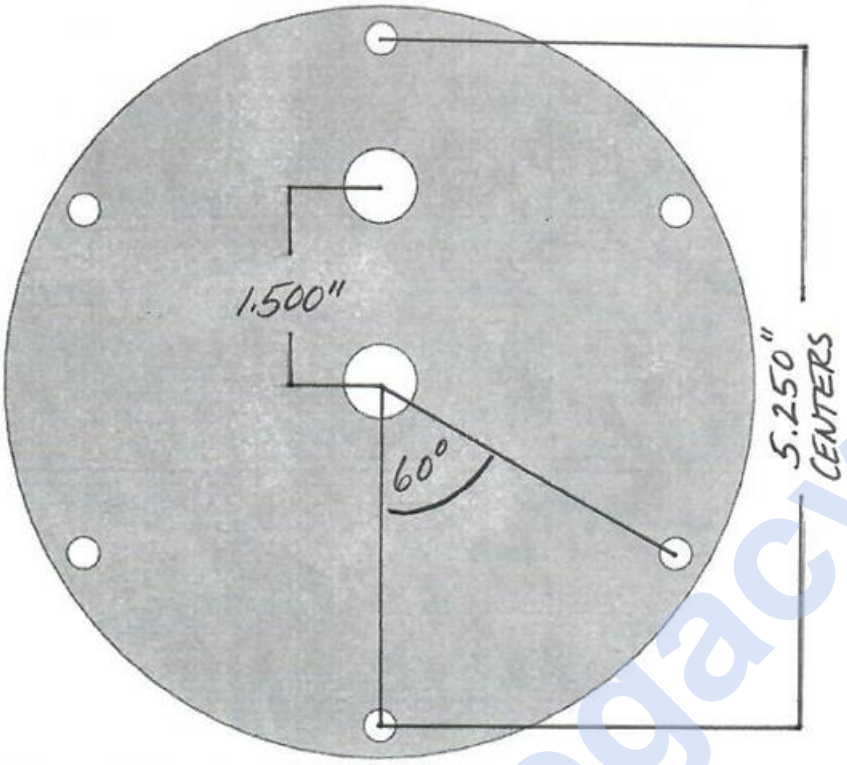

Top Cap – Bottom View

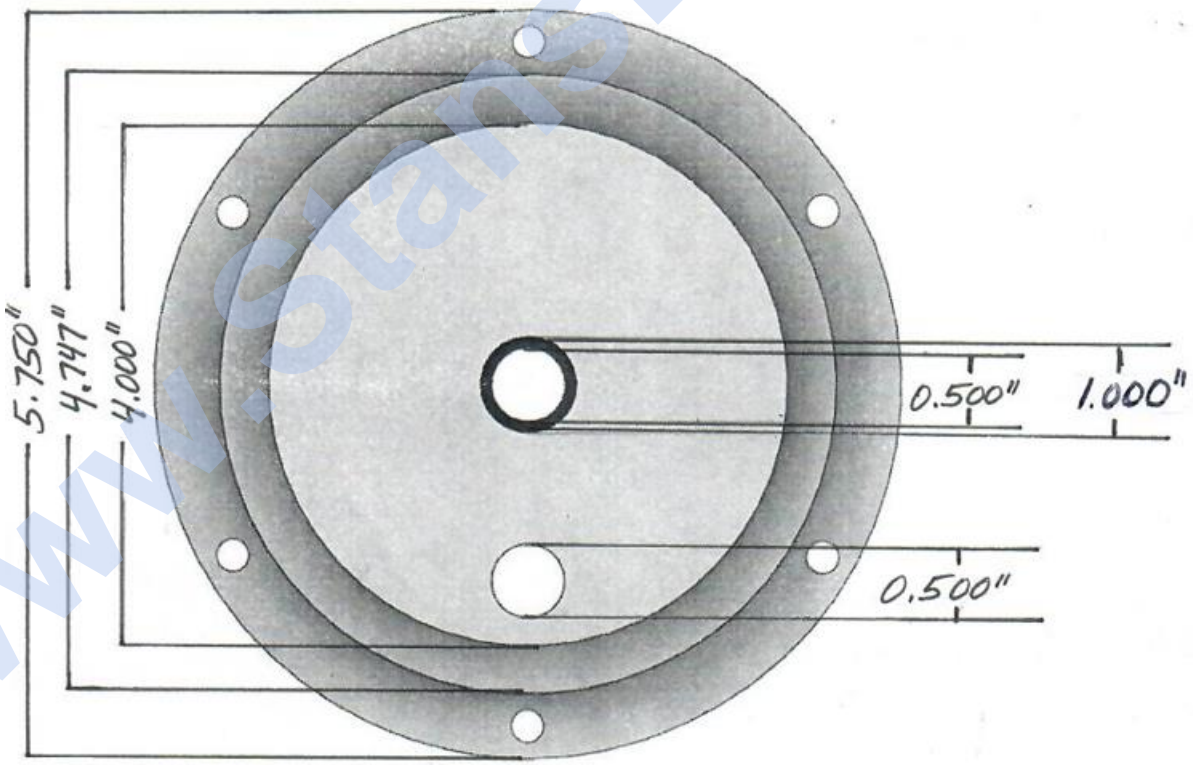

Bottom Cap – Cutaway View

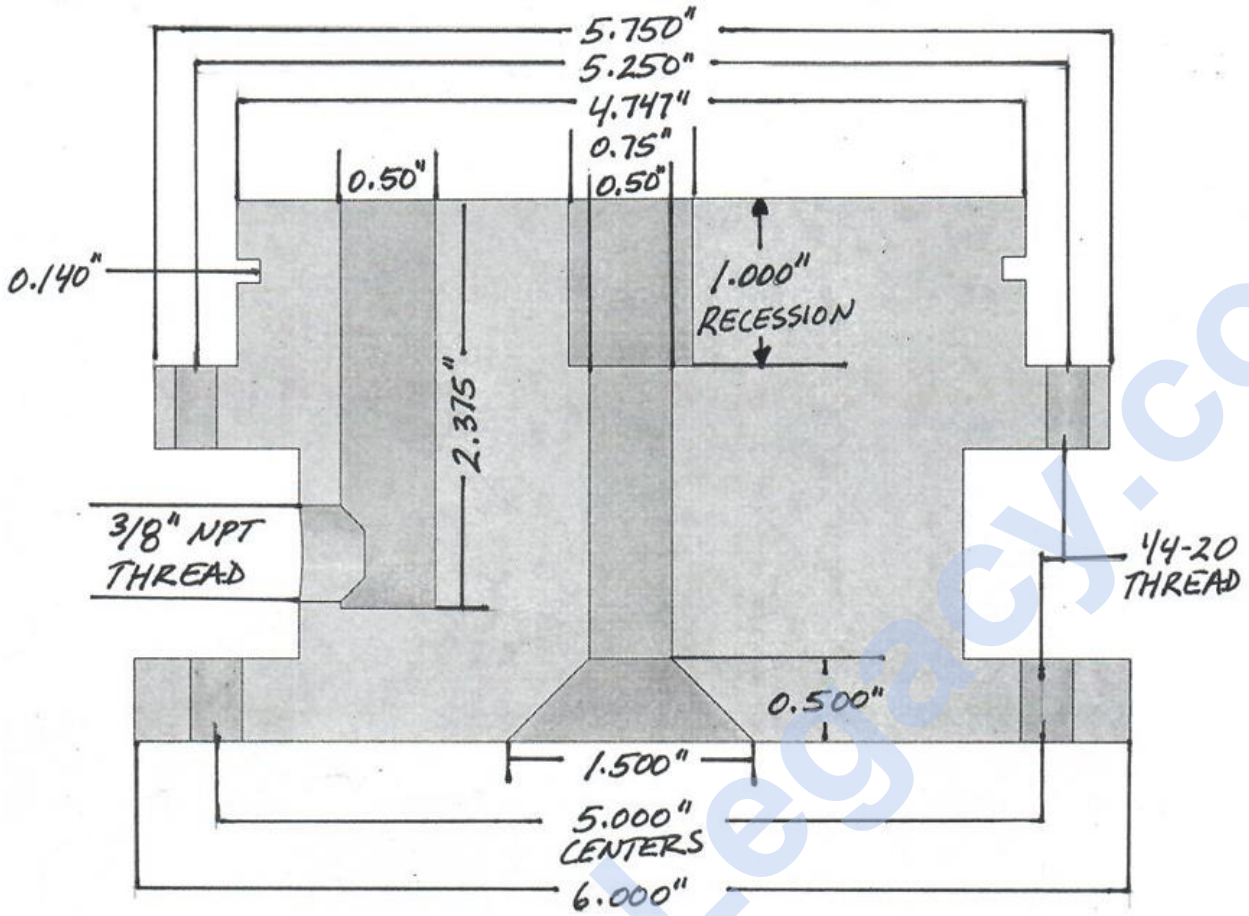

Side View

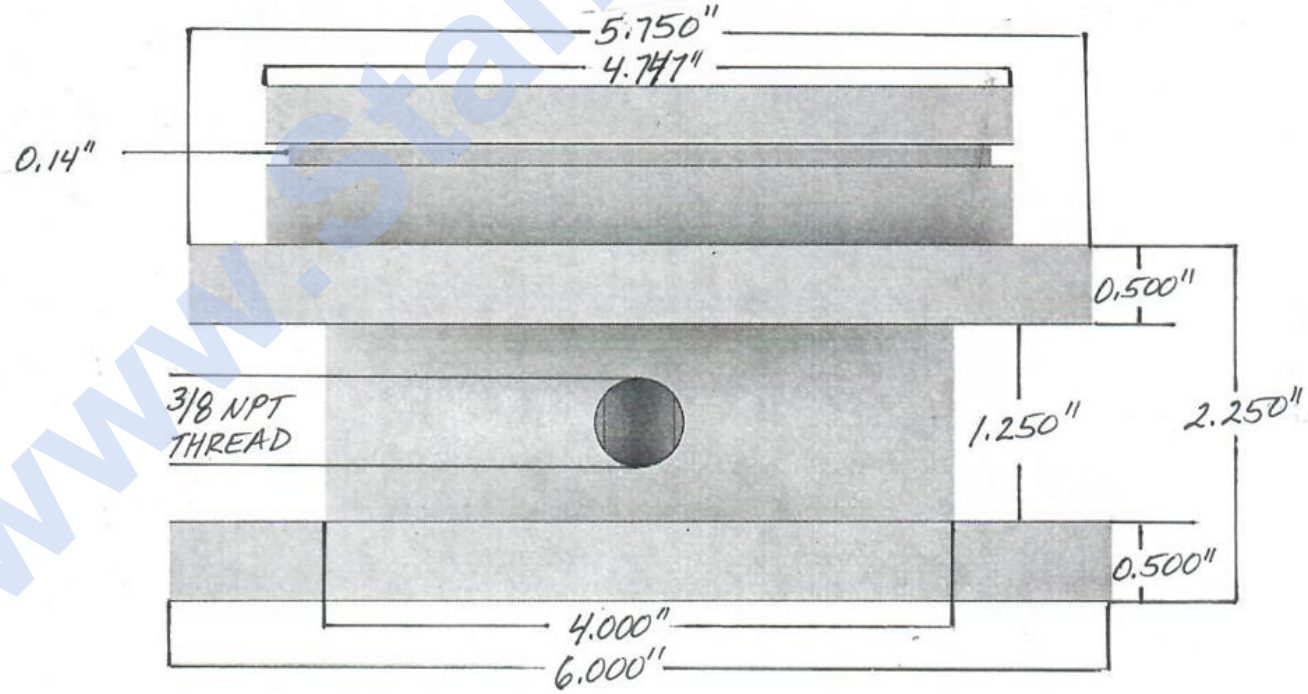

Bottom Cap – Top View

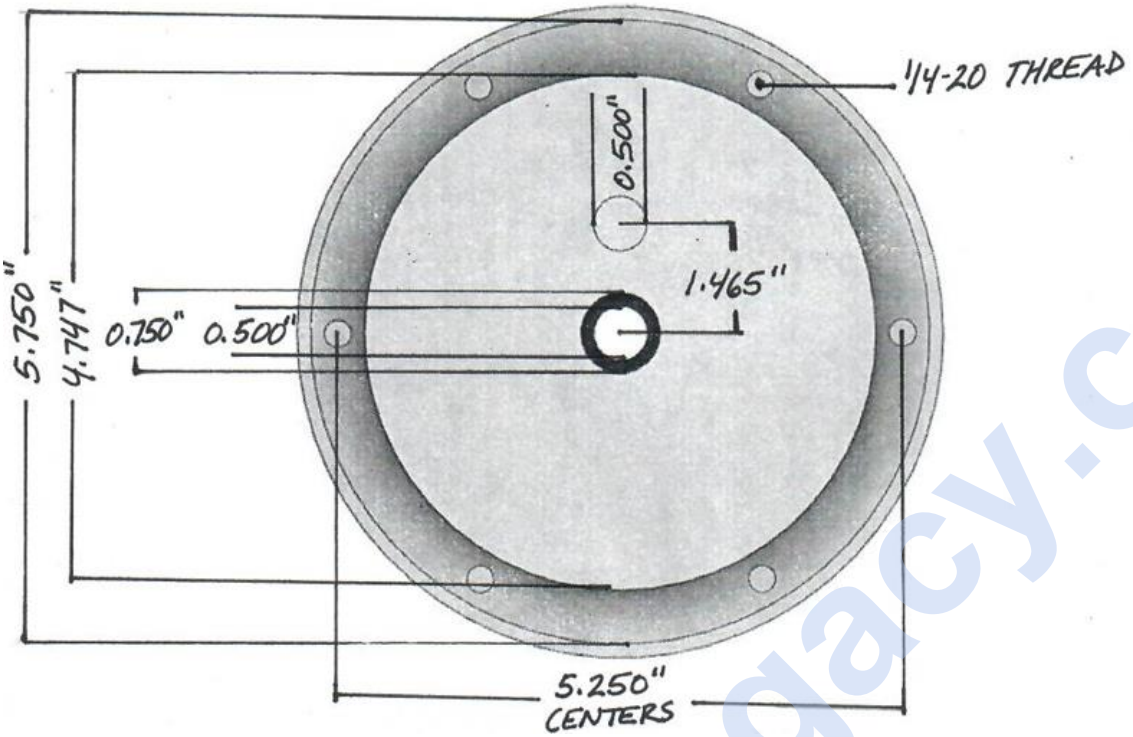

Bottom Cap – Bottom View

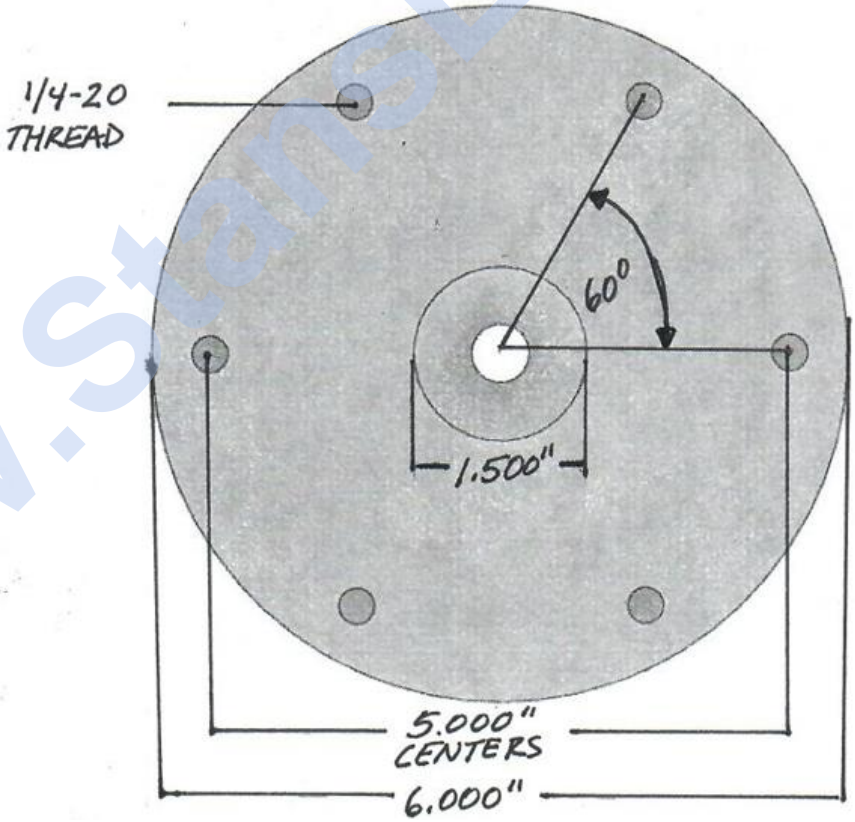

O-rings

(Thickness – 0.14”)

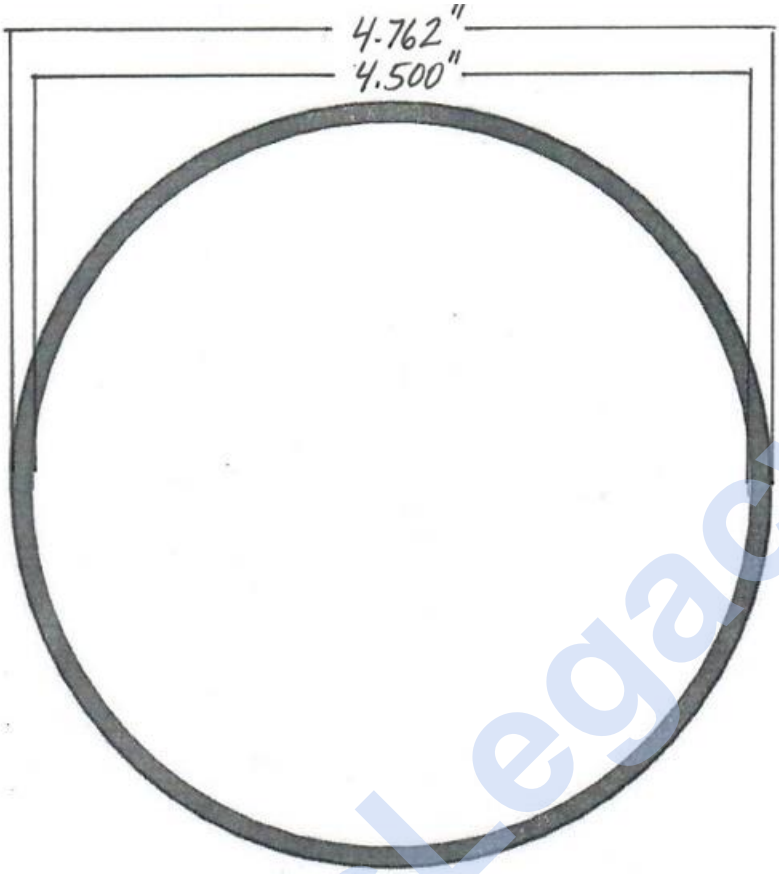

(Thickness – 0.070”)

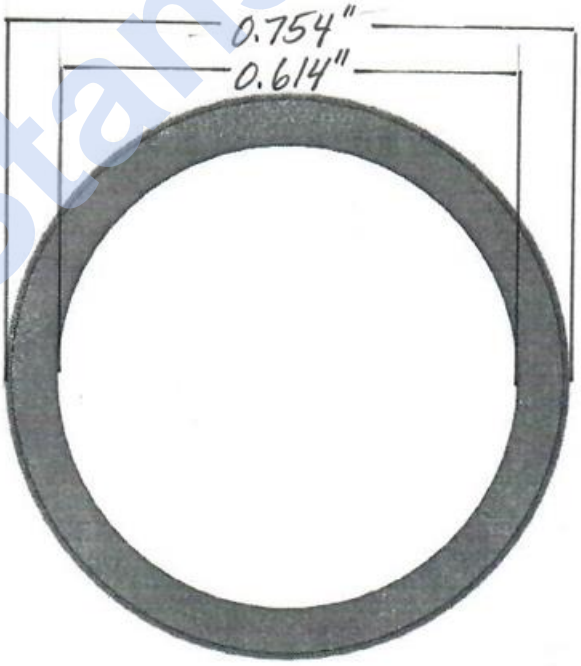

Center Tube – Side / Cutaway / Top & Bottom View